Synthesis, Characterisation and Thermal Degradation Studies of Carborane Containing Siloxane Elastomers:

Alistair Apedaile

A thesis submitted to the Department of Pure and Applied Chemistry, University of Strathclyde, in part fulfilment of the requirements for the degree of Doctor of Philosophy

March 2012

Declaration

This thesis is the result of the author's original research. It has been composed by the author and has not been previously submitted for examination which has led to the award of a degree.

The copyright of this thesis belongs to the author under the terms of the United Kingdom Copyrights Act as qualified by the University of Strathclyde Regulations 3.50. Due acknowledgement must always be made of the use of any material contained in or derived from this thesis.

Signed: Date:

Acknowledgements

Abstract

The investigation of model siloxane then subsequent *m*-carborane, 1,7-bis(dimethylmethoxysilyl)-*m*-carborane-carborane and 1,7-diallyl-*m*-carborane filled siloxane elastomer systems was undertaken. Thermal degradation studies showed little difference in the degradation profile of all carborane containing elastomers compared to the model system. The major degradation products of these materials are siloxane ring structures. Use of different cross-linkers also showed little difference in the thermal degradation properties of both materials.

Investigation of poly(dimethylsiloxane) (PDMS) polymerised by Lewis acid condensation catalysts to obtain a replacement catalyst for $FeCl_3$ has been undertaken. Both $FeCl_3$ and $GaCl_3$ give rise to vulcanized material in which the catalyst is trapped in the matrix. $AlCl_3$ and $ZnCl_2$ give high molecular mass material determined by both GPC and NMR spectroscopy. Kinetic studies have been undertaken to determine the activation energy for the $FeCl_3$ catalysed reaction. Carborane-siloxane network polymers have been produced using $FeCl_3$ as the catalyst. These materials display unusually high thermal stability and have been shown to be crystalline in nature by DSC analysis. Thermal volatilisation studies show carborane dehydrogenates during thermal decomposition.

Hydrosilylation has been employed to produce novel network carborane-siloxane materials. Samples have been produced where the molar ratio of carborane to PMDS has been varied from 1:1 to 6:1. Higher carborane containing materials have problems with volatile loss of unbound monomer. The materials have been studied using thermal volatilisation analysis and their degradation has changed remarkably from what was observed previously for carborane-siloxane elastomers. The majority of the degradation products observed are low molecular mass silanes. These form in part by the demethylation of the siloxane polymer promoted by platinum catalyst residues in the material.

In conclusion the incorporation of carboranes in siloxane elastomers does not improve the thermal stability of these materials significantly.

Table of Contents

Chapter 1: Literature Review

Chapter 4: Carborane Containing Polydimethylsiloxane Polymers and Elastomers Formed *Via* Lewis Acid Catalysis

Chapter 5: Carborane Containing Polydimethylsiloxane Elastomers Formed *Via* Hydrosilylation

Chapter 6: Conclusion and Appendix

List of Figures

xix

List of Reaction Schemes

List of Abbreviations Used

2D COSY – two dimensional correlation spectrometry

AIBN - azobisisobutyronitrile

DSC - differential scanning calorimetry

FID – free induction decay

GC - gas chromatography

GPC - gel permeation chromatography

HSAB – hard and soft acids and bases

HTV - high temperature vulcanization

IPN - interpenetrating polymer network

MAS – magic angle spinning

MALDI-TOF - matrix-assisted laser desorption/ionization-time of flight

m-Carborane - meta-carborane ($1,7$-$C_2B_{10}H_{12}$)

MS - mass spectrometry

NMR - nuclear magnetic resonance

o-Carborane - ortho-carborane ($1,2$-$C_2B_{10}H_{12}$)

p-Carborane - para-carborane ($1,12$-$C_2B_{10}H_{12}$)

PDMS – poly(dimethylsiloxane)

PMMA – poly(methylmethacrylate)

POSS - polyhedral oligomeric silsesquioxane

PPMS – poly(phenylmethylsiloxane)

RTV - room temperature vulcanization

SATVA – sub-ambient thermal volatilisation analysis

SEM – scanning electron microscopy

TEOS - tetraethyl orthosilicate

TfOH - trifluoromethanesulphonic acid (Triflic acid)

TGA - thermogravimetric analysis

THF – tetrahydrofuran

TVA – thermal volatilisation analysis

VOC- volatile organic compound

Chapter 1

Literature Review

1.0 Chapter Introduction

In this project the starting point is to repeat and investigate the classical routes to incorporation of carboranes into siloxanes. Transition metal Lewis acid catalysts have been the catalyst of choice since the discovery of these novel copolymer systems in the 1970s, e.g. $FeCl_3$ etc. Even recent developments in this area still involve the use of transition metal complexes with carbonaceous ligands. The advantage of these systems is the reactivity can be tuned and generally leads to high yields of product. However, the metal centre can act as a reducible site for promoting degradation of composite materials and polymers. This project will allow us to investigate the synthesis of poly(dimethylsiloxane) networks with a variety of catalysts and then elucidate the degradation pathways of the materials which can be influenced heavily by the catalysts remaining *in situ*.

With the reintroduction of thermal volatilisation analysis (TVA) at the University of Strathclyde the assessment of the degradation of materials produced in this project will be more comprehensive than if undertaken by TGA-MS. The advantage of our technique is it uses sub-ambient trapping of the volatiles that are evolved during degradation. This trapping technique allows us to distil the degradation products to allow a more quantitative measure of each major degradation component. From these data it is hoped the investigation of carborane-siloxane polymers will reveal the reason for the increased stability of carborane containing silicones, as previously it has been thought to be due to the electron withdrawing nature of the carborane moiety.

The aim of the research is to develop siloxane elastomers with nanoscale modifiers which complements the investigation by Lewicki, work that involved the ageing of novel polydimethylsiloxane (PDMS) nanocomposites.[1] The research carried out with polyhedral oligomeric silsesquioxane (POSS) systems dispersed throughout the polymer were shown to be stabilising upon ageing, but the POSS needs to be bound to the polymer to prevent leaching and aggregation of the filler. A system was

created that allowed for accurate modelling of the polymers' ageing due to the fillers used.

This investigation of PDMS elastomers will be focusing on the addition of novel boron containing nanocomposites, in particular functionalised carboranes. Carboranes will be included in the polymer backbone, bonded onto the polymer or added as dispersions. The main objective of the work is to maximise the boron content while retaining the elastomeric properties of the cross-linked polymer. Characterisation by thermal degradation analysis and mechanical property testing will allow modelling of the new system and comparisons can be drawn with known data for the unmodified systems.

This review will cover discussions on PDMS polymers, PDMS elastomers, thermal stability, an overview of carborane chemistry and composite boron containing silicones.

1.1 Synthesis of Poly(dimethylsiloxane)s

Friedel and Crafts discovered the first siloxanes in 1866 by the partial oxidation of tetraethylsilane.[2] In 1874 Ladenurg fully polycondensated a silicon ester when he added aqueous hydrogen iodide to form a siloxane and water shown in Scheme 1.1:[3]

$$n\ Si(C_2H_5)_2(OR)_2 + 2n\ HI \longrightarrow [(C_2H_5)_2SiO_2]_n + 2n\ RI + n\ H_2O$$
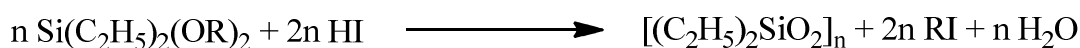
Scheme 1.1: Condensation of an organosilicate to a siloxane polymer. R group = alkyl

During the Second World War American scientists further developed poly(siloxanes) as a replacement material for natural rubber since rubber was sourced mainly from Asia whose countries were mostly under Japanese occupation at the time. After the war elastomeric poly(siloxane) materials were used as gaskets and have found uses in medical science, for example silicone breast implants. This is owed to the low toxicity, chemical inertness and flexibility of these materials. More recently they are finding uses in the electronics industry as housing for electrical components due to their insulating properties. In laboratories they can be found in vacuum lines as o-rings to provide a barrier seal as the material can withstand large pressure differences. In the home they can be found in the freezer as flexible ice trays; their low T_g allows the ice tray to remain elastomeric so that the ice can be "popped" out of the tray once ready. Since the days of Friedel and Crafts a more commercially viable synthesis of these siloxane polymers has been discovered. The monomer unit of PDMS is synthesised *via* the Rochow process where elemental silicon is added to methyl chloride in the presence of a copper catalyst (Scheme 1.2) to afford the intermediate (dichlorodimethyl)silane:[4]

$$2\ CH_3Cl + Si \xrightarrow[200\ -\ 300\ ^oC]{Cu\ Catalyst} (CH_3)_2SiCl_2 \quad \sim (70\text{-}90\%)$$
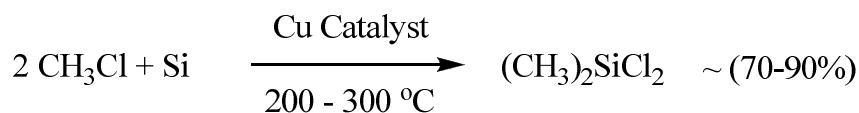
Scheme 1.2: Overview of the Rochow process

1.1 Synthesis of Poly(dimethylsiloxane)

The reaction does not lead to exclusive formation of (dichlorodimethyl)silane and further purification is required. The next step in the synthesis of PDMS is to hydrate the (dichlorodimethyl)silane with loss of hydrogen chloride. Upon hydration the compound undergoes a series of condensation reactions when heated. Distillation produces low molar mass cyclic oligomers with rings that contain 3 or 4 silicon atoms.[5] This is shown in reaction Scheme 1.3:

$$(CH_3)_2SiCl_2 + 2\,H_2O \xrightarrow{\text{- 2 HCl}} (CH_3)_2Si(OH)_2 \xrightarrow[\text{- 2 H}_2\text{O} \ \ k_2]{\Delta \ \ k_1} [(CH_3)_2SiO]_n$$
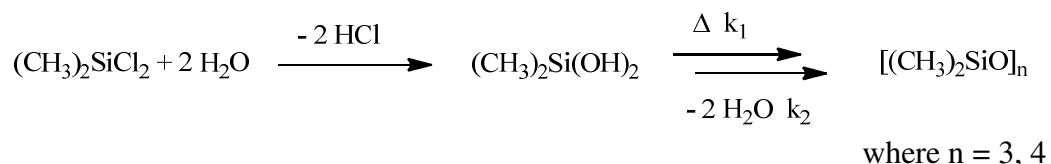
where n = 3, 4

Scheme 1.3: Cyclic oligomers and polymers of siloxanes are denoted as D_n where n is the number of siloxane repeat units

A noticeable feature of this reaction is the formation of oligomers over a polymer chain. This is due to the polymer not conforming to the Flory model of polycondensation.[6] This model predicts that functional groups on the polymer will act similarly to those of the monomer but this is not the case for poly(dimethylsiloxanes). The consequence of this is that the rate of condensation of the monomer and dimer are different by a factor of 35 (k_1/k_2 in Scheme 1.3). Also formation of water favours the equilibrium of the reaction towards the starting material after each successive condensation.

The silicone oligomers from this reaction are then carried forward into ring opening polymerisation reaction to form poly(siloxane) polymers. These reactions are thermally controlled, anionic or cationic ring opening polymerisations. Most commercial syntheses use anionic ring opening reactions as the final molecular mass of the polymer can be more intimately controlled. This is achieved by using alkyl-lithium reagents or alkali metal hydroxides as initiators.[7-8]

Using alkyl-lithium initiators polymerisation is carried out at –78 °C in the presence of a Lewis base such as tetrahydrofuran (THF). THF is an aprotic solvent that lowers the aggregation of the alkyl lithium cages, increases the reactivity and rate of

reaction of the alkyl lithium reagent. A general reaction Scheme for a D_3 siloxane is this is shown in reaction Scheme 1.4:
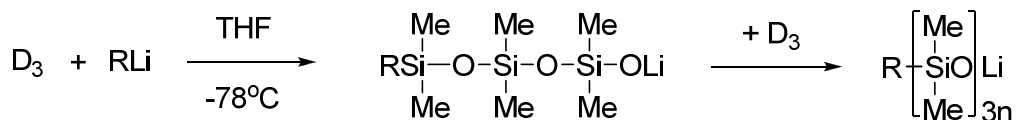
Scheme 1.4: Anionic Ring opening polymerisation of siloxane oligomers to PDMS

Alternatively by adding an alkali metal hydroxide instead of an alkyl lithium reagent the same ring opening reaction can be carried out. Initiation of this reaction is the opening of the SiOSi linkage by nucleophilic attack of ⁻OH forming a silanolate anion, which then propagates the formation of the polymer. The reaction is terminated by the addition of a capping group such as trimethylsilyl, stopping any further condensation reactions occuring.[9]

With regard to rheology, poly(siloxane)s display typical extensional viscosity and non-Newtonian behaviour at high molecular masses; at low molecular mass materials will commonly show Newtonian behaviour as the polymer is very flexible with few entanglements. When buying poly(siloxane) materials from companies like Sigma Aldrich, it is common to base the choice on their average viscosity rather than by molecular mass averages. This is mainly due to the use of poly(siloxane)s as rheological calibration standards. However, it is possible to determine the molecular mass of the material from the viscosities quoted on the bottle. The Mark-Houwink-Sakurada equation is a relationship that links the intrinsic viscosity η of a polymer to the molecular mass, M, *via* equation 1.1:[10]

$$[\eta] = KM^{a}$$

Equation 1.1: Mark-Houwink-Sakurada equation where a > 0.5 and K is a constant

From the data supplied with the polymer (temperature at which viscosity measurement was taken), values of *a* and *K* can be obtained from the polymer handbook;[11] subsequently molecular mass can be determined. More commonly some of the average molecular masses are supplied and a graph can be plotted as the log of

viscosity against molecular mass. An example using data from Sigma Aldrich website is shown in Figure 1.1 for poly(dimethylsiloxane) (PDMS):[12]

The plot shows log Viscosity (cSt) on the y-axis against Molecular Mass (M_n) on the x-axis, with the fitted equation $y = 0.7832\ln(x) - 4.7309$ and $R^2 = 0.9743$.
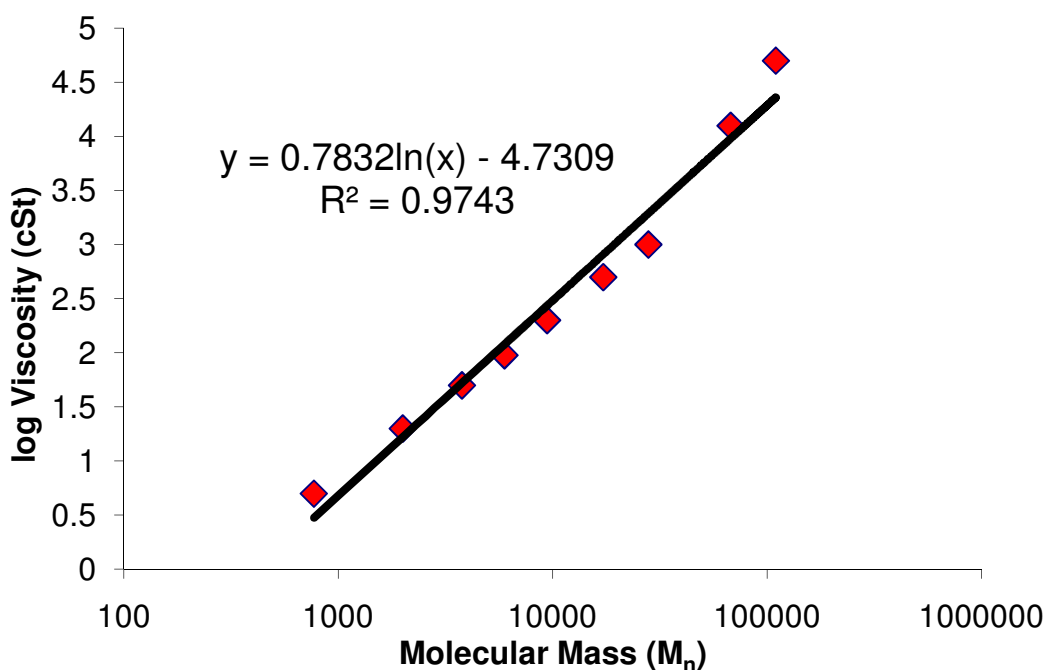
Figure 1.1: A plot of the log of intrinsic viscosity against average molecular mass for a series of poly(dimethylsiloxane) polymers available from Sigma Aldrich

The plot is useful for estimating the molecular mass of PDMS where only the viscosity is quoted when purchased, removing the need for GPC analysis. The graph gives reasonable agreement with the Mark-Houwink-Sakurada equation but at higher molecular masses the viscosity starts to rise in a non-linear manner due to increased number of entanglements between polymer chains increasing frictional flow of the polymer.

1.1.1 Formation of Cross-linked Siloxane Elastomers

In order for the poly(dimethylsiloxane) to have desirable properties in this project the polymer must be cross-linked to form an elastomer. The process of cross-linking the polymer is known as vulcanisation, a process that has been in commercial use since the 19th century. In this process the polymer chains are brought together *via* chemical bonds that give greater mechanical reinforcement to the polymer and create a more organised system. An example of vulcanisation is shown in Scheme 1.5:
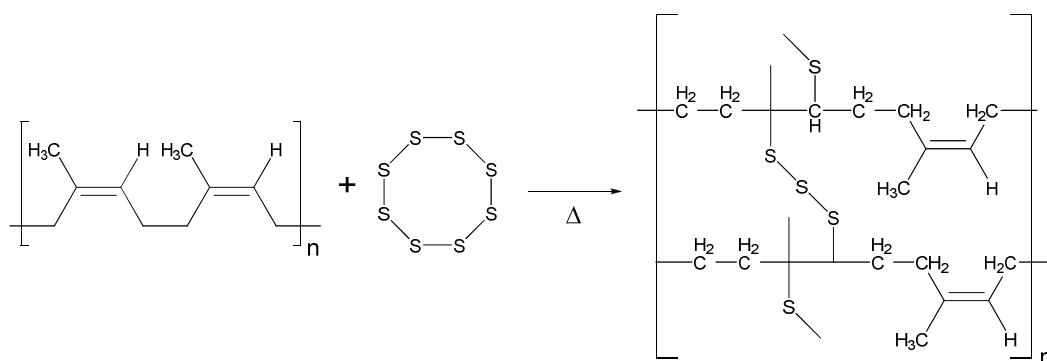
Scheme 1.5: Vulcanisation of poly(isoprene) using sulphur to form rubber

To facilitate the vulcanisation reaction functionality on the cross-linker and polymer must be compatible. The presence of a catalyst is usually required to propagate the reaction although certain reactions can also occur uncatalysed as thermal processes.

The cross-linking of the elastomer will be achieved by using room temperature vulcanisation (RTV). In this process a cross-linker and catalyst are dispersed throughout the polymer and upon activation of the catalyst the liquid polymer starts to form an elastomeric network. The use of small amounts of tri- or tetra-functional cross-linker allows a high level of cross-linking to be achieved. Tetraethyl orthosilicate (TEOS) is one of many cross-linkers used in siloxane elastomers and when present with tin 2-ethylhexanoate acid activated with water the RTV occurs as in reaction 1.6:
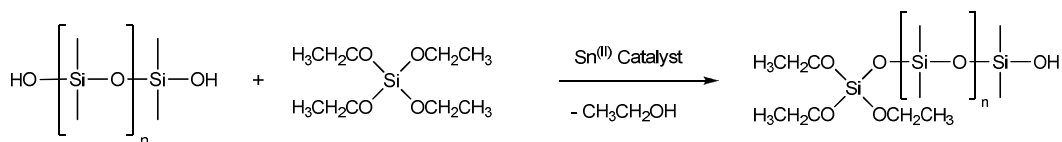
Scheme 1.6: Condensation of hydroxy end capped siloxane polymer and TEOS cross-linker

As the vulcanisation proceeds the elastomer is usually cured in an oven to promote a faster rate of reaction and evaporation of unwanted ethanol. As the reaction proceeds to completion the elastomer gels and no further cross-linking takes place. It is important that the level of cross-linker is controlled so that no unbound TEOS species are left un-reacted. Tang *et al.* have shown that although using more cross-linker does indeed speed up rate of vulcanization, the degree of vulcanisation is lowered and longer cure times are required.[13] When an excess of cross-linker is used the hydrolysis of untreated alkoxy-orthosilane will also produce silica particles. Another consequence of using an excess of cross-linker is that residues left *in situ* promote thermal degradation of the product.

The role of the tin catalyst during these reactions is subject to conjecture. Generally it is accepted that upon addition of water the tin is hydrated to R_xSnOH (R = $CH_3(CH_2)_3CH(C_2H_5)CO_2$ and x = 1 or 2) with this product being prone to condensation, hence activated. Van der Weij discusses the mechanism in which he infers a catalytic cycle involving various organic tin compounds. The active hydrolysed tin is first to react with the cross-linker liberating ethanol and forming a Sn-O-Si bond.[14] When the target Si-OH end group from the polymer reacts with this intermediate a new Si-O-Si linkage is made and the hydrolysed catalyst is regenerated. The cycle is shown in reaction Scheme 1.7:

1.1.1 Formation of Cross-linked Siloxane Elastomers
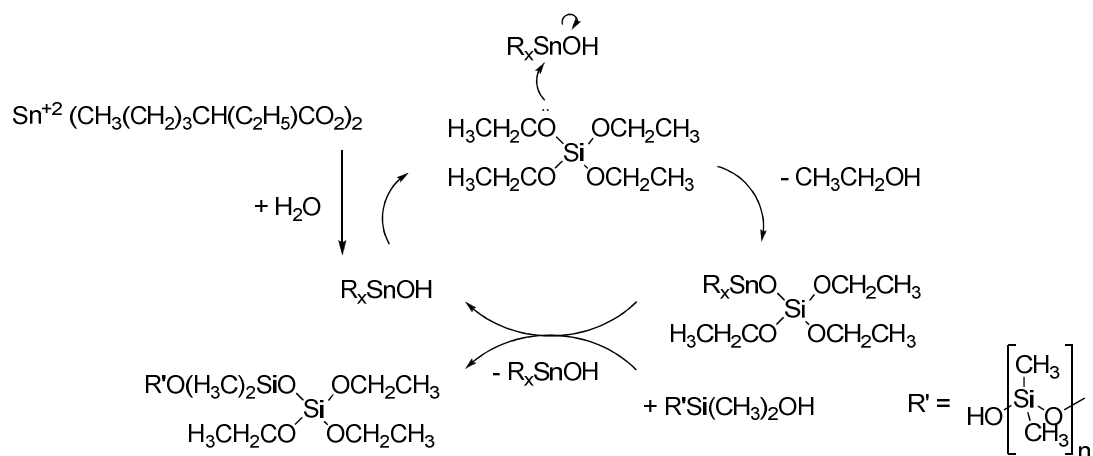
Scheme 1.7: Tin(II) 2-ethylhexanoate acid catalyst cycle

Another method of producing siloxane elastomers involves the incorporation of vinyl end capped siloxane polymers cross-linked in the presence of free radical initiators. By use of cross-linking agents for vinyl end groups, a solid elastomeric network can be synthesised similar to that of Scheme 1.5. The free radical initiator is usually a compound with a leaving group that is activated by either heat or UV light. Traditionally azobisisobutyronitrile (AIBN) was an initiator of choice and degraded under heating to form two 2-cyanopropyl radicals with the evolution of nitrogen gas.[15] However, the compound had an inherent risk of explosion if not handled correctly and has been phased out of production. More commonly, peroxide initiators are used since they have a more stable storage life and are easier to handle. An example of high temperature vulcanization (HTV) initiation reaction of a siloxane polymer is shown in Scheme 1.8:
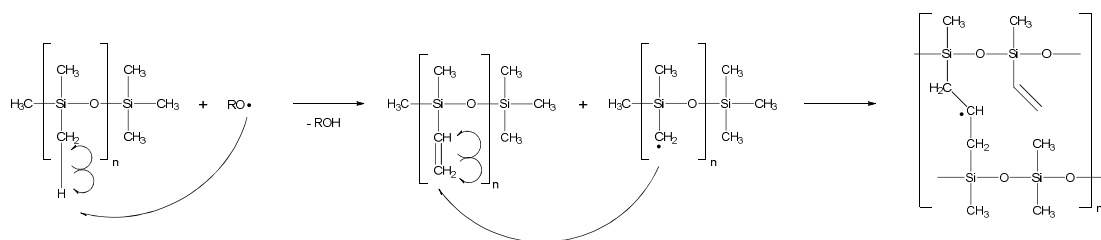
Scheme 1.8: Formation of a HTV siloxane elastomer network using a free radical initiator

1.1.1 Formation of Cross-linked Siloxane Elastomers

The newly formed free radical on the initiator abstracts hydrogen from a methyl side group on the siloxane polymer which then propogates by opening the vinyl side group. The resulting network forms *in situ* and does not require any further curing, however end capping is used to terminate the polymerisation process and prevent free radicals in the polymer matrix from back biting the elastomer. The reactions are carried out under non-oxidising conditions as elemental oxygen is a reactive spieces in the presence of free radicals lowering yield and also may form unwanted peroxide side products.

1.1.2 Interpenetrating Siloxane Polymer Networks

Interpenetrating polymer networks (IPN's) are the combination of two or more vulcanized polymers held together by physical interactions at the boundary interface between each polymer. The polymers must be cross-linked either simultaneously or sequentially which gives rise to interpenetration of each polymer and can be achieved by using different cross-linking chemistries that are non-competing. The phase separation between the two polymers is microscopic in size, which leads to a "dual phase continuity" as this separation is not observable on a macroscopic level.[16]

The main problem to be overcome in forming an IPN is that the solubility parameters of one polymer in another may cause phase-separation, that is unfavourable for formation of a network. Solubility parameter is usually a function of molecular size and also end group functionality on a polymer. The system employed must be chosen carefully to avoid to large differences in these parameters, and therefore inadequate mixing of each polymeric system. There is also a dependency on the thermodynamic treatment of the ΔH of mixing of the two polymers. The arguments for this are beyond the scope of this literature review and the reader is directed to Chapter 8 of "Polymer Structure Characterisation" by R. A. Pethrick, P. G. Hodge and R. Wang, also Chapter 8 of "Polymers: Chemistry and Physics of Modern Materials" by J. M. G. Cowie and V. Arrighi. Essentially there is not just a dependence on heat of mixing but also molar mass considerations in determining the miscibility of two phases. Part of this problem arises from entropic penalties for large molecular mass polymers mixing with each other.

IPN's can provide an alternative route to incorporation of carboranes. Carboranes as cross-linkers or creation of an unreported polymer system that will allow for novel boron dispersions while retaining the elastomeric properties of siloxanes could be synthesised.

1.2 Alternative Synthesis of PDMS Polymers/Networks

In this Section other methods of forming siloxane elastomer networks are considered.

1.2.1 Formation of PDMS Networks Using Lewis Acid Catalysis

Another method that is less commonly used in the formation of high molecular mass PDMS polymers/networks but will be investigated in the course of the project is Lewis acid catalysed polymerisation. A Lewis acid is defined as a compound that an electron acceptor, a Lewis base is an electron pair donor.[17] Unlike a Brønsted-Lowry acid in which the strength is quantifiable by measuring pK_a values, the strength of a Lewis acid depends on the adduct formed with the Lewis base electron pair donor.

Hard and soft acids and bases (HSAB) theory was developed in 1963 by Ralph G. Pearson as an attempt to bridge a gap in understanding between inorganic and organic reaction chemistry.[18] The theory attempted to classify various chemical species in the periodic table as "hard or soft" based on the reactivity of these species to the Lewis base pair. By comparative studies of reaction rates the Lewis acid species could be classed as either type "a" or type "b". Examples of each are shown in the Table below:

Type "a"	Type "b"
H^+, Li^+, Na^+, Mg^{2+}, BX_3, AlX_3, Sn^{2+}, Ga^{3+}, La^{3+}, VO^{2+} …*	Cu^+, Ag^+, Pd^{2+}, Pt^{2+}, CH_3Hg^+, Tl^{3+}, RS^+, I_2, Br_2 …*

* A full list can be found in reference 17

The species that are classified as type "a" are hard acids and those that fall into type "b" are soft acids. It is also to be noted that there are borderline species that are neither hard nor soft but they will not be discussed further. The properties of hard and soft Lewis acids are distinct and are listed below:

1.2.1 Formation of PDMS Networks Using Lewis Acid Catalysts

Hard Acid

- Small atomic radii

- Non polarisable

- Ionic bonding character

- High electronegativity

- High oxidation states

Soft Acid

- Large atomic radii

- Polarisable

- Covalent bonding interaction

- Low electronegativity

- Low oxidation states

This is an important point to consider when choosing a Lewis acid reagent for a reaction. The strongest interactions of a Lewis acid and substrate come from either hard-hard or soft-soft interactions as they lead to stabilising interactions.

In terms of catalysts for a reaction, other design motifs may need to be considered. Introduction of different ligands at the metal centre will influence the donor properties of these metals in a reaction. Thus, the electron donating/withdrawing properties of a ligand will influence the hardness of the Lewis acid. For example, AlX_3 reactivity decreases in the following way $F^- > Cl^- > Br^- > I^-$ as the electron withdrawing ability of the halogen decreases. Another consideration is designer ligands that impart stereochemical control as well as enhanced reactivity of the metal.[19] This is usually achieved by introduction of chiral ligands which give exclusively one conformation (R or S) over the other.

These catalyzed reactions fall into either reaction type 1 or reaction type 2 Lewis acid mediated reactions.[20] Type 1 is the addition of a Lewis acid to a substrate that causes a rearrangement of the starting material to the desired product. Type 2 which is more common is the addition of a Lewis acid to the substrate and then attack by a reagent to form a product.

For a PDMS system Lewis acid catalysis can be used to create a network polymer by the addition of $FeCl_3$ to a reaction vessel containing a methoxy capped PDMS and (dichlorodimethyl)silane in the bulk condensation shown in Scheme 1.9:
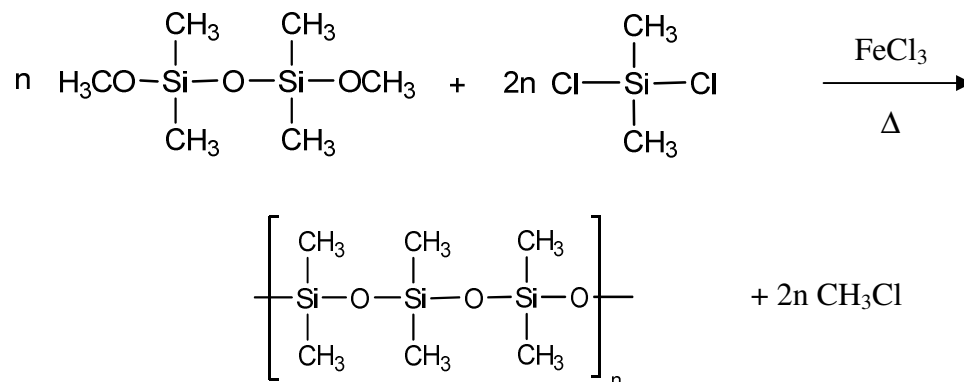
Scheme 1.9: Lewis Acid catalysis of methoxy-capped siloxane to a PDMS polymer

The ferric chloride also initiates a cross-linking pathway by replacement of some of the side CH_3 groups on the polymer with Cl then condensation with newly formed OH groups to provide new SiOSi links.[21]

$FeCl_3$ can be directly prepared by dissolution of elemental iron in liquified chlorine. Industrially the catalyst is prepared by dissolving iron ore in hydrochloric acid, where Fe^{2+} and Fe^{3+} are then present in solution. The reaction is completed by adding an excess of chlorine to the solution forcing the equilibrium towards $FeCl_3$.

In terms of Lewis acid strength $FeCl_3$ lies fairly central in the hardness scale. The qualitative sequence for the catalysts has been suggested for metal halides $BX_3 > AlX_3 > FeX_3 > GaX_3 > SbX_5 > SnX_4 > AsX_5 > ZnX_2 > HgX_2$.[22] It is hoped by replacement of the catalyst in this reaction instead of networks that high molecular mass polymers will be created instead of networks. This will be investigated by altering the Lewis acid used to see what effect acceptor strength has in these reactions.

1.2.2 Formation of PMDS Networks Using Hydrosilylation

Most recent developments in PDMS network formation have been focused on hydrosilyation chemistry. Hydrosilylation can be defined simply as the formation of a bond between a silicon and a carbon atom, more explicitly it is the addition of a silane (Si-H) group across an olefinic double bond.[23] This is acheived by using a platinum(0) catalyst; typically Karstedt's or Speier's catalyst is used. An overview of hydrosilylation is shown in Scheme 1.10:
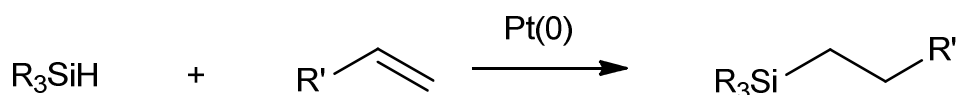
Scheme 1.10: Overview of Hydrosilylation

Karstedt's catalyst was developed in 1979 and patented by B.D. Karstedt.[24] The catalyst is prepared using chloroplatinic acid as shown in Scheme 1.11:[25]
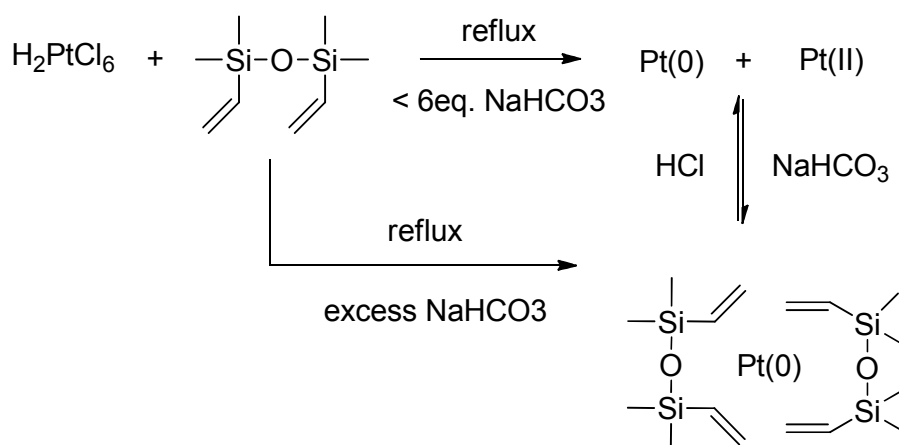
Scheme 1.11: Preparation of Karstedt's catalyst

By use of excess base the platinum is converted to its zero oxidation state and is then stabilised by the 1,1,3,3-divinyltetramethyldisiloxane ligand. The final step once all the acid has been neutralised is to filter out the sodium carboanate and wash with more siloxane ligand. Karstedt's catalyst solutions which are commercially available are often either dissolved in vinyl terminated PDMS or as molar solutions in xylene.

1.2.2 Formation of PMDS Networks Using Hydrosilylation

Hydrosilylation addition reactions occur by the Chalk-Harrod mechanism where the platinum catalyst undergoes oxidative addition, alkane insertion and reductive elimination.[26] The catalytic cycle is shown in Scheme 1.12:
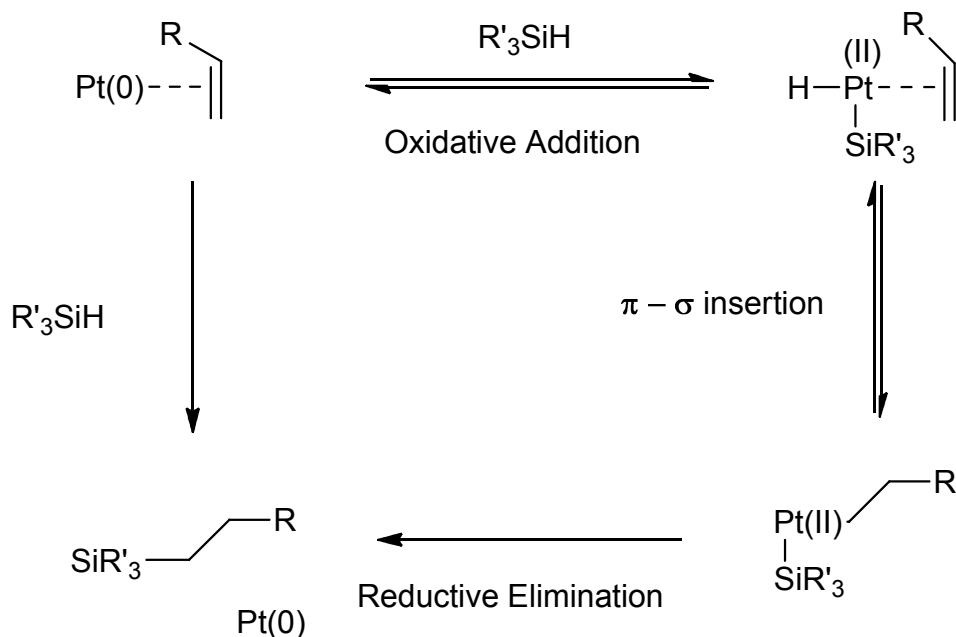
Scheme 1.12: Chalk-Harrod Mechanism

Addition across the olefinic double bond is not exclusive to one end of the double bond. The silane group can either undergo α or β addition across the vinyl bond. The reaction is thought to proceed with the formation of platinum colloids which has been investigated further by UV-vis spectroscopy.[27] As the colloids form in solution the oxidation state change in the catalyst leads to a change in colour, an intense yellow brown colour which is also dependant on how much platinum is present during the hydrosilylation step. The reaction step is further complicated by the suggestion that there is an induction period based on the activation of the catalyst by oxygen. The following addition to the cycle has been suggested in Scheme 1.13:

$$—Si—O—Si—$$

Pt(0)

INDUCTION PERIOD

O_2

$Pt_x(0)\ (O\text{-}O)$

$HSiR_3$

R' ⟶ SiR_3

$R' \Vert$ ⟶ $H \overset{}{\underset{R_3Si}{\diagdown}}\ Pt_x(0)\ (O\text{-}O)$

$H \overset{}{\underset{R_3Si}{\diagdown}}\ Pt_x(0)\ (O\text{-}O)$

R'
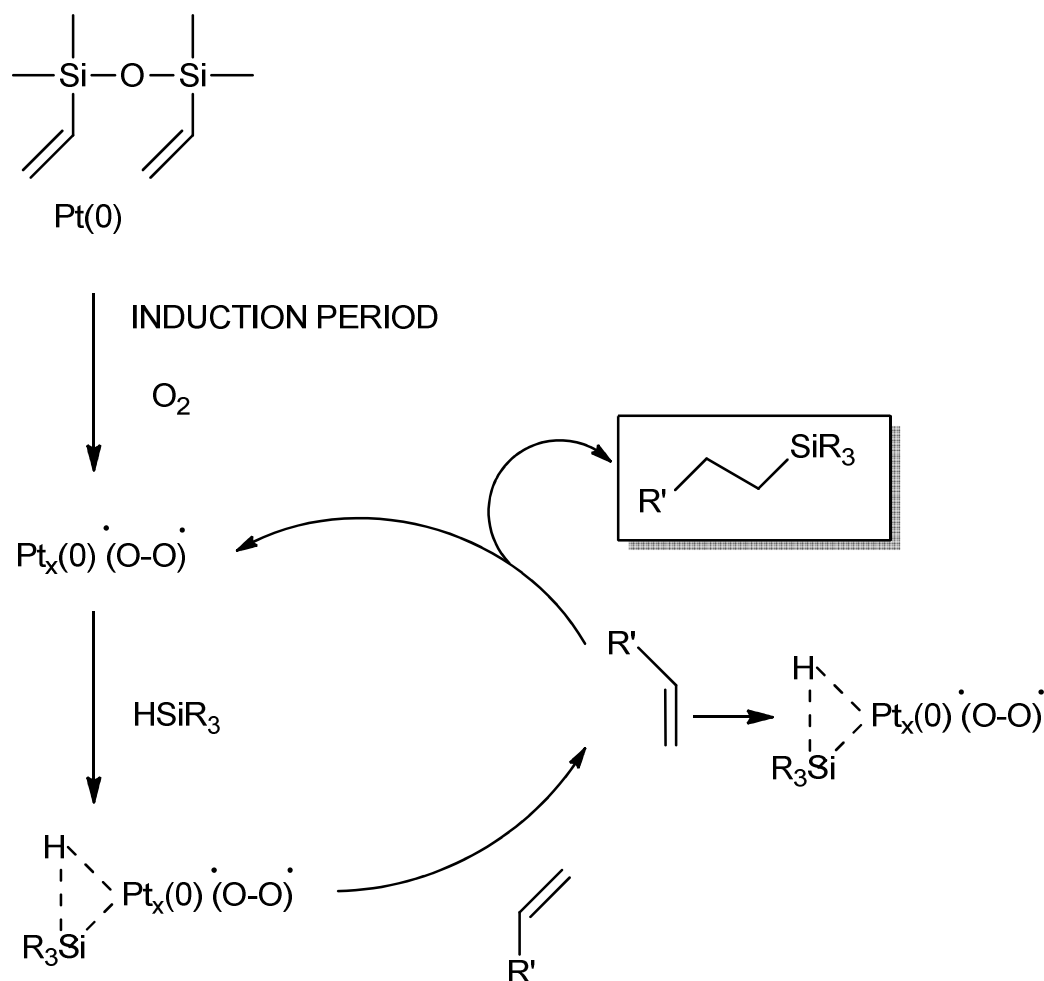
Scheme 1.13: Proposed cycle for Karstedt's catalyst

Experimental evidence in the laboratory confirms this with colour changes appearing after short delays and development of colour top down in solution. Hydrosilylation offers an alternative route to siloxane elastomer network formation and is an efficient process, with high yields obtained.

Palladium(0) and platinum(0) metals are used as heterogeneous catalysts for hydrogenation and dehydrogenation reactions. Hydrogenation usually occurs when there is a positive hydrogen pressure over the reaction otherwise the equilibrium lies to the metal catalysing removal of hydrogen in a dehydrogenation process. Potential problems with the catalyst could be the release of hydrogen from the silane rather than addition of the vinyl group or further reduction of the vinyl bond. Again this

1.2.2 Formation of PMDS Networks Using Hydrosilylation

must be assessed when considering transition metal catalysts as surfaces to perform polymerisation reactions with silicones and carboranes.

1.2.3 Formation of PDMS Polymers/Networks Using Wilkinson's Catalyst

Most recently a catalyst known industrially for hydrogenation reactions has found interest in the field of sol-gel silicone chemistry. Wilkinson's catalyst has traditionally been used to catalyse the hydrogenation of alkenes. The synthesis of Wilkinson's catalyst is based on a ligand exchange process at the metal centre.[28] In this instance the (triphenyl)phosphine ligands have a stronger affinity for the Rh(I) centre and replace the coordinate chloride and water on the reduced metal centre. The reaction is summarised in Scheme 1.14:

$$RhCl_3(H_2O)_3 \; + \; 4\,PPh_3 \; \xrightarrow[\Delta]{CH_3CH_2OH} \; RhCl(PPh_3)_3 \; + \; OPPh_3 \; + \; 2\,HCl \; + \; 2\,H_2O$$
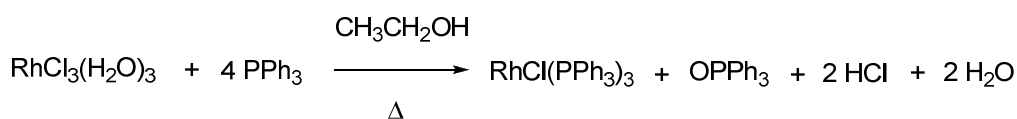
Scheme 1.14: Synthesis of Wilkinson's catalyst

An orange precipitate appears in solution and further heating takes the reaction to completion. The product is a red salt that can be filtered and then collected. Solvent choice when using the catalyst is important as the triphenylphosphine ligands are labile and their loss leads to dimerisation of the rhodium metal centre via chlorine-bridge formation.

In 2000 Zhang *et al.* described a reaction in which a (trimethyl)silane condensed with (trimethyl)silanol, with loss of hydrogen, using Wilkinson's catalyst.[29] The reaction is shown in Scheme 1.15:

Scheme 1.15: Synthesis of siloxane bonds using Wilkinson's catalyst

The reaction requires a donor solvent to break down any dimer structure the catalyst may adopt and the reaction times are generally slow. Also hydrogen is evolved so slow reactions in this instance are a benefit as to keep the concentration of gas evolved at safe levels. This catalyst could be used in the formation of network siloxane elastomers with the correct number of tri- or tetra-functional cross-linkers. These are most likely to be -OH functional as multifunctional hydride materials are unstable in the presence of water and convert to the alcohol.

In the next Section the discussion will focus on the thermal degradation of a PDMS elastomer, mechanisms on how this is proposed to occur and the routes by which the thermal stability of PDMS elastomers can be increased.

1.3 Thermal Degradation of PDMS Elastomers

In this Section the thermal degradation of PDMS under non-oxidative and oxidative environments will be considered. The first report of the investigation into the thermal stability of PDMS was by Adrianov in the 1950s.[30] He noted that the flexibility and structure of the elastomers were the cause of the main mechanisms behind the degradation of the material. In particular side groups on the silicone polymer were shown to be important, as methyl groups in PDMS were more reactive than phenyl side groups in poly(phenylmethylsiloxane) (PPMS), especially under oxidative environments.

Focusing on non-oxidative degradation of PDMS elastomers, using thermogravimetric analysis PDMS elastomers start degrading around 350 °C and char residues at 800 °C are typically about 5%, where most of the polymeric material has been volatilised.[31] The most important paper to discuss the mechanism and degradation products formed during non-oxidative heating was by Grassie and MacFarlane.[32] They used thermal volatilisation analysis and sub-ambient trapping of volatiles that formed. The collected volatiles were then dissolved in chloroform where GPC analysis revealed that the main degradation products of PDMS were cyclic oligomers from D_3 to D_{10} in size. The following yields were obtained from the GPC analysis shown in Table 1.1:

Cyclic Observed	Yield %	Cyclic Observed	Yield %
Trimer	73	Heptamer	1
Tetramer	13	Octomer	0.9
Pentamer	4	Nonamer	0.3
Hexamer	6	Decamer	0.2

Table 1.1: GPC analysis of degradation products collected from TVA run of PDMS

The mechanism for formation of the cyclic oligomers is known as "reversion". In this process once the polymer chain has broken due to thermal decomposition it is

able to backbite and eliminates cyclic species. The initiation is usually activated by water or catalyst residues, as shown in Scheme 1.16:
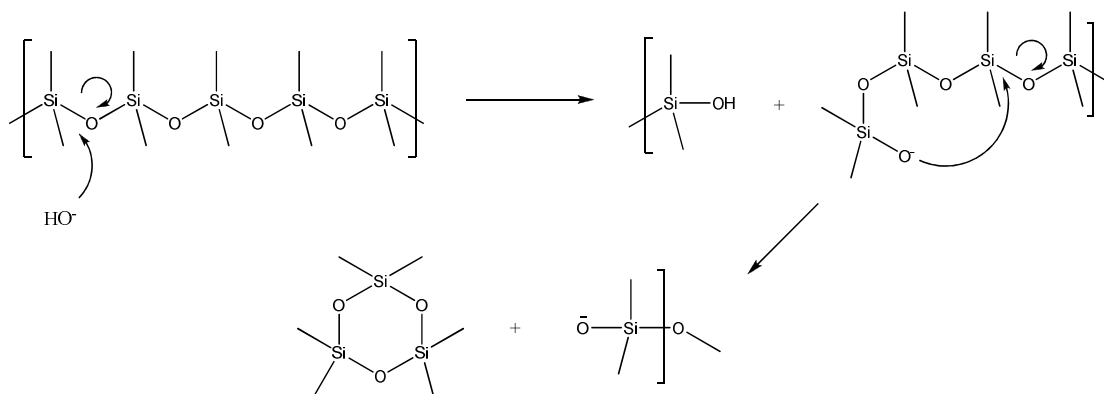
Scheme 1.16: Reversion of PDMS to cyclic species during thermal decomposition under a non-oxidative environment to form a D_3 cyclic species. A silanolate anion is also formed which continues to self catalyse the reversion process

The char residue of 5% is made up of silicon dioxide that has most probably formed from the decomposition of the cross-linking TEOS units.

Under oxidative conditions the onset of degradation is slightly lowered by 20 °C and the char residue at 800 °C is also higher between 20-30%. In this mechanism it is proposed that elemental oxygen is active in reacting with side chain methyl groups. A proposed mechanism is shown in reaction 1.17.
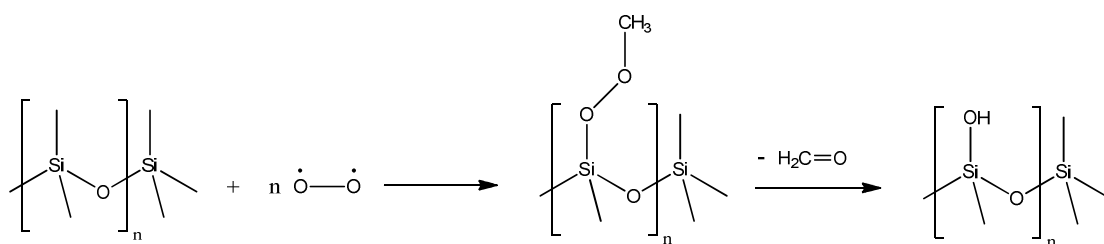
Scheme 1.17: Oxidative addition and thermal decomposition of side methyl groups on PDMS under oxidative environments. Mechanism is not proven but formaldehyde is known to be evolved during heating

1.3 Thermal Degradation of PDMS Elastomers

The elevated amount of hydroxy groups on the backbone of the polymer also promotes cross-linking in the material which leaves more char residue behind while retarding the reversion process.

1.3.1 Routes to Highly Thermally Stable Siloxane Elastomers

In the previous Section the two major degradation processes of PDMS elastomers have been identified as reversion and oxidation. In order to create a siloxane elastomer that will have a higher thermal resistance one or both of these problems must be eradicated as far as possible from the material.

Reversion can be firstly lowered by scrupulous drying of the materials using post-curing and also inclusion of drying agents into the elastomeric network. Also extracting of the elastomer with solvents that will swell the network then removing catalyst residues is also recommended. Again care must be taken to then dry the elastomer to remove any remaining solvent molecules. In doing this the onset of degradation temperature is raised.

Another tactic for reduction of reversion is to include more cross-links to lower the mobility of the polymer backbone. However, care must be taken as not to increase the glass temperature to such a point the material is no longer elastomeric.

Oxidation of the material can be lowered by incorporation of antioxidants into the elastomer network.[33] Polymeric aryl amine compounds have been used to protect silicone networks but phosphorus based antioxidants may also be considered. The incorporation of Fe^{2+} into PDMS has also been shown to reduce the level of free radical degradation on networks and works by reduction of a siloxane free radical to form the silanolate anion, shown in Scheme 1.18:

$$\equiv SiO \bullet \ + \ Fe^{2+} \longrightarrow \equiv SiO^{-} \ + \ Fe^{3+}$$
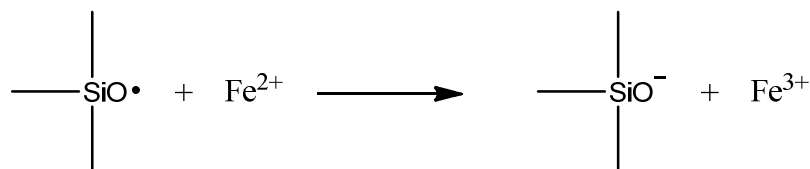
Scheme 1.18: Fe^{2+} can be used as an antioxidant to convert siloxane radicals into the silonate anion

1.3.1 Routes to Highly Thermally STable Siloxane Elastomers

Recently Yoshida *et al.* incorporated montmorillonite clay into PDMS to investigate its effect on the thermal stability of the material.[34] In the study the addition of clay led to no significant increase in onset temperature of degradation. However, increased the loading led to higher char residues. The presence of the clay slows down the formation of cyclic species, acting as a barrier to degradation which in turn allows higher chars due to higher more material left at high temperature then able to cross-link. Although the addition of clay may not be as important for thermal stability it is useful when designing flame retardant polymers and elastomers. The barrier properties of clay slow down both the rate of transport of oxygen into the material and the flow of fuel to the source of ignition.[35]

Another possible approach to enhancing the thermal stability of siloxanes is to include carboranes into the backbone of the polymer. In doing this, unusual thermal stabilisation properties are observed. In order to understand why this is the case, it is important to gain an understanding of what carboranes are, how they are synthesised and what are their physical properties. This is discussed in the next Section.

1.4 Introduction to Carborane Chemistry

Carboranes are borane clusters that have been derivatised by replacement of $[BH]^-$ units with -CH. The carboranes of interest are based on the parent icosahedron of $[B_{12}H_{12}]^{2-}$ and the structure is shown in Figure 1.2. Boron clusters involve multicentre 2-electron bonds which lead to the formation of polyhedral structures:
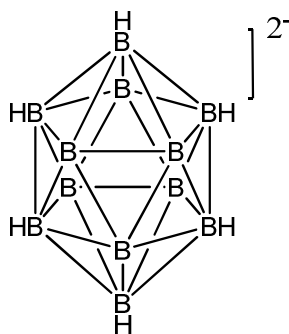
Figure 1.2: Icosahedral structure of $[B_{12}H_{12}]^{2-}$ with some of the hydrogen atoms removed for clarity. The cage comprises twelve boron cluster vertices consisting of two opposing faced pentagons capped by a boron atom each side.

The icosahedral borane cluster is electron deficient, there are 20 B-B bonds which require 40 electrons. In total there are 12 B-H bonds which give rise to 24 electrons plus 2 electrons for charge give 26 electrons. Carboranes differ from alkyl borane units in the sense that the carbon atoms are involved in the bonding of the boron cluster unit.[36] The condition for replacement of a -BH unit in the cluster with -CH is that the fragments must be isolobal with each other. The -CH unit having the same hybridisation of orbitals as -BH as shown in Figure 1.3 meets this requirement:

Figure 1.3: Isolobal fragments -BH and -CH. The frontier orbitals presented into the cluster by both molecules are the same hybridisation, sp^3, hence isolobal.

The carborane of interest is $C_2B_{10}H_{12}$, and its structure is similar to that shown in Figure 1.2. Comparing against the parent $[B_{12}H_{12}]^{2-}$ molecule it is noted that there is no formal charge on the carborane. This is due to the replacement of two anionic $[BH]^-$ units with a neutral isoelectronic CH units. The complete filling of all low lying, delocalised molecular orbitals are what give carborane clusters their high chemical inertness.

Even although there is no formal charge on a carborane the structure is still electron deficient. When a cage structure is electron precise the number of valence electrons is equal to 5n where n = number of vertices in the cage structure. Electron counting for *m*-carborane leads to a shortfall in the number of electrons needed:

5n rule: $5 \times 12 = 60e^-$ required

Atom	Electron Configuration	Valence electrons (e$^-$)
Carbon	s^2p^2	4
Boron	s^2p^1	3
Hydrogen	s^1	1

B-H vertex = 4e$^-$ and C-H vertex = 5e$^-$

Total valence electrons = $(10 \times 4) + (2 \times 5) = 50e^-$

50 e$^-$ < 60 e$^-$ therefore electron deficient

Another property most recently discovered is that carboranes are amongst the strongest acids known to science.[37] Juhasz *et al.* have attempted to quantify the

Hammet values for carboranes versus other known superacids. For example, the following protonation has been shown to occur at room temperature using $H[CHB_{11}H_5Cl_6]$ in Scheme 1.19.

$$C_{60} \ + \ H[CHB_{11}H_5Cl_6] \ \rightleftharpoons \ [HC_{60}] \ + \ ^-[CHB_{11}H_5Cl_6]$$
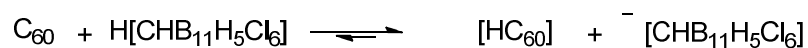
Scheme 1.19: Acid-base equilibrium of $H[CHB_{11}H_5Cl_6]$ and fullerene

The carborane is both a soft but strong protic acid where triflic acid decomposes fullerenes in this instance. The high acidity of carboranes can be important when considering functionalising of the surface of a carborane cluster and avoiding basic solutions which may damage the carborane.

1.4.1 Synthesis of 1,2-$C_2B_{10}H_{12}$ (*o*-Carborane)

The addition of carbon into the borane cluster requires manipulation of the polyhedral structure of $[B_{12}H_{12}]^{2-}$. The *arachno* structure of the parent icosahedral borane is $B_{10}H_{14}$ and known as decaborane. In this structure two boron vertices have been removed. Decaborane is susceptible to attack by Lewis bases which provide extra electrons to the decaborane cluster:[38]

$$B_{10}H_{14} + 2L \longrightarrow B_{10}H_{12}L_2 + H_2$$

where L = Lewis Base
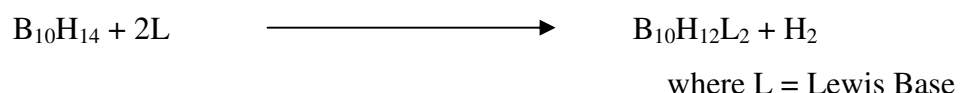
Scheme 1.20: Addition of a Lewis Acid to decaborane with evolution of hydrogen

Over seventy five Lewis bases are known to react with decaborane. The next step in the synthesis is to introduce acetylene to the ligated product and the reaction proceeds with the formation of white crystalline product in high yield:

$$B_{10}H_{12}L_2 + HCCH \longrightarrow C_2B_{10}H_{12} + 2L + H_2$$
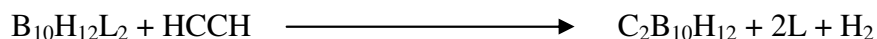
Scheme 1.21: Replacement of Lewis Acid in decaborane complex with acetylene and loss of hydrogen

This product is 1,2-$C_2B_{10}H_{12}$ (*o*-carborane) and is a chemically inert species. This carborane however can undergo re-arrangement at higher temperatures (400-500°C) in inert atmospheres to form the 1,7-$C_2B_{10}H_{12}$ (*m*-carborane) and under even higher temperatures (620°C) to form 1,12-$C_2B_{10}H_{12}$ (*p*-carborane). The structure of these carboranes are shown in Figure 1.4:

Figure 1.4: Isomers of C$_2$B$_{10}$H$_{12}$. From left to right *o*-carborane, *m*-carborane and *p*-carborane. Hydrogen atoms have been removed for clarity. C-H vertices are shown as large black spheres, other vertices are B-H units.

The consequence of this is that different functionalities of *o*-carborane can be produced by use of derivatised acetylenes and re-arranged by heating to give a wide range of functionalised carboranes.

Carboranes behave like aromatic compounds as they can undergo electrophilic substitution on the cage.[39] The reaction is carried out using one equivalent of butyl lithium deprotonating the face and then electrophilic attack can take place and is demonstrated in Scheme 1.22:

Scheme 1.22: Electrophilic attack of chlorosilane to 1-dehydro-*o*-carborane

The verticies of the carborane structure may be modified by refluxing the carborane in hydrogen peroxide to form a per-hydroxy functionalised derivatives of the carborane, as described by Bayer and Hawthorne.[40] From this work it was then shown that these carboranes could be further modified to give a carborane with twelve equivalent reactive sites for binding of peptides.[41] The numbers of permutations of different multifunctional surfaces are endless and the carborane is a stable motif on which to support the chemistry taking place at the new reactive surfaces.

1.4.2 Development of Carborane-Siloxane Copolymers

The initial studies of carborane-siloxane copolymers were varied out in the 1960s. American and Soviet scientists were competing to discover new chemically inert and thermally stable polymers for use in their "space race" research programs. Siloxane polymers and elastomers had potential as they were chemically inert but were only thermally stable to about 350-400°C, as confirmed in later work by Grassie and MacFarlane.[42] However it was hoped that incorporating the carborane unit into the backbone of the siloxane would greatly increase the thermal stability of the polymer.

To form a carborane-siloxane elastomer the starting monomer must be constructed from a functionalised carborane of which alkoxysilyl carborane is the starting monomer of choice.[43] This starting monomer is synthesised by lithiation of *m*-carborane and then reaction with (chlorodimethylmethoxy)silane, as shown in Scheme 1.23:
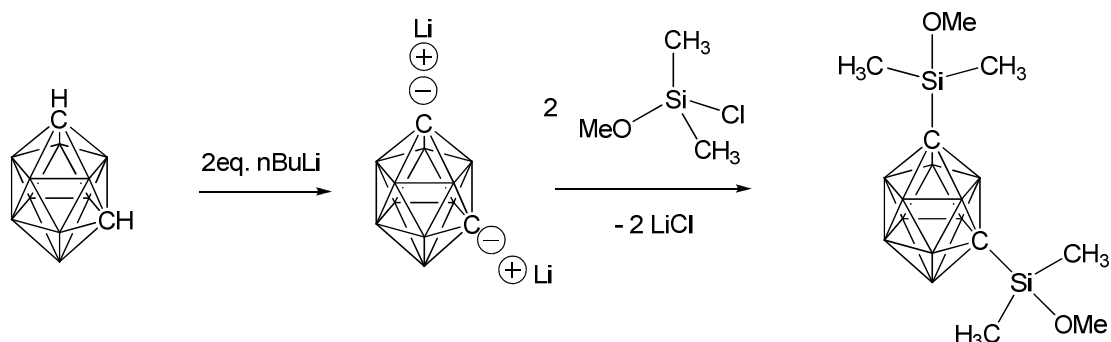
Scheme 1.23: Synthesis of 1,7(dimethylmethoxy)-*m*-carborane

Some of the first syntheses of carborane-siloxane polymers in the 1960s involved the formation of cyclic *o*-carborane-siloxanes instead of polymers due to condensation of the type in reaction Scheme 1.3 (Chapter 1.1). Ring opening polymerisation of these cyclic carborane-siloxanes using acid catalysis produced linear polymers containing carborane units.[44]

The way to avoid cyclo-condensation of the carborane-siloxane monomers was to prepare the *m*-carborane isomer of the monomer as spatial separation between the functional groups prevented this occuring.[45] Lewis acid catalysis of the *m*-carborane monomer with (dichlorodimethyl)silane was employed as shown in reaction 1.24 instead of using condensation polymerisation to form the carborane-siloxane polymer:
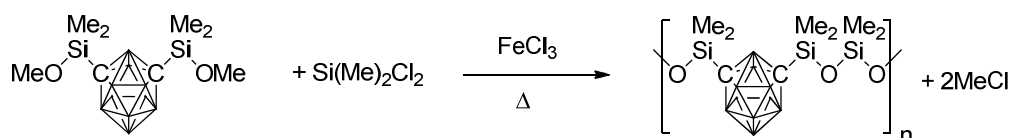
Scheme 1.24: Polycondensation of 1,7(dimethylmethoxy)*m*-carborane and dichlorodimethylsilane in the presence of $FeCl_3$

Research groups reported the most comprehensive work on synthesising and investigating these copolymers only in the 1970s, mainly due to the secrecy during the cold war preventing earlier publication. Roller and Gillham published first in the 1970s studying linear polycarboranesiloxanes for their structure-property relationship.[46-47] They compared *m*- and *p*-carborane-containing polysiloxanes for thermal and mechanical properties and found that on increasing the carborane: siloxane ratio, T_g and stiffness of the polymer increased linearly. They also noted that replacing methyl groups on the siloxane with phenyl increased thermal stability and left a synthetic route for cross-linking of the polymer chains.

Research in the USSR at the time by Andrianov *et al.* was investigating the degradation of these carborane siloxane copolymers in more detail.[48] What they observed was that, as the number of carborane cages in the backbone increased, the rate of generation of siloxane rings in the breakdown of the material decreased and that larger amounts of hydrogen and methane were evolved. The experimental rationale for this was the formation of methylene and ethylene cross-links during thermal degradation, but evidence was lacking due to limitations in testing.

Another group at this time (Peters *et al.*) was investigating synthesis of various linear, high molecular mass *m*-carborane-siloxane polymers.[50] The initial work carried out was to form a D_2-*m*-carborane-siloxane copolymer (D nomenclature is discussed in Chapter 1.1) and was achieved by the same Lewis acid catalysis as described in reaction 1.24. The group also went onto synthesise linear carborane-siloxanes by reverse condensation of bis(ureido)silanes with carborane disilanols as shown in reaction 1.25:[49]
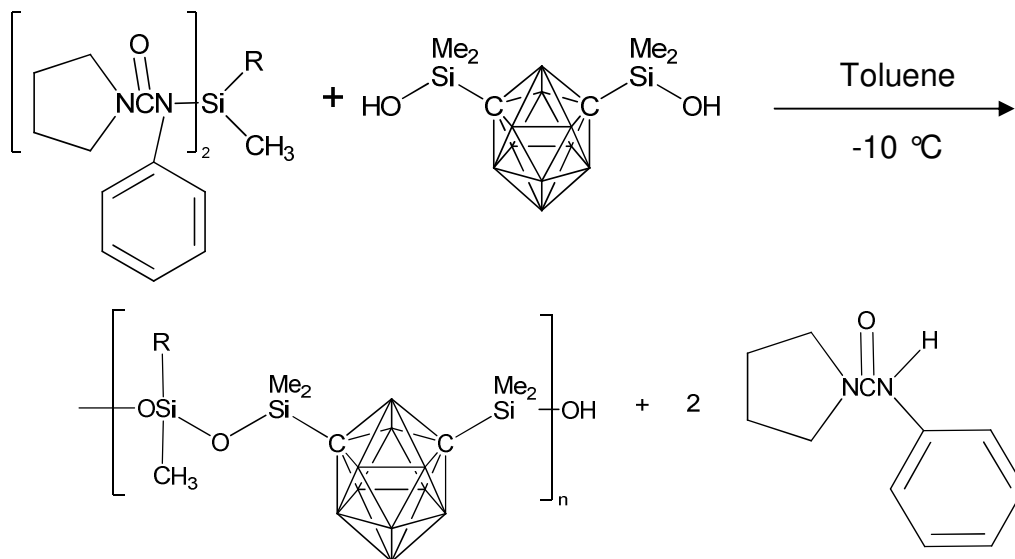
Scheme 1.25: Reverse condensation of bis(ureido)silane with carborane disilanol

This work was completed with an overview of the synthesis of carborane-siloxane elastomers from D_1-D_6.[51] The preferred method of synthesis for these polymers was Lewis acid catalysis or acid catalysed condensation. D_1 polymers are crystalline in nature with D_2-D_6 polymers having elastomeric properties. The outcome of this work showed that carborane-siloxane elastomers had a high thermal stability and flame retardant properties.

The next significant contribution to the field of carborane-siloxane copolymers came in the 1990s from a group (Keller *et al.*) investigating the properties of carborane-siloxane-diacetylene copolymers. The synthesis involves the addition of 1,4,-dilithio-1,3-butadiyne to varying mixtures of 1,7-bis(chlorotetramethyldisiloxy)-*m*-carborane and 1,3-dichlorotetramethyldisiloxane in THF at –78 °C.[52-53] The new polymer was

found to retain about 80% weight in a TGA at temperatures above 1000 °C and DSC analysis showed cross-linking of acetylene groups at 300 °C. These properties formed the basis of producing a polymer that was a precursor for ceramic material.

Most recently Patel and Swain carried out work on synthesising a D_3 carborane-siloxane polymer in 2003. The purpose of this work was to maximise the boron content while controlling the elastomeric properties of the polymer.[54] The formation of the polymer was achieved by Lewis acid catalysed chemistry as shown in reaction 1.24. The work also included synthesising a phenyl-modified elastomer.

The outcome of this work showed that a boron content of 30% by weight was achieved and that the polymer remained an elastomer. This was demonstrated by DSC analysis that showed the T_g of the polymer was only raised slightly. The thermo-oxidative properties show that decoupling of the *m*-carborane unit from the polymer occurs at temperatures of 580 °C.[55]

Other current developments include a carborane branched PDMS where the carborane is attached using hydrosilylation chemistry.[56] Kolel-Veetil and Keller have produced a network material based on a vinyl terminated 1,7-bis(dimethylmethoxysilyl)-*m*-carborane-carborane and a hydride-containing PDMS as shown in reaction Scheme 1.26:
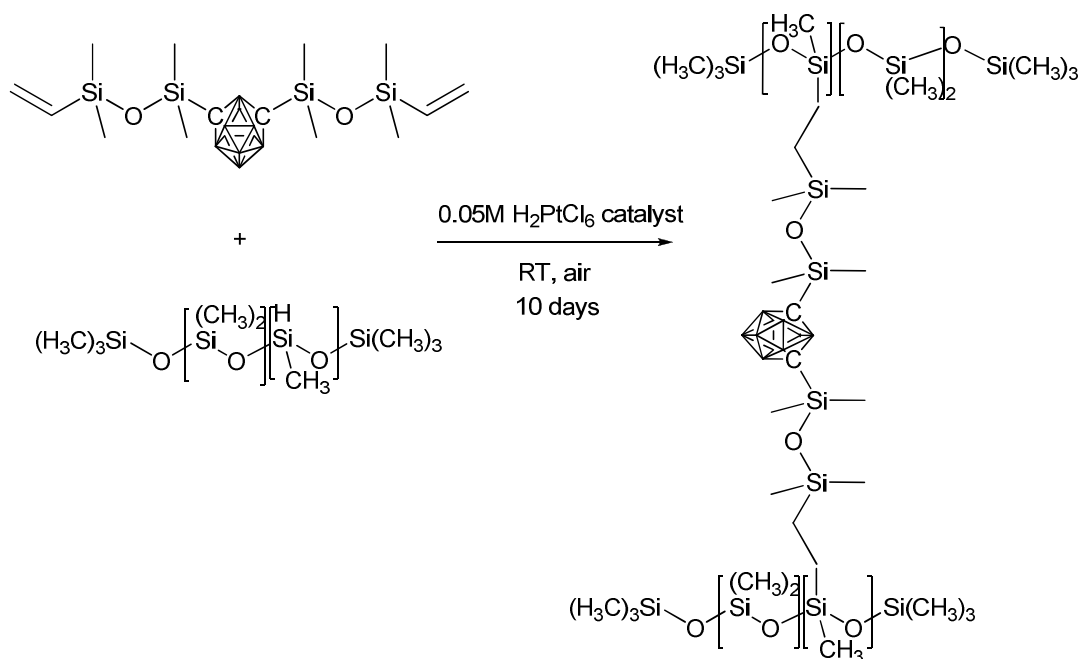
Scheme 1.26: Addition of vinyl capped carborane and poly(dimethylsiloxane-*co*-methyhydroxysiloxane) using chloroplatinic acid

The chemistry is quite straightforward to perform with reagents added neat. The reaction can be done in a beaker in the open lab and moulding of the product is also possible. Some disadvantages with this synthesis are the reaction itself is quite slow and the overall weight of boron in the final product is not very high due to the bulky siloxane side group on the carborane monomer.

However, the use of transition metal chemistry with carboranes should be undertaken with caution. Gaines and Steehler demonstrated that decaborane is highly reactive with metal centres and can yield metal substituted borane structures.[57] More worryingly for hydrosilylation chemistry is the dehydrogenation of *m*-carborane due to the presence of platinum catalyst. Tillekaratne *et al.* have demonstrated at temperatures lower than 300 K under vacuum that hydrogen is released from carborane that is on a platinum(111) surface.[58] The consequence of this is that other transition metal catalysts may also damage the carborane cage in a similar way and care should be taken in this circumstance.

1.4.3 Other Carborane-Containing Polymers

The thermal and chemical inertness of carboranes have made them of interest for inclusion in other polymer systems. This stability is lent to poly(ether-ketone)s which themselves are thermally oxidative stable compounds. Colquhoun *et al.* worked on producing a series of different polyaryl(ether-ketone-carbaborane) polymers using *o*-carborane units in the backbone.[59]

There are two ways in which to synthesise this polymer; nucleophilic condensation of a phenol and phenone or electrophilic attack of an aromatic carboxylic acid with an aromatic ether. The nucleophilic condensation route is unfavourable as carboranes are susceptible to degradation in the presence of alkoxide ions.[60] The consequence of this limits carboranes use in condensation chemistry, an important synthetic point when considering polysiloxane systems. The electrophilic attack route is by far a more suitable reaction and was used in the formation of these new polymers. The reaction between the aromatic carboxylic acid and aromatic ether is performed in trifluoromethanesulphonic acid (TfOH) shown in Scheme 1.27:
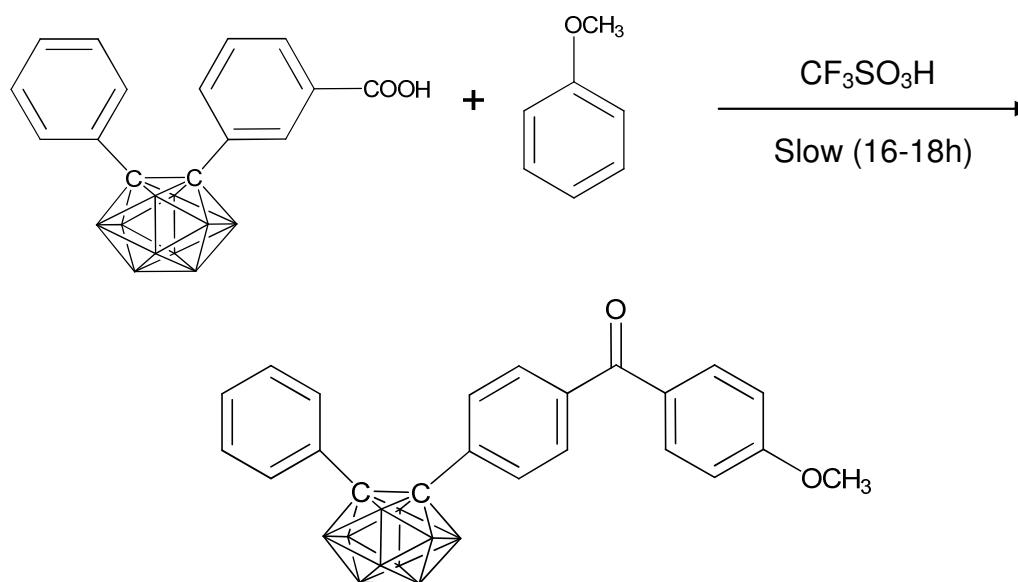
Scheme 1.27: Reaction of 1-phenyl,2-(phenyl-2-carboxclic acid)*o*-carborane and methoxybenzene in the presence of TfOH

1.4.3 Other Carborane Containing Polymers

This reaction is slow due to the electron-withdrawing properties of the carborane unit and is why the reaction must be carried out in super-acid media. The Hammet σ value of *o*-carborane is +0.49; c.f. -CF$_3$ +0.54 that indicates the carborane unit is highly electron withdrawing. By using the di-acid and di-ether of the compounds shown in Scheme 1.27 polymers were formed that contained carborane in the backbone. The inclusion of carboranes in this polymer system was shown to significantly decrease the weight loss of the polymer by pyrolysis at high temperatures (1000 °C).

More recently carboranes have been incorporated into dendronized polymer networks as the carborane moiety offers an easy route to functionalisation and relatively high boron content. The dendronized networks themselves are usually well reinforced and end groups leave room for further chemical interactions.[61]

A group led by Adronov *et al.* has recently made polyesters which contain pendant carborane units.[62-63] These carboranes have been further modified to include branching dendrimer units containing OH functionality. The interest for this revolves around making the carborane unit more receptive for use in drug delivery and by using OH functionalised dendrimers the polymer is more water soluble. Also the use of polyester backbone to house the carborane moiety should reduce the overall toxicity of the carborane.

Hydrosilylation chemistry is another possible option for binding of carboranes to POSS molecules to form new hybrid materials. Recent studies by Keller *et al.* have looked at the use of vinyl carboranes and hydride functionalised POSS to form a reinforced network material.[64] Synthesis of the network was achieved by use of small quantities of catalyst with heating of the mixture and setting in a mould. The thermal stability of this new hybrid material is considerably similar to that of other carborane containing silicones. These materials could be of interest due to their mouldability and ease of processing.

1.5 Composite Polymer Systems

Composite comes from the Latin word *compositus* meaning "to put together".[65] In a sense the composites under investigation will be put together in order to interact with each other. The components however will be differing, an organic siloxane polymer and an inorganic carborane cluster unit. In composite chemistry the synergistic effects of the unmodified material with the added filler material are under investigation.

The correct definition for these systems would also include the word hybrid as neither component is of the same type of material. For example it can be assumed that the organic siloxane polymer will interact with the inorganic fragment of the carborane unit to form a synergistic effect. Quite often these interactions give unexpected increases in the properties of new materials.[66-67]

A micro filler material will interact with the host polymer by physical interactions as well as chemical bonding. These interactions are mainly regional due to the size of the filler particles. Fillers can inhibit polymer chain movement and potentially hinder their overall mechanical movement. They also require less preparation and can be easily dispersed through a polymer system.

Nanocomposites have one dimension that is on the nanometre scale and the move from micro to nanoscale modifiers is no surprise given that the nanoscale is more easily detected with recent developments in technology. The advantage to using these nanoscale modifiers is that the surface area interactions with the host polymer are much greater which leads to much stronger chemical interactions while reducing the steric constraint on the polymer.[68] These increases in interaction are what give the nanocomposites the advantage over conventional microcomposites. The key to unlocking the potential of these nanocomposites lies in homogeneous dispersion and chemical control of the functionality of the composite material.

1.5.1 Composite Dispersions and Impact on Rheology

Many polymers applied in materials technology are rarely used without some form of blending or addition of a filler to stabilise the polymer and also to impart increased chemical properties on the material. Some of these may include flame retardancy, impact properties, optical clarity and conductivity. Since this is the case it is important that the rheology of the blends are understood to allow correct processing parameters for extrusion and casting to be obtained.

In terms of adding carboranes to a poly(dimethylsiloxane) blend then the rheological properties will depend on the functionality of the cluster unit. For example a blend of a bis-vinyl carborane will lead to an emulsion (liquid-liquid mix) where as an *m*-carborane or silyl carborane blend will lead to a suspension (liquid-solid mix). Described in Figure 1.5 are all the possible structures that may exist in a suspension:[69]
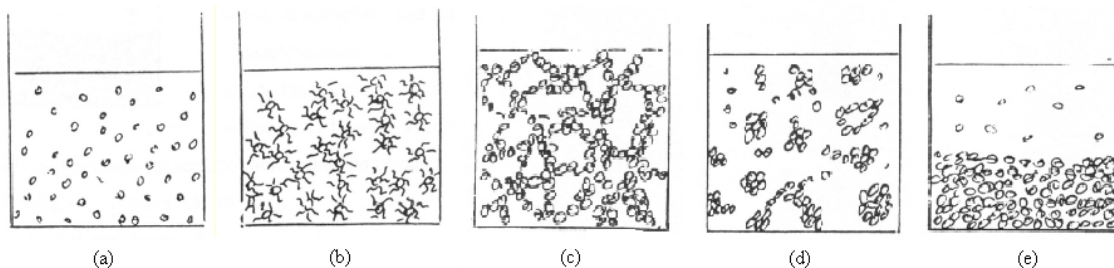
Figure 1.5: Filler particles in solution where (a) dilute with no particle/particle interactions (b) sterically stable (c) flocculation with agglomerate structures formed (d) partial structure formation (e) sedimenting

The viscosity of the suspended solution is a reflection of the viscosity of the continuous phase and also the nature of the interactions of the particles in the dispersion. However it is not just the nature of the interactions but also the shape of the particles that can also affect the change in viscosity shown in Figure 1.6. The change in volume fraction of the filler particles will affect the viscosity and also the maximum loading of a particle inside the free volume of the continuous phase. This is described in the form of the Krieger-Dougherty equation shown in Equation 1.2:

$$\eta = \eta_0 \left(1 - \frac{\Phi}{\Phi_m} \right)^{-[\eta]\Phi_m}$$

Equation 1.2: Where η is measured viscosity, η_0 is viscosity of continuous phase, $[\eta]$ is the intrinsic viscosity, Φ is the phase volume and Φ_m is the maximum phase volume
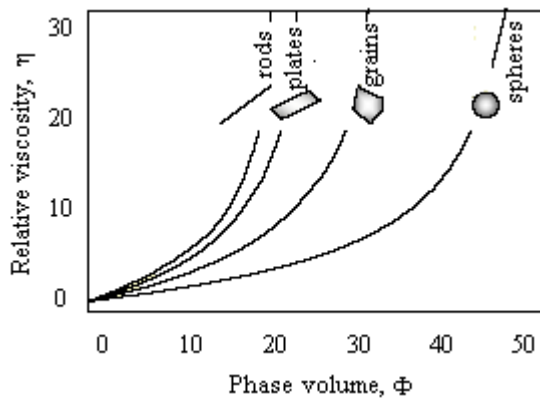
Figure 1.6: Suspension type as a function of phase volume showing change in viscosity for various shapes of particle[70]

For carboranes the material can be considered as regular sphere (the carborane cluster unit is actually icosahedral; two anti-symmetric pentagons capped at each end) due to its small size and the only major effect on its overall structure is dependent on the functionality at the carbon atoms. The loading of carborane in a PDMS blend will therefore be limited by the structures that the carborane will adopt in solution due to the functionalisation of the material.

1.5.2 Effects of Fillers on Polymer Relaxation Behaviour

For siloxane elastomer systems where the polymer has been cross-linked to form a network the relaxation properties are a good indication of the true network properties of an unfilled system (ignoring catalyst residues). As nanoscale filler is added the filler-particle interaction with the polymer changes the physical properties of a system. Most filler particles reduce the mobility of the backbone of the polymer in a bulk elastomer. This local change can lead to a change in the bulk properties of the sample.

This observation forms the basis of the Struik restricted mobility model shown in Figure 1.7.[71] The observation is that the T_g of a material is broadened when filler particles are present in an elastomer or semi-crystalline system. The reason for this is that the filler particle acts as a steric hindrance to the polymer backbone which would normally rotate freely above its glass transition. The broadening of the T_g occurs at the high temperature end of the endotherm. Where the filler and polymer are interacting the local T_g will be raised, leading to a change in the physical properties of the elastomer.
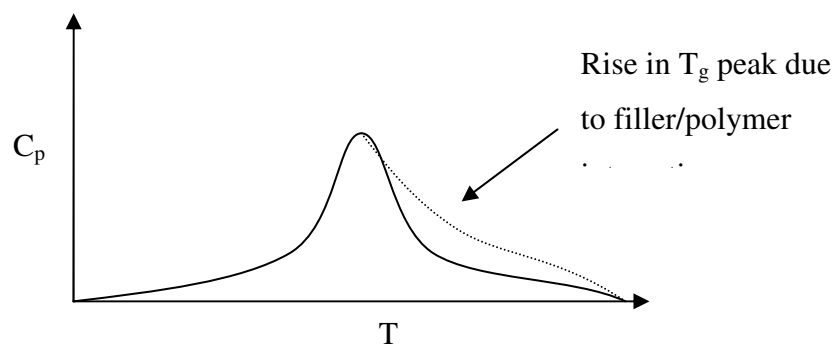
Figure 1.7: Broadening of T_g due to filler-particle interaction with polymer as described by the Struik restricted mobility model

More often with PDMS nanocomposite materials the most important relaxation data comes from DMTA and dielectric analysis. In the literature investigating specifically

1.5.2 Effects of Composites on Polymer Relaxation Behaviour

both siloxane nanocomposite material and relaxation spectrometry there are surprisingly few major publications.

1.5.3 Desirable Properties of a Composite Material

Use of a filler in a host polymer can lead to enhanced performance in a few or all of the following characteristics:

- Increase in mechanical modulus of the polymer
- Increase in thermal stability, flame retardancy and a greater resistance to thermal degradation
- Increase in electrical conductivity of the polymer
- Improvement of surface appearance
- Decrease in permeability to gases, water and hydrocarbons

An example of a new and interesting type of nanoscale filler are carbon nanotubes. Carbon nanotubes are among some of the strongest and stiffest materials known to modern science. The conductivity of their derived nanocomposites is also high as these materials are good semiconductors. There is even a proposal that carbon nanotube structures may have self-healing properties when exposed to photon irradiation.[72] With these interesting properties it is clear to see why this class of nanocomposite material is a popular and interesting research field.

In this project it is hoped that inclusion of carboranes into siloxane elastomers may also lead to the discovery of improved and unexpected properties. In the next Section possible routes to high boron-content composites are discussed.

1.5.4 Boron Composites in PDMS Systems

The incorporation of carborane units into the backbone of the polymer is one way of including boron in the PDMS systems. The project dictates that the maximum loading of boron must be achieved and nanoscale boron fillers offer a way to load the host polymer network without modification of the polymer. Also the opportunity for loading of a poly(carborane-siloxane) with boron fillers can potentially give an even larger percentage weighting of boron whilst retaining the elastomeric properties of the cross-linked polymer.

The first and probably easiest way would be to try and disperse elemental boron throughout the host polymer. The advantage would be no functionalisation required and could be as simple as sonicating a powdered sample to disperse it into the polymer. However aggregation of the boron particles could make it difficult to incorporate it in this manner. Boron comes in three forms, crystalline, rhombohedral α and β phases and as an amorphous solid.[73] The amorphous solid is random in its boron-boron bonding pattern with large particle size distributions. The α-crystalline structures of boron contain regular B_{12} icosahedral fragments surrounded by six other icosahedral cages, with a unit cell dimension of ~50 Å. The β-crystalline structure consists of a B_{84} cage (an icosahedron inside 12 pentagonal pyramids of boron atoms) with a unit cell dimension of ~101 Å. Some of the properties of elemental boron do not lend it well to dispersion. The melting points are extremely high (~2000 °C), they are relatively insoluble and have hardnesses second to diamond.

Another way of trying to incorporate boron would be to use functionalised carboranes and attach them to known polymer dispersants. Recently work by Lewicki showed that POSS could be dispersed throughout a siloxane polymer system and could be achieved without binding of the filler.[1] It is already know that using POSS is a favourable route into nanocomposite dispersion so rather than disregarding this work it should be developed further. The general structure of a POSS is shown in Figure 1.8:
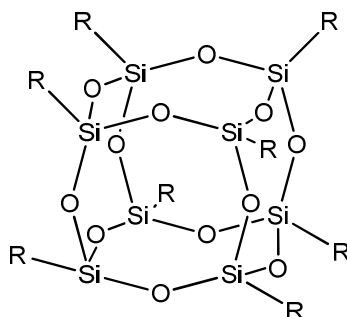
Figure 1.8: General Structure of POSS. The R groups on POSS can be interchanged with different functionalities

By selecting the right functionality on the POSS and then synthesising a carborane with the correct functionality the two units could be brought together.

Recently Adronov *et al.* have carried out work on synthesising a carborane with OH functionality to add it pendant on the backbone of poly(ethylene glycol).[74] The synthesis of the (hydroxypropyl)carborane is carried out in THF and is shown in reaction 1.28:
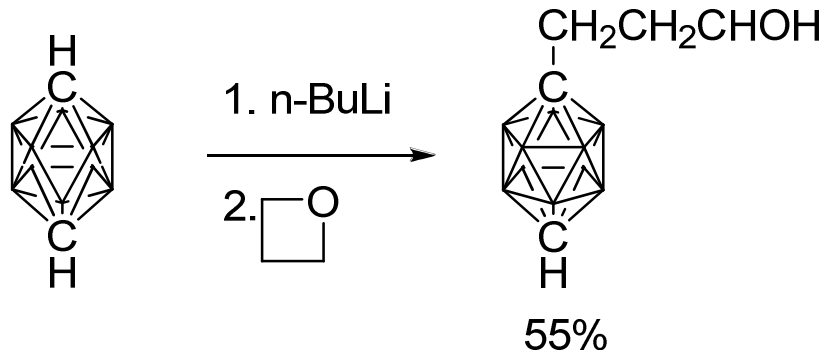
Scheme 1.28: Synthesis of 1-(hydroxypropyl)*p*-carborane

The resulting 1-(hydroxypropyl)carborane could have synthetic use for this project. The OH group is now away from the electron withdrawing carborane centre and could be used in condensation chemistry of the type used in polysiloxane elastomer synthesis. If a POSS containing OH or silanol groups at the R group were brought together with this functionalised carborane in the presence of a tin catalyst

condensation of the two reactants might occur. This could be done in situ with the formation of a PDMS elastomer in one reaction.

The other way of modifying Scheme 1.28 would be to introduce a POSS with eight epoxy groups in the R position and in an 8:1 ratio of carborane to POSS, a new carborane containing POSS superstructure could be formed. The loading of carborane in the polymer could then be maximised without the need for high levels of POSS in the elastomeric system.

Another boron based nanoscale modifier could be synthesised out of the condensation of TEOS with 1-(hydroxypropyl)carborane. TEOS is a known cross-linking agent as previously discussed and is a more economical way to incorporate carboranes than using POSS. By combination of alkoxycarborane and TEOS in a 4:1 ratio in the presence of a tin catalyst a new tetra-functional carborane orthosilicate molecule could be synthesised as shown in Scheme 1.29.
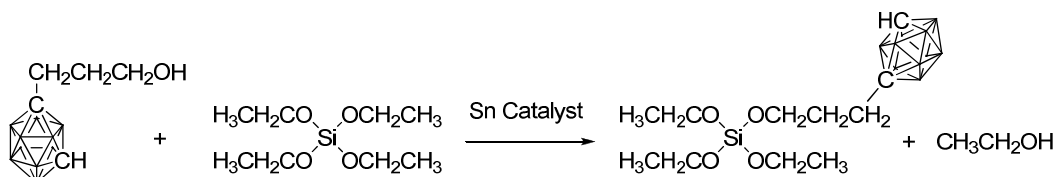
Scheme 1.29: Using a tin catalyst to incorporate a mono hydroxy functional carborane into a TEOS unit

Other methods of attaching alcohol-functionalised carboranes could be achieved by conversion of the OH unit into an alkene-containing ether which could be coupled to a silane in the presence of a platinum catalyst. This is the basis of the work by Métivier *et al.* where they attempted to graft a pyrene unit onto an aluminium surface.[75-76] The initial functionalised pyrene was readily available commercially and the conversion reaction was a simple alkyl bromination as shown in Scheme 1.30.
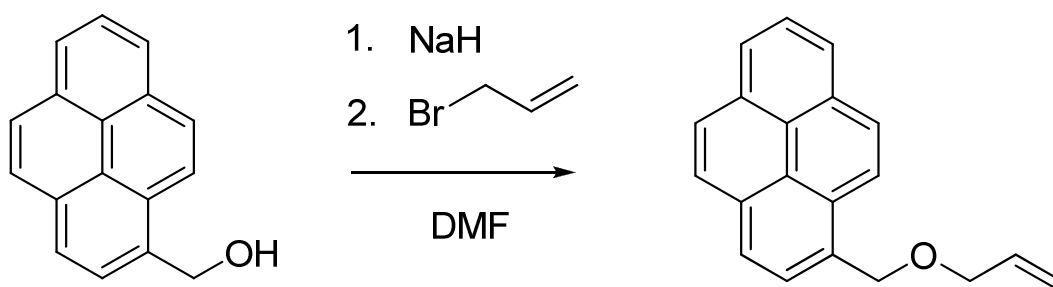
Scheme 1.30: Conversion of pyrenemethanol to 1-allyloxymethylpyrene

This was then coupled in the presence of a platinum catalyst to triethoxysilane to form a new nanoscale modifier for grafting onto the surface of aluminium. The remaining ethoxysilane groups could be used to bind into the siloxane elastomer networks to control where the carborane is bound.

By replacing the pyrene in the product with carborane the following addition reaction could be performed shown in rection 1.31.
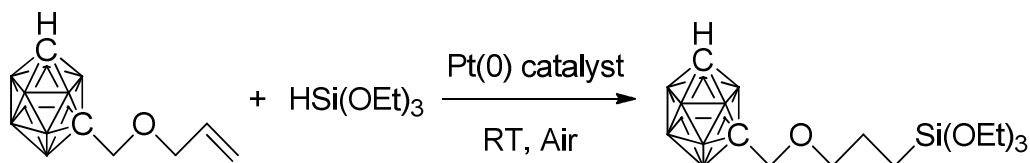
Scheme 1.31: Hydrosilylation coupling of 1-(allyloxymethyl)*m*-carborane to triethoxysilane using a Pt(0) catalyst

The available silyl ether groups could then be condensed into a siloxane network in the presence of the Sn^{2+} catalyst.

1.6 Chapter Conclusion

In summary the questions of how much boron can be incorporated into the PDMS elastomeric system and which method of thermal stabilisation works best are still to be answered. The addition of carboranes into the backbone of PDMS has been comprehensively researched and is by far the optimal way to incorporate boron in order to vastly improving thermal stability of these polymers. The past work gives a solid starting point for synthesising a new elastomeric system.

The question remains as to what sort of carborane composites can be synthesised? Although carboranes are chemically stable clusters they can undergo a wide variety of transformations in functionality on the carbon atoms and less commonly on the boron atoms. With this in mind the research field is essentially open to exploration. By combining functionalities on known nanocomposites with carboranes new boron containing nanocomposites could be formed. Hopefully this will lead to new and interesting thermal degradation properties in the development of the current siloxane elastomer technology.

In the next Chapter the discussion will now focus on the theory behind the experimental techniques that will be used during the course of the project.

1.7 References

1. Lewicki, J.P. *"Ageing studies of novel polydimethylsiloxane nanocomposites"* University of Strathclyde 2008

2. Archer, R. D., *"Inorganic and organometallic polymers"* Wiley-VCH 2001: 54

3. Seyferth, D., *"Dimethyldichlorosilane and the direct synthesis of methylchlorosilanes. The key to the silicones industry"* Organometallics 2001, **20** (24): 4978

4. Patai, S., Rappoport, Z. *"The chemistry of organic silicon compounds"* The Chemistry of Functional Groups 1989 **2** (38): 1290

5. Mark, H. F., Kroschwitz, J. I. *"Silicones"* Encyclopaedia of Polymer Science and Engineering, Wiley Interscience, New York 1989 **15**: 205

6. Chojnowski, J., *"The behaviour of the silanol function in polycondensation systems"* Silicon Containing Polymers 1995: 59

7. Archer, R. D., *"Inorganic and organometallic polymers"* Wiley-VCH 2001: 75

8. Tsuruta, T., Kawakami, Y., *"Anionic ring-opening polymerization: General aspects and initiation"* Comprehensive Polymer Science 1989 **7**: 464-465

9. Chojnowski, J., *"Ring opening polymerizations of cyclosiloxanes"* Silicon Compounds: Silanes and Silicones 2004: 390

10. Hudson, N.E. *"Process Rheology"* 2009 Lecture 6: 19

11. Brandrup, J., Immergut, E.H., Crulke, E.A. *"Polymer Handbook: 4th Edition"* Wiley Interscience, New York 1999 **VII**: 40

12. http://www.sigmaaldrich.com/materials-science/material-science-products.html?TablePage=20204347 (correct as of 21st July 2010)

13. Tang, Y., Tsiang, R. *"Rheological, extractive and thermal studies of the room temperature vulcanized polydimethylsiloxane"* Polymer 1999 **40**: 6135

14. Van der Weij, F. W., *"The Action Of Tin-Compounds In Condensation-Type Rtv Silicone Rubbers"* Makromolekulare Chemie - Macromolecular Chemistry And Physics 1980 **181** (12): 2541

15. Walton, D., Lorimer, P., *"Polymers"* Oxford University Press 2000: 59

16. Bischoff, R., Cray, S.E. *"Polysiloxanes in macromolecular architecture"* Progress in Polymer Science 1999 **24**: 185

17. March, J. *"Advanced organic chemistry: Reactions, mechanism and structure"* Wiley Interscience 1992: 260

18. Person, R.G, *"Hard and soft acids and bases"* Journal of the American Chemical Society 1963 **85** (22): 3533

19. Yamamoto, H. *"Lewis acid reagents: A practical approach"* Oxford University Press 1999: 1-3

20. Yamamoto, H. *"Lewis acids in organic synthesis: Vol.1"* Wiley-VCH 2001: 5

21. Peters, E.N., *"Poly(dodecacarborane-siloxanes)"* Journal of Macromolecular Science – Reviews 1979 **C17** (2): 177

22. March, J. *"Advanced organic chemistry: Reactions, mechanism and structure"* Wiley Interscience 1992: 261

23. Lewis, L.N., Lewis, N., *"Platinum-catalyzed hydrosilylation – colloid formation as the essential step"* Journal of the American Chemical Society 1986 **108**: 7228

24. Karstedt, B.D., US Patent (3 775 452) 1973

25. Lewis, L.N., Stein, J., Gao, Y., Colborn, R.E, Hutchins, G., *"Platinum catalysts used in the silicones industry"* Platinum Metals Review 1997 **41** (2): 68

26. Lewis, L.N, *"On the mechanism of metal colloid catalyzed hydrosilylation: Proposed explanations for electronic effects and oxygen cocatalysis"* Journal of the American Chemical Society 1990 **112**: 5998

27. Duff, D.G., Edwards, P.P., Johnson, B.F.G., *"Formation of a polymer-protected platinum sol: A new understanding of the parameters controlling morphology"* Journal of Physical Chemistry 1995 **99**: 15934

28. Osborn, J.A., Jardine, F.H., Young, J.F., Wilkinson, G., *"The preparation and properties of tris(triphenylphosphine)halogenorhodium(1) and some reactions thereof including catalytic homogeneous hydrogenation of olefins and acetylenes and their derivatives"* Journal of the Chemical Society 1966 **A**:1711

29. Zhang, R., Mark, J.E., Pinhas, A.R., *"Dehydrocoupling polymerization of bis-silanes and disilanols to poly(silphenylenesiloxane) as catalyzed by rhodium complexes"* Macromolecules 2002 **33**: 3508

30. Wright, W.W., Lee, W.A, *"The search for thermally stable polymers"* Iliffe Books Ltd. 1968: 8

31. Critchley, J.P., Knight, G.J., Wright, W.W *"Heat resistant polymers"* Plenum Press 1983: 332

32. Grassie, N., MacFarlane, I. G. *"The thermal degradation of polysiloxanes – 1"* European Polymer Journal 1978 **14**: 875

33. Critchley, J.P., Knight, G.J., Wright, W.W *"Heat resistant polymers"* Plenum Press 1983: 335

34. Kaneko, M.L.Q.A., Yoshida, I.V.P., *"Effect of natural and organically modified montmorillonite clays on the properties of polydimethylsiloxane rubber"* Journal of Applied Polymer Science 2008 **108**: 2587

35. Morgan, A.B., Wilkie, C.A, *"Flame retardant polymer nanocomposites"* Wiley Interscience 2007: 116

36. Grimes, R. *"Carboranes"* Academic Press 1970: 2

37. Juhasz, M., Hoffman, S., Evgenii, S., Kim, K.C., Reed, C.A., *"The strongest isolable acid"* Angewandte Chemie 2004 **43**: 5352

38. Casanova, J. *"The borane, carborane, carbocation continuum"* Wiley Inter-Science 1998: 203

39. Nunez, R., Gonzalez-Campo, A., Vinas, C., Teixidor, F., Sillanpaa, R., Kivekas, R., *"Boron-functionalized carbosilanes: insertion of carborane clusters into peripheral silicon atoms of carbosilane compounds"* Organometallics 2005 **24**: 6351

40. Bayer, M.J., Hawthorne, M.F., *"An improved method for the synthesis of [closo-$B_{12}(OH)_{12}]^{-2}$"* Inorganic Chemistry 2004 **43**: 2018

41. Li, T., Jalistgi, S.S., Bayer, M.J., Maderna, A., Khan, S.I., Hawthorne, M.F., *"Organic syntheses on icosahedral borane surface: Closomer structures with twelvefold functionality"* Journal of the American Chemical Society 2005 **127**: 17832

42. Grassie, N., MacFarlane, I. G. *"The thermal degradation of polysiloxanes – 1"* European Polymer Journal 1978 **14**: 875

43. Grimes, R. *"Carboranes"* Academic Press, Oxford 1970: 183

44. Mayes, N., Green, J., Cohen, M.S., *"Carborane polymers. IV. Polysiloxanes"* Journal of Polymer Science: Part A-1 1967 **5**: 365

45. Papetti, S., Schaeffer, B.B., Gray, A.P., Heying, T.L. "*A new series of organoboranes. VII. The preparation of poly-m-carboranylenesiloxanes*" Journal of Polymer Science: Part A-1 1966 **4**: 1623

46. Roller, M.B., Gillham, J.K., "*High temperature elastomers: A systematic series of linear poly(carborane-siloxane)s containing icosahedral ($-CB_{10}H_{10}C-$) cages. II. Thermo-oxidative behavior* " Journal of Applied Polymer Science 1973 **17**: 2623

47. Roller, M.B., Gillham, J.K., "*Linear polycarboranesiloxanes*" Polymer Engineering and Science 1974 **14** (8): 567

48. Andrianov, K.A., Pavlova, S.-S.A., Zhuravleva, I.V., Tolchinskii, Yu.I., Astapov, B.A., "*Thermal breakdown of polydi-organocarborane siloxanes*" Polymer Chemistry in the USSR 1976 **19** (9): 1037

49. Hedaya, K., Kawakami, J.H., Kopf, P.W., Kwiatkowski, G.T., McNeil, D.W., Owen, D.A., Peters, E.N., Tulis, R.W., "*D_2-meta-carborane-siloxanes. IV. Synthesis of linear, high molecular weight polymers*" Journal of Polymer Science 1977 **15**: 2229

50. Stewart, D.D., Peters, E.N., Beard, C.D., Dunks, G.B., Heydaya, E., Kwiatkowski, G.T., Moffitt, R.B., Bohan, J.J., "*D_2-m-carborane-siloxanes. 7. Synthesis and properties of ultra-high molecular weight polymer*" Macromolecules 1978 **12** (3): 373

51. Peters, E.N., "*Poly(dodecacarborane-siloxanes)*" Journal of Macromolecular Science – Reviews 1979 **C17** (2): 173

52. Son, D.Y., Keller, T.M. "*Oxidatively stable carborane-siloxane-diacetylene copolymers*" Journal of Polymer Science: Part A 1995 **33**: 2969

53. Sundar, R.A., Keller, T.M. "*Linear diacetylene polymers containing bis(dimethylsilyl)phenyl and/or bis(tetramethyldisiloxane)carborane residues: Their synthesis, characterization and thermal and oxidative properties*" Journal of Polymer Science: Part A 1997 **35**: 2387

54. Patel, M., Swain, A.C., Skinner, A.R., Mallinson, L.G., Hayes, G.F, "*Synthesis and properties of poly(m-carborane-siloxane) elastomers*" Macromolecular Symposia 2003 **202**: 47

1.7 References

55. Patel, M., Swain, A.C. "*Thermal stability of poly(m-carborane-siloxane) elastomers*" Polymer Degradation and Stability 2004 **83**: 539

56. Kolel-Veetil, M.K., Keller, T.M., *"Formation of elastomeric network polymers from ambient heterogeneous hydrosilations of carboranylenesiloxane and branched siloxane monomers"* Journal of Polymer Science Part A: Polymer Chemistry 2006 **44**: 147

57. Gaines, D.F., Steehler, G.A., *"Oxidation of elemental transition metals by decaborane to form metalloboranes"* Journal of the Chemical Society Chemical Communications 1982: 122

58. Tillekaratne, A., Siap, D., Trenary, M. *"Adsorption and dehydrogenation of ortho-carborane on the Pt(111) surface"* Journal of Physical Chemistry C 2008 **112**: 8682

59. Colquhoun, H.M., Daniels, A.J., Stephenson, I.R., Wade, K., "*Polyaryl(ether-ketone-carbaborane)s: A new class of hybrid polymers*" Polymer Communications 1991 **32** (9): 272

60. Wiesboeck, R.A., Hawthrone, M.F. "*Dicarbaundecaborane(13) and derivatives*" Journal of the American Chemical Society 1964 **86**: 1642

61. Beletskaya, I.P., Chuchurjukin, A.V., "*Synthesis and properties of functionalised dendrimers"* Russian Chemical Reviews 2000 **69** (8): 639

62. Benhabbour, S. R., Gratton, S.E.A, Parrott, M.C., Adronov, A. *"Synthesis and properties of carborane-containing dendronized polymers"* Macromolecules 2007 **40**: 5678

63. Parrott, M.C., Marchington, E.B., Valliant, J.B., Adronov, A. *"Synthesis and properties of carborane-functionalised aliphatic polyester dendrimers"* Journal of the American Chemical Society 2005 **127**: 12081

64. Kolel-Veetil, M. J., Dominguez, D.D., Keller, T.M., *"Dendritic networks containing polyhedral oligomeric silsesquioxane(POSS) and carborane clusters"* Journal of Polymer science: Part A 2008 **46**: 2581

65. Online Etymology Dictionary @ http://www.etymonline.com (correct as of 21st July 2010)

66. Joshi, M., Bhupendra, S. B., "*Polymeric nanocomposties – polyhedral oligomeric silsesquioxanes (POSS) as hybrid nanofiller*" Journal of Macromolecular Science 2004 **44** (4): 393

67. Kickelbick, G., "*Concepts for the incorporation of inorganic building blocks into organic polymers on a nanoscale*" Progress in Polymer Science 2003 **28**: 83-114

68. Fedullo, N., Sorlier, E., Sclavons, M., Bailly, C., Lefebvre, J.M., Devaux, J., "*Polymer-based nanocomposites: Overview, applications and perspectives*" Progress in Organic Coatings 2007 **58**: 87

69. Hudson, N.E. *"Process Rheology"* 2009 Lecture 9: 3-5

70. Hudson, N.E. *"Process Rheology"* 2009 Lecture 2

71. Lewicki, J.P. *"Aspects of molecular motion in polymeric systems"* 2009 Lecture 4: 9

72. Miyamoto, Y., Berber, S., Yoon, M., Rubio, A., Tomanek, D., "*Can photo excitations heal defects in carbon nanotubes?*" Chemical Physical Letters 2004 **392** (1-3): 209

73. Greenwood, N.N., Earnshaw, A. "*Chemistry of the Elements*" Permagon Press 1984: 142

74. Gratton, S.E.A, Parrott, M.C., Adronov, A. "*Preparation of carborane-containing polymers by atom transfer radical polymerisation*" Journal of Inorganic and Organometallic Polymers and Materials 2006 **15** (4): 469

75. Metivier, R., Leray, I., Roy-Auberger, M., Zanier-Szydlowski, N., Valeur, B. "*Characterization of alumina surfaces by fluorescence spectroscopy. Part 1. Grafting a pyrene derivative on c- and d-alumina supports*" New Journal of Chemistry 2002 **26**: 413

76. Metivier, R., Leray, I., Lefevre, J.P., Roy-Auberger, M., Zanier-Szydlowski, N., Valeur, B. "*Characterization of alumina surfaces by fluorescence spectroscopy. Part 2. Photophysics of a bound pyrene derivative as a probe of the*

spatial distribution of reactive hydroxyl groups" Physical Chemistry Chemical Physics 2003 **5**: 758

Chapter 2

Theory of Instrumental Analyses

2.0 Theory of Instrumental Analyses

This Chapter is intended to provide an outline of the theory associated with some of the instrumental analysis techniques used during this project.

2.1 Thermogravimetric Analysis

Thermogravimetric analysis (TGA) is a technique used to monitor the degradation of a polymer sample with either increasing temperature or isothermal hold by recording the mass of the sample during heating. The sample is placed in a pan that is attached to a sensitive electromagnetic balance, which is counter-balanced. The furnace is then sealed and air or argon is allowed to flow through the chamber. This provides an environment that is either oxidising or non-oxidising respectively. Figure 2.1 shows the experimental setup of a typical TGA instrument:[1]

Figure 2.1: Design of a typical TGA instrument showing the sample pan, furnace, gas flow and auto-sampler

Once the run has completed a graph of percentage mass of sample versus temperature is drawn and a degradation profile is obtained. A typical model poly(siloxane) elastomer TGA thermogram is shown in Figure 2.2:
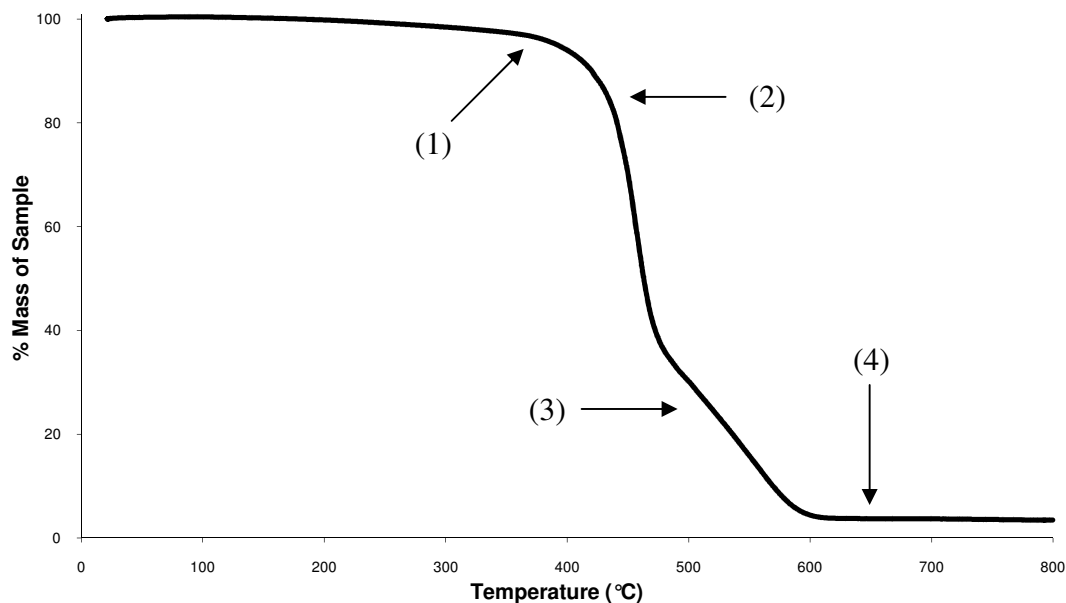
Figure 2.2: TGA plot of a model poly(siloxane) elastomer under argon

As the polymer sample is heated, low molecular mass volatiles, trace amounts of solvent and surface water are removed from the polymer (1). The sample then reaches an onset degradation temperature and the sample starts to release low molecular mass volatiles from the polymer (small siloxane cyclic species volatilised); the primary degradation process (2). The mass of the sample is then reduced further to a point where the remaining material starts to volatilise (heavier siloxane cycles volatilised) and formation of a cross-linked char residue (silicon dioxide residues); this is a secondary degradation process (3). The mass loss then ceases as no further degradation occurs and char residue is left in the pan (4). Onset degradation temperature, percentage char of polymer, and (by integration of the slope) the rate of change of the mass with respect to temperature can all be extracted from the graph (Figure 2.3).
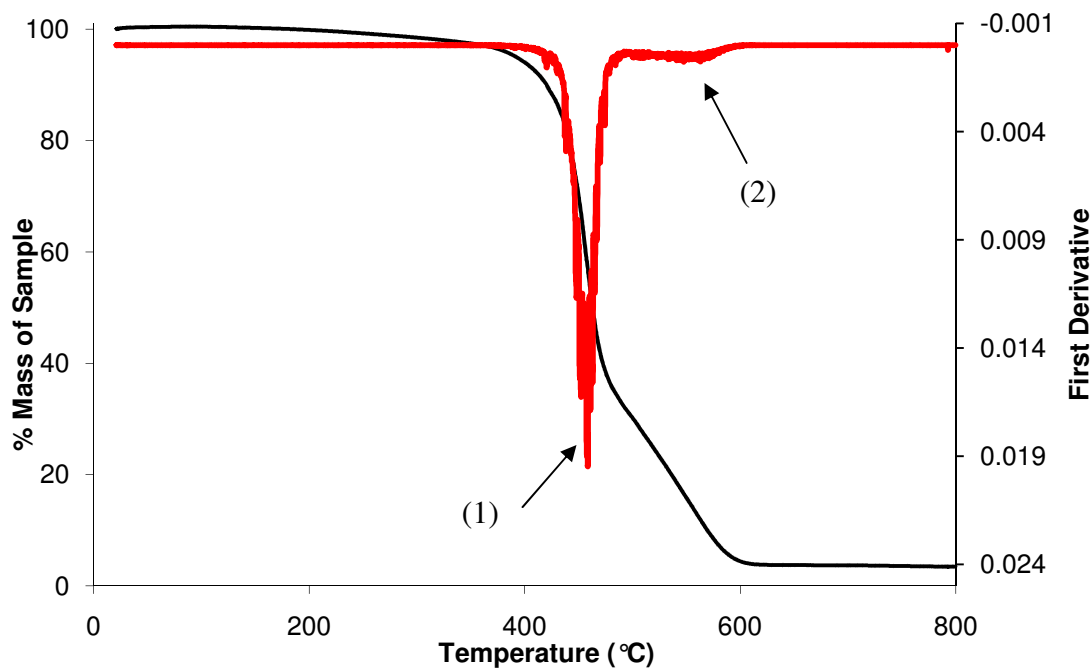
Figure 2.3: Replot of Figure 2.2 with first derivative included (red line). Two peaks indicate two main degradation processes are occurring

The first derivative is useful as it shows more clearly where each degradation process occurs. It also shows at which temperature the maximum loss of volatiles happens for each process and the relative rate of loss in comparison to other peaks present. Peak (1) is the main degradation process with a fast rate of evolution of volatiles and peak (2) is a secondary process with a slow rate of volatilisation.

TGA can be coupled with mass spectrometry (MS) to further investigate the volatiles that are released during degradation. Argon is a carrier gas for MS and as each major degradation analyte is released the mass spectrometer records spectra in real time. By use of NIST library searches and knowledge of the chemical structure of the sample it is possible to use this information to identify the analyte then propose a degradation mechanism which leads to the formation of the analyte observed. The drawback of using coupled mass spectrometry is that anything smaller than argon ($M/z = 40$) will not be observed easily; for example it will not be able to detect methane or hydrogen off-gassing from the sample as degradation products will also

ionise whilst in the quadrupole of the mass spectrometer, producing hydrogen and methane peaks.

2.2 Differential Scanning Calorimetry

Differential scanning calorimetry (DSC) is a technique that is used to determine the temperature and enthalpy change associated with phase transitions which occur as a polymer is heated or cooled.[2] During heating a polymer may undergo several readily observable phase changes such as melting and volatilisation to a gas measurable by various techniques. Polymers may contain crystalline regions within amorphous regions that melt and secondary phase transitions also occur such as the glass transition. These phase changes can be observed by measuring the heat flux through the sample as the phase change occurs. The setup for a typical DSC is shown below in Figure 2.4:[3-4]
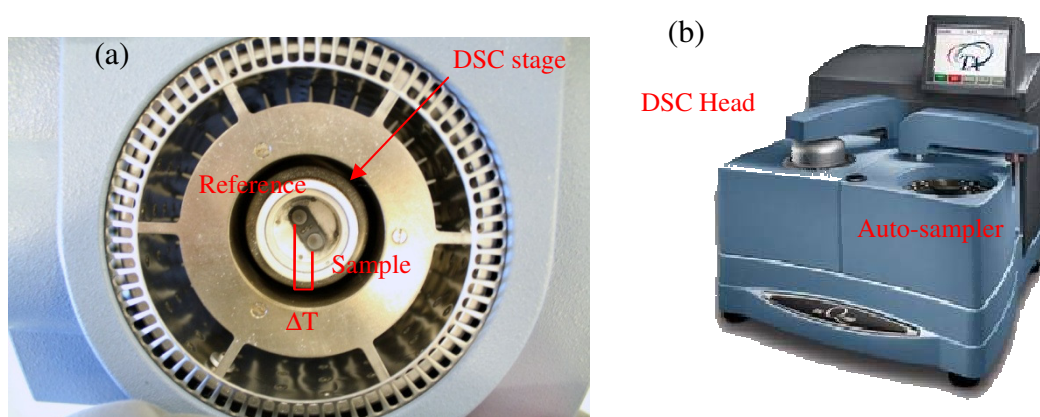
Figure 2.4: Design of a typical DSC instrument (a) inside the heating chamber (b) overview of the instrument

The reference pan and sample pan are subjected to the same temperature program so that the rate of change in temperature is always the same for both pans. When a sample starts to undergo a phase transition the temperature of that pan varies with respect to the reference pan and the computer measures the change in heat flux. For processes such as melting, endothermic peaks are obtained where as during crystallisation the phase transition is exothermic. During a materials' glass transition the sample undergoes a change in specific heat which results in a shoulder in the DSC trace. Also, degradation can be observed which can be either endothermic or

exothermic dependant on the chemistry involved. The resulting differences give rise to a DSC trace that shows the temperature at which the phase transitions occurs and can be integrated to find the specific enthalpy of the transition. A DSC trace for a typical siloxane elastomer material is shown in Figure 2.5:
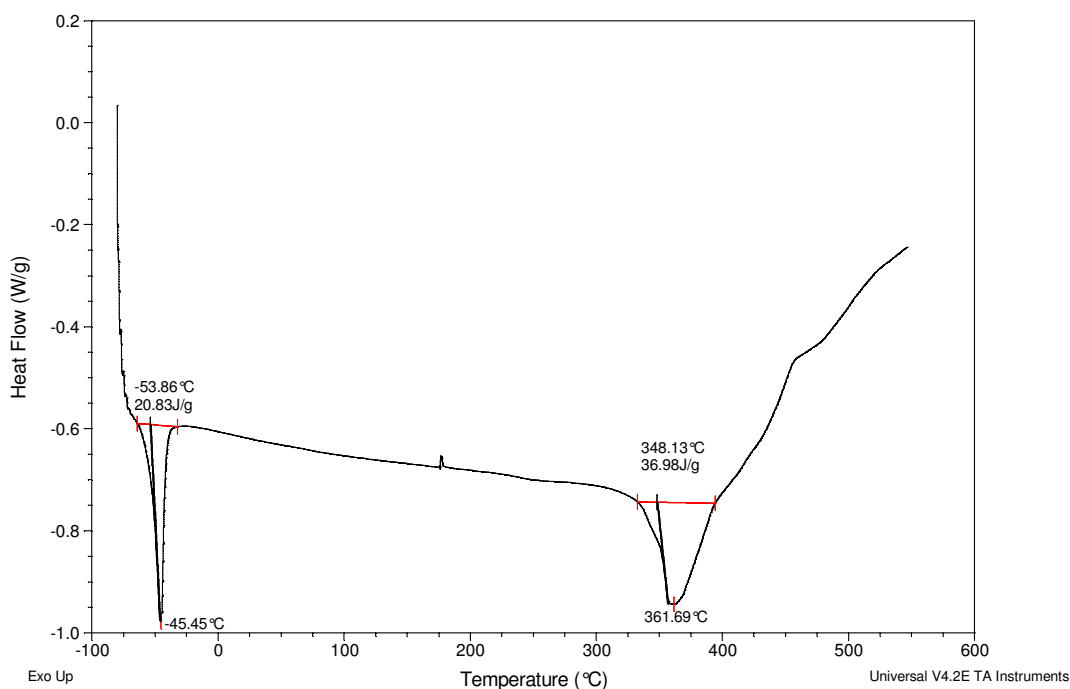
Figure 2.5: DSC plot of a typical PDMS elastomer material. Melt transition occurs at -45 °C and onset of degradation occurs at 348 °C

There is no T_g present on the plot above as siloxane elastomers have some of the lowest T_g transitions for any elastomer type. On DSC instruments with liquid nitrogen cooled heads the glass transition can be observed at around -120 °C.

The technique can be used under oxidising or non-oxidising conditions which may indicate a difference in the chemical behaviour of the sample. The sample can be heated to melting and then cooled to observe the enthalpy of crystallisation of a polymer and the temperature at which this occurs.

2.3 Thermal Volatilisation Analysis

The first example of trapping of volatiles that lead to elucidation of a polymer's thermal degradation mechanism was in 1949 by Grassie. He described an experiment where the degradation products from a thermally-degraded poly(vinylchloride) were trapped in a molecular still.[5] Thermal volatilisation analysis (TVA) is a technique that was developed by McNeill at the University of Glasgow in the late 1960s, based on Grassie's original design, in which the investigation of degradation products from thermally decomposing polymers was enabled by sub-ambient trapping of volatiles under vacuum. One of the pioneering papers was on the degradation of vinyl chloride copolymers,. Other polymer systems analysed using this technique included polyacrylonitrile, polysiloxanes and polyurethanes to name but a few.[6-9]

The technique has been subsequently introduced here at the University of Strathclyde by Liggat, Lecomte and Lewicki in 2005-07. The principal use of the technique is in the study of polymer degradation by distillation of volatiles produced from a sample in a furnace under high vacuum. The volatiles are condensed in a sub-ambient trap, distilled and analysed by mass spectrometry, gas phase IR and GC-MS. The sub-ambient TVA trace is split between two experiments. First the degradation run in which pressure data for the total volatiles evolved and non condensable volatiles during thermal degradation are plotted against time with furnace temperature on a secondary y-axis. Secondly the sub-ambient distillation step in which pressure data of distilled volatiles under vacuum are plotted against either time or temperature of the still. The experimental design is shown in Figure 2.6:
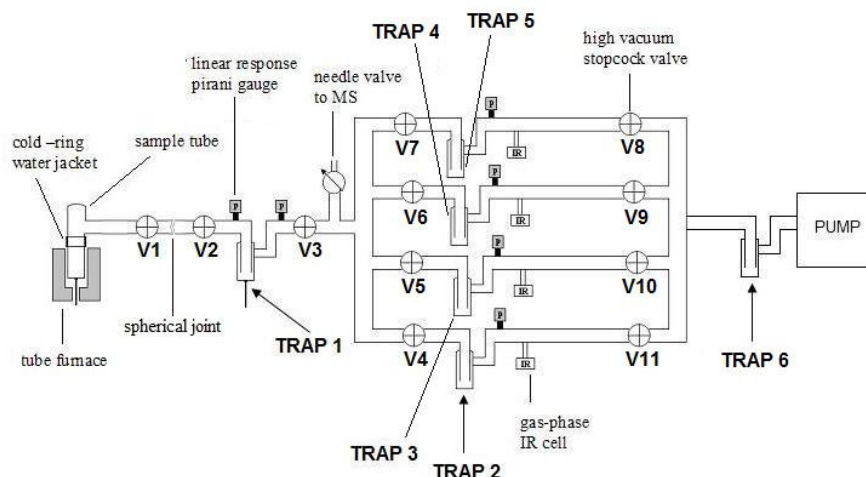
Figure 2.6: Design of a sub-ambient thermal volatilisation analysis vacuum line

The sample is placed in either a borosilicate or quartz tube which is placed into the tube furnace. Valve 1 (V1) and valve 2 (V2) are opened allowing the sample to reach vacuum (typical 1×10^{-4} Torr). The oven is then heated up to degradation temperature (isothermal hold) or above degradation temperature (degradation run) at 10 °C per minute. As volatiles leave the sample they pass the cold ring which captures high molar mass species and room temperature vaporisable volatiles, other volatiles move past a Pirani gauge and into a cold trap (trap 1) held at liquid nitrogen temperature. Any non-condensable species (hydrogen, methane etc) pass straight though the trap, are detected by the trap exit Pirani gauge and into the online mass spectrometer. After the degradation run the cold trap is then heated from -196 °C to 40 °C at typically around 4 °C min^{-1}. As each volatile is distilled from the trap the pressure on the exit Pirani gauge rises and the online mass spectrometer records the ion fragment pattern. Further down the line the volatiles corresponding to each pressure peak can be selectively isolated in limbs where the trapped volatile is then transferred to a gas IR cell and gas GC cell so each component can be analysed in further detail.

2.3 Thermal Volatilisation Analysis

The measured output (in mV) from the Pirani gauges must be converted to pressure and this is achieved by using the following equation:

$$P = e^{((VxCf)-6.125)}$$

Equation 2.1: Conversion of voltage (V) to pressure (P) using set equation from Pirani handbook and additional correction factor (C_f). To prevent voltage overloading to the data-logger, resistors are installed in the circuit and therefore a correction factor is applied.

The pressure plots for both the degradation run and sub-ambient distillation are plotted against temperature and time. An example of a typical SATVA run on a model PDMS is shown in Figure 2.7:
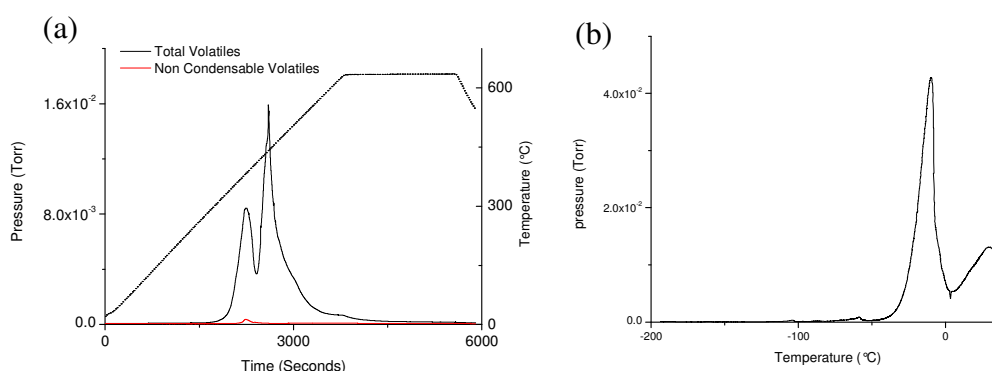
Figure 2.7: Degradation run and sub-ambient distillation of a model PDMS elastomer. In (a) the pressure both in and out of the trap is recorded. Pressure out peaks can be assigned from mass spectrometry data; in (b) sub-ambient run, each peak can be isolated in limbs further down the line and analysed by mass spectrometry, IR and GC-MS

By setting the online mass spectrometer to single-ion monitoring on the repeat run the total pressure obtained for each volatile evolved during both degradation and distillation step can be measured. This can lead to elucidation of the all the thermal degradation mechanisms occurring in the material that is being studied.

Thermal volatilisation analysis has been combined with TGA in an experiment described by Camino, Grassie and McNeill.[10] In this setup a pan was sealed in the

sample tube and balanced using an external electromagnetic balance which allowed simultaneous monitoring of mass loss in the sample with pressure data from Pirani gauges. This allows a more in-depth study of where volatile fractions appear with respect to the degradation processes occurring in the sample during mass loss.

Degradation studies using the thermal volatilisation analysis apparatus are not limited to thermal degradation of a sample. Other methods of sampling may be constructed by alteration of the furnace end of the TVA line. One of the first alterations noted in literature was photothermal degradation of methacrylate polymers by Grassie *et al.*. By combination of thermal heating and UV light it was shown the degradation temperature of these polymers could be lowered by 200 °C.[11] The theory behind this observation was the energy of the UV light was able to break bonds that are normally homolytically broken at higher temperatures when only thermally degraded. A study using only photochemical degradation was carried out in a special cell built by McNeill in which many parameters were investigated to determine optimum molar release of volatiles from degrading polymer samples. It was shown that increasing exposure time, film thickness and decreasing distance of the lamp from sample lead to greater levels of detectable degradation products.[12] Potentially it would also be possible to use laser ablation in order to understand degradation of polymers at high energies, something that has not been considered before.

The most recent application of TVA at Strathclyde that has been published has focused on the conservation of books.[13] By use of TVA and multivariate analysis it was shown that certain volatile organic compounds (VOCs) are consistently found leeching from old library books as they age. This was studied in further depth by Lewicki *et al.* by use of desiccation of old library books and collection of off gases by connecting the desiccator to the high vacuum line.[14] Not only can library books provide VOCs but other objects such as leather covers, tobacco pipes and bowling balls have all been studied.

2.4 Gel Permeation Chromatography

Gel permeation chromatography (GPC) is a non-destructive separation technique which is used in the determination of molecular mass distributions of polymers and proteins. A flow diagram describing the experimental setup is shown in Figure 2.8:
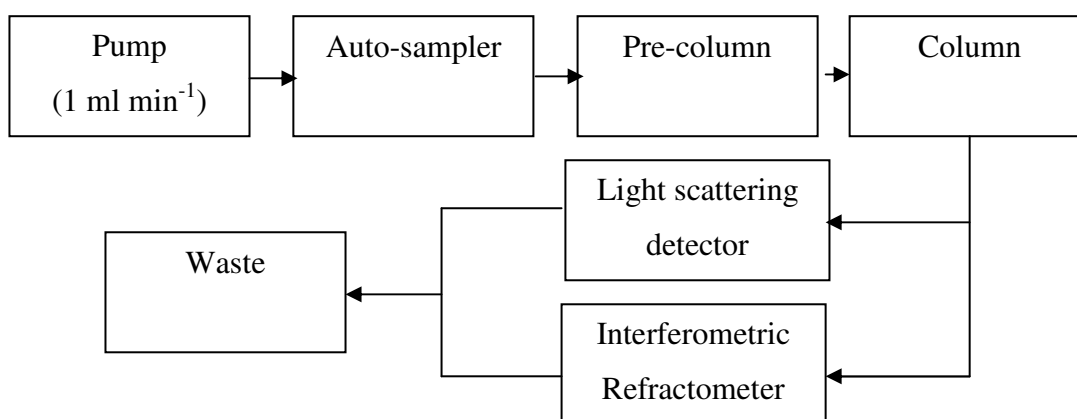
Figure 2.8: A flow diagram showing the general setup of a GPC system

The polymer sample is dissolved into the mobile phase at a concentration of 10 mg ml^{-1}. The auto-sampler then injects the sample onto the top of the pre-column which protects the main column from unsuitably sized analytes. From the pre-column the sample is then passed onto the column. The technique works by separating the analyte species by size exclusion, this is achieved by passing the material through a column filled with porous polymer beads. These polymer beads are usually made of cross-linked polystyrene. Large species will be unable to permeate into the beads and will elute first (void volume) and small species will be able to migrate into the beads and will take longer to elute (total volume).[15] Intermediate-sized species will be able to enter large pores on the beads and will elute somewhere between the void volume and the total volume of the column. The molar mass range of a typical column is about 1,000 – 2,000,000 g mol^{-1}.

As the analytes elute from the column they are passed into a detector which analyses the species present based on the difference in refractivity of light between the solvent

and analyte. The detection of the analyte is dependent on the dn/dc value and this is characteristic of the solvent/analyte combination. For PDMS this value is 0.098 (λ = 546 nm) in benzene where as the value is 0.0446 (λ = 633 nm) in THF.[16-17] The consequence of having a low dn/dc value is that the analyte may not be observed by the detector and therefore no peak will be found. For PDMS based analytes it is critical that an appropriate mobile phase is used as they tend to have low dn/dc values in certain solvents such as THF.

The interferometric refractometer is used to detect the concentration of the peaks and is based on the mass recovery of the sample. This concentration peak can be integrated with the peak from the light scattering detector to give an average molecular mass of the analyte. These peaks are normally Gaussian in shape and the sharper the peak the narrower the polydispersity index of the polymer. For PDMS systems the polymers tend to have low polydispersity indices.

UV light detectors can also be used to monitor the analytes as they elute if the sample contains a chromophore. As with refractometry, the use of this type of detector requires standards of known molecular mass to be run so that the detector can be calibrated to the polymer that is being used. The mobile phase must be non-fluorescing in the region of the analytes so as not to mask the UV absorption peaks.

2.5 Matrix-Assisted Laser Desorption/Ionization Time of Flight Mass Spectrometry

Matrix-assisted laser desorption/ionization time-of-flight (MALDI-TOF) uses a laser to ablate a sample and the fragments are separated using a time-of-flight mass spectrometer. The technique is a soft ionisation technique that is useful at detecting mass fragments from 1-150,000 atomic mass units. This technique can be used to characterise small molecules, large organic polymers and proteins. It is complementary to GPC analysis in determining molecular mass and polydispersity of a polymer however, unlike GPC, this technique is qualitative and destructive.

Samples are prepared by dissolving standards and analytes separately in a solvent containing a host matrix. The final concentration of these samples are usually in the pico molar range as the technique is very sensitive and only requires a small sample size so as to avoid overloading the ion detector. The matrix will then crystallise out of solution and the sample will be contained within it. The matrix is used to allow for good coupling of the laser with the sample in the formation of ions. More complex sample preparations can utilised if direct crystallisation methods are problematic.[18] The experimental setup is shown in Figure 2.9:
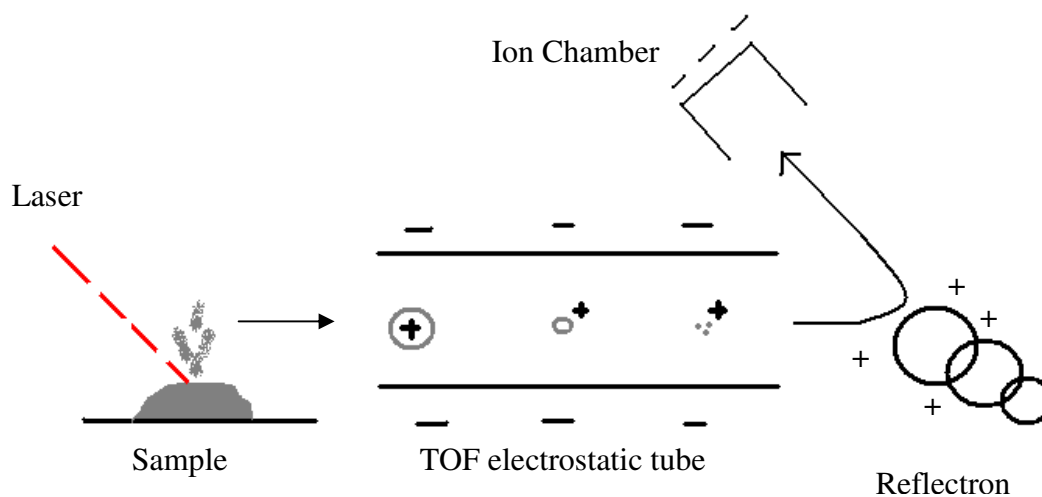
Figure 2.9: Experimental overview of a MALDI-TOF instrument

The evolution of ions is achieved by firing a laser onto the sample. The matrix absorbs the incoming photons and then vaporises and ionises the sample. To collect enough data, 100 shots are carried across the surface of the sample and rastering of the laser is used to obtain a representative spectrum. The ions leave the surface of the sample and are accelerated electrostatically down the time-of-flight tube; large molecules move slower than the smaller molecules and their difference in flight time determines their mass. The use of standards allows the mass spectrometer to be calibrated such that compounds of known molecular mass are timed in flight. Resolution can be increased by reflectron mode where the ions are reflected back to the detector which increases sensitivity of separation of small molecules. Once in the ion chamber they hit the detector and the mass spectrum is recorded.

MALDI-TOF MS has been used to investigate poly(siloxane) polymers of low molecular mass and the conditions required for analysis have been established. The matrix of choice is dithranol and the concentration of the polymer in the sample should be in the region of 10^{-4} M.[19]

In general the use of MALDI-TOF in the determination of molecular mass distribution of a polymer should always be complemented by GPC data. In comparing the results of the MALDI-TOF with GPC analysis it was noted that the average molar mass and the polydispersity when comparing MALDI to GPC. This underestimation was due to the loss of higher molar mass components of the Gaussian distribution which is visible if the MALDI data is overlaid onto the GPC data. It has been suggested that this is due to ion suppression of the larger molar mass species.[20]

2.6 Nuclear Magnetic Resonance Studies of Both Polymer and Carborane Solutions

Rather than discuss the origin of NMR spectroscopy and line signal generation this Section is designed to address some of the aspects of NMR relating to polymer characterisation in terms of theory and its practical applications. For discussions on nuclear spin, chemical shift, coupling effects of nuclei and splitting patterns the reader is directed to Chapter 3 of "Spectroscopic Methods in Organic Chemistry" by Williams and Fleming. This book covers the basics of NMR spectroscopy from Larmor precession through to nuclei decoupling sequences.

One use of NMR spectroscopy employed in polymer characterisation is the analysis of stereochemical differences that arise within synthesised polymer materials.[21] Vinyl polymers and copolymers generally add in head-to-tail fashion when polymerising, although, as this process terminates at high molecular masses other conformations will arise. In the example of poly(methylmethacrylate) changes between isotatic and syndiotactic form give rise to changes in the ^{1}H C$\underline{H}_2$ signal in the NMR spectrum.[22] The monomer unit is shown in Figure 2.10.
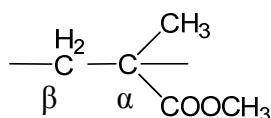
Figure 2.10: Repeat unit of PMMA

The α and β splitting pattern will change depending on the configuration the polymer adopts. Isotactic configuration will lead to a AB system (pseudo quartet) in the NMR spectrum where as syndiotactic conformation leads to a singlet for the β protons. This is because in the isotactic conformation the methylene protons are no longer in equivalent environments. Symmetry effects can be subtle but have to be considered when assigning NMR data. For PMDS no such issues with regard to conformation arise but phenyl substituted siloxanes such as poly(phenylmethylsiloxane) (PPMS) may have a degree of stereoisomerism.

[11]Boron NMR spectroscopy of carboranes requires knowledge of the symmetry environments that the cage structure of the molecule adopts, especially the isomer of the material. In particular *meta*-carborane gives rise to 4 signals in the ^{11}B NMR spectrum due to 4 symmetry environments for boron being present in the molecule. Also the carbon atoms are slightly more electronegative and will increase *J* coupling values of the neighbouring boron atoms. As the B-H vertices have relatively high δ+ charge in the cage system the shifts in the [11]B-^{1}H couplings decrease in order of *ortho* > *meta* > *para* as the electronegative carbons are rearranged as first postulated by Lipscomb.[23] Comparison of *ortho*, *meta* and *para* carboranes calculated *J*-values and those observed experimentally is shown in Table 2.1:

Compound	BH Vertex	Δ	$J(^{11}B\text{-}^1H)$exp	$J(^{11}B\text{-}^1H)$cal
ortho-Carborane	3,6	-15.8	178	180
	4,5,7,11	-14.7	165	165
	8,10	-10.3	151	150
	9,12	-3.4	150	148
meta-Caborane	2,3	-18.0	180	180
	4,6,8,11	-14.3	165	165
	5,12	-7.7	163	163
	9,10	-11.5	150	150
para-Carborane	2-11	-15.8	164	165

Table 2.1: Calculated and experimental *J*-values for *o*-, *m*- and *p*-carborane

To obtain the ^{11}B-^{1}H coupling values 2D COSY NMR is required as it is not possible to observe the multiplets in 1D as they overlap. In doing this a 2D plot reveals 4 doublet peaks which by further interrogation of the spectra prove actually to be quadruplets where the two inner peaks are suppressed.[24] The splitting of the individual symmetries on the *J*-tree is 3:1:1:3. To obtain accurate values for the [11]B-^{1}H coupling constants the separation of the two outer points are measured and the result divided by 3. An example of a 2D COSY spectrum of *m*-carborane is shown in Figures 2.11 and 2.12:
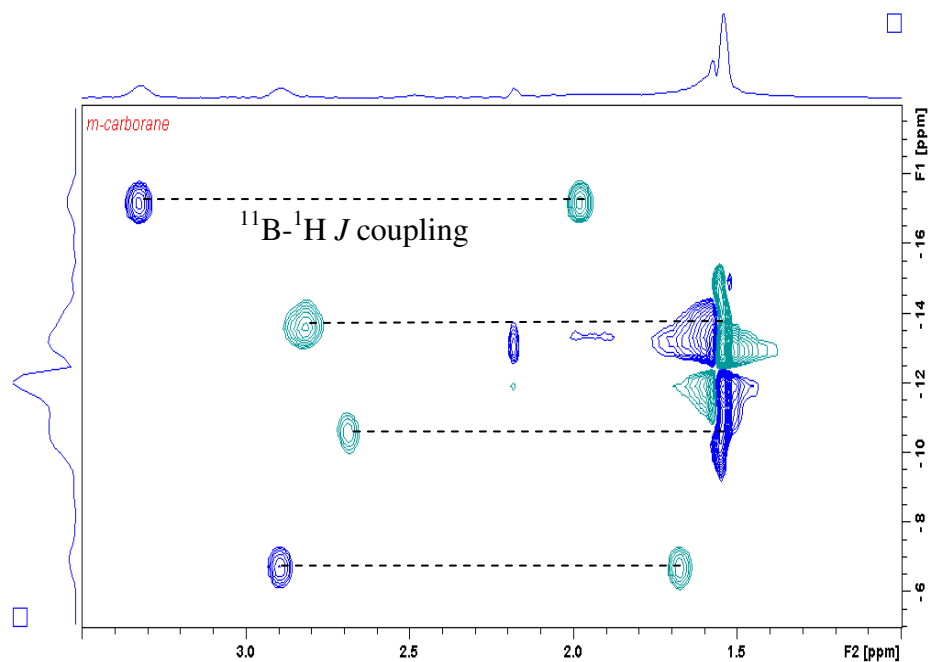
Figure 2.11: 2D ^{11}B NMR COSY plot for *m*-carborane. Each dotted line on the spectrum indicates the ^{11}B-^{1}H *J* coupling distance between outer most peaks
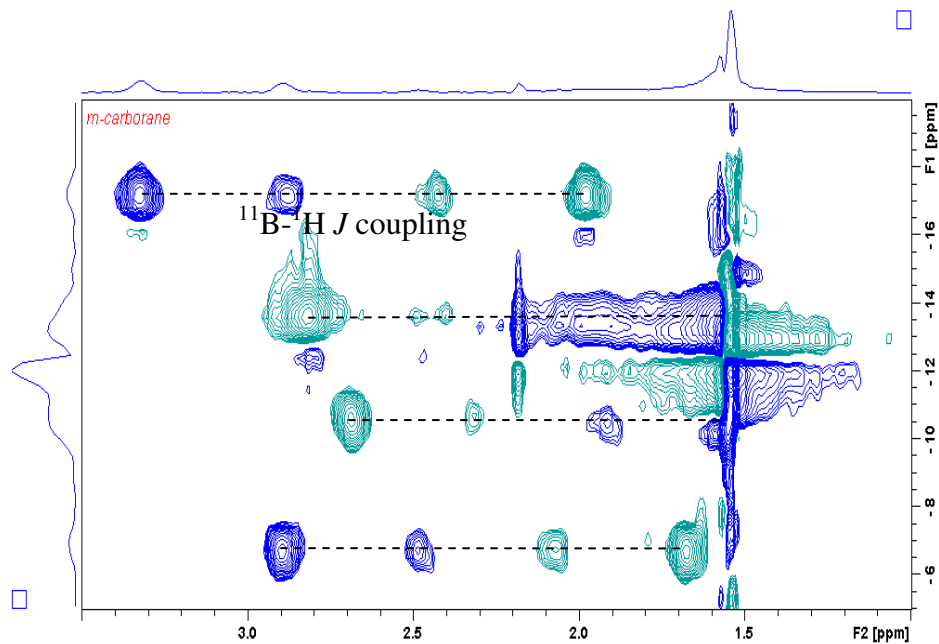
Figures 2.12: Replot of Figure 2.16 showing the expanded spectrum containing quadruplet peaks, therefore measured value is divided by 3

2.7 Solid State Nuclear Magnetic Resonance Studies of Polymer Materials

Solid state NMR of polymer and elastomer materials can not only help characterise the functional groups present in a material, but it can also be used to assess the phase behaviour of polymers. Solid state NMR has incorporated time as a function of the free induction decay (FID) so phase behaviour of both short and long relaxations may be observed.[25] In solution phase NMR all of these interactions are averaged so no phase behaviour can therefore be observed. The main problem that had to be overcome in the transition from solution NMR to introducing solid state NMR was the broad signals that were initially observed when attempting to accumulate spectra.[26] The main reason for the broad signals observed was due to the strong dipolar couplings that occur in the solid phase.

This hurdle was overcome by using Magic Angle Spinning (MAS) where the NMR sample is orientated at an angle of 54.7° to the direction of the magnetic field. The magic angle is the root of the Legendre polynomial and any interaction dependant on the polynomial will equal zero at the magic angle. The relationship between dipolar coupling constant and angle is shown in equation 2.2:

$$D(\emptyset) \propto 3cos^2\emptyset - 1$$

Equation 2.2: Relationship between dipolar coupling constant and an external magnetic field. D is the dipolar coupling constant.

The consequence of orientating the sample at 54.7° was to diminish the effect of dipolar coupling to zero, and allow collection of a cleaner FID signal with respect to all nuclei other than ^{1}H. Protons are too mobile and unfortunately there is no suitable way of resolving the broad signals even after adjustment for broadening due to dipolar coupling.

The signals obtained for ^{13}C etc. after this step are very weak due to the low gyromagnetic ratios in the NMR relaxation so further adjustment must be made. Cross polarisation is a process in which magnetism from the protons is transferred to neighbouring nuclei of interested in order to generate a stronger line signal in the FID. The pulse sequence is shown in Figure 2.13:

Frequency Channel 1 ^{1}H

Frequency Channel 2 ^{13}C
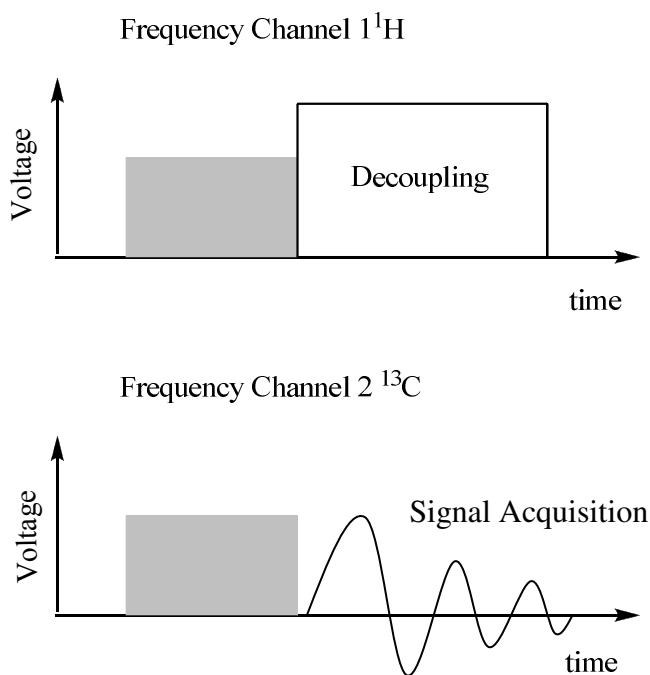
Figure 2.13: Example of a pulse sequence used to obtain a ^{13}C solid state NMR spectrum

In order to achieve a spectrum a low energy ^{1}H pulse is used in frequency channel 1 which matches the energy of the pulse that is used in the second frequency channel which is used to collect the spectrum. This then gives rise to a stronger signal that is similar to the spectra obtained in solution NMR. An example of an ^{11}B NMR of *m*-carborane is shown in Figure 2.14:
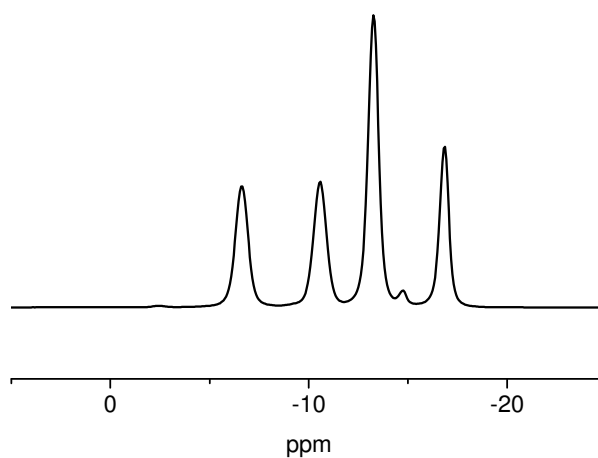
Figure 2.14: ^{11}B solid state NMR spectrum of *m*-carborane showing the four-peak splitting pattern arising from the symmetry of the carborane cage

Another use of solid state NMR relating to polymer and elastomer materials is in contact time experiments. As mentioned previously, polymer materials may have both amorphous and crystalline regions, also cross-linked and entangled polymer chains. These regions relax on different time scales so by collecting the FID at different time intervals the information collected depends on the environment that the nuclei are in. At short contact times the more rigid part of the polymer material is observed whereas at longer contact times the more flexible parts start to appear in the spectrum. This can be important when identifying the reasons why a material may have rigid and flexible regions and for identifying flexible pendent groups or chains on a polymer backbone for example. Solid state NMR will help in the study of carborane-siloxane hybrid materials by not only identifying how the carborane is incorporated but also by what degree the carborane is influencing the polymer chain dynamics.

2.8 Cyclic Voltammetry

Cyclic voltammetry is a type of potentiodynamic electrochemical measurement which is used to study the electrochemical properties of an analyte in solution. In this case, the analyte is an electroactive species, for example a species which can undergo reduction or oxidation at the electrode surface.

In a typical cyclic voltammetry experiment, potential limits are set within which the electroactive species can undergo reduction or oxidation at the electrode surface. The voltage is scanned at a defined rate known as the scan rate v (mV s^{-1}). Voltage limits are set between which the voltage is varied. When scanning in a positive direction an oxidation wave is seen for the compound and when this is reversed the reduction wave is observed, the half cycles link at both ends completing the voltammogram. Each wave indicates either the loss or gain of one or more electrons by the compound in the solution. The current at the working electrode is plotted against the applied voltage to give the cyclic voltammogram trace. By taking the measured voltages at the peak maximum heights, the redox potential of the compound can be calculated by using the Nernst equation shown in equation 2.3.[27]

$$E = E^0 + 2.3RT/nF \log[Red]/[Ox]$$

Equation 2.3: The Nernst Equation where E is the cell potential, E^0 is standard cell potential, R is the gas constant, T is absolute temperature, n is the number of electrons, F is the Faraday constant, [Red] is the concentration of the reduced species and [Ox] is the concentration of the oxidising species

The solvents used are not charge carriers so a salt must be added to conduct the charge between the electrodes. A calibration standard must also be used to act as a reference to the electrochemical experiment. Ferrocene is commonly used and is made up in the stock solution to 5 mM concentration (25 mg, 25 mL). An example of a ferrocene voltammogram is shown in Figure 2.15.
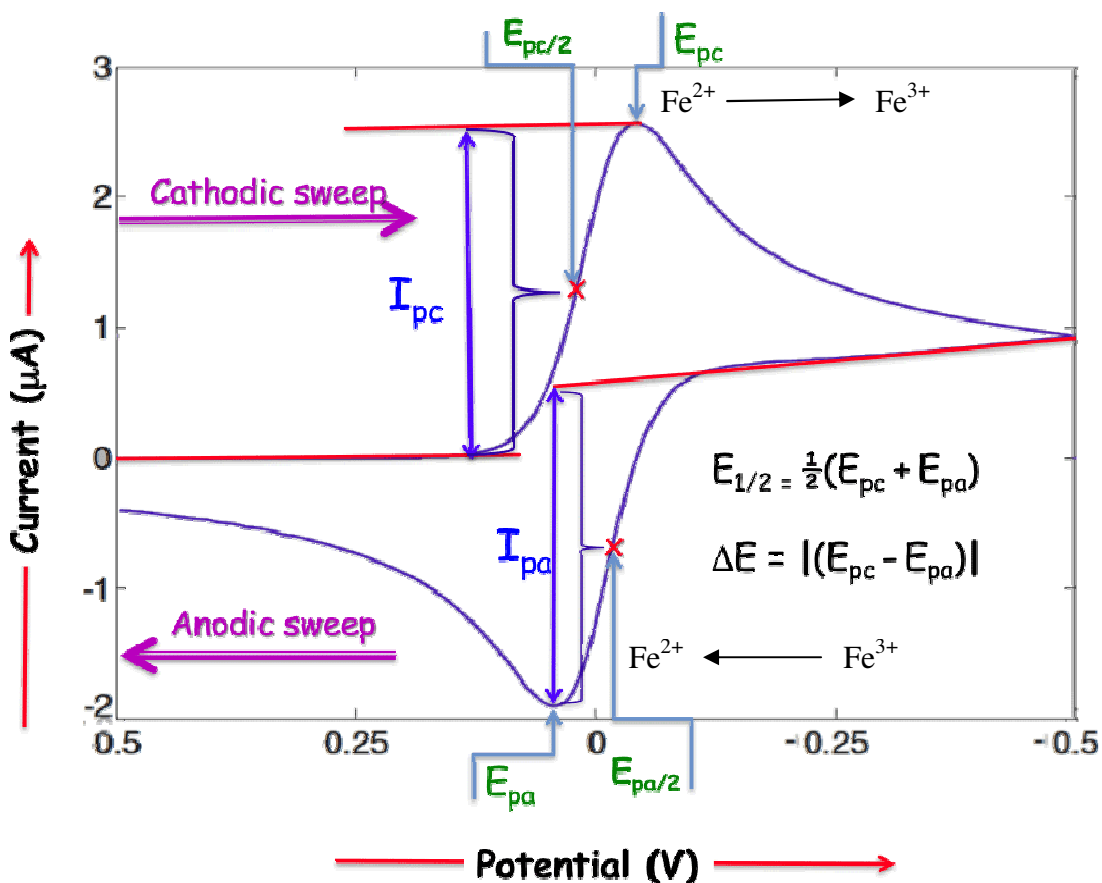
Figure 2.15: Voltammogram of ferrocene showing both an oxidation and reduction wave of the iron metal centre vs AgCl reference electrode. Extraction of $E_{1/2}$ gives a value of 59 mV showing reversibility in the system[28]

The compounds of interest are made up as millimolar solution in the solvent with typically 0.1 M electrolyte. The molecular size of the compounds will require the scan rate to be adjusted because larger molecules will have slower diffusion rates at the electrodes. Scanning at very slow scan rates may not reveal the oxidation wave of the compounds that are tested, so different scan rates are introduced.

A solution is normally scanned at multiple different scan rates so a test for reversibility can be performed. If the system is fully diffusion controlled and reversible it will obey the Randles Sevcik equation as shown in Equation 2.4:[29]

$$I_p = -(2.69x10^5)n^{3/2}c_o^{\infty}D^{1/2}v^{1/2}$$

Equation 2.4: Randles Sevcik equation where I_p is peak current (A), n is number of electrons, c_o is concentration of analyte (mol cm^{-3}), D (cm^2 sec^{-1}) is diffusion coefficient and v is scan rate (V sec^{-1})

The peak current density is proportional to the concentration of electro-active species and the square root of the sweep rate and diffusion coefficient. The system is reversible if: $\Delta E_p = E^A_p - E^C_p = 0.059/n$ V, $|i^C_p|/i^A_p = 1$ and E_p is independent of v. Furthermore, a plot of i_p versus $v^{1/2}$ is linear and passes through the origin. Also, from the gradient of the linear graph the diffusion coefficient can be calculated. The diffusion coefficient can be measured for a range of samples to determine the rate at which the species of interest are moving on to the surface of the electrode. The size of the diffusion coefficient can also validate what is being observed in the cyclic voltammogram.

2.9 References

1. Image from http://www.apmtesting.com/testing-services/test-methods/ASTM-E1131.php (21st July 2012)

2. Walton, D., Lorimer, P. "*Polymers*" Oxford University Press 2000: 53

3. Image from http://mse.cornell.edu/mse/undergrad/lab/dsc.cfm (10th September 2010)

4.Image from

http://164.15.112.38/ULB-GALENIQUE/appareillage.php?page=appareillage_EN

(21st July 2012)

5. Grassie, N., Meville, H.W. *"The thermal degradation of polyvinyl compounds I – IV"* Proceedings of the Royal Society of London A, 1949, **199**:1-13, 14-23, 24-39, 40-55

6. Grassie, N., McLaren, I. F., McNeill, I. C. *"Thermal degradation of vinyl chloride-vinyl acetate copolymers"* European Polymer Journal 1970 **6**: 679

7. Grassie, N., McGuchan, R., *"Pyrolysis of polyacrylonitrile and related polymers – III"* European Polymer Journal 1971 **7**: 1357

8. Grassie, N., MacFarlane, I.G., Francey, K.F., *"The thermal degradation of polysiloxanes – II"* European Polymer Journal 1978 **15**: 415

9. Grassie, N., Zulfiqar, M., Guy, M.I. *"Thermal degradation of a series of polyester polyurethanes"* Journal of Polymer Science 1980 **18**: 265

10. Camino, G., Grassie, N., McNeill, I.C. *"Influence of the fire retardant, ammonium phosphate, on the thermal degradation of poly(methyl methacrylate)"* Journal of Polymer Science: Polymer Chemistry Edition1978 **16** (1): 95

11. Grassie, N., Scotney, A., Mackinnon, L., *"Observation of the photothermal degradation of polymethacrylates by using thermal volatilisation analysis"* Journal of Polymer Science: Polymer Chemistry Edition 1977 **15** (1): 251

12. McNeill, I.C., Zulfiqar, S., *"Photolysis of polymers using the medium pressure mercury lamp: Part 1 – photolysis and product analysis apparatus and the effect of some experimental variables"* Polymer Degradation and Stability 1985 **10**: 147

13. Gibson, L.T., Robertson, C., *"Analysing smelly old books"* Advances in Paper Conservation Research 2009 May: 40

14. Lewicki, J.P., Todd, D., Redon, P., Liggat, J., Gibson, L. *"Thermal volatilisation analysis – The development of a novel technique for the analysis of conservation artefacts"* Materials Research Society Symposia Proceedings 2008: (1047-Y04-05)

15. Dean, J. R., Jones, A.M., Holmes, D., Reed, R., Jones, A., Weyers, J. *"Practical skills in chemistry"* Prentice Hall 2002: 206

16. Brandrup, J., Immergut, E.H., *"Polymer handbook: Third edition"* Wiley Interscience 1989 **VII**: 465

17. Hwang, Y.H., Yang, M.H. *"Determination of molecular weight of PDPS modified copolymers"* Journal of the Chinese Chemical Society 2000 **47**: 187

18. Hillenkamp, F., Karas, M., *"The MALDI process and method"* Wiley Interscience 2007: 18

19. Haddleton, D.M., Bon, S.A.F, Robinson, K.L., Emery, J.N., Moss, I., *"Matrix-assisted laser desorption ionization time-of-flight mass spectrometry of polydimethylsiloxanes prepared via anionic ring-opening polymerization"* Macromolecular Chemistry and Physics 2000 **201**: 694

20. Lui, M. X., Maziarz, P.E., Heiler, D.J., Grobe, G.L. *"Comparative studies of poly(dimethylsiloxanes) using automated GPC-MALDI-TOF MS and on-line GPC-ESI-TOF MS"* Journal of American Society for Mass Spectrometry 2003 **14**: 195

21. Campbell, D., Pethrick, R.A., White, J.R., *"Polymer characterization – Physical Techniques"* Stanley Thornes 2000: 134

22. Cowie, J.M.G., Arrighi, V., *"Polymers: Chemistry and physics of modern materials"* CRC press 2008: 260

23. Hermanek, S., Machacek, J., Fusek, J., Bletcher, V. *"Importance of ^{11}B-^{1}H coupling constants in assigning the ^{11}B signals"* Wiley Interscience 1998: 370

24. Hermanek, S., Machacek, J., Fusek, J., Bletcher, V. *"Importance of ^{11}B-^{1}H coupling constants in assigning the ^{11}B signals"* Wiley Interscience 1998: 378

25. Mirau, P.A., *"A practical guide to understanding the NMR of polymers"* Wiley Interscience 2005: 361

2.9 References

26. Campbell, D., Pethrick, R.A., White, J.R., *"Polymer characterization – Physical Techniques"* Stanley Thornes 2000: 146

27. Pletcher, D. *"A first course in electrode processes"* Alresford Press 1991: 7

28. Image from http://faculty.sdmiramar.edu/fgarces/LabMatters/Instruments/eDaq/eDaq_Operation/eDaq_PotentioStat_Operations.htm (21st July 2012)

29. Greef, R., Peat, R., Peter, L.M., Pletcher, D., Robinson, J., *"Instrumental methods in electrochemistry"* Ellis Horwood Limited 1990: 183

Chapter 3

Incorporation of Carboranes into Polydimethylsiloxane Elastomers Formed *Via* Tin-Catalysed Condensation

3.0 Chapter Introduction

In this Chapter the first set of experiments are described in which a tin(II) 2-ethylhexanoate catalyst is used to synthesise all network PDMS materials for analysis. Before incorporating carboranes into the networks to improve thermal stability a material must be synthesised that will act as a control for the rest of the study. Previous work by Lewicki in this field included formation of well defined PDMS elastomers using a tetra-functional cross-linkers and di-functional end capped siloxane polymers catalysed by a RTV process to form a network PDMS. These materials will act as the control in this study where all subsequent improvement in properties and behaviour will be compared to this.

The incorporation of carboranes as dispersions into PDMS will be considered in this Chapter. By assessing the solubility, stability and ease of processing of *m*-carborane filled PDMS elastomers improvement in thermal stability may be obtained as a composite material. Adjustment of the functional groups on the carborane cage will help determine the optimum functionalisation for compatibility. Subsequent routes to binding of carborane moieties to PDMS will be described in later Chapters.

3.1 Instrumentation

This Section outlines the instrumentation used in the collection of all data during the course of the project. All instruments are detailed below to allow for reproduction of the analyses and cover all work described in Chapters 3 - 6.

All synthesis used standard laboratory glassware and equipment. Solution nuclear magnetic resonance (NMR) measurements were made using either a Bruker Avance 400 or a Bruker Avance DRX500 instrument, ^{1}H NMR signals were collected at 400 MHz, ^{13}C collected at 100.5 MHz and ^{11}B at 128 MHz. Solid state NMR measurements were carried out by the University of Durham NMR service (Dr David Appley) on a Varian VNMRS spectrometer, with ^{13}C data collected at 100.5 MHz and ^{11}B at 128 MHz. Infra red spectra were recorded from KBr discs using a Perkin Elmer Spectrum One FT-IR spectrometer. Gas phase FTIR was carried out using a Nicolet FTIR spectrometer. 45° reflectance FTIR and ATR probed FTIR was performed using an A2 Technologies Exoscan handheld spectrometer. X-ray fluorescence measurements were performed by PANalytical, Netherlands, using an AXIOS XRF spectrometer. Scanning electron microscopy (SEM) was carried out in-house on a Cameca SX100. Microanalysis was carried out in-house using a Perkin Elmer series II CHNS/O 2400 analyser. Gas chromatography (GC) was completed using a ThermoQuest Trace GC and Finnagan Polaris Q mass spectrometer (MS). MALDI-TOF measurements were made using a Kratos Analytical AXIMA-CRF. GPC was carried out in either THF or methylene chloride with an Ultimate 3000 pump into Waters columns connected to an Optilab DIP interferometric refractometer and Tri Star light scattering detector. TGA analysis was carried out using a Shimadzu TGA-51 thermogravimetric analyzer. DSC analysis was completed using a TA instruments DSCQ1000. Sub-ambient thermal volatilisation analysis was performed on a vacuum line built in-house.

3.2 Materials for Synthesis

Most of the chemicals used in this project (unless otherwise stated) were obtained from Sigma Aldrich (United Kingdom). Methoxy end-capped silicones were bought from Fluorochem (United Kingdom). Carboranes and their derivatives were purchased from Katchem (Czech Republic). The most important chemicals used during this project are discussed further in the next few Sections.

3.2.1 Poly(dimethylsiloxane)
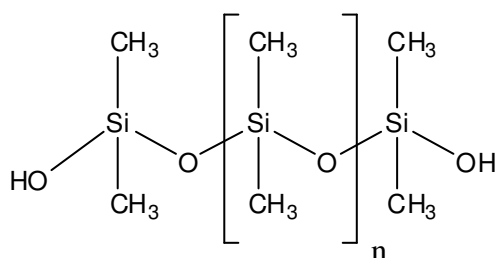
Figure 3.1: Chemical structure of poly(dimethylsiloxane) (OH terminated)

Linear PDMS is a viscous liquid at room temperature. In this form the polymer has limited thermal stability until cross-linked to form a solid elastomer. The polymer can be bought with a variety of starting molar masses and functionalities capping the terminal position on the polymer end. Another important siloxane in this project is a 1:1 copolymer of PDMS with a methylhydrosiloxane chain, shown in Figure 3.2.
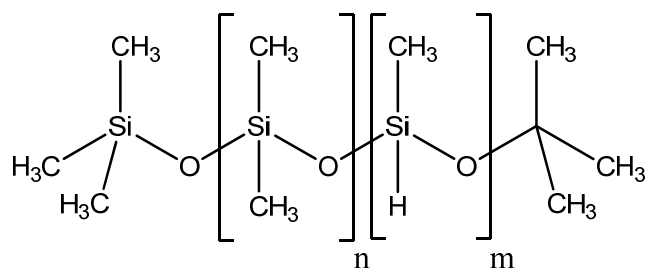
Figure 3.2: Chemical structure of poly(dimethylsiloxane-*co*-methylhydrosiloxane) (tri-methylsilyl end capped)

3.2.1 Poly(dimethylsiloxane)

PDMS elastomers will act as a baseline material for this project and all results from modified PDMS systems will be compared to these.

3.2.2 Tetraethyl orthosilicate, TEOS

$$H_3CH_2CO \diagdown \quad \diagup OCH_2CH_3$$
$$Si$$
$$H_3CH_2CO \diagup \quad \diagdown OCH_2CH_3$$
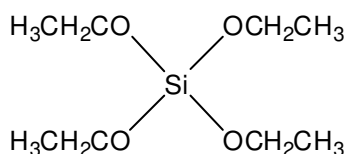
Figure 3.3: Chemical structure of tetraethyl orthosilicate

TEOS is a cross-linking agent that also promotes nucleation of PDMS in the formation of elastomers by solution-gel chemistry. The compound is also used as a synthetic intermediate en route to silicon dioxide. The small molecular size and liberation of ethanol from the product during condensation chemistry increases the reactivity of this species over the slightly larger tetrapropyl orthosilicate alternative. When using this compound for cross-linking the temperature of the reaction must be lowered as not to cause rapid vulcanization of the polymer. The molecular size means it could also be coupled to a carborane to possibly form a new boron based modifier.

3.2.3 Tin(II) 2-ethylhexanoate
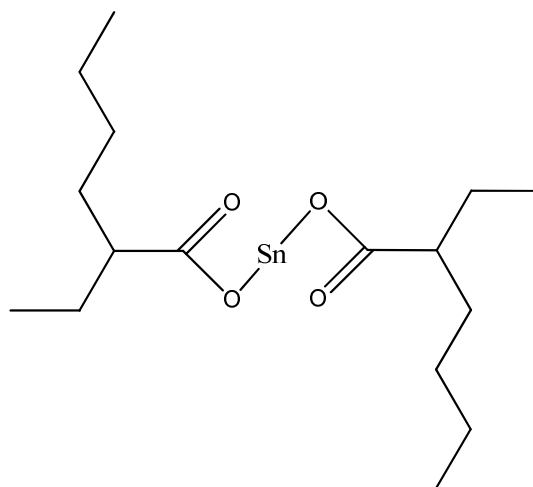
Figure 3.4: Chemical structure of tin(II) 2-ethylhexanoate

Tin(II) 2-ethylhexanoate is a catalyst that is commonly used in condensation chemistry. This is due to the compound's activation in the presence of water to a hydrolysed form that will propagate condensation reactions and regenerate the catalytically active tin hydrate species.

3.2.4 *m*-Carborane and Derivatives

Figure 3.5: Structure of 1,7 *m*-carborane. Carbon atoms are explicitly shown and hydrogen atoms have been removed for clarity

m-Carborane is an isomer of *o*-carborane and is based on the parent icosahedron of $[B_{12}H_{12}]^{2-}$ borane cluster. The carborane unit is very stable and has a high resistance to chemical degradation. The hydrogen atoms attached at the carbons may be

3.2.4 m-Carborane and Derivatives

deprotonated using organo-lithium reagents and subsequently functionalised by reactions with electrophiles. Some of the carboranes used in this project will be supplied already functionalised. However, the *m*-carborane unit may be functionalised in-house to give a wide variety of possible synthetic routes to a new nanoscale modifier. However, the one drawback of using these cluster molecules is their cost which can run into thousands of pounds for a few hundred grams of material.

3.3 Synthesis of a PDMS Elastomer

Synthesis of a PDMS elastomer was based on a standard formulation used by AWE, Aldermaston and previously studied by Lewicki *et al*. The use of two different molar masses of PDMS was to exert control of the viscosity of the reactant solution and control gelation time. To a 100 ml beaker was added 24 g of PDMS hydroxy terminated with an average molar mass (M_n) ~76,000 g mol^{-1}, and followed by 8 g of hydroxy terminated PDMS with an average molar mass (M_n) ~550 g mol^{-1} was then added. The resulting mixture was then stirred using a high speed blender at 2000 rpm for 30 minutes to ensure good mixing of the two liquids. While the liquids were mixing, TEOS cross-linker (3.10 g, 14.8 mmol) was weighed out in a small vial, enough to ensure 1:1 molar ratio of bonding of the hydroxyl groups on the polymer and ether groups in the cross-linker. The TEOS was then added to the reaction mixture drop-wise by pipette whilst stirring continued. The resulting blend was then de-gassed in a vacuum desiccator until the liquid was void of air bubbles. The beaker was then placed in an ice bath and the liquid was mixed again this time at 200 rpm. During this time tin(II) 2-ethylhexanoate catalyst (0.702g, 1.73 mmol) was weighed out in a small vial such that the mass was 2% of the total resin mass in the beaker. This was then returned to the fridge to cool for five minutes. After this time the stirring rate was increased to 2000 rpm and the catalyst was added to the solution drop-wise by pipette. After the addition was complete the mixing was stopped and the contents of the beaker were poured into a mould. Moulds used in the project are shown in the Figure 3.6 below:

Figure 3.6: On left an aluminium mould with an internal depth of 5 mm and on the right hand side a nylon mould with an internal depth of 2mm

Prior to using the moulds they are lined with either beeswax or PTFE spray to help release the samples once cast. After the contents of the beaker had been emptied into the mould, the mould was placed into a vacuum desiccator and the air removed from the sample. Once this was complete the mould was removed from the desiccator, the lid was placed on the mould and the mould was placed in an oven to cure the reacting mixture at 80 °C for 15 minutes. The mould was then taken from the oven and the sample was removed from the mould. The sample was post-cured in the oven at 60 °C for 16 hours.

The elastomer synthesis was repeated using tetrapropyl orthosilicate (3.92 g, 14.8 mmol) as the cross-linker to observe the effect of changing the cross-linker.

Experimental Data:

Siloxane elastomer with tetraethyl orthosilicate cross-linker (2% catalyst)

FTIR 45° reflectance (v/cm^{-1}): 2975 (aliphatic CH_3); 1275 ($Si-CH_3$); 1100($Si-O$ stretch); 800($Si-(CH_3)_2$);

3.3.1 Synthesis of a PDMS Elastomer Containing *m*-Carborane

To a 100 ml beaker *m*-carborane (1.755 g, 12.2 mmol) and 36 g of PDMS with an average molar mass (M_n) ~76,000 g mol^{-1} were added. To the mixture 12 g of PDMS with an average molar mass (M_n) ~550 g mol^{-1} was added. The resulting mixture was then stirred using a high speed blender at 2000 rpm for 30 minutes to ensure good mixing. While the solution was mixing TEOS cross-linker (4.64 g, 22.2 mmol) was weighed out in a small vial, enough to ensure 1:1 molar ratio of bonding of the functional groups on the polymer and ether groups on the cross-linker. This was then added to the reaction mixture drop wise by pipette whilst stirring continued. The resulting solution was then de-gassed in a vacuum desiccator until the solution was free of air bubbles.

m-Carborane is soluble with difficulty in PDMS so to assist the dissolution process sonication methods were employed. The ultrasonic probe was immersed into the 100 ml beaker and the solution was stirred at 800 rpm. The probe was set to amplitude of 35% for 40 minutes with the probe set to pulse for eight seconds on and nine seconds off. The amplitude was set such to promote good coupling of poly(dimethylsiloxane) to the sonic probe. If the amplitude is not set correctly the solution is vibrated away from the surface of the probe and not the desired effect of the sonication is lost.

The beaker was then placed in an ice bath and the solution was mixed again this time at 200 rpm. During this time tin(II) 2-ethylhexanoate catalyst (1.503 g, 3.71 mmol) was weighed out in a small vial such that the mass was 2% of the total resin mass in the beaker. This was then returned to the fridge to cool for 5 minutes. After this time the stirring rate was increased to 2000 rpm and the catalyst was added to the solution drop-wise by pipette. After the addition was complete the mixing was stopped and the contents were poured into a mould.

After the contents of the beaker had been emptied into the mould it was placed into a vacuum desiccator and the air removed from the sample. Once this was complete the lid was placed on the mould and the mould was placed in the oven to cure at 80 °C

3.3.1 Synthesis of a PDMS Elastomer Containing m-Carborane

for 15 minutes. The mould was then taken from the oven and the sample was removed from the mould. The sample was post-cured in the oven at 60 °C for 16 hours.

The *m*-carborane dispersed elastomer synthesis was repeated using tetrapropyl orthosilicate (5.89 g, 22.2 mmol) as the cross-linker.

3.3.2 Synthesis of a PDMS Elastomer Containing 1-,7 Bis(methoxydimethylsilyl)-*m*-Carborane

To a 100 ml beaker 1,7-bis(dimethylmethoxysilyl)-*m*-carborane (1.34 g, 4.18 mmol) and 18 g of PDMS with an average molar mass (M_n) ~76,000 g mol^{-1} were added. To the mixture 6 g of PDMS with an average molar mass (M_n) ~550 g mol^{-1} was added. The resulting mixture was then stirred using a high speed blender at 2000 rpm for 30 minutes to ensure good mixing of the two solutions. While the solution was mixing TEOS cross-linker (2.32 g, 11.1 mmol) was weighed out in a small vial, enough to ensure 1:1 molar ratio of the hydroxyl functional groups on the polymer and ether groups on the cross-linker. This was then added to the reaction mixture drop-wise by pipette whilst stirring continued. The resulting solution was then de-gassed in a vacuum desiccator until the solution was void of air bubbles.

The beaker was then placed in an ice bath and the solution was mixed again this time at 200 rpm. During this time tin(II) 2-ethylhexanoate catalyst (0.526 g, 1.30 mmol) was weighed out in a small vial such that the mass was 2% of the total resin mass in the beaker. This was then returned to the fridge to cool for 5 minutes. After this time the stirring rate was increased to 2000 rpm and the catalyst was added to the solution drop-wise by pipette.

A new design of mould was developed to shape the reactant material to give rise to regular three dimensional architectures. In place of a flat metal casting tray an injection moulded plastic capped cylinder was used. The cylinder has one end that has a ridge to attach a lid and the other end was band-sawed off in house to give rise to a vertical pour mould. This is shown in Figure 3.7 below.

3.3.2 Synthesis of a PDMS Elastomer Containing Bis(methoxydimethylsilyl)-m-Carborane

Figure 3.7: On the left a grey plastic cylinder of length 7 cm and internal volume of 198 cm^3 next to a white cap with a plastic release mechanism on rear with an internal diameter of 3 cm. The construction of the pour mould is shown on the right

The cap was attached to the cylinder and the reactant material poured into the open end of the mould. After the contents of the beaker had been emptied into the mould it was placed into the oven to cure at 80 °C for fifteen minutes. The mould was then taken from the oven and the sample was removed from the mould. The sample was post-cured in the oven at 60 °C for sixteen hours.

The (dimethylmethoxysilyl) *m*-carborane dispersed elastomer synthesis was repeated using tetrapropyl orthosilicate (5.89 g, 22.2 mmol) as the cross-linker.

Experimental Data:

5% (dimethylmethoxysilyl) *m*-carborane dispersed siloxane elastomer with tetraethyl orthosilicate cross-linker (2% catalyst)

FTIR (v/cm^{-1}[ATR diamond]): 2975, 2925 (aliphatic CH$_3$); 2600 (B-H); 1250 (Si-CH$_3$); 1100, 1025 (Si-O stretch); 860 (Si-(CH$_3$)$_2$); 800 (C-H); 700 (Si-CH$_3$);

5% (dimethylmethoxysilyl) *m*-carborane dispersed siloxane elastomer with tetrapropyl orthosilicate cross-linker (2% catalyst)

The sample failed to cure due to slow reactivity of the cross-linker against the faster reacting silyl ether carborane which bound faster to the PDMS polymer blocking network formation. When the reaction is repeated removing the *m*-carborane filler, the reaction proceeds to completion.

3.3.3 Synthesis of a PDMS Elastomer Containing 1,7-diallyl-*m*-Carborane

To a 100 ml beaker 1,7-bis(allyl) *m*-carborane (1.34 g, 4.18 mmol) from Katchem (Czech Republic) and 18 g of PDMS with an average molar mass (M_n) ~76,000 g mol^{-1} was added. To the mixture 6 g of PDMS with an average molar mass (M_n) ~550 g mol^{-1} was added. The resulting mixture was then stirred using a high speed blender at 2000 rpm for 30 minutes to ensure good mixing of the two solutions. While the solution was mixing TEOS cross-linker (2.32 g, 11.1 mmol) was weighed out in a small vial, enough to ensure 1:1 molar ratio of the hydroxyl functional groups on the polymer and ether groups on the cross-linker. This was then added to the reaction mixture drop-wise by pipette whilst stirring continued. The resulting solution was then de-gassed in a vacuum desiccator until the solution was void of air bubbles.

The beaker was then placed in an ice bath and the solution was mixed again this time at 200 rpm. During this time tin(II) 2-ethylhexanoate catalyst (0.526 g, 1.30 mmol) was weighed out in a small vial such that the mass was 2% of the total resin mass in the beaker. This was then returned to the fridge to cool for 5 minutes. After this time the stirring rate was increased to 2000 rpm and the catalyst was added to the solution drop-wise by pipette.

The reactant material was poured into the open end of the cylindrical vertical pour mould. After the contents of the beaker had been emptied into the mould it was placed into the oven to cure at 80 °C for 15 minutes. The mould was then taken from the oven and the sample was removed from the mould. The sample was post-cured in the oven at 60 °C for 16 hours.

The bis(allyl) *m*-carborane dispersed elastomer synthesis was repeated using tetrapropyl orthosilicate (5.89 g, 22.2 mmol) as the cross-linker.

3.3.3 Synthesis of a PDMS Elastomer Containing Allyl m-Carborane

Experimental Data:

5% bis(allyl) *m*-carborane dispersed siloxane elastomer with tetraethyl orthosilicate cross-linker (2% catalyst)

FTIR (v/cm^{-1}[ATR diamond]): 2975, 2925, 2840 (aliphatic CH$_3$); 2600 (B-H); 1250 (Si-CH$_3$); 1100, 1025 (Si-O stretch); 820 (C-H bend); 795 (Si-CH$_3$);

30% bis(allyl) *m*-carborane dispersed siloxane elastomer with tetraethyl orthosilicate cross-linker (2% catalyst)

FTIR (v/cm^{-1}[ATR diamond]): 2975, 2900 (aliphatic CH$_3$); 2600 (B-H) 1250 (Si-CH$_3$); 1075, 1000 (Si-O stretch); 875 (Si-(CH$_3$)$_2$); 780 (Si-CH$_3$);

5% bis(allyl) *m*-carborane dispersed siloxane elastomer with tetrapropyl orthosilicate cross-linker (2% catalyst)

FTIR (v/cm^{-1}[ATR diamond]): 2975, 2925, 2850 (aliphatic CH$_3$); 2600 (B-H); 1260 (Si-CH$_3$); 1090, 1010(Si-O stretch); 875 (Si-(CH$_3$)$_2$); 800 (C-H bend);

3.4 Base Siloxane Elastomer Networks

To gain an understanding of poly(dimethylsiloxane) networks it was important to be able to create a model elastomer that can be used for comparison with the boron filled systems. Two model networks were successfully created using either TEOS or TPOS as the cross-linking agent. The TEOS cross-linker was more reactive than the TPOS and the temperature had to be controlled to stop rapid gelation of the material before it was transferred to the mould. Data collected by TGA and DSC analyses was in good agreement with previous data for these types of networks.[1] The thermal degradation behaviour of the TEOS and TPOS PDMS networks are shown in Figures 3.8-3.10:
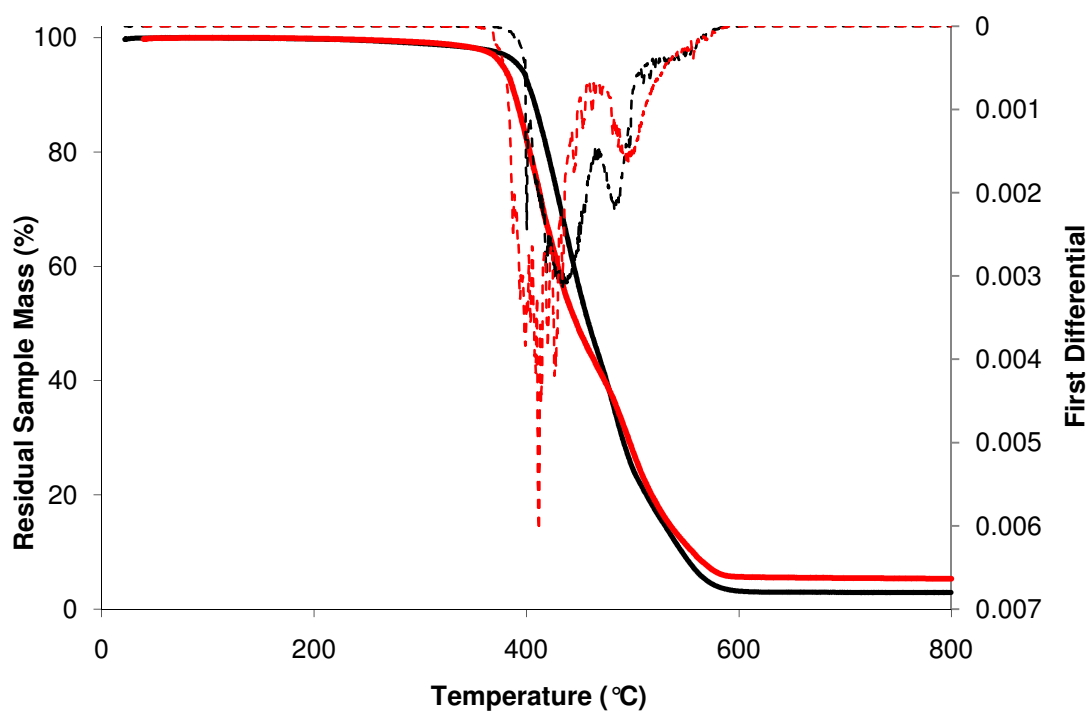
Figure 3.8: Non-oxidative TGA analysis of TEOS (black line) and TPOS (red line) PDMS elastomers including derivatives (dotted lines)

Run	Onset Degradation Temperature / °C	Temperature Maximum Mass Loss / °C	Char Residue / % @ 800 °C
TEOS	384	432	3
TPOS	373	411	5
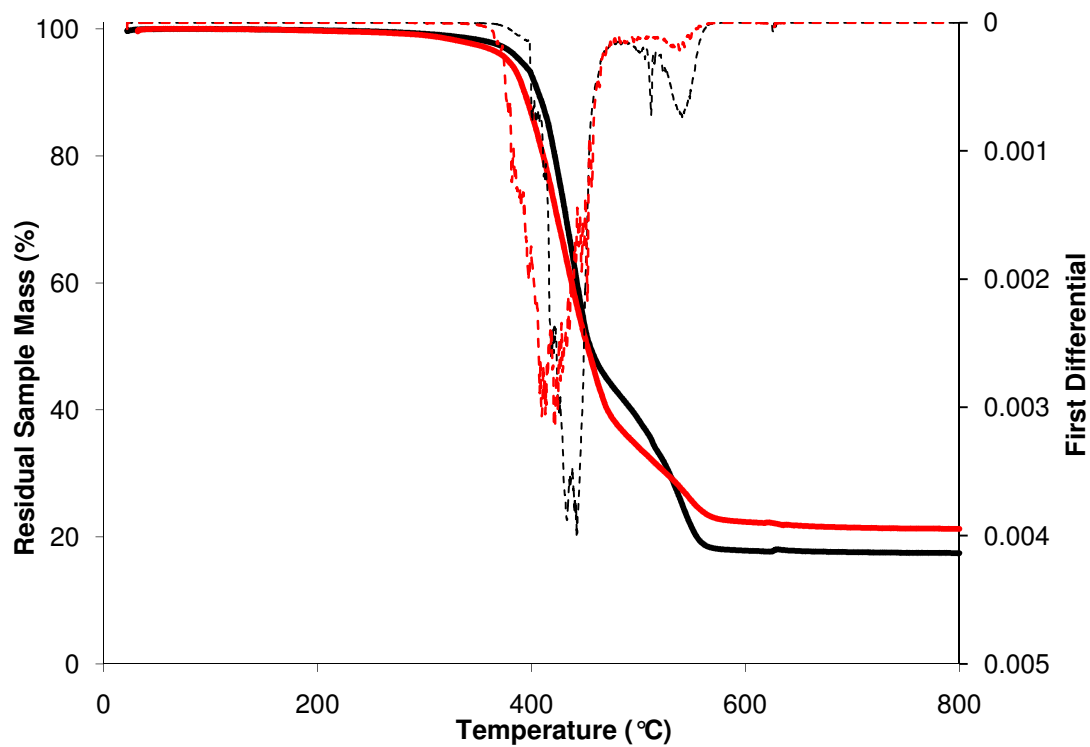
Figure 3.9: Oxidative TGA analysis of TEOS (black line) and TPOS (red line) PDMS elastomers including derivatives (dotted line)

Run	Onset Degradation Temperature / °C	Temperature Maximum Mass Loss / °C	Char Residue / % @ 800 °C
TEOS	383	449	18
TPOS	373	430	21
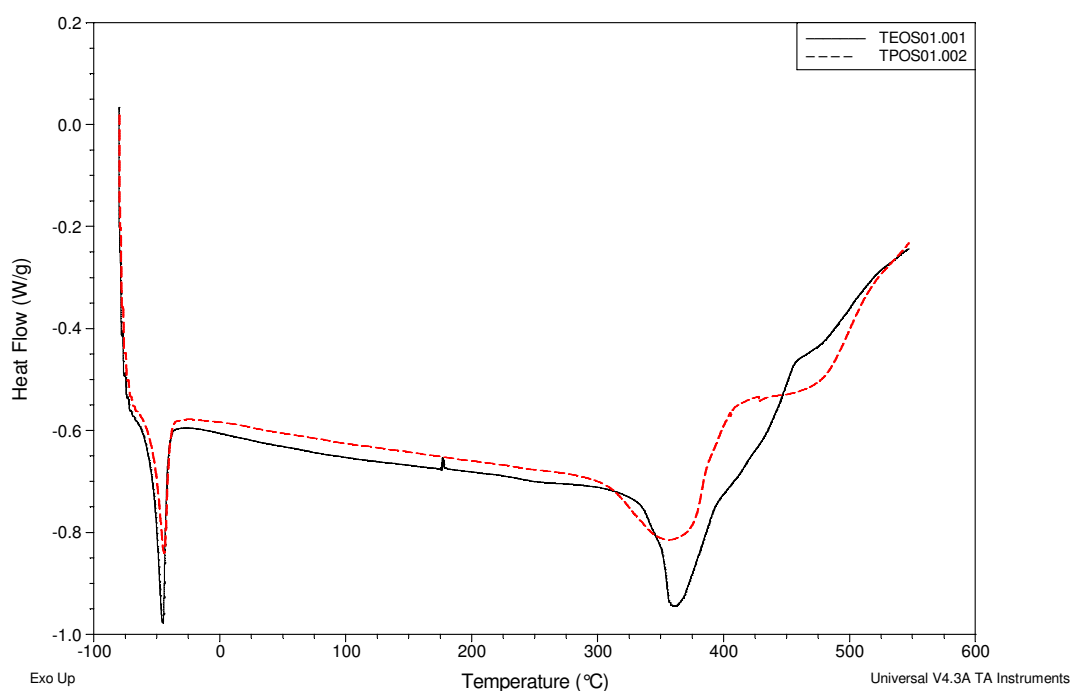
Figure 3.10: DSC analysis of TEOS (black line) and TPOS (red line) containing PDMS elastomers under nitrogen

DSC analysis of TEOS siloxane network (non-oxidative):

Transition	Onset Temperature / °C	Peak Maximum / °C	Enthalpy of Transition / J g^{-1}
T_m	-53.9	-45.5	20.8
T_d	348	361	40.6

DSC analysis of TPOS bound siloxane network (non-oxidative):

Transition	Onset Temperature / °C	Peak Maximum / °C	Enthalpy of Transition / J g^{-1}
T_m	-53.8	-44.5	14.9
T_d	312	356	30.7

From the data the onset degradation of the TPOS sample occurs at slightly lower temperatures than for the TEOS. However, the melting transitions for the two materials are very similar showing that the cross-linker has no significant effect on the melting point of the material. The degradation of both the TEOS and TPOS silicone elastomers is a two step process. The non-oxidative degradation steps happen at around 400 °C then 500 °C, whereas the oxidative steps occur at 400 °C then 550 °C. However, the increase in char residue at the end of the run is a significant indicator to the chemistry occurring in the sample. Oxygen is likely reacting with the sample which will be causing two effects. First an oxidative barrier could form on the surface retarding the release of volatiles. Secondly the formation of formaldehyde under oxidative addition, as shown previously in Scheme 1.17, leads to formation of silanol bonds on the polymer which may react and cross-link the material which reduces the amount of volatilisation.

3.4.1 Thermal Volatilisation Analysis of TEOS Bound Network

The TVA of the TEOS bound siloxane elastomer network has been carried out successfully. The data collected during the run was comparable to previously investigated siloxane elastomer materials.[2] The degradation run is shown in Figure 3.11 and the sub-ambient distillation is shown in Figure 3.12:
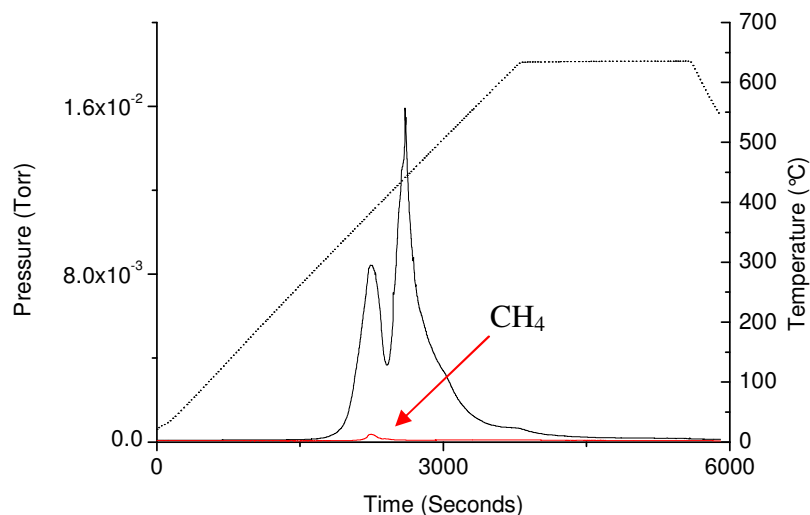
Figure 3.11: TVA degradation run of TEOS bound siloxane elastomer network. Total pressure of volatiles into trap (black line) and non-condensable volatiles (red line) shown against time with furnace temperature shown on secondary axis (dotted line)

The degradation run shows that the degradation of the TEOS bound siloxane elastomer is a two step process, as observed in the TGA of these materials. The two degradation temperatures at which maximum pressure of volatiles generated are similar to that of the two temperatures of maximum mass loss of sample in the non-oxidative TGA. This strongly indicates that the two techniques are complementary. The only non-condensable volatile detected by mass spectrometry is methane and is detected in small quantities. The main degradation process is thought to be the formation of siloxane ring cycles which form without the loss of methane.
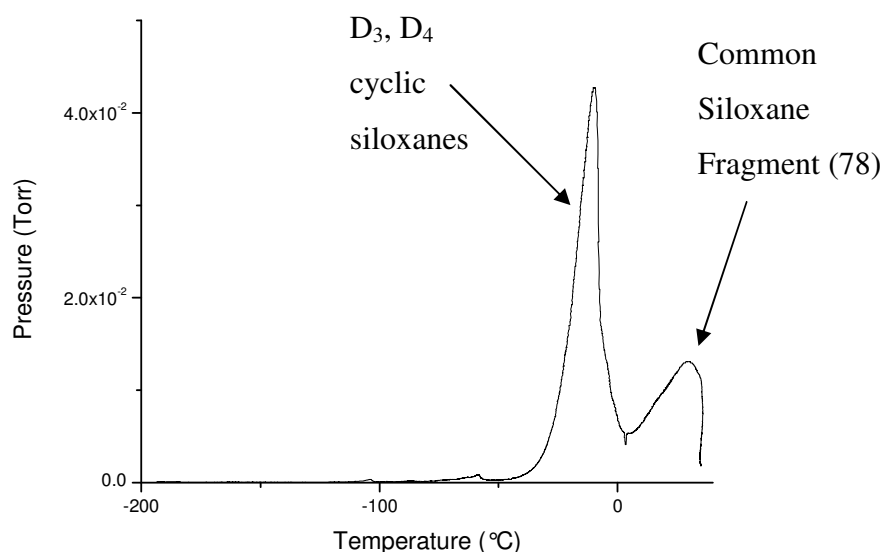
Figure 3.14: Sub-ambient distillation of volatiles from TEOS siloxane elastomer sample

In the sub-ambient distillation curve there are two major distillation peaks as detected by the online mass spectrometer. The first peak comprises of small siloxane ring structures and the second major peak contains larger siloxane rings, again consistent with what is believed about the degradation of this material. This is then further confirmed by the FTIR data and GC-MS data in tables 3.1-3.2 that confirm the presence of various silicone ring structures.

Limb No.	Wavenumber (cm^{-1})	Peak Identities
1	2925, 2850, 2350	aliphatic CH_3, CO_2
2	2925, 2850, 2300	aliphatic CH_3, CO_2
3	2975, 2925, 2850, 1275, 1100, 1025, 825	aliphatic CH_3, Si-CH_3, Si-O stretch, Si-$(CH_3)_2$
4	2975, 2925, 2850, 2375	aliphatic CH_3, CO_2

Table 3.1: FTIR (v/cm^{-1}[NaCl]):

Retention Time	Molar Mass	Identity
Cold Ring Fraction		
11.61	461.0	D_3 ring-D_3 linear-D_3 ring
12.51, 13.31	535.0	D_{10} siloxane ring
Limb 3		
4.94	207.2	D_3 siloxane ring
6.75	281.1	D_4 siloxane ring
Limb 4		
6.76	281.1	D_4 siloxane ring
8.10	355.3	D_5 siloxane ring
8.89	415.0	dimer of cross-linker
9.36	429.2	D_6 siloxane ring

Table 3.2: GC Mass Spectrometry (m/e, M+):

The degradation of the material is thought to occur with depolymerisation of the polymer backbone and then formation of the cyclic siloxane species. How big the cyclic structure that is volatilised during degradation depends on how far round the polymer backbone the tail wraps before recombination. A general diagram showing distance along polymer chain and formation of size of cyclic is shown in Figure 3.13. A degradation Scheme of how such a ring structure may form is shown in Scheme 3.1 and another plausible mechanism is shown in Scheme 3.2:
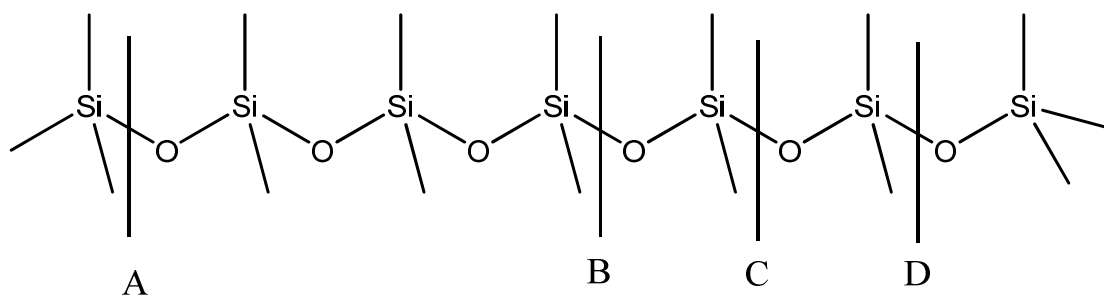
Figure 3.13: A PDMS polymer prior to thermal depolymerisation. If depolymerisation occurs at bond A, different size rings will form depending on which bond is opened upon attack of silanolate anion. At B a D_3 siloxane ring, at C a D_4 siloxane ring and at D a D_5 siloxane ring will be formed
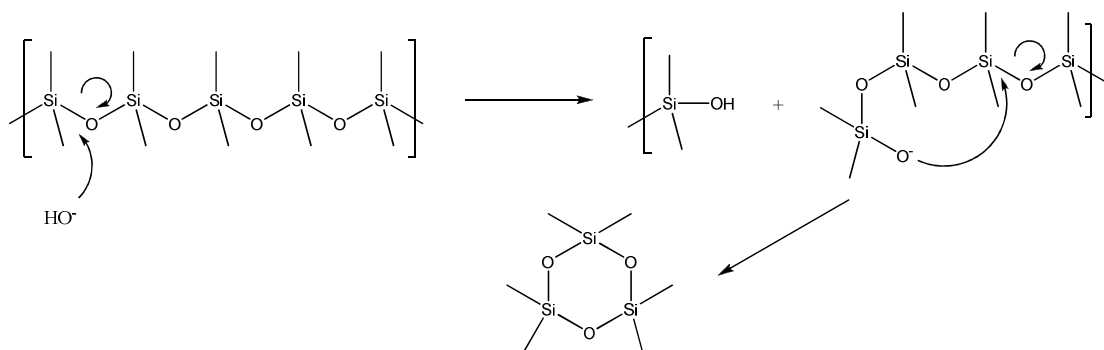
Scheme 3.1: Mechanism for the breakdown of a siloxane into a D_3 siloxane ring the presence of a base.[3]
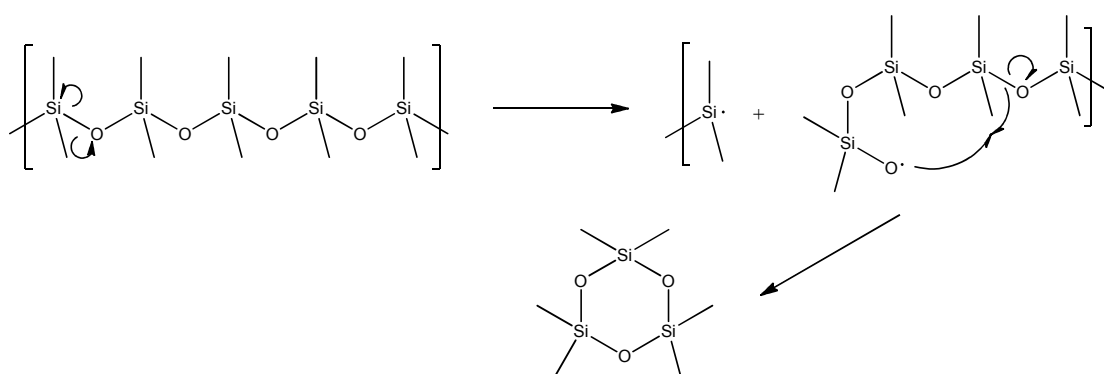
Scheme 3.2: Mechanism of how a D_3 siloxane ring might construct if free radicals form during thermal degradation

3.4.1 Thermal Volatilisation Analysis of TEOS Bound Network

The mechanism in Scheme 3.1 is the accepted process in which degradation of these networks containing tin catalyst residues with hydroxyl anions[3] degrade and is most likely the mechanism by which the PDMS degraded in the TVA experiment. Scheme 3.2 is less likely as the bond dissociation energy of a Si-O bond ($\Delta H^{\emptyset}$ = 466 kJ mol^{-1}) is greater than that of a C-C homolytic bond scission ($\Delta H^{\emptyset}$ = 348 kJ mol^{-1}) which normally occurs between 450 – 750 °C.[4] As degradation of the elastomer starts about 400 °C the dominant process is most likely reversion by depolymerisation via nucleophilic attack of hydroxy anions.

3.4.2 *m*-Carborane PDMS Elastomer Composites

The inclusion of *m*-carborane into the TEOS and TPOS PDMS elastomer systems was also completed. The loading of the carborane was 5% (w/w) and the carborane was found to be only partially soluble in the PDMS homopolymer. By use of sonication methods dissolution of the *m*-carborane was further improved. However, not all the carborane aggregates were able to be broken down in the TPOS sample. The material was tested for its thermal degradation properties, results of which are shown in Figures 3.14-3.16.
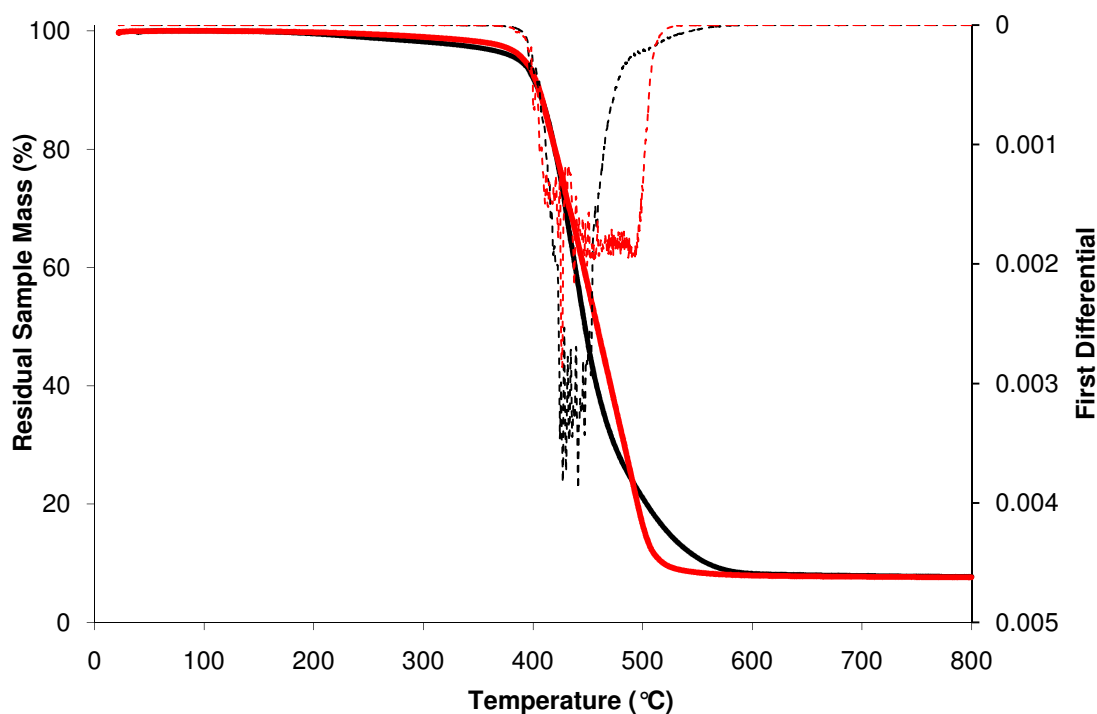
Figure 3.14: Non-oxidative TGA analysis of 5% *m*-carborane-containing, TEOS (black line) and TPOS (red line) cross-linked PDMS elastomers including derivatives (dotted lines)

Run	Onset Degradation Temperature / °C	Temperature Maximum Mass Loss / °C	Char Residue / % @ 800 °C
TEOS	384	426	8
TPOS	383	425	7
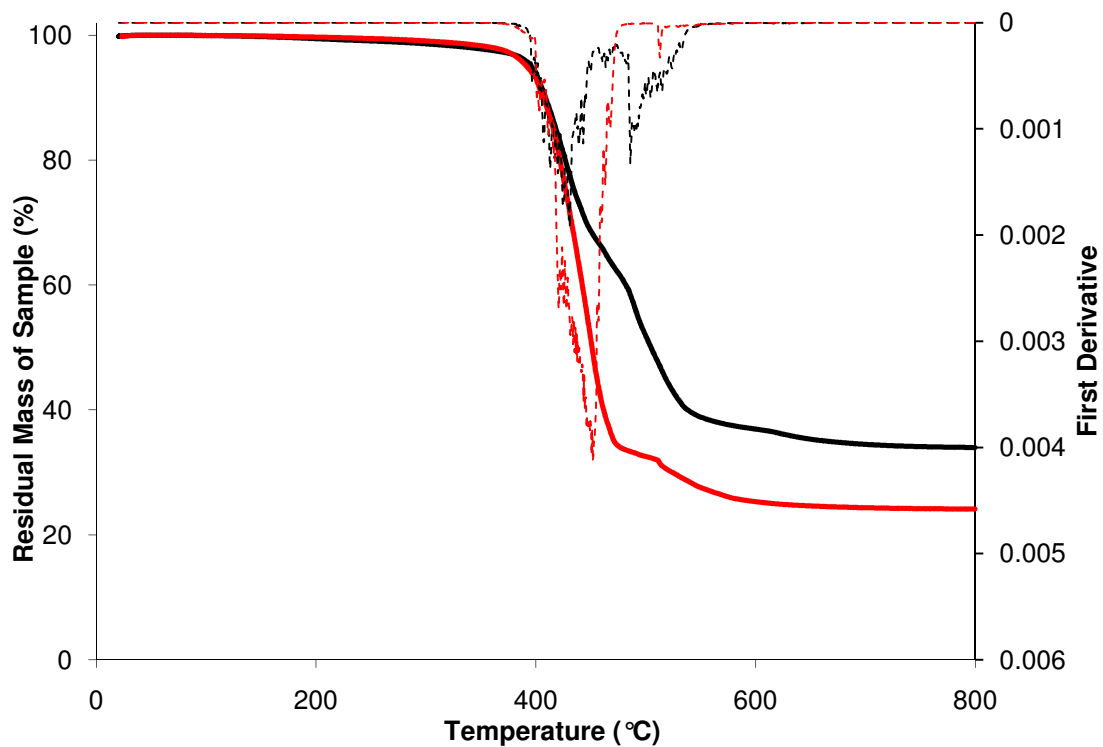
Figure 3.15: Oxidative TGA analysis of 5% *m*-carborane-containing, TEOS (black line) and TPOS (red line) cross-linked PDMS including derivatives (dotted lines)

Run	Onset Degradation Temperature / °C	Temperature Maximum Mass Loss / °C	Char Residue / % @ 800 °C
TEOS	387	430	34
TPOS	379	449	24
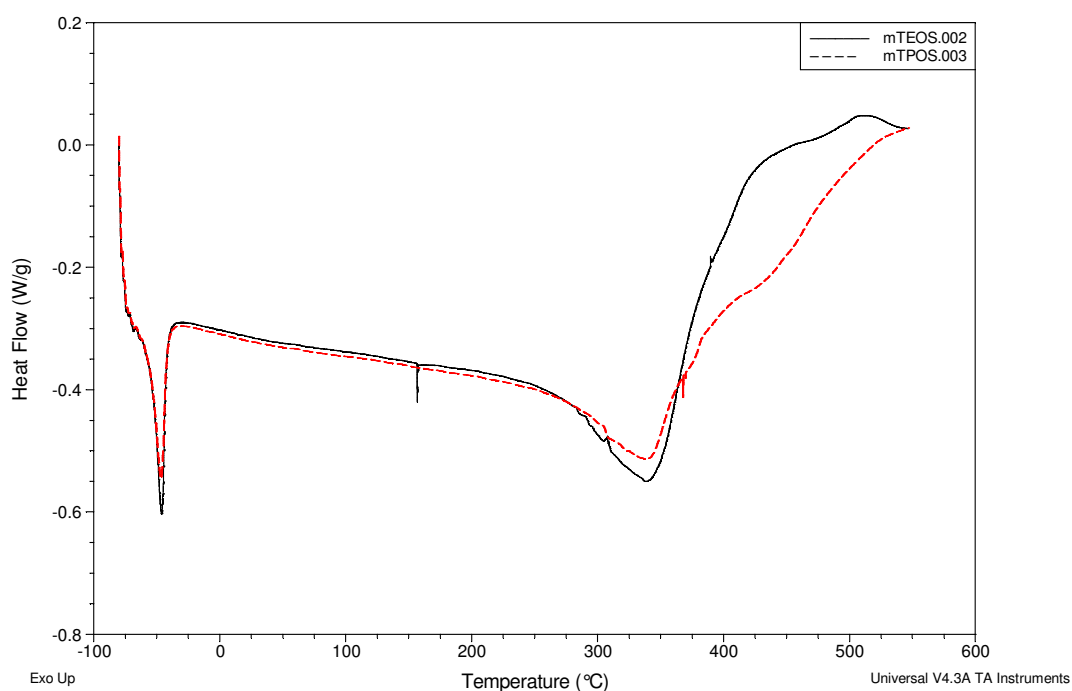
Figure 3.16: DSC analysis of 5% *m*-carborane-containing, TEOS (black line) and
TPOS (red line) cross-linked PDMS elastomers under nitrogen

DSC analysis TEOS bound siloxane network (non-oxidative):

Transition	Onset Temperature / °C	Peak Maximum / °C	Enthalpy of Transition / J g^{-1}
T_m	-54.8	-46.3	17.5
T_d	303	339	32.4

DSC analysis TPOS bound network (non-oxidative):

Transition	Onset Temperature / °C	Peak Maximum / °C	Enthalpy of Transition / J g^{-1}
T_m	-56.5	-47.1	15.4
T_d	301	338	17.6

From the thermal degradation behaviour it can be seen that the incorporation of *m*-carborane in the network has no significant effect on the onset degradation temperature of the TEOS and TPOS network. The temperatures at which maximum mass loss occurs increased, which could be due to the carboranes acting as a physical barrier to the removal of volatiles from the degrading material, or possibly physically impeding the reversion process from occurring as easily as in the unfilled PDMS samples. Also noted is the higher char residue in both sample run in air and argon, probably due to carbonaceous carborane residues left behind causing borate glass formation. The DSC run shows no significant change in the phase transition behaviour of the two materials.

3.4.3 1,7-bis(dimethylmethoxysilyl)-*m*-carborane-Carborane PDMS Elastomer Composites

Addition of silyl carborane to the PDMS pre-blend reveals the carborane is more soluble within the host polymer as the solid carborane forms a clear solution with the host PDMS polymer. The methoxy-capped carborane will be in competition within the cross-linker to form links with the hydroxy terminated PDMS. The TPOS cross-linker was unable to compete with the more reactive methoxy-capped carborane. This is confirmed by the lack of network formation where the material failed to vulcanise. Although TGA data are not available for this system the thermal properties of the TEOS bound material are shown in Figures 3.17-3.18:
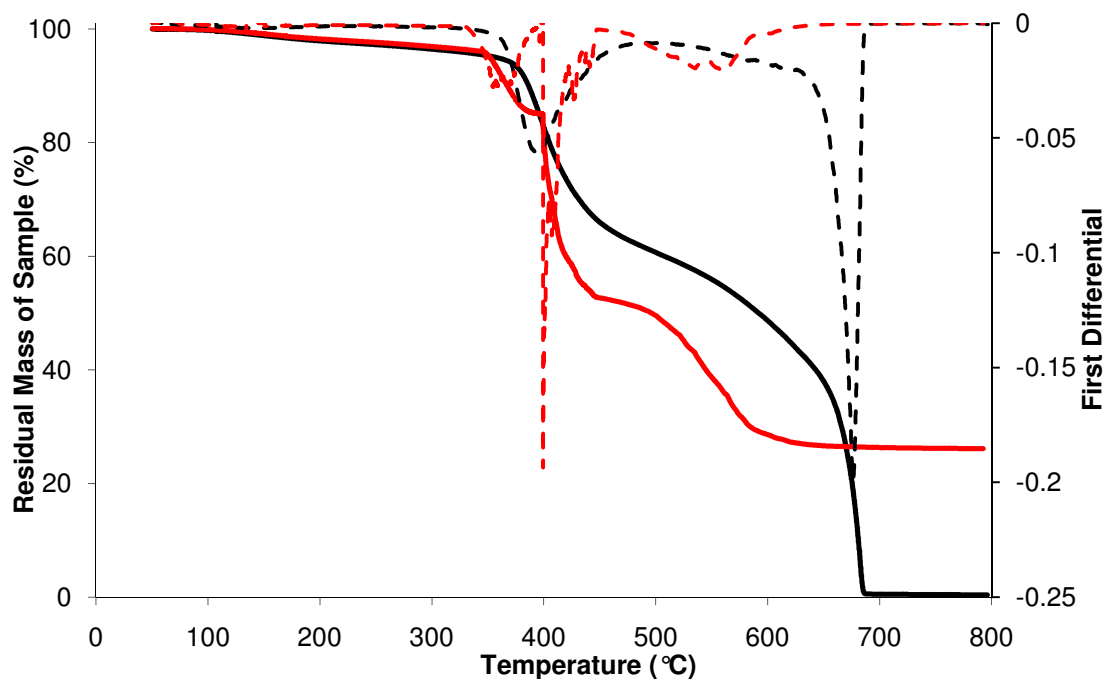
Figure 3.17: TGA of TEOS bound PDMS containing 5% (w/w) 1,7-bis(dimethylmethoxysilyl)-*m*-carborane. Non-oxidative (black line) degradation reveals a secondary degradation process. Oxidative (red line) degradation reveals rapid sample decay around 400 °C. Derivatives are also shown (dotted lines)

Run	Onset Degradation Temperature / °C	Temperature Maximum Mass Loss / °C	Char Residue / % @ 800 °C
Non-oxidative	375	676	0.5
Oxidative	383	399	26
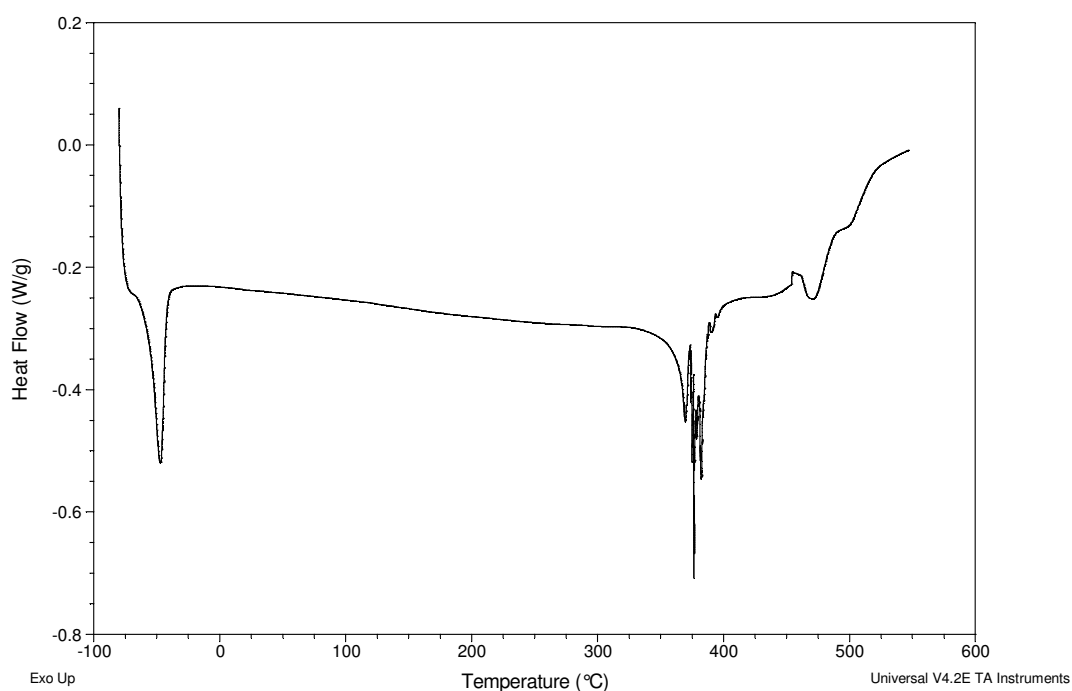
Figure 3.18: DSC of TEOS bound PMDS containing 5% 1,7-bis(dimethylmethoxysilyl)-*m*-carborane-carborane. Trace reveals that incorporation of silyl carborane complicates degradation of the material

DSC analysis (non-oxidative):

Transition	Onset Temperature / °C	Peak Maximum / °C	Enthalpy of Transition / J g^{-1}
T_m	-56.9	-47.2	17.5
T_d	329	376	18.9

The oxidative TGA behaviour of the 1,7-bis(dimethylmethoxysilyl)-*m*-carborane-carborane PDMS elastomer has not altered significantly *versus* the *m*-carborane containing PDMS elastomer material (ref. Figure 3.15). However, the non-oxidative behaviour of the 1,7-bis(dimethylmethoxysilyl)-*m*-carborane-carborane material shows a difference where char residue at 800 °C is less than 1% of original mass of material. The 1,7-bis(dimethylmethoxysilyl)-*m*-carborane-carborane can only react

3.4.3 1,7-bis(dimethylmethoxysilyl)-m-Carborane PDMS Elastomer Composites

with end group on the PDMS polymer in the vulcanisation reaction. Most char residues left behind after thermal decomposition in PDMS systems are SiO_2 arising from the cross-link sites. The carborane has decreased the amount of available end – OH groups on the polymer, reducing the amount of cross-links due to the competing reaction with the TEOS, which may lead to the increased volatilisation observed.

3.4.4 1,7-Diallyl-*m*-Carborane PDMS Elastomer Composites

Vinyl carborane is very compatible with PDMS pre-blend and forms a pure dispersion. This has been studied by measuring the viscosity with changing shear rate on a number of PDMS pre-blends containing vinyl carborane, the results of which are shown in Figure 3.19:
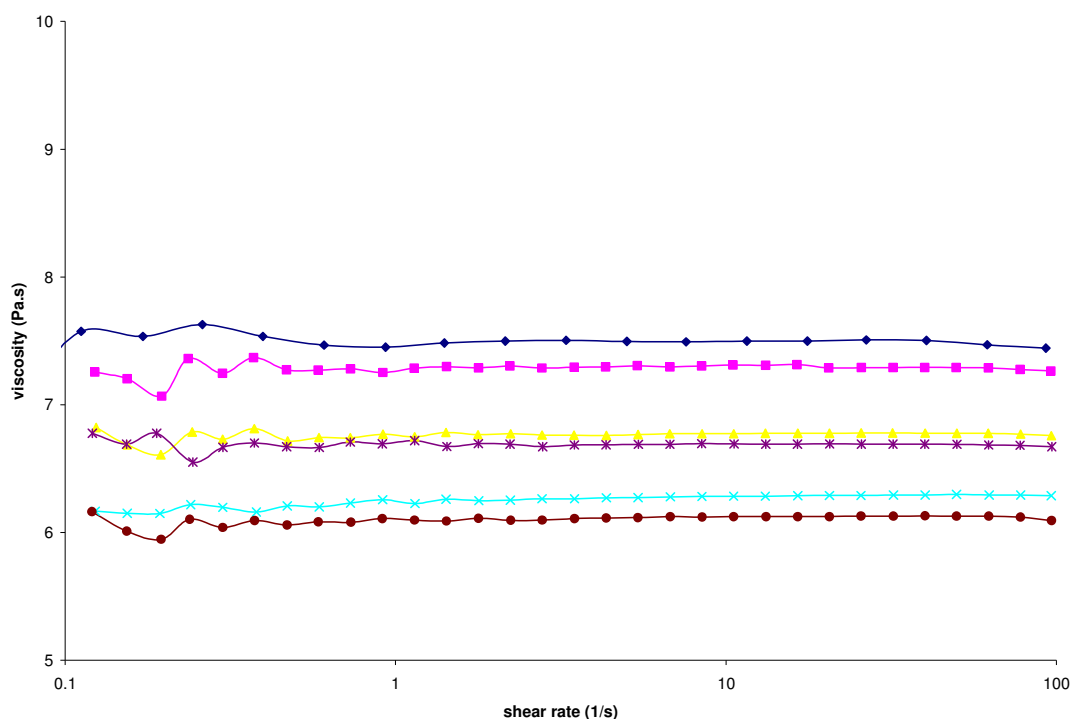
Figure 3.19: Plot of viscosity against shear rate for various PDMS blends containing vinyl carborane. 0% (blue line), 0.1% (pink line), 0.5% (yellow line), 1% (purple line), 2% (aqua line) and 4% (brown line) (w/w) 1,7-diallyl-*m*-carborane

As the vinyl carborane content is increased the viscosity is reduced but upon increasing shear rate the loadings show no change in viscosity. This shows that there is no aggregation of the carborane molecules with either themselves or the polymer.

The vinyl carborane blends were then successfully vulcanised. To confirm the presence of boron in these blends XRF analysis was conducted. Table 3.3 shows

115

3.4.4 1,7-Diallyl-m-Carborane PDMS Elastomer Composites

expected % boron values and % values found using both fixed and gonio channel. The tolerance for the analysis is +/- 0.5%.

	Fixed Channel		Gonio Channel	
Standard	B% (expected)	B% (found)	B% (expected)	B% (found)
Sample 1	15	14.2	15	14.3
Sample 2	6	6.9	6	6.9
Sample 3	3	2.5	3	2.3
Sample 4	1.5	1.6	1.5	1.7

Table 3.3: XRF analysis of PDMS elastomers containing 1,7-diallyl-*m*-carborane

The XRF result shows that the 1,7-diallyl-*m*-carborane filler material is present in the siloxane elastomer network. At the 15% (w/w) loading the % boron found is less than predicted which could indicate the filler material is leaching from the material at high loadings where the result is close to the tolerance allowed for the experiment.

TGA of vinyl carborane systems against the unfilled PDMS elastomers shows problems with dispersion of these materials. TGA of 5% (w/w) 1,7-diallyl-*m*-carborane filled PDMS and 30% (w/w) 1,7-diallyl-*m*-carborane filled PDMS are shown in Figures 3.20-3.22. DSC analysis is shown in graphs Figures 3.23-25. A comparison of the unfilled PDMS and 30% (w/w) *m*-vinyl carborane using non-oxidative TGA is shown in Figure 3.26:
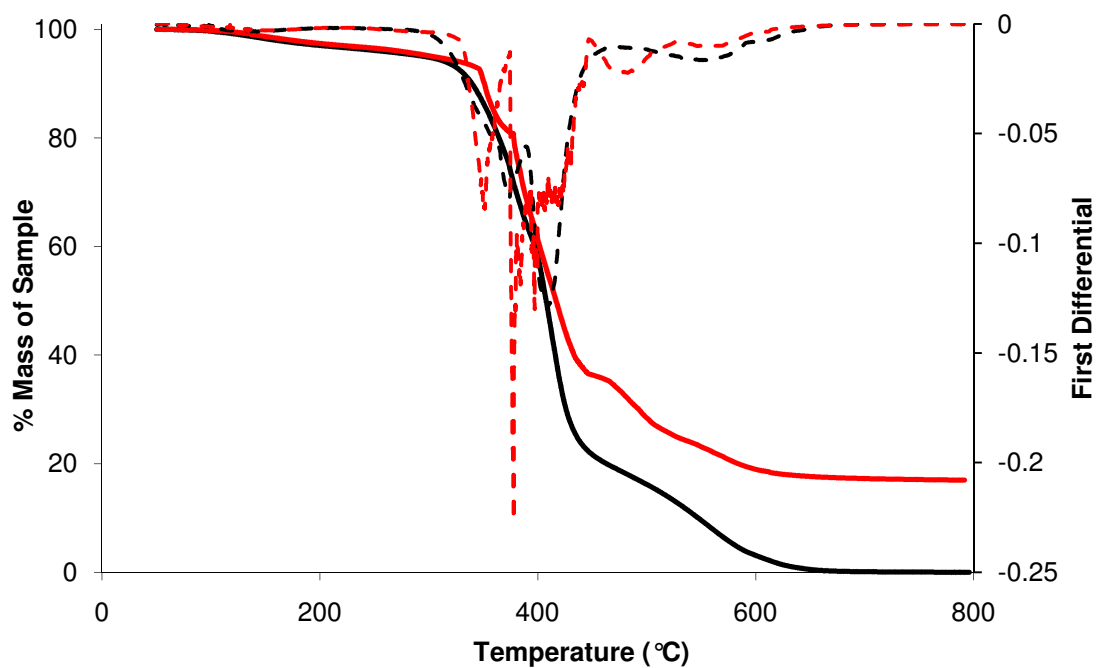
Figure 3.20: TGA of 5% (w/w) 1,7-diallyl-*m*-carborane in TEOS bound PDMS elastomer. Both performed under non-oxidative (black line) and oxidative (red line) conditions

Run	Onset Degradation Temperature / °C	Temperature Maximum Mass Loss / °C	Char Residue / % @ 800 °C
Non-oxidative	324	408	0.05
Oxidative	337	377	17
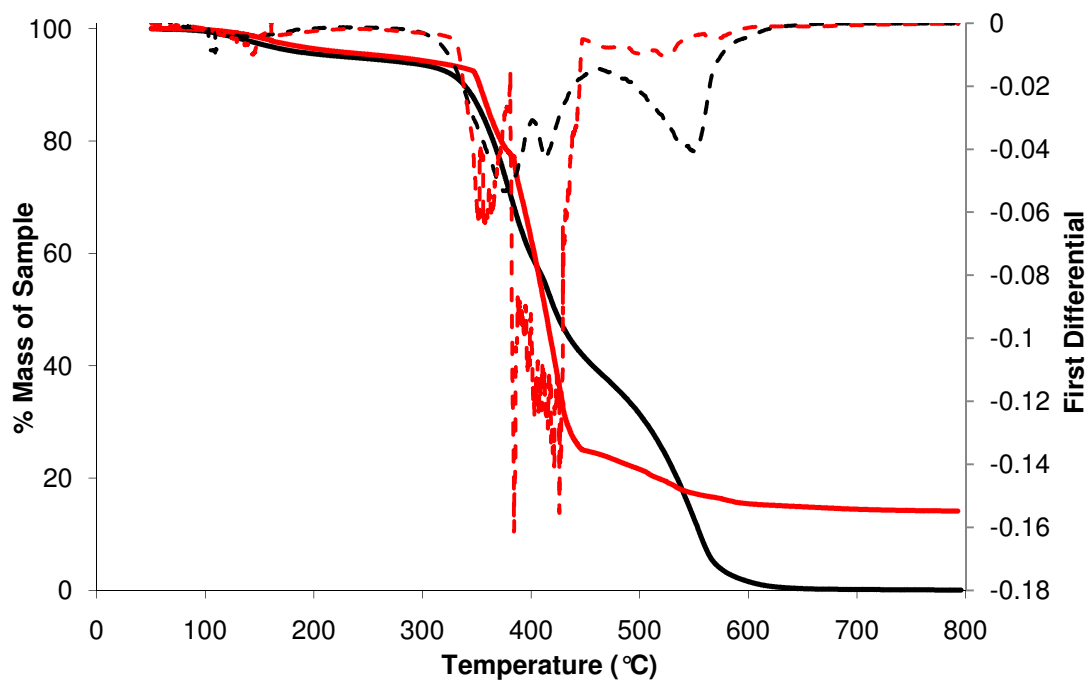
Figure 3.21: TGA of 5% (w/w) 1,7-diallyl-*m*-carborane in TPOS bound PDMS elastomer. Both performed under non-oxidative (black line) and oxidative (red line) conditions

Run	Onset Degradation Temperature / °C	Temperature Maximum Mass Loss / °C	Char Residue / % @ 800 °C
Non-oxidative	327	376	0.6
Oxidative	368	384	14
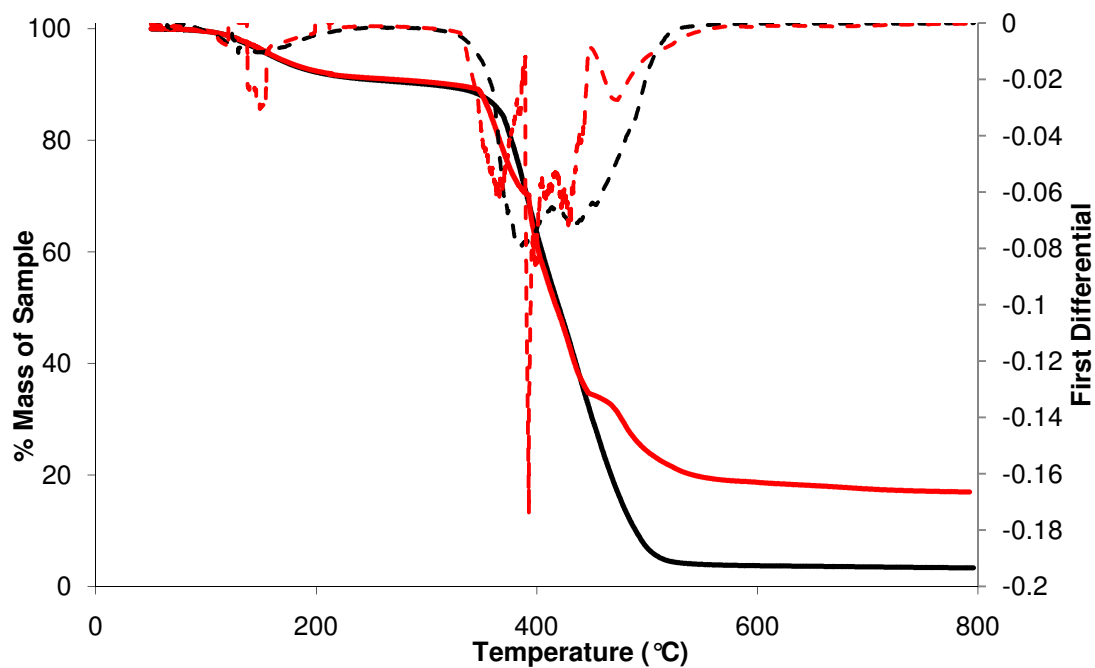
Figure 3.22: TGA of 30% (w/w) 1,7-diallyl-*m*-carborane in TEOS bound PDMS elastomer. Both performed under non-oxidative (black line) and oxidative (red line) conditions

Run	Onset Degradation Temperature / °C	Temperature Maximum Mass Loss / °C	Char Residue / % @ 800 °C
Non-oxidative	366	385	1
Oxidative	373	392	17
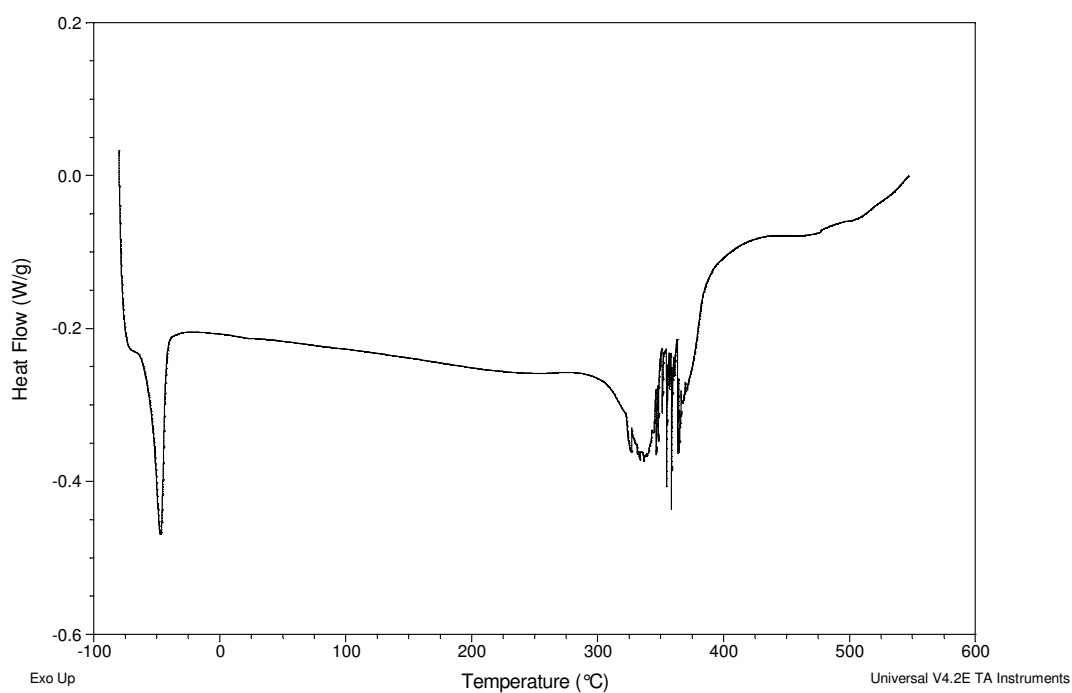
Figure 3.23: DSC of 5% (w/w) 1,7-diallyl-*m*-carborane in TEOS bound PDMS

elastomer

DSC analysis (non-oxidative):

Transition	Onset Temperature / °C	Peak Maximum / °C	Enthalpy of Transition / J g^{-1}
T_m	-56.1	-47.0	14.0
T_d	306	359	15.1

3.4.4 1,7-Diallyl-m-Carborane PDMS Elastomer Composites
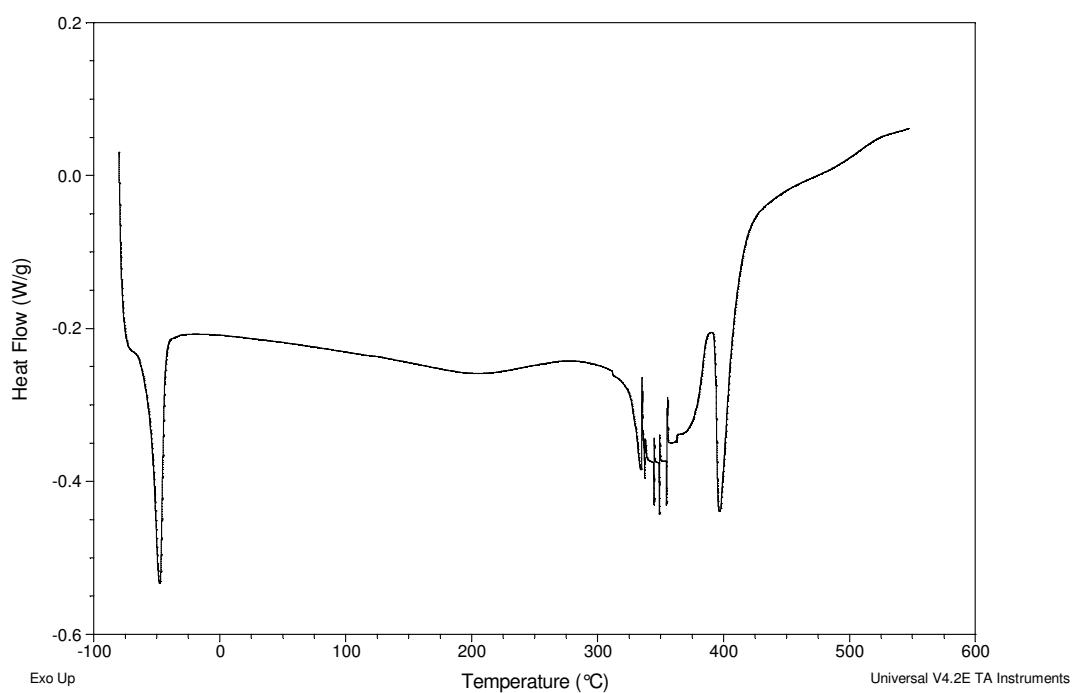
Figure 3.24: DSC of 5% (w/w) 1,7-diallyl-*m*-carborane in TPOS bound PDMS elastomer

DSC analysis (non-oxidative):

Transition	Onset Temperature / °C	Peak Maximum / °C	Enthalpy of Transition / J g^{-1}
T_m	-56.3	-47.9	17.2
T_d	335	349	30.5
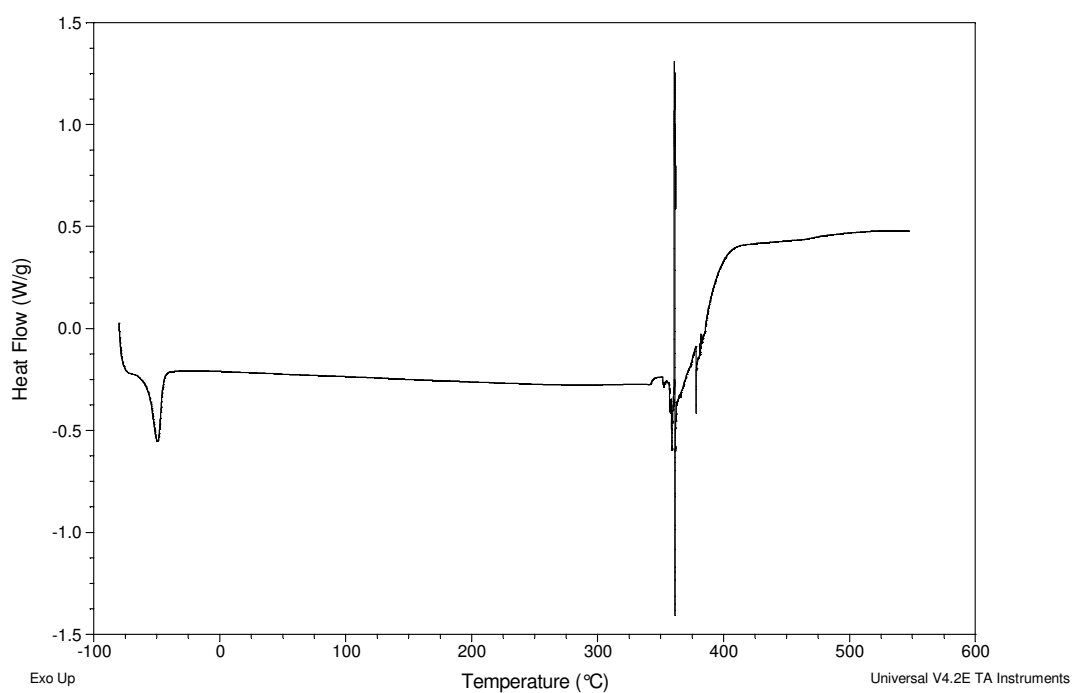
Figure 3.25: DSC of 30% (w/w) 1,7-diallyl-*m*-carborane in TEOS bound PDMS

elastomer

DSC analysis (non-oxidative):

Transition	Onset Temperature / °C	Peak Maximum / °C	Enthalpy of Transition / J g^{-1}
T$_m$	-57.4	-49.3	18.00
T$_d$	359	359	12.8

3.4.4 1,7-Diallyl-m-Carborane PDMS Elastomer Composites
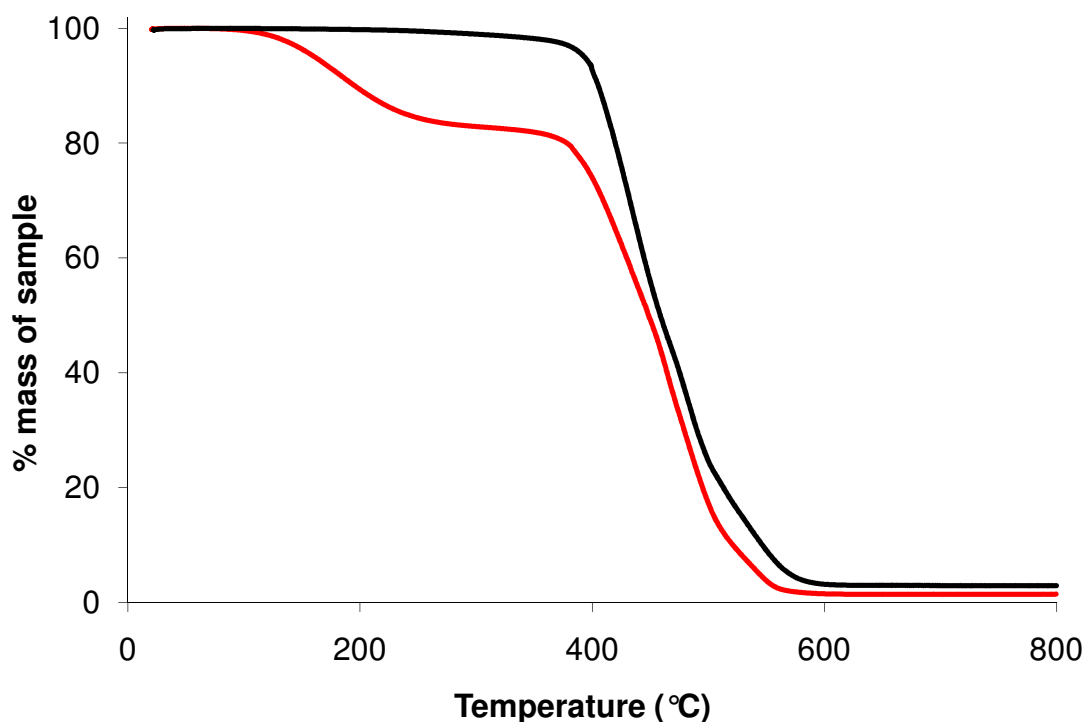
Figure 3.26: Non-oxidative TGA comparing unfilled PDMS elastomer (black line) and 30% (w/w) 1,7-diallyl-*m*-carborane in PDMS elastomer (red line)

The TGA data in Figures 3.20 to 3.22 show that the inclusion of vinyl carborane is not significantly improving the thermal degradation properties of the siloxane elastomer. The char residues are slightly lower in the non-oxidative TGA compared to the model PDMS system shown in Figure 3.8. DSC data shows no change in morphology but again more complex degradation behaviour is observed. The comparison of the model PDMS and 30% (w/w) 1,7-diallyl-*m*-carborane material in Figure 3.26 shows the filler is subliming from the material at reduced temperatures and is not significantly increasing the thermal degradation temperature of the network. Approximately two thirds of the filler material has sublimed out of the elastomer before degradation occurs. Carborane dispersions, although simple to prepare, do not provide the significant increases in thermal stability required of a composite material.

3.5 Chapter Conclusion

A PDMS material has been synthesised and characterised that will give a standard by which to thermally improve the properties of PDMS elastomers using carboranes. Using urea prills it is also possible to create an open pore PDMS elastomer network. The thermal degradation cycle of the material is also well defined by use of thermal volatilisation analysis. The main degradation process is "reversion" in which the polymer chain backbites and forms cyclic species. The challenge will be to prevent this process from occurring and thus obtain greater thermal stability.

The incorporation of *m*-carborane materials to form composites has little effect on the thermal stability of the elastomer network. However, by changing the functionalisation on the carborane unit *m*-carborane fillers with improved solubility in PDMS are obtained. 1,7-bis(dimethylmethoxysilyl)-*m*-carborane-carborane does lead to a small increase in thermal stability as the carborane is involved in the reaction with the polymer and is incorporated into the network. 1,7-diallyl-*m*-carborane has the advantage of improved solubility at high loadings, but 1,7-diallyl-*m*-carborane fails to thermally stabilise the network as a composite material. The satisfactory compatibility of this carborane moiety with the polymer will be of use when designing a way of incorporating this carborane into a network in later Chapters. The next Chapter now turns to focus on the classical method of grafting carboranes to PDMS by the use of Lewis acids in order to understand their thermal stabilisation behaviour.

3.6 References

1. Lewicki, J.P. *"Ageing studies of novel polydimethylsiloxane nanocomposites"* PhD Thesis, University of Strathclyde 2008

2. Grassie, N., MacFarlane, I. G. *"The thermal degradation of polysiloxanes – 1"* European Polymer Journal 1978 **14**: 875

3. Van der Weij, F. W., *"The Action Of Tin-Compounds In Condensation-Type Rtv Silicone Rubbers"* Makromolekulare Chemie-Macromolecular Chemistry And Physics 1980 **181** (12): 2541

4. Atkins, P., De Paula, J *"Physical Chemistry – 8th Edition"* Oxford Press 2006: 1012

Chapter 4

Carborane Containing Polydimethylsiloxane Polymers and Elastomers Formed *Via* Lewis Acid Catalysis

4.0 Chapter Introduction

In the last Chapter it was shown that the production of composite siloxane elastomers containing carborane with high loadings of carborane filler was possible. However, there was no significant gain in the thermal stability of the material. Even worse in the case of the 1,7-diallyl-*m*-carborane, the filler can sublime out of the material at temperatures lower than the degradation temperature of a standard PDMS elastomer. The question is then asked as to why we are incorporating carboranes to thermally stabilise PDMS?

The answer is because of previous examples in the literature which show copolymers of carborane siloxane repeating units have produced materials with high thermal oxidative stability. Classically these copolymers were synthesised using $FeCl_3$ Lewis acid catalysts which later became a commercialised process.[1] Polymerizing under oxidative conditions leads to the formation of elastomers but the cross-linking is a side reaction and is not necessarily desirable when synthesising these materials. In this Chapter this classic reaction is re-investigated by studying D_2-copolymers containing *m*-carborane Their synthesis and thermal stability will be studied first and then by replacing the expensive methoxy capped carborane with a PDMS alternative a series of different Lewis acid catalysts will be used to determine whether it is possible to create similar polymeric materials. Finally the kinetics of the classical Lewis acid reaction will be studied to further investigate the role of $FeCl_3$, to measure the activation energy and the entropy of the rate determining step.

4.1 Synthesis of a Carborane-Siloxane Copolymer Using FeCl₃

To a 250 ml round bottom flask was added 1,7 bis(dimethylmethoxysilyl)*m*-carborane (6.0 g, 18.7 mmol). In a fume hood (dichlorodimethyl)silane (2.41 g, 18.7 mmol) was weighed out and added to the reaction vessel. To this FeCl₃, catalyst (0.061 g, 0.37 mmol) was subsequently added. The reaction vessel was placed in an oil bath and refluxed gently at 140 °C while stirring. During the course of the reaction chloromethane was evolved and the reaction was carried out for 3 hours until no more effervescence was observed. Once the reaction product had cooled sufficiently and solidified the polymer was extracted using an acetone/water mix overnight to remove as much catalyst from the polymer as possible. After extracting the product a light brown opaque rubber was obtained.

Experimental Data:

Mass of polymer recovered = 5.750g
Yield = 68.4%

FTIR (ν/cm⁻¹[ATR diamond]): 3400 (b) (-OH stretch); 2970 (aliphatic CH_3); 2600 (B-H); 1600 (H-O-H); 1415(O-H bend); 1275 (Si-CH_3); 1100 (Si-O stretch); 880 (Si-(CH_3)₂); 800 (C-Cl);

4.1.1 Synthesis of a Carborane-Siloxane Copolymer Using BF$_3$

To a 250 ml round bottom flask was added 1,7 bis(dimethylmethoxysilyl)*m*-carborane (6.0 g, 18.7 mmol). In a fume hood (dichlorodimethyl)silane (2.41 g, 18.7 mmol) was weighed out and added to the reaction vessel. To this BF$_3$.ethylamine catalyst (0.042 g, 0.37 mmol) was subsequently added. The reaction vessel was placed in an oil bath and refluxed gently up to 140 °C while stirring. The reaction was carried out under dry nitrogen to avoid an unwanted side reaction shown below in Scheme 4.1:

$$4BF_3 + 3H_2O \longrightarrow 3HBF_4 + B(OH)_3$$
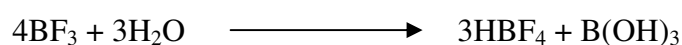
Scheme 4.1: Decomposition of boron trifluoride in water with release of hydrogen fluoride gas and formation of boric acid

To ensure no release of HF into the fume hood (1.0 M) NaOH solution was used to scrub the outgoing nitrogen gas and fluorinated grease was used to seal glass joints and glass flanges.

The reaction was completed in three hours and left to cool. The solution was then collected and extracted with 20 ml (1.0 M) NaOH solution to remove the catalyst and quench any HF that may have formed. The reaction was repeated using BF$_3$.THF complex (0.052 g, 0.37 mmol) as the catalyst.

Experimental Data:

BF$_3$.ethylamine catalyst:

^{1}H NMR data (400 MHz, CDCl$_3$; δ): 0.27 (t, 15H, CH$_3$); 3.49 (t, 1H, OCH$_3$)

GPC data (THF): M_n = 6,031; M_w = 6,645; polydispersity (M_n/M_w) = 1.102

4.1.1 Synthesis of a Carborane-Siloxane Copolymer Using BF₃

MALDI-TOF m/z (dithranol): 666.2, 900.7

<u>BF$_3$.THF catalyst:</u>

^{1}H NMR data (400 MHz, CDCl$_3$; δ): 0.25 (t, 7H, C<u>H</u>$_3$); 3.49 (t, 1H, OC<u>H</u>$_3$)

4.2 Synthesis of a Model PDMS Network Using a FeCl$_3$ Catalyst

To a 250 ml round bottom flask was added 6.0 g of methoxy end capped poly(dimethysiloxane) with an average molar mass (M$_n$) ~1174 g mol^{-1}. In a fume hood (dichlorodimethyl)silane (2.00 g, 15.3 mmol) was weighed out and added to the reaction vessel. To this, FeCl$_3$ catalyst (0.06 g, 0.372 mmol) was subsequently added. The reaction vessel was placed in an oil bath and refluxed gently up to 140 °C while stirring. During the course of the reaction chloromethane was evolved and the reaction was carried out for 3 hours until no more effervescence was observed. Once the reaction had cooled sufficiently and solidified it was extracted using an acetone/water mix overnight to remove as much catalyst from the polymer as possible. After extracting the product a black/brown rubber was obtained.

Experimental Data:

FTIR (ν/cm^{-1}[ATR diamond]): 3400 (b) (-OH stretch); 2970 (aliphatic CH$_3$); 1600 (H-O-H); 1415(O-H bend); 1275 (Si-CH$_3$); 1100 (Si-O stretch); 880 (Si-(CH$_3$)$_2$); 800 (C-Cl);

GPC data (CHCl$_3$): M$_w$ = 129,000; M$_n$ = 55,200; polydispersity (M$_n$/M$_w$) = 2.3

4.2.1 Synthesis of a Model PDMS Using a BF$_3$ Catalyst

To a 250 ml round bottom flask 6.0 g of methoxy end capped poly(dimethysiloxane) with an average molar mass (M$_n$) ~1174 g mol^{-1} was added. In a fume hood (dichlorodimethyl)silane (2.00g, 15.3 mmol) was weighed out and added to the reaction vessel. To this BF$_3$.ethylamine complex catalyst (0.06 g, 0.535 mmol) was subsequently added. The reaction vessel was placed in an oil bath and refluxed gently up to 140 °C while stirring. The reaction was carried out under dry nitrogen to ensure no unwanted side reactions occurred. During the course of the reaction chloromethane was evolved and the reaction was carried out for 3 hours until no more effervescence was observed.

Once the reaction was completed the solution was allowed to cool to room temperature and the catalyst quenched by extracting with 20 ml (1.0M) NaOH solution. The resulting solution was separated in a separating funnel, washed further and the organic fraction collected. The resulting solution was a viscous opaque liquid. The reaction was repeated using BF$_3$.THF complex (0.06 g, 0.432mmol) as the catalyst.

Experimental Data:

BF$_3$.ethylamine catalyst:

^{1}H NMR data (400 MHz, CDCl$_3$; δ): 0.09 (t (b), 202H, CH$_3$); 3.49 (s, 1H, OCH$_3$)

Integration of 202:1 gives ~MW 15,809

The calculation of molar mass by nmr is discussed in the appendix

BF$_3$.THF catalyst:

^{1}H NMR data (400 MHz, CDCl$_3$; δ): 0.09 (t (b), 10H, CH$_3$); 0.21 (d, 1H, CH$_2$)

4.2.2 Synthesis of PDMS Using a AlCl$_3$ catalyst

To a 250 ml round bottom flask 6.0 g of methoxy end capped poly(dimethysiloxane) with an average molar mass (M$_n$) ~1174 g mol^{-1} was added. In a fume hood (2.00 g, 15.3 mmol) (dichlorodimethyl)silane was weighed out and added to the reaction vessel. To this (0.06g, 0.453 mmol) AlCl$_3$ catalyst was subsequently added. The reaction vessel was placed in an oil bath and refluxed at to 140°C while stirring. During the course of the reaction chloromethane was evolved and the reaction was carried out for 3 hours until no more effervescence was observed. Once the reaction had cooled sufficiently the product was obtained as a viscous opaque liquid.

Experimental Data:

^{1}H NMR data (400 MHz, CDCl$_3$; δ): 0.09 (t, 660H, CH$_3$); 3.50 (t, 1H, OCH$_3$)

Integration of 660:1 gives polymer 44 chains in length ~MW 51,656

GPC data (CHCl$_3$): M$_w$ = 61,400; M$_n$ = 39,600; polydispersity (M$_n$/M$_w$) = 1.5

4.2.3 Synthesis of PDMS Using a ZnCl$_2$ Catalyst

To a 250 ml round bottom flask 6.0 g of methoxy end capped poly(dimethysiloxane) with an average molar mass (M_n) ~1174 g mol^{-1} was added. In a fume hood (dichlorodimethyl)silane (0.65 g, 5.11 mmol) was weighed out and added to the reaction vessel. To this, ZnCl$_2$ catalyst (0.06 g, 0.443 mmol) was subsequently added. The reaction vessel was placed in an oil bath and refluxed gently up to 140 °C while stirring. The reaction was carried out under dry nitrogen to stop deactivation of the catalyst by atmospheric moisture. The reaction was left for 3 hours and in this time it was observed that the solution started to increase in viscosity. The solution was then allowed to cool and the white viscous product was collected for analysis.

Experimental Data:

^{1}H NMR data (400 MHz, CDCl$_3$; δ): 0.08 (t, 654H, CH$_3$); 3.49 (s, 1H, OCH$_3$)

Integration of 654:1 gives ~MW 51,186 g mol^{-1}

GPC data (CHCl$_3$): M_w = 308,000; M_n = 136,000; polydispersity (M_n/M_w) = 2.3

4.2.4 Synthesis of PDMS Network Using a GaCl$_3$ Catalyst

To a 250 ml round bottom flask was added 6.0 g of methoxy end capped poly(dimethysiloxane) with an average molar mass (M$_n$) ~1174 g mol^{-1}. In a fume hood (dichlorodimethyl)silane (0.65 g, 5.11 mmol) was weighed out and added to the reaction vessel. To this, GaCl$_3$ catalyst (0.06 g, 0.343 mmol) was subsequently added. The reaction vessel was placed in an oil bath and refluxed gently up to 140 °C while stirring. During the course of the reaction chloromethane was evolved and the reaction was carried out for 3 hours until no more effervescence was observed. Also over time the colourless solution turned yellow and then to red. As it turned red the solution thickened and upon cooling a solid soft rubber material was obtained for analysis.

Experimental Data:

FTIR (ν/cm^{-1}[ATR diamond]): 3400 (b) (-OH stretch); 2970 (aliphatic CH$_3$); 1600 (H-O-H); 1415(O-H bend); 1275 (Si-CH$_3$); 1100 (Si-O stretch); 880 (Si-(CH$_3$)$_2$); 800 (C-Cl);

4.2.5 Attempted Synthesis of PDMS Network Using Other Lewis Acid Catalysts

To a 250 ml round bottom flask was added 6.0 g of methoxy end capped poly(dimethysiloxane) with an average molar mass (M_n) ~1174 g mol^{-1}. In a fume hood (dichlorodimethyl)silane (2.00 g, 15.3 mmol) was weighed out and added to the reaction vessel. To this, a catalyst listed in the table below was subsequently added, the weighing data of each is in Table 4.1. The reaction vessel was placed in an oil bath and heated slowly up to 140 °C while stirring. The reactions were completed within 3 hours; all solutions were then left to cool before the products collected for analysis.

Experimental Data:

Catalyst	Mass (g)	Moles catalyst (mmol)	SiCH$_3$ integral	OCH$_3$ integral	Molar Mass (M_n) of Polymer (g mol^{-1})
SnCl$_2$	0.06	0.313	3	?*	?
CuCl$_2$.2H$_2$O	0.06	0.354	41	1	3,029
PbCl$_2$	0.06	0.217	21	1	1,644
LaCl$_3$.7H$_2$O	0.06	0.180	23	1	1,800
EuCl$_3$.6H$_2$O	0.06	0.182	36	1	2,818
DyCl$_3$	0.06	0.247	29	1	2,270
SnCl$_4$	0.06	0.256	91	1	7,110
HgCl$_2$	0.06	0.245	35	1	2,734
TiCl$_3$	0.06	0.432	92	1	7,188

Table 4.1: ^{1}H NMR data (400 MHz, CDCl$_3$; δ) *peak too small to see hydrogen ratio

4.3 Kinetic Study of FeCl₃ Reaction via NMR Spectroscopy

To a 250 ml round bottom flask 8.0 g of methoxy end capped poly(dimethylsiloxane) was added. In a fume hood (dichlorodimethyl)silane (0.890 g, 6.81 mmol) was weighed and added to the reaction vessel. The reaction vessel was heated up to 80 °C in a heating block whilst stirring. Once equilibrated, FeCl₃ (0.0900 g, 0.547 mmol) catalyst was added such that the total amount was 1% of the total mass of the reactants. At this point an aliquot of the supernatant solution (0.1 ml) was removed, mixed into deuterated chloroform (2 ml) and filtered into a NMR tube using a pipette filter. During the course of the reaction similar aliquots were extracted at regular intervals (5, 10, 20, 30, 40, 50, 60, 70, 80, 90, 120, 150, 180, 210 minutes). Once the reaction had cooled sufficiently the remaining material was filtered and collected. The fifteen NMR samples were then run on a Bruker 500 NMR spectrometer. 1H data were collected at 400 MHz, examining the loss of the -OC$\underline{H}_3$ peak against reaction time. An example of the data collected at time zero is shown in Figure 4.1 with interpretation shown in the Table 4.2 below.
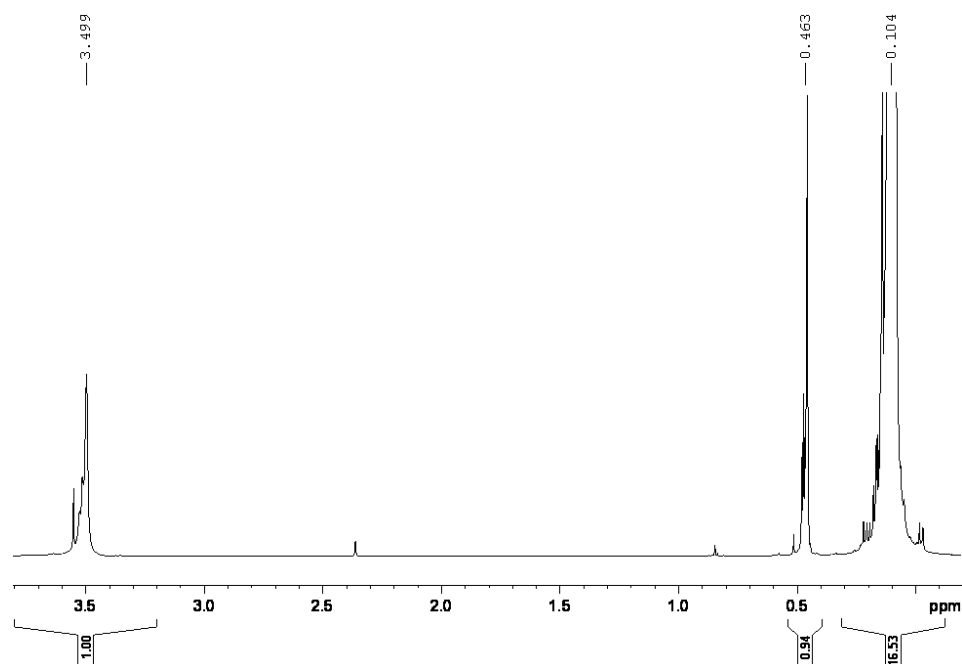
Figure 4.1: ^{1}H NMR plot of reaction solution at time t = 0

4.3 Kinetic Study of FeCl₃ Reaction via NMR Spectroscopy

^{1}H NMR Chemical Shift (δ)	Integral Value	Peak identification
3.49 (s)	1.00	-OC$\underline{H}_3$ terminal group
0.46 (s)	0.94	SiCl$_2$(C$\underline{H}_3$)$_2$ reactant
0.11 (multi)	16.53	SiO-(C$\underline{H}_3$)$_2$ backbone

Table 4.2: Assignment of ^{1}H NMR for spectrum shown in Figure 4.1

The change in integral against time was plotted on a graph. The experiment was repeated and data collated showing error between experiments. The experiments were repeated at temperatures varying from 40 °C to 120 °C.

The processing of data was carried out using a batch method as to avoid biasing the integrals obtained in the experiment. The resulting integrals are treated as a quantitative measure of the concentration of the methoxy group in the NMR solution. The change in concentration values are averaged between two experiments, then converted to a natural logarithm and plotted against time. In plotting the graph this way the gradient is equal to the rate constant for the experimental temperature used in the polymerization step.

In order to determine the kinetics of the reaction NMR spectroscopy was chosen as the method of analysis. The signal at 3.5 ppm lies distinctly away from other peaks and can be easily monitored. NMR analysis of the resulting polymer can be achieved by dissolving an aliquot of the reacting polymer into CDCl$_3$ and filtering. Monitoring of the reaction by NMR could be achieved by choosing any of the various active nuclei (^{13}C, ^{29}Si and ^{17}O). However, for reduced analysis time ^{1}H NMR is selected. The reaction progress is followed by the loss in the -OC$\underline{H}_3$ peak signal with respect to time. Although not a direct measure of concentration, the resulting integrals give rise to the following relationship:

$$R_{OMe} = \frac{I_t}{I_0}$$

where R_{OMe} is the relative concentration of methoxy group, I_t is the integral at time t and I_o is the integral at time zero. The results are discussed in section 4.5.1.

4.3.1 Preparation of FeCl$_2$ solutions for electrochemical kinetic study

To be able to determine the reversibility of the initial reaction step electrochemistry was chosen. Although the initial reaction step does not involve a redox reaction, in generating FeCl$_3$ from FeCl$_2$ the presence of (dichlorodimethyl)silane the important reverse oxidation step for Fe^{3+} to Fe^{2+} should remain symmetrical at similar scan rates even if any subsequent reaction intermediate is generated.

Five solutions were made up in separate 50 ml standard flasks for the electrochemical study. A 20.0 mM aqueous solution of FeCl$_2$ (0.127 g) in 0.100 M KCl (0.745 g); a 0.100 M solution of tetrabutylammonium chloride (TBACl) (0.829 g) in THF; a 0.100 M solution of TBACl (0.829 g) with 0.100 M (dichlorodimethyl)silane (0.605 ml) in THF; a 20.0 mM solution of FeCl$_2$ (0.127 g) with 0.100 M of TBACl (0.829 g) in THF and a 20.0 mM solution of FeCl$_2$ (0.127 g) with 0.100 M of TBACl (0.829 g) and 0.100 M (dichlorodimethyl)silane (0.605 ml) in THF. The cyclic voltammetry was carried out using an Autolab eco-chemie PSTAT10 and GPES3 software package. The working electrode used was a platinum disc, the counter electrode was a platinum mesh and the reference electrode was an Ag/AgCl electrode. Each solution was degassed in the electrochemical cell before the experiment was begun and the solutions were scanned at various rates from 10 mVs^{-1} through to 1.6 Vs^{-1} between the voltage limits of -0.5 V to +1.75 V. The data was then plotted as voltage (ref. Ag/AgCl) against current. The results obtained in the electrochemical experiments using cyclic voltammetry were analysed using the Randles-Sevcik equation[2] at 298K described as:

$$i_p = -(2.69 \times 10^5) \times n^{3/2} \times C_o \times D^{0.5} \times v^{0.5}$$

where i_p is the peak current density (A cm^{-2}), n is the number of electrons, C_o is the concentration of electro-active species (mol cm^{-3}), D is the diffusion coefficient (cm^2 s^{-1}) and v is the scan rate (V s^{-1}).

The diffusion coefficients were measured for a range of samples to determine the rate at which the species of interest were moving on to the surface of the electrode. The shape of the cyclic voltammogram helps determine the reversibility of the system. The results are discussed in section 4.5.1.

4.4 Lewis Acid Catalysis of a Carborane-Siloxane Copolymer

One of the ways to achieve high thermal stability of siloxane elastomer networks is to incorporate carboranes into the backbone of the polymer. Previously, there have been many publications describing the production of carborane-siloxane networks using $FeCl_3$ as a catalyst. In this Chapter the re-investigation to assess thermal stability started by repeating this classical synthesis. The $FeCl_3$ catalysed carborane-siloxane network was successfully synthesised. However, a noticeable problem with the material was the encapsulation of the catalyst in the host elastomer matrix. Attempts to wash this out with acetone/water were only partly successful and most of the catalyst could not be removed by this method. The thermal stability of this material was tested and is shown in Figures 4.2-4.3:
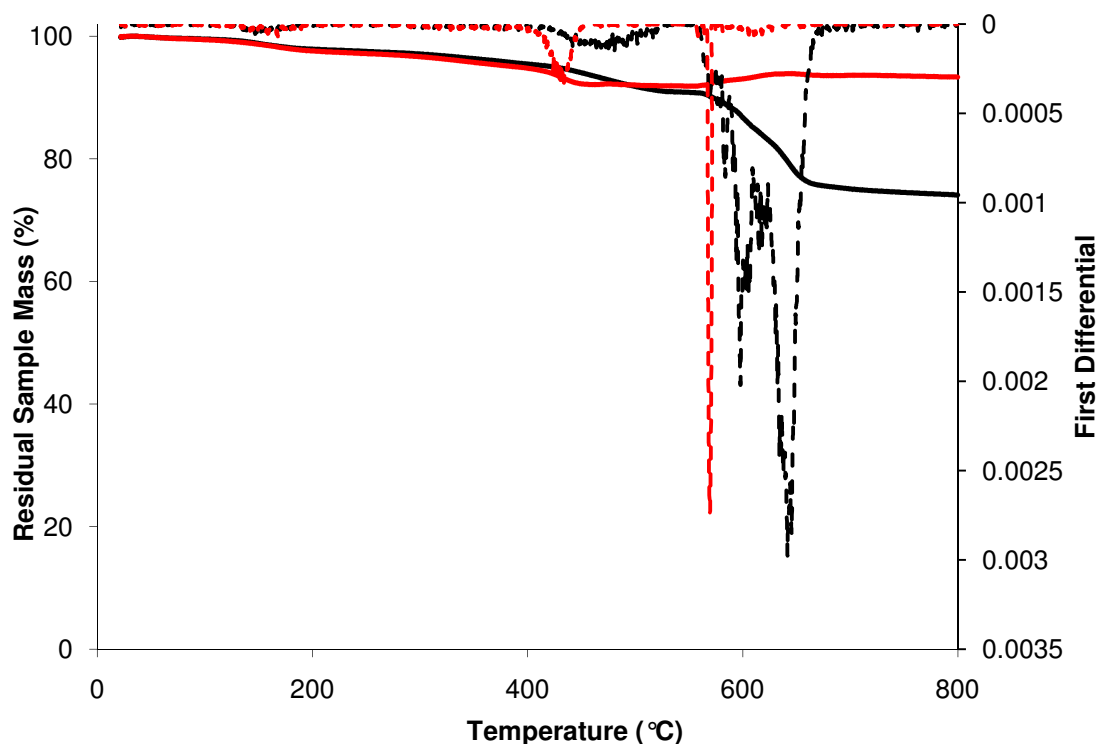
Figure 4.2: TGA analysis of a carborane-siloxane network containing 1% $FeCl_3$ catalyst; non-oxidative run (black line) and oxidative run (red line) including derivatives (dotted lines)

Run	Onset Degradation Temperature / °C	Temperature Maximum Mass Loss / °C	Char Residue / % @ 800 °C
Non-oxidative	567	641	74
Oxidative	-	-	93
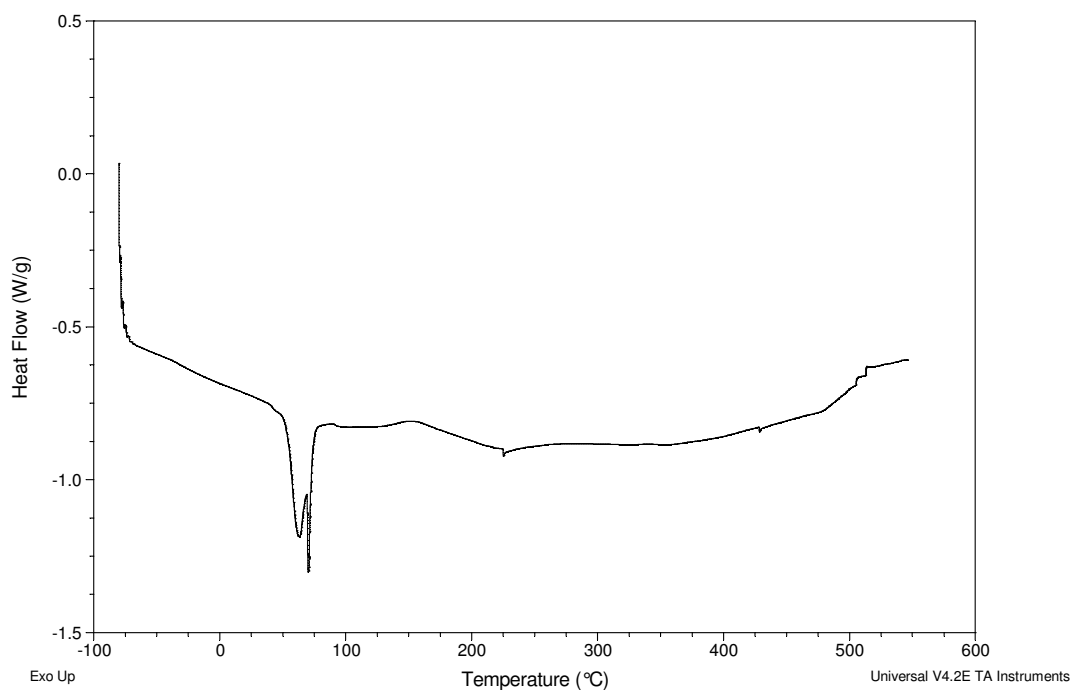
Figure 4.3: DSC analysis of carborane-siloxane copolymer catalysed by FeCl$_3$ run under nitrogen

DSC analysis (non-oxidative):

Transition	Onset Temperature / °C	Peak Maximum / °C	Enthalpy of Transition / J g^{-1}
T$_m$	69.1	70.4	35.1

The TGA data shows that the carborane-siloxane copolymer networks have remarkable thermal stability compared to PDMS elastomer networks. High char residues are also obtained showing that the carborane is severely restricting the reversion degradation processes observed in the PDMS materials. The DSC data

reveals that the properties of the material have been radically altered and that the carborane-siloxane network is more crystalline in nature. The endotherm in the DSC plot is also unusual as it appears as a double peak which could indicate a chemical change in the material. To determine whether this was the case the DSC run was repeated heating, cooling then re-heating the product to see if the peak is reversible or not. The result is shown in Figure 4.4:
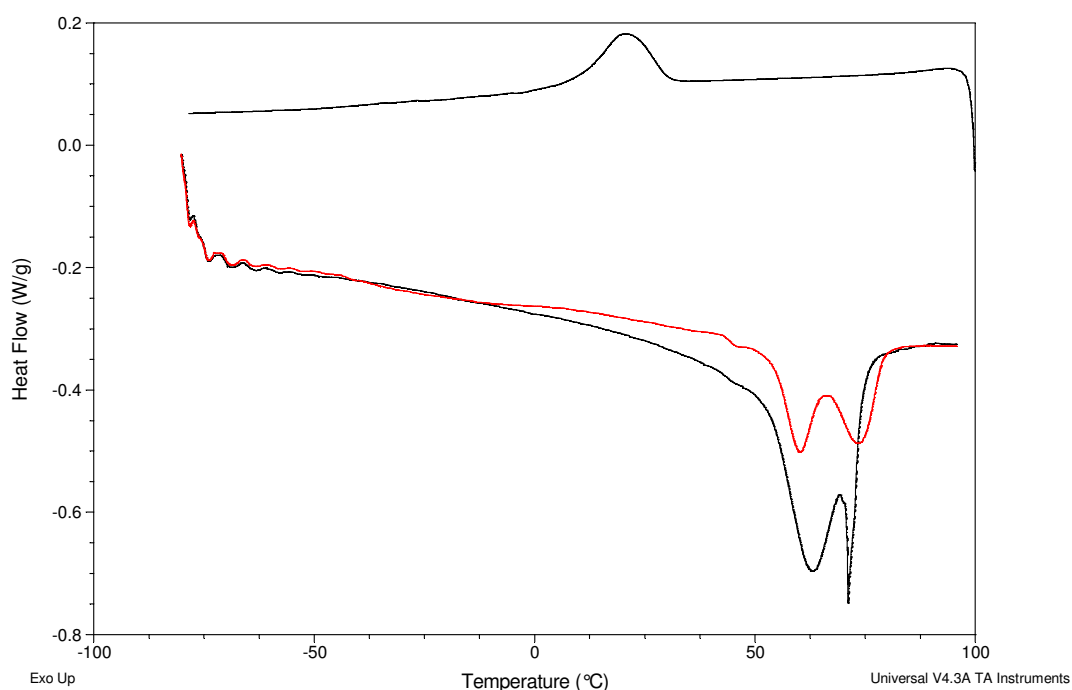
Figure 4.4: DSC heat, cool, reheat analysis of carborane-siloxane copolymer catalysed by FeCl$_3$ run under nitrogen. Heating cycle (lower black line), cooling cycle (higher black line) and reheat cycle (red line)

The result obtained shows that the initial thoughts that it was a chemical change in the material were not correct. What is observed is a splitting of the melting transition which could indicate two separate crystalline regions. The polymer could contain both α and β crystalline regions which X-ray diffraction studies of the material would confirm.

The BF$_3$ catalysts resulted in crystalline products which were analysed by NMR spectroscopy. The NMR data were disappointing and suggested that the reaction had not proceeded. However, data from the GPC of the BF$_3$.amine complex catalysed carborane-siloxane copolymer revealed a M$_w$ of 6,645 with a polydispersity of 1.102. The low molecular mass change observed in the GPC study could suggest that the catalyst does indeed work, however, is deactivated during the reaction. MALDI-TOF measurements did not reveal a high MW polymer but small mass fragments of carboranes coupled with silanes, most likely due to poor coupling of the sample to the host dithranol matrix.

In the next subchapter the role of the FeCl$_3$ in the degradation of a D$_2$ carborane-siloxane copolymer is investigated using sub-ambient thermal volatilisation analysis.

4.4.1 Thermal Volatilisation Analysis of a FeCl$_3$ Catalysed Carborane-Siloxane Copolymer

The TVA of FeCl$_3$ catalysed carborane-siloxane elastomer has been carried out successfully as described in Section 4.1. So far there has been no data in the literature confirming the degradation cycle of these materials combined with the use this technique. The degradation run is shown in Figure 4.5 and an expansion of the lower degradation peak in Figure 4.6:
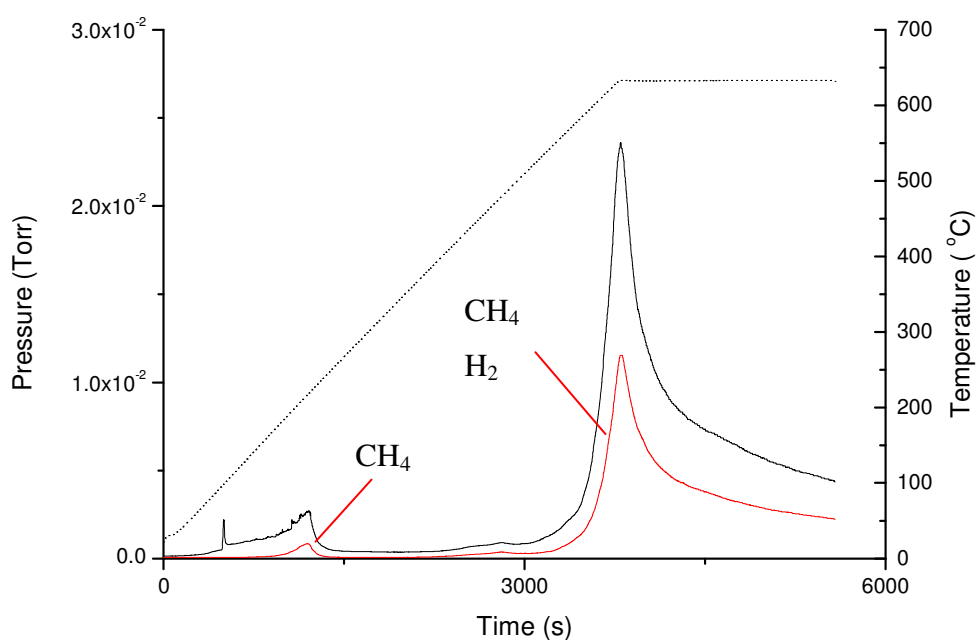
Figure 4.5: TVA degradation run of FeCl$_3$ catalysed carborane-siloxane elastomer. Total pressure of volatiles into trap (black line) and non-condensable volatiles (red line) shown against time with furnace temperature shown on secondary axis (dotted line)
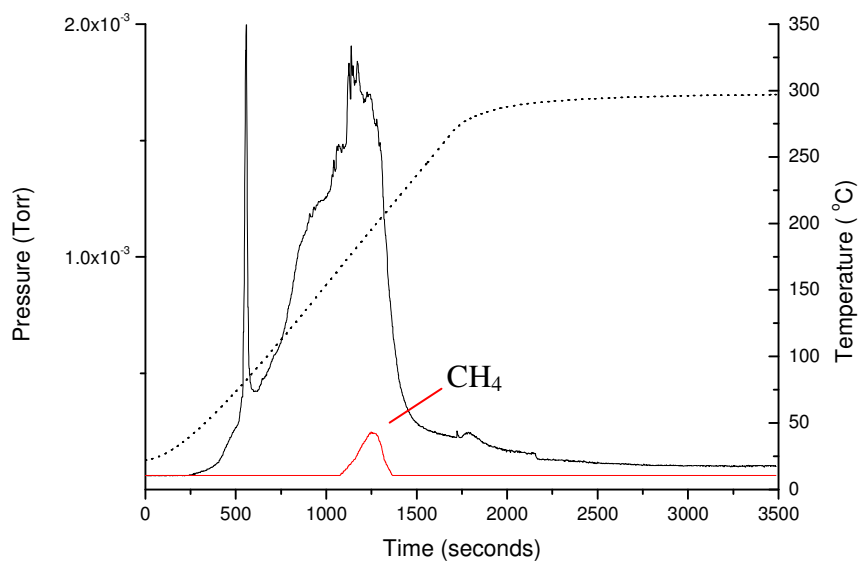
Figure 4.6: FeCl₃ catalysed carborane-siloxane elastomer degradation run to 300 °C.
Plot shows total pressure evolved (black line) and non condensable volatiles (red line)

The degradation plot in Figure 4.5 reveals there are two major degradation steps. The first pressure peak at 150 °C and the second process is the dominant process occurring at close to 600 °C. The major gas fraction that is obtained in the degradation step is hydrogen. By running the mass spectrometer in Faraday mode the amount of each component of each gas can be detected as shown in Figure 4.7:
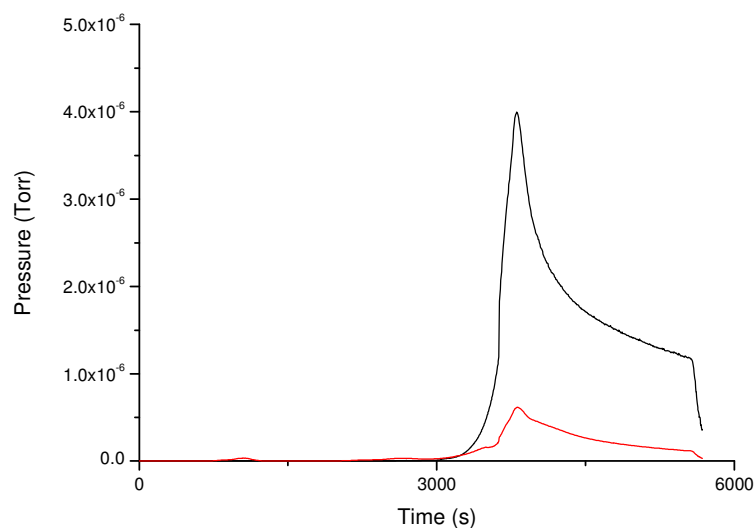
Figure 4.7: Faraday scanning mode on the mass spectrometer for the degradation step of the FeCl₃ catalysed PDMS elastomer, running to 650 °C. Total amount of hydrogen m/z 2 (black line) and methane m/z 16 (red line) evolved is shown

In the GC degradation run trace there are two degradation products observed, methane and hydrogen where hydrogen is given off in significant quantities (peak evolution 7 times greater than methane. In the last Chapter it was noted that it is unusual for a siloxane to undergo dehydrogenation so the presence of the carborane could be responsible for this observation. The carborane has ten hydrogen atoms per cage and could be forming boron carbide (B_4C) at these reduced pressures and elevated temperatures. Other work supporting this hypothesis has been carried out by Tillekaratne, Siap and Trenary where they observed dehydrogenation of *o*-carborane adsorbed on platinum surfaces at low pressures and elevated temperatures up to 430 °C.[3] The resulting dehydrogenation left boron carbide *in situ* as observed by reflection adsorption infra red (RAIR) where the intensity of B-H peaks were reduced in size with increasing temperature.

This evidence is then further backed up by recent work by Rhül *et al.* where dehydrogenation of *o*- and *m*-carborane was observed under synchrotron vacuum

4.4.1 Thermal Volatilisation Analysis of a FeCl₃ Catalysed Carborane-Siloxane Copolymer

ultra violet (VUV) conditions.[4] The main process for the degradation was believed to be as shown:

$$B_{10}C_2H_{12} \; + \; h\nu \; \longrightarrow \; B_{10}C_2H_{10}{}^{\oplus} \; + \; H_2 \; + \; e^{-}$$

Scheme 4.2: UV degradation and dehydrogenation of carborane

The decomposition was then modelled using hybrid density functional theory (DFT) and it was determined that the B-H bonds were most favourable for dehydrogenation and most probably the ones furthest away from the carbons in the cage structure.

In the D_2 carborane-siloxane copolymer the ratio of methyl side groups on the siloxane polymer to hydrogen atoms on the carborane is 2:5. The Faraday scanning mode shows that the ratio of methane to hydrogen produced during degradation is 1:8. This molecular ratio indicates the amount of dehydrogenation is significantly large, indicating that boron carbide formation in the char is highly likely. Solid state ^{11}B NMR was carried out on the char residue and the spectrum arising is shown in Figure 4.8. Figure 4.9 shows an expanded view of the B-H chemical shift region.
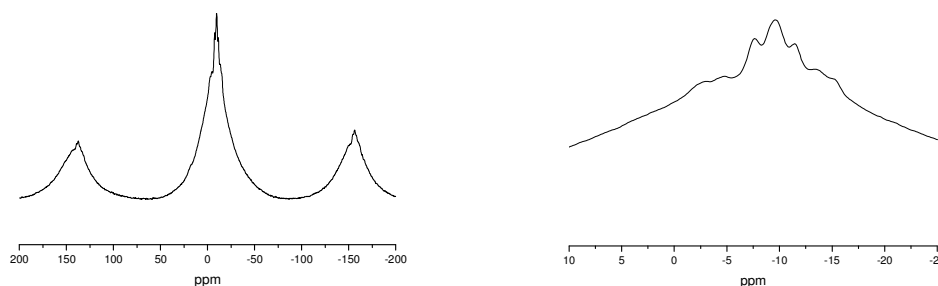
Figures 4.8 (Left): ^{11}B solid state NMR spectrum of TVA char residue of FeCl₃ catalysed carborane siloxane copolymer

Figure 4.9 (Right): Magnified spectrum of Figure 4.8 between limits of 10 and -25 ppm

The presence of paramagnetic iron (III) in the char residue broadens the peaks in the spectrum and is the result of the side bands shown in Figure 4.10 at 150 ppm and -150 ppm. Figure 4.11 reveals that the number of B-H peaks is reduced to 3. The peak

4.4.1 Thermal Volatilisation Analysis of a FeCl$_3$ Catalysed Carborane-Siloxane Copolymer

at -16 has disappeared which is the B-H peaks at positions 2 and 3 on the carborane cage. The dehydrogenation will most likely have been mediated where iron chloride would be able to bridge the face at position 2 and 3 on the carborane.

The majority of the other species generated in the degradation run were isolated in the liquid nitrogen trap. Figure 4.10 shows the sub-ambient distillation of the degradation products and Figure 4.11 shows the GC Faraday mode collecting amount of each component distilled.
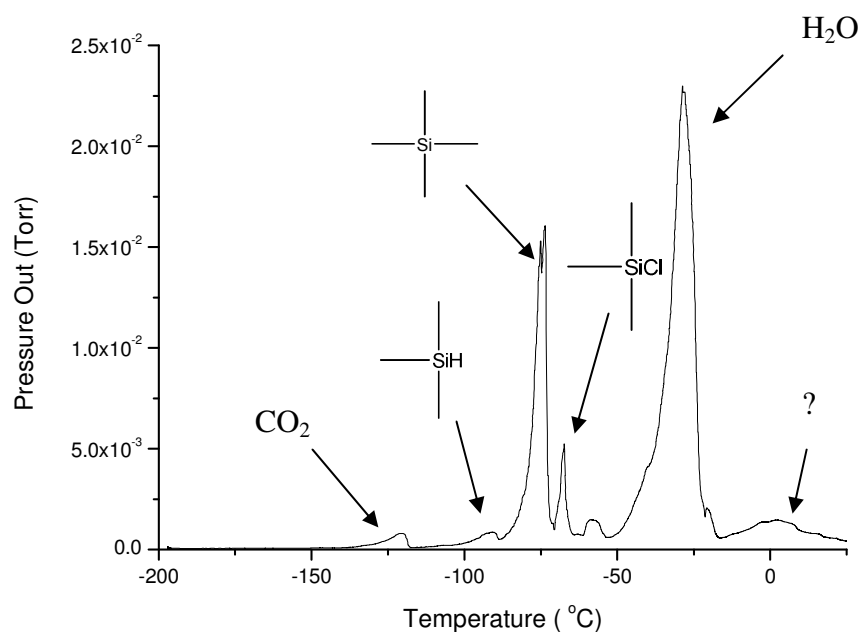
Figure 4.10: Sub-ambient distillation of volatiles from FeCl$_3$ catalysed carborane-siloxane elastomer sample. The black line is output from exit Pirani gauge on trap
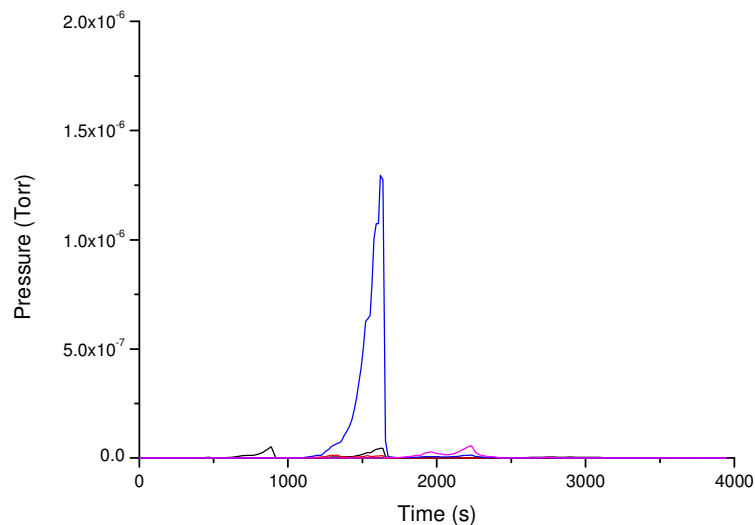
Figure 4.11: Faraday scanning mode on the mass spectrometer for sub-ambient distillation step of the FeCl$_3$ catalysed PDMS elastomer. Total amount of CO$_2$ m/z 44 (black line), silane m/z 58 (red line), silane 2 m/z 73 (blue line) and siloxane m/z 147 (pink line) evolved is shown

The sub-ambient run shows that a significant amount of low molecular mass silane material is given off, most probably due to the carborane blocking the reversion process. The inclusion of *m*-carborane in the backbone of the polymer most likely stops the polymer chain from backbiting due to the steric restriction of the polymer to bend back on itself as shown in Figure 3.16. The high water background is probably from the extracting procedure used to remove excess FeCl$_3$ from the material and could be the cause of the peak at 150 °C in the degradation run. Morgenstern-Badarau *et al.* have characterised cryptand ligand systems where coordinated Fe^{3+} metals can be reduced, dehydrogenating the cryptand ligand.[5] FeCl$_3$ coordinated in the presence of the carborane could undergo a similar dehydrogenation as shown in Scheme 4.3:

151

4.4.1 Thermal Volatilisation Analysis of a FeCl$_3$ Catalysed Carborane-Siloxane Copolymer
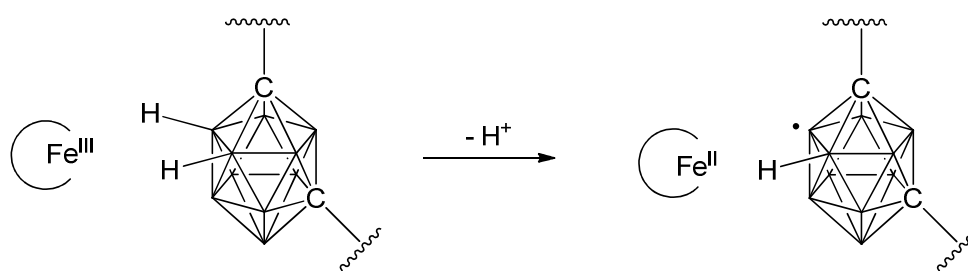
Scheme 4.3: Reduction of Fe^{+3} to Fe^{+2} dehydrogenating *m*-carborane

This evidence suggests the iron is responsible for the dehydrogenation of the carborane under thermal degradation whilst suggesting the iron centre is reduced in the process.

There is an unknown peak in the pressure trace as the mass spectrometer did not detect an analyte, however, experimentally this is believed to be *m*-carborane volatiles that have formed during thermal degradation which are detected using GC mass spectrometry.

The following FTIR data and GC data was obtained for the trapping of the volatiles in the limbs further up the TVA line shown in Tables 4.3-4.4.

Limb No.	Wavenumber (cm^{-1})	Peak Identities
1	3350(b), 2920, 2850, 1750, 1600, 1100	OH signal, aliphatic CH$_3$, C=O, C-O
2	2965, 2920, 2850, 2125, 1255, 870, 700	aliphatic CH$_3$, Si-H stretch, Si-O, Si-(CH$_3$)$_2$
3	3350(b), 2975, 2920, 2850, 1600, 1475, 1380, 1260, 860	water, aliphatic CH$_3$, Si-CH$_3$, C-H stretch, Si-O stretch, Si-(CH$_3$)$_2$
4	3350(b), 2920,, 2850, 2340, 1460, 1380	water, aliphatic CH$_3$, CO$_2$, C-H stretch

Table 4.3: FTIR (v/cm^{-1}[NaCl]):

4.4.1 Thermal Volatilisation Analysis of a FeCl₃ Catalysed Carborane-Siloxane Copolymer

Retention Time	Molar Mass	Identity
Cold Ring Fraction		
4.78	207.0	D_3 siloxane ring
6.70	281.1	D_4 siloxane ring
7.62	355.3	D_5 siloxane ring
8.09	142.2	*m*-carborane
9.23	429.0	D_6 siloxane ring
10.34	503.0	D_7 siloxane ring
16.19	478.4	*m*-carborane structure
17.96	608.6	*m*-carborane structure
18.70	592.5	*m*-carborane structure
Limb 4		
4.78	207.0	D_3 siloxane ring
6.76	281.1	D_4 siloxane ring
7.62	355.3	D_5 siloxane ring
8.09	142.2	*m*-carborane
9.23	429.0	D_6 siloxane ring
10.34	503.0	D_7 siloxane ring

Table 4.4: GC Mass Spectrometry (m/e, M+):

Carborane structures are found in the cold ring fraction, the structures contain multiple carboranes and are confirmed by the boron isotope pattern in the mass spectrum. However, more work is required to determine the exact structure of these degradation residues. The majority of volatiles formed during degradation are low molar mass silanes and siloxane ring structures. Silanes are most probably formed by the reduction of the Si-O bond adjacent to the carborane by hydrogen radicals as shown in Scheme 4.4:

4.4.1 Thermal Volatilisation Analysis of a FeCl₃ Catalysed Carborane-Siloxane Copolymer
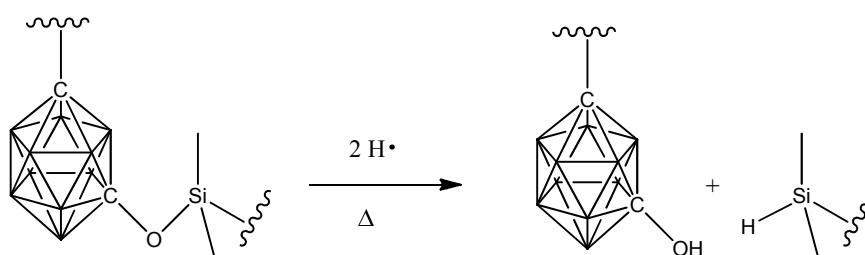
Scheme 4.4: Proposed reduction of carborane siloxane bond with hydrogen radicals

Unfortunately the true mechanism of how this disconnection may occur is unknown. The proposed disconnection is the reverse process to that of the Wilkinson's catalyst polymerisation reaction. Therefore, it is probably the FeCl₃ catalyses this degradation step. Additional TVA experiments are required where no metal is present in the material to determine the catalyst's role in the thermal degradation of carborane siloxane copolymers.

There is also lack of evidence for -OH groups on the carborane in the char residue, however, these could be consumed by hydrogen ions to form water from the degradation step as described in Scheme 4.4. The presence of the carboranes in the GC trace show that the carborane cage structure is stable under thermal degradation and the presence of *m*-carborane in limb 4 most likely indicates the unknown pressure spike in the sub-ambient run is *m*-carborane. The percentage char residue for the material left in the quartz glass tube from the furnace is 27.9%. Comparing this to the char residue under non-oxidative TGA of 74% reveals that the reduced pressure in the TVA is having a more significant effect on revealing the true nature of the degrading material. High vacuum in the TVA can remove degradation products that would normally stay in the pan at atmospheric pressure in a TGA.

4.5 Lewis Acid Catalysis of a Model PDMS Polymer

The purpose of this work is to investigate the following reaction which was previously shown in Chapter 1, Scheme 1.9 to consider replacement of ferric chloride with an alternative Lewis Acid catalyst:

$$n \ H_3CO-\underset{\underset{CH_3}{|}}{\overset{\overset{CH_3}{|}}{Si}}-O-\underset{\underset{CH_3}{|}}{\overset{\overset{CH_3}{|}}{Si}}-OCH_3 \ + \ 2n \ Cl-\underset{\underset{CH_3}{|}}{\overset{\overset{CH_3}{|}}{Si}}-Cl \xrightarrow[\Delta]{FeCl_3}$$

$$\left[\underset{\underset{CH_3}{|}}{\overset{\overset{CH_3}{|}}{Si}}-O-\underset{\underset{CH_3}{|}}{\overset{\overset{CH_3}{|}}{Si}}-O-\underset{\underset{CH_3}{|}}{\overset{\overset{CH_3}{|}}{Si}}-O \right]_n + 2n \ CH_3Cl$$
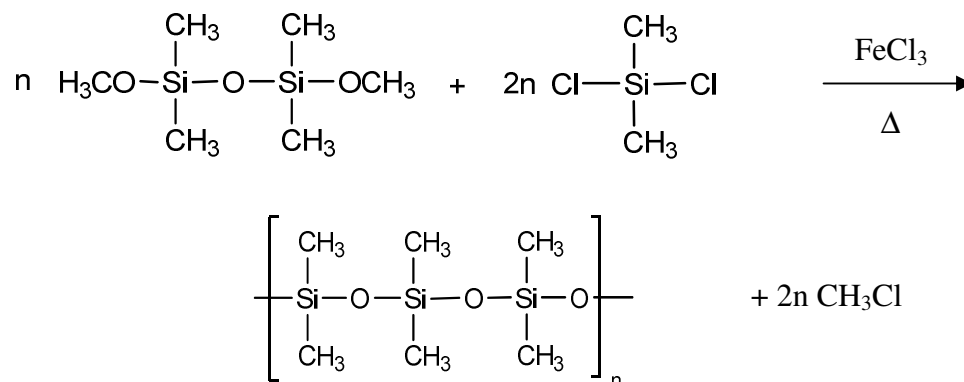
As mentioned before this is not a common route to synthesis of PDMS polymers and is more commonly associated with the formation of carborane-siloxane copolymers. The first reaction involved repeating the above synthesis with methoxy end capped PDMS material. The reaction was successful and led to the formation of a network polymer, so changing the Lewis Base from bis-1,7-dimethylmethoxysilylcarborane to methoxy end capped PDMS did not significantly alter the outcome of the reaction. The thermal stability of the material was tested by TGA and DSC and is shown in Figures 4.12-4.13:

Figure 4.12: TGA analysis of PDMS elastomer containing 1% FeCl$_3$ catalyst; non-oxidative run (black line) and oxidative run (red line) including derivatives (dotted lines)

Run	Onset Degradation Temperature / °C	Temperature Maximum Mass Loss / °C	Char Residue / % @ 800 °C
Non-oxidative	341	521	2
Oxidative	298	538	30

Figure 4.13: DSC analysis of PDMS elastomer containing 1% FeCl$_3$ catalyst under nitrogen

DSC analysis (non-oxidative):

Transition	Onset Temperature / °C	Peak Maximum / °C	Enthalpy of Transition / J g^{-1}
T$_m$	-48.7	-41.4	24.8
T$_d$	479	479	26.7

The addition of the ferric chloride has significantly altered the thermal degradation profile *versus* PDMS elastomers synthesised in Chapter 3 (ref. Figure 3.8) using the tin(II) 2-ethylhexanoate catalyst. The TGA samples in both air and nitrogen show onset of degradation sooner and this can be attributed to the presence of low molecular mass materials, however, the dominating process in both air and nitrogen is at elevated temperatures (~520 °C) much changed from the conventional siloxane elastomers (~390 °C). The DSC data confirm the massive change in T$_d$ where the T$_m$

157

transition remains relatively unchanged. The reason for this change is maybe cross-linking resulting from an unwanted side reaction which increases the resistance to volatilisation of the material.

The $GaCl_3$ catalyst was the only other catalyst used that led to the formation of an elastomeric network. This was to be expected as gallium(III) has a similar ionic radius to iron(III).[6] The network that was formed was not very stable in air due to the sensitivity of the $GaCl_3$ to atmospheric moisture and the outer portion of the material formed an oxidised layer. This was evident as the sample was being prepared for TGA and DSC analysis because part of the material on the inside was still a viscous liquid that solidified as it was exposed to air. The thermal degradation properties of the material are shown below in Figures 4.14-4.15:
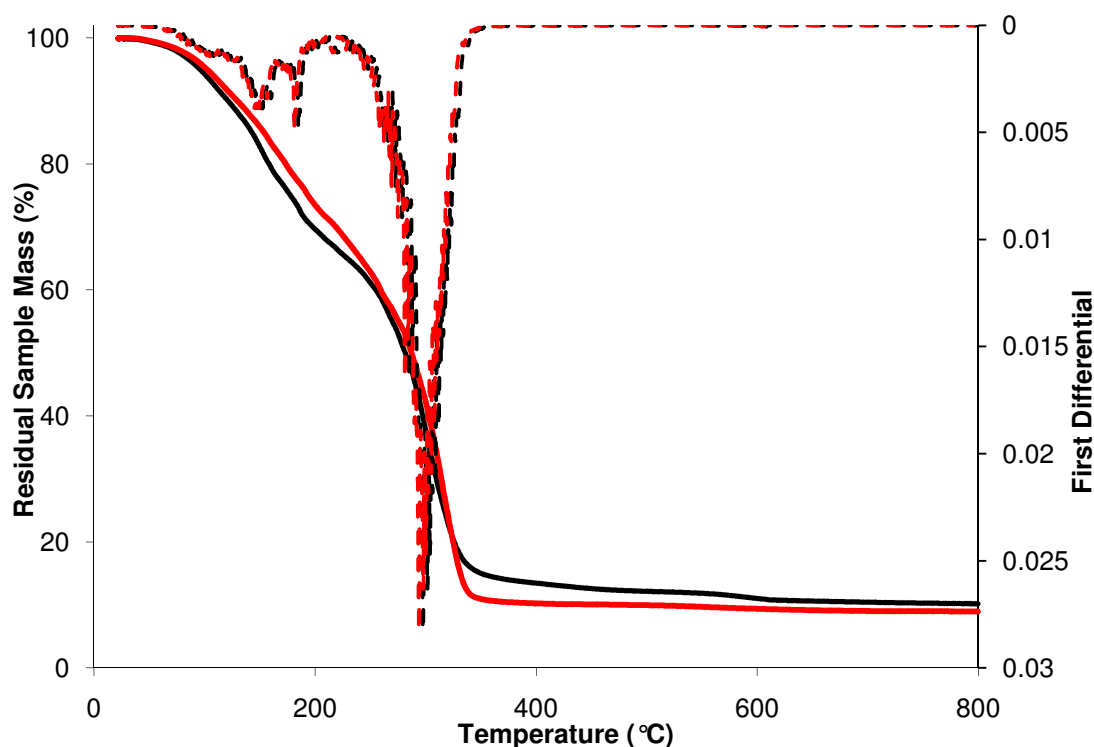
Figure 4.14: TGA analysis of PDMS network formed using $GaCl_3$ catalyst; non-oxidative run (black line) and oxidative run (red line) including derivatives (dotted lines)

Run	Onset Degradation Temperature / °C	Temperature Maximum Mass Loss / °C	Char Residue / % @ 800 °C
Non-oxidative	73	293	10
Oxidative	86	313	9
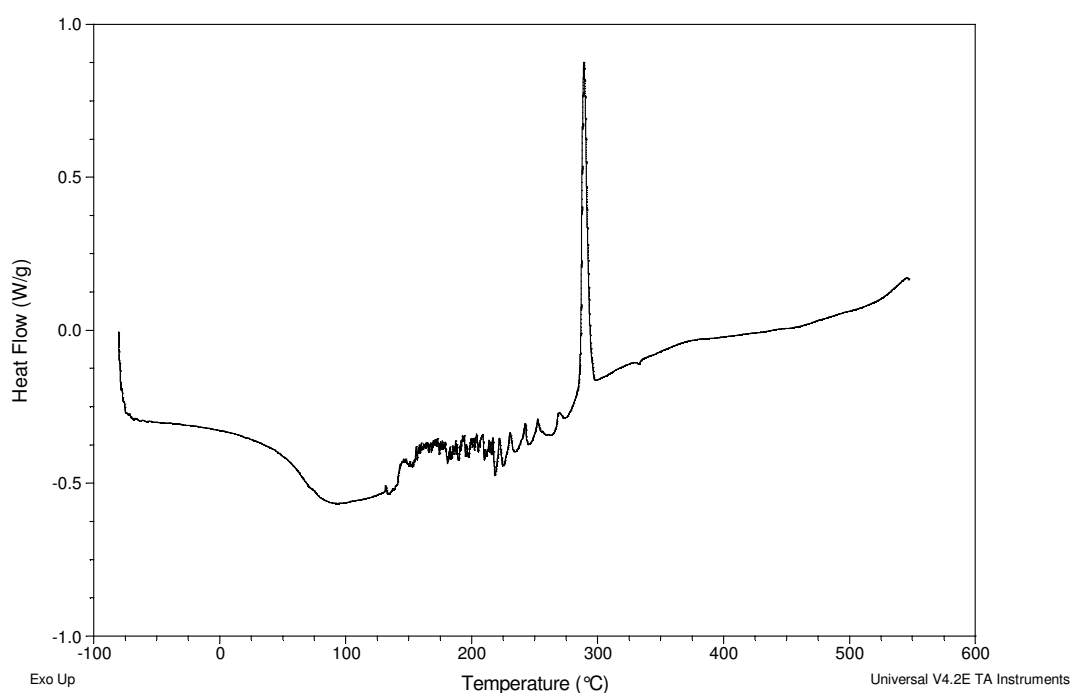
Figure 4.15: DSC analysis of PDMS network formed from GaCl$_3$ catalyst run under nitrogen

DSC analysis (non-oxidative):

Transition	Onset Temperature / °C	Peak Maximum / °C	Enthalpy of Transition / J g^{-1}
T$_d$	64.5	93.4	35.2

The use of GaCl$_3$ as a catalyst has had a significant effect on the thermal stability of the PDMS elastomer. The material is highly unstable at slightly elevated

temperatures and most of the material is lost to vaporization. Although effective as a catalyst, $GaCl_3$ produces polymer which is too unstable for practical use. The exothermic spike in the DSC is both highly interesting and unusual. The peak occurs around 300 °C where about 40% of the material would remains in the TGA pan under non-oxidative degradation. Large exotherms observed when heating a sample usually indicate a bond forming process or crystallisation event in the material. Unfortunately, the origin of this process occurring in the $GaCl_3$ sample is outwith the scope of the thesis. Reduction of $GaCl_3$ and evolution of Cl_2 may be a possibility during degradation.

In general the use of other catalysts did result in a successful reaction where the product was a viscous material. The products of these reactions were monitored initially by the use of ^1H NMR spectroscopy. The starting PDMS polymer material was determined to be ~1174 g mol^{-1} as the -OC$\underline{H}_3$: C$\underline{H}_3$ integral was 1:15. What was noticeable about the NMR results for the polymer systems is the reduction in size or disappearance altogether of the –OC$\underline{H}_3$ peak and the relative increase in size of the C$\underline{H}_3$ peak. For the $AlCl_3$ catalyst the integration shifted to 1:660 which was indicative of 44 oligomer chains coming together and this was the same for the $ZnCl_2$ catalyst. For the other catalyst systems it was not possible to determine this as the –OC$\underline{H}_3$ peak was not observed.

Initial GPC analysis was carried out on the BF_3 and $AlCl_3$ catalysed polymers but unfortunately this failed. It was believed this happened because the dn/dc values of PDMS in THF are too low for the light scattering detector to sense the compound. Also the interferometric refractometer struggled to detect the compound leading to broad and flat looking peaks that are uncharacteristic of PDMS polymers. The more successful samples were sent for analysis at RAPRA where access to a GPC with a more appropriate eluting solvent, methylene chloride, was available. The $FeCl_3$, $AlCl_3$ and $ZnCl_2$ materials were tested and molar masses (M_w) of 129,000, 61,400 and 308,000 g mol^{-1} were found respectively. This proves that changing the catalyst

still leads to significant polymerisation with $ZnCl_2$ forming the longest linear polymers that could be of synthetic value.

Other Lewis Acid catalysts failed to produce high molecular mass polymers when used. This is possibly due to the poor stability of the intermediate species formed between the catalyst and the dicholodimethylsilane.

4.5.1 Kinetic Study of Formation of a PDMS polymer using FeCl$_3$

The literature covering the reaction between a methoxy capped carborane and a (dichlorodimethyl)silane to form a copolymer is extensive, however, there is an absence of kinetic data which studies the role of FeCl$_3$ in the reaction. In this Section the activation energy and reaction steps are interrogated.

In this study we focus on the FeCl$_3$ system using a model reaction as carborane monomers are highly expensive and the cost of completing such a comprehensive study would be excessive. To determine the kinetics, the reaction was carried out using a methoxy-capped PDMS, to determine the optimum conditions in which to evaluate the energy of activation for this reaction. The reaction is shown in Scheme 4.5:
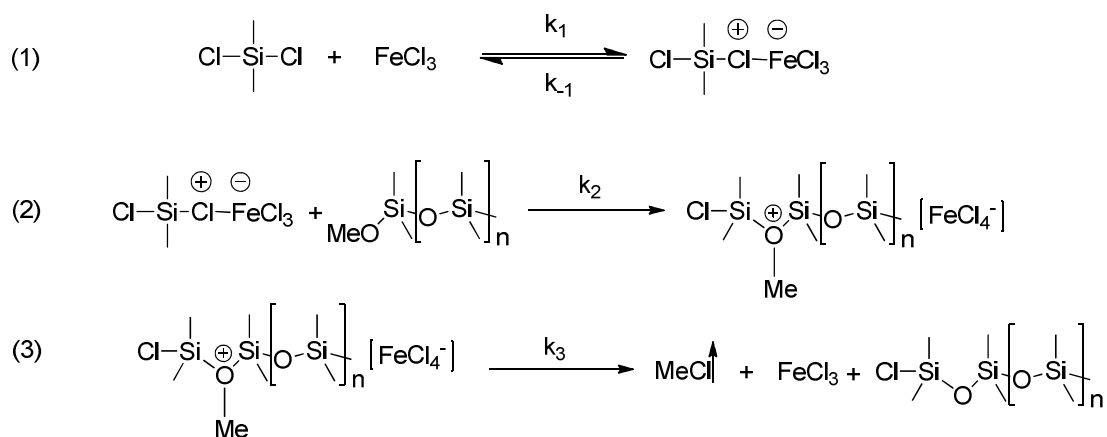
Scheme 4.5: Possible kinetic steps in the polymerization of (dichlorodimethyl)silane and methoxy terminated poly(dimethylsiloxane) polymer mediated by FeCl$_3$

To be able to determine the activation energy, the rate determining step must be studied so it is important to discount the least likely rate determining steps first. The third reaction step involving k$_3$ can be immediately rejected as gas formation will be rapid. The reaction step involving k$_1$ and k$_{-1}$, although not a redox process, requires the use of electrochemistry to investigate the equilibrium and subsequently determine reversibility of the system. However, during the reaction the catalyst and (dichlorodimethyl)silane will approach equilibrium quickly. This is due to the low

levels of catalyst present in the solution restricting the amount of electrophile that can be present at any one time. Reaction step 2 is most likely to be the rate determining step as it requires the electrophile to be in the vicinity of the methoxy end-capped group and the electrophile to propagate for longer times as the viscosity of the solution rises with increasing molar mass of poly(siloxane) polymer. Also electrophile formation at lower temperatures might be less likely so the intermediate species could be reduced in concentration further. This would suggest that reaction step 2 will be the rate determining step.

There are a few complications that should be noted. First, the polymer is also the solvent for the reaction which complicates the measuring of the kinetic behaviour. In addition, when measuring the rate constant, normal solution kinetic assumptions may not apply due to the change in viscosity as the reaction proceeds. Moreover, the stability of the electrophile may vary with temperature but this is not predictable and can only be determined by experimentation.

In terms of defining the complex reaction rate the following kinetic analysis may be envisaged, based on the overall reaction.[7]

$$A + B \underset{k_{-1}}{\overset{k_1}{\rightleftharpoons}} I + C \overset{k_2}{\longrightarrow} P$$
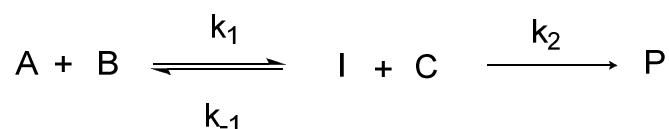
A simplified reaction rate Scheme for the polymerization is shown above where A is (dichlorodimethyl)silane, B is FeCl$_3$, I is the electrophile intermediate formed and C is the methoxy capped PDMS. Assuming that [A], [B] and [I] are in equilibrium, the following assumption is then

$$k' = \frac{k_1}{k_{-1}} = \frac{[I]}{[A][B]}$$

and therefore the rate of generation of the product can be described as

$$\frac{d[P]}{dt} = k_2[I][C] = k_2 k'[A][B][C]$$.

This can be simplified further to the following

$$\frac{d[P]}{dt} = k''[A][B][C]$$

where the complex rate constant is described as

$$k'' = \frac{k_1 k_2}{k_{-1}}$$

Our model predicts that the formation of the intermediate species is reversible and this needs to be confirmed for our hypothesis to be valid. Also, in the predicted kinetic model the rate constant obtained in the NMR study will also depend on k_1 and k_{-1} if the hypothesis is valid. This is due to the existence of the pre-equilibrium in the formation of an electrophile intermediate that is only quantifiable through the mathematical model outlined.

To obtain any meaningful data from an electrochemical study it is important that the species of interest will give a peak that is definable before investigating any peak responsible for interrogating the behaviour of the intermediate formed. In this instance generation of $FeCl_3$ electrochemically would be ideal as firstly we could observe a reproducible oxidation of $FeCl_2$ to $FeCl_3$ and also $FeCl_2$ does not react with (dichlorodimethyl)silane so we can be confident that any peaks after the oxidation are solely due to the removal of Fe^{3+} by the (dichlorodimethyl)silane to form the intermediate species as predicted. One problem that becomes apparent from attempting to make electrochemical solutions is the insolubility of $FeCl_2$ in pure (dichlorodimethyl)silane; in this instance we have to use a solvent to help solvate the chloride salt. This will mean that k_1 will be determined in a electrolytic solvent which will differ from the actual reaction in which the poly(dimethylsiloxane) acts as its own solvent.

Another reason for generating the $FeCl_3$ from $FeCl_2$ is that ferric chloride will form an equilibrium with itself and complex to form the $[Fe_2Cl_6]$ dimer.[8] In generating small amounts of $FeCl_3$ it is hoped that such an equilibrium will not have time to

form as the solution will have an excess of (dichlorodimethyl)silane which will react with all the $FeCl_3$ generated at the electrode.

The results obtained from the NMR integrations were then plotted for different temperatures as shown in Figure 4.16. Table 4.5 shows the rate constants obtained and error in best fit line for each pair of runs.
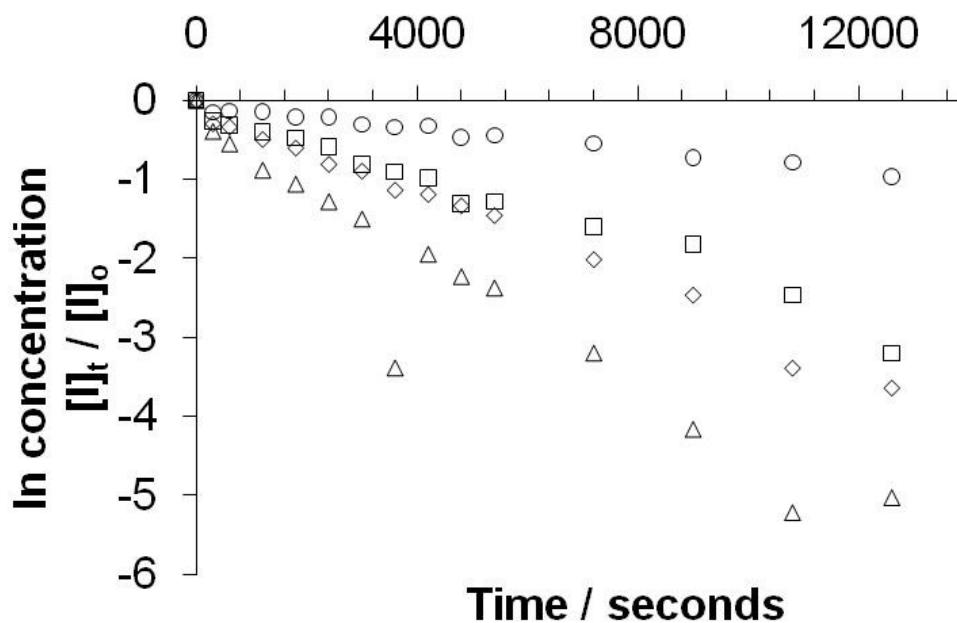
Figure 4.16: Plot of natural log of the fraction of the -OC<u>H</u>₃ integral present at time t as a function of reaction time. Circles are reaction at 60 °C, squares are reaction at 75 °C, diamonds are reaction at 80 °C and triangles are reaction at 90 °C

4.5.1 Kinetic Study of Formation of a PDMS polymer using FeCl₃

Temperature (°C)	Rate constant k 1×10^{-4} (s^{-1})	R^2 best fit value
40	0.50	0.79
60	0.69	0.98
75	2.55	0.90
80	2.92	0.92
90	5.10	0.75
100	6.62	0.74
120	6.89	0.75

Table 4.5: Rate constants at various temperatures including best fit constant

NMR studies of the copolymerization revealed that the concentration of methoxy group on the PDMS reduced over time according to first order kinetics. Only the first nine data points of the experiment were carried forward into these plots as the initial rate method applied to these results. At reaction times greater than one hour undesirable effects start to occur. The viscosity of the solution becomes significant and this has a greater influence on the mobility of electrophile, reducing the reaction rate. At higher temperatures (dichlorodimethyl)silane can distil from the reaction vessel. In addition, a temperature study was conducted and an Arrhenius plot was obtained that encompassed data points from 40 through to 120 °C as shown in Figure 4.17.
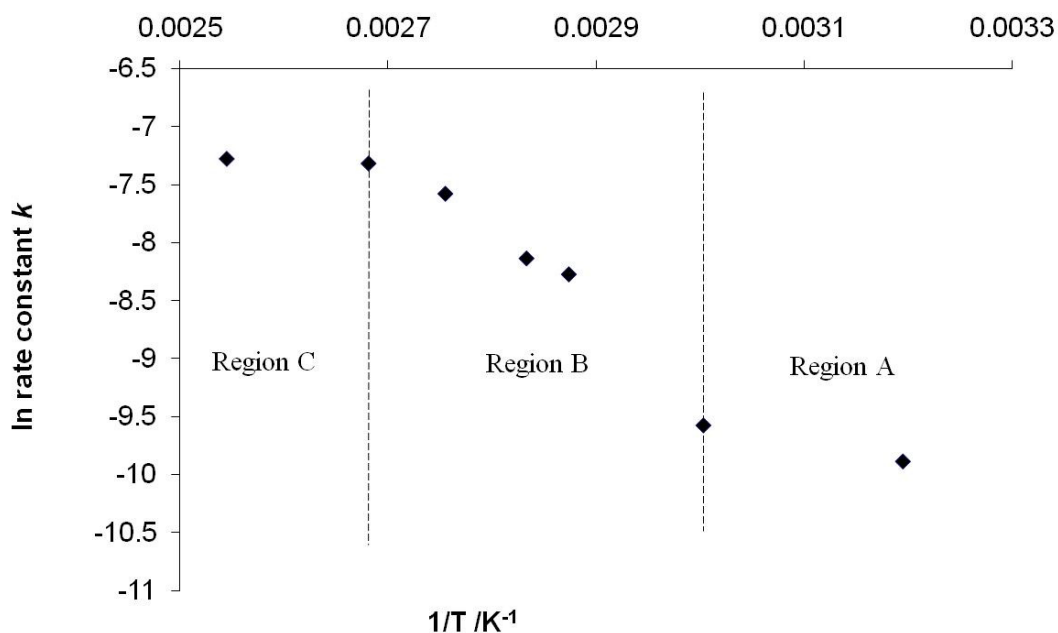
Figure 4.17: Overall Arrhenius plot of rate constant from 40 °C through to 120 °C against reaction rate

In the plot three regions were observed which could each be explained by experimental observation. In region A there is a slow increase in the rate constant where it was observed that the catalyst was only partially soluble at lower temperatures which lead to slower reaction rates. Region B is the Arrhenius region in which the reaction rate almost doubles with each 10 °C increase in temperature. In region C the reaction rate significantly fails to increase further, most likely caused by the distillation of reactant material at elevated temperature.

The Arrhenius region was extracted from the data, re-plotted as shown in Figure 4.18, and the activation energy obtained.
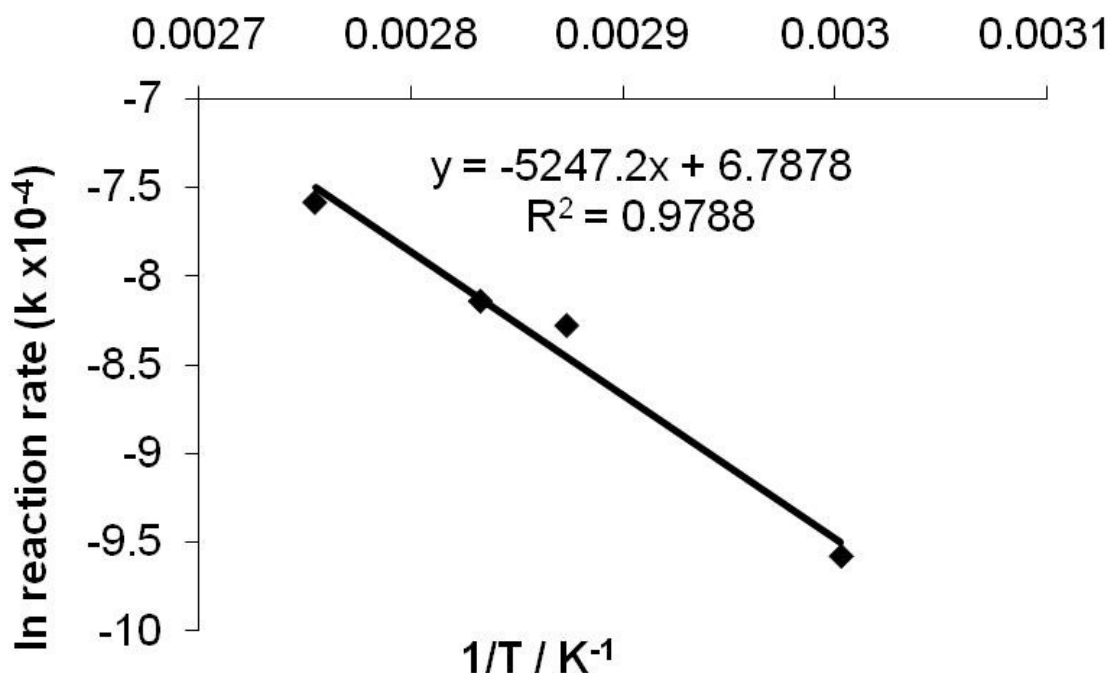
Figure 4.18: Arrhenius region plotted between the temperature range of 60 °C to 90 °C against natural log of reaction rate

The activation energy of the reaction was found to be +43.6 kJ mol⁻¹. Further extrapolation of the data back to the y-axis reveals the frequency factor for the reaction defined as ln A. This was used to calculate the activation entropy of the reaction according to the following equation[9]

$$\Delta S^{\ddagger} = R\left(\ln A - \ln\left(\frac{kT}{h} \right) - 1 \right)$$

The value calculated for the reaction was taken from a temperature in the Arrhenius region (80 °C) giving a value for $\Delta S\ddagger$ = -198.2 J K⁻¹ mol⁻¹. The value is large and negative which indicates that the transition state is much more ordered than the original reactants, as befits the proposed mechanism in reaction step 2.

To complete the kinetic study, an analysis of reactions involving steps of k_1 and k_{-1} were investigated. The first electrochemical study involved testing the reversibility of $FeCl_2$ to $FeCl_3$ in aqueous KCl solution. Figure 4.19 shows the oxidation and reduction peaks at various scan rates. Clear diffusion controlled peaks were obtained

for both oxidation and reduction reactions with a peak to peak separation of 120 mV (independent of scan rate). The latter indicates that the electron transfer process is slow for this reaction. The diffusion coefficient for the Fe^{2+} was obtained using Randles-Sevcik equation and is shown in Table 4.6:
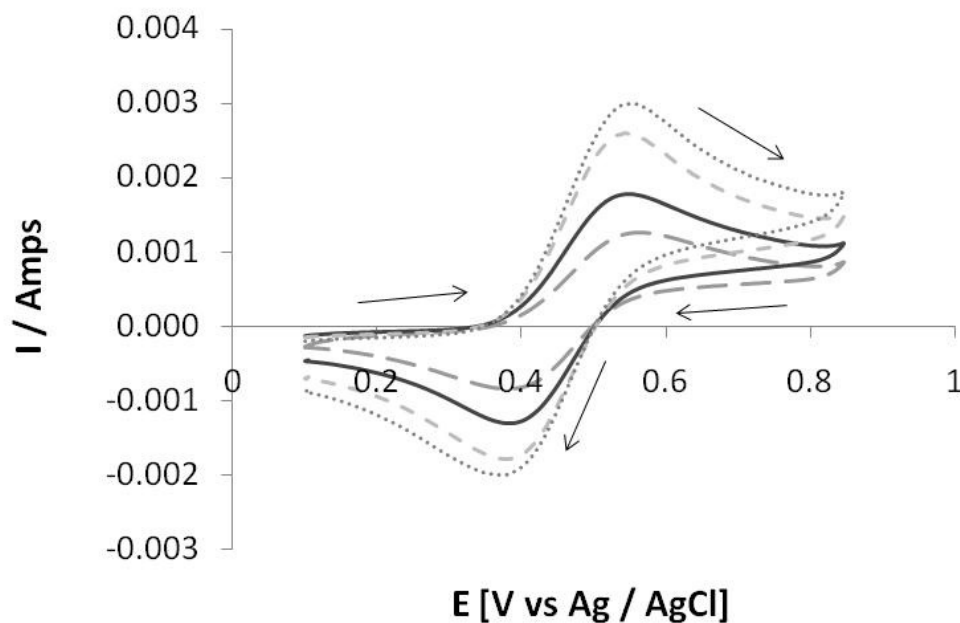
Figure 4.19: 20 mM solution of $FeCl_2$ in 0.1 M KCl solution. Scan rates show are 20 mVs^{-1} (long dash), 40 mVs^{-1} (solid line), 80 mVs^{-1} (short dash) and 120 mVs^{-1}(dotted line). The cyclic voltammogram shows the oxidation of $FeCl_2$ to $FeCl_3$ and its reduction in the reverse peak

Solution	Electrode Area (cm^2)	Diffusion Coefficient cm^2 s^{-1} (1x10^{-7})	Error +/- cm^2 s^{-1} (1x10^{-7})
20 mM FeCl$_2$ in 0.1M KCl	0.38	22.4	1.25
20 mM FeCl$_2$ and 0.1M TBACl in THF	0.002	0.415	0.00689
20 mM FeCl$_2$, 0.1M Si(Me$_2$Cl$_2$) and 0.1M TBACl in THF Peak A	0.002	0.578	0.00875

Table 4.6: Diffusion coefficients and associated errors for varying solutions containing FeCl$_2$

Ideally for the next series of cyclic voltammetry experiments the solubility of the FeCl$_2$ in (dichlorodimethyl)silane would allow us to measure the cyclic voltammogram without an additional solvent. However, the solubility of the FeCl$_2$ is poor in (dichlorodimethyl)silane even at elevated temperatures > 80 °C. To overcome this THF was used as the solvent to ensure dissolution of the electrolyte and electro-active analyte. A background scan using a solution of TBACl electrolyte in THF was produced to show that no peaks appear in the voltage limits of interest. Again, a second background scan using a THF solution incorporating (dichlorodimethyl)silane and TBACl shows that no peaks are observed in the voltage range of interest. When 20 mmol of FeCl$_2$ was added to a solution containing the electrolyte in THF peaks for the oxidation and for reduction of the Fe^{2+}/Fe^{3+} centre were observed similar to that of Figure 4.19. As before the diffusion coefficient was extracted from a voltage scan rate dependence and application of the Randles-Sevcik equation. The value obtained is given in the above Table. The decrease in D here compared to that in aqueous solution suggests that the diffusion species in the less polar THF solvent is much larger than in water.

When (dichlorodimethyl)silane, FeCl$_2$ and electrolyte are present in the same solution the oxidation of Fe^{2+} to Fe^{3+} is observed (peak A) and in continuing to scan

in a positive direction a second peak is observed which is only present when $FeCl_3$ and (dichlorodimethyl)silane are present (peak B), shown in Figure 4.20.
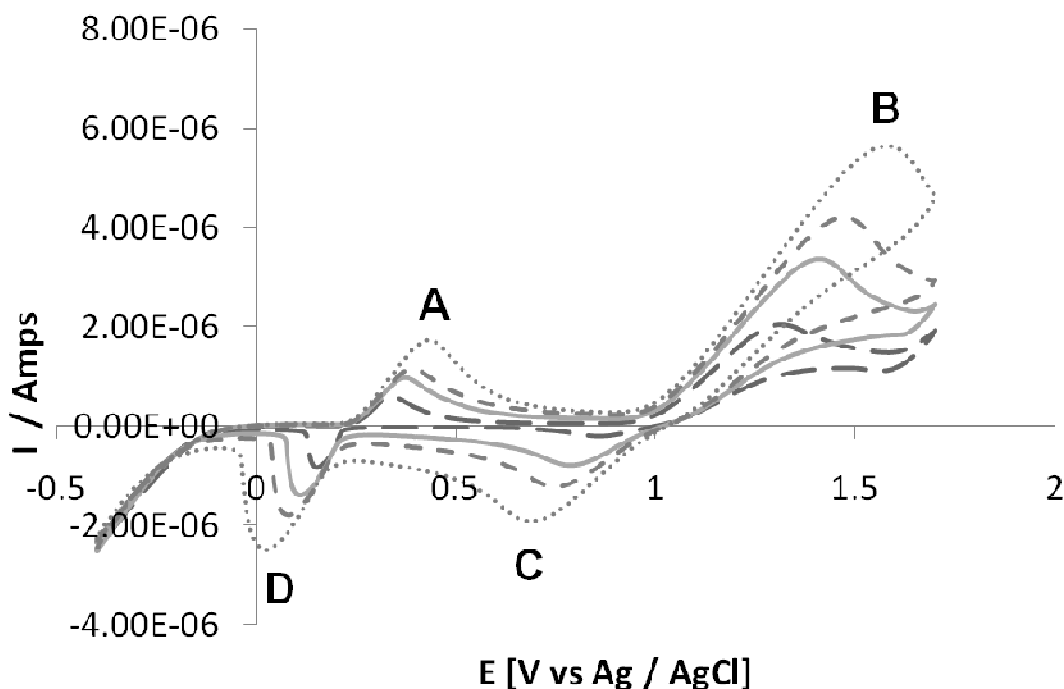
Figure 4.20: 20 mM $FeCl_2$, 0.1 M (dichlorodimethyl)silane and 0.1 M TBACl in THF. Scan rates shown are 40 mVs^{-1} (long dash), 120 mVs^{-1} (solid line), 200 mVs^{-1} (short dash) and 400 mVs^{-1}(dotted line)

Here the oxidation and reduction peaks associated with Fe^{2+}/Fe^{3+} (at 0.3 V and 0.15 V respectively) are still present peak to peak separation increases substantially with scan rate, giving a 500 mV separation at a scan rate of 400 mV s^{-1}. This indicates that the reaction has become even more electrochemically irreversible in the medium (THF). Furthermore, although the shape of the oxidation peak at A retains the diffusion controlled reaction shape, the reverse reduction reaction at D does not. The shape of the peak at D suggests that the Fe^{3+} species generated at the electrode surface in this region becomes rapidly exhausted, due to continuing chemical reaction with the (dichlorodimethyl)silane.

The size of peak B is three times greater than peak A which indicates it could be associated with a multi-electron process. This could be due to the destabilisation of

171

the iron centre by the (dichlorodimethyl)silane liberating the three chloride ligands on the metal centre. The oxidation process peak B is linked to the reverse reduction process at peak C, both which give diffusion controlled shapes. In such a case we can normalise the curves by dividing by $v^{1/2}$ in which case, all the curves should superimpose shown in Figure 4.21.
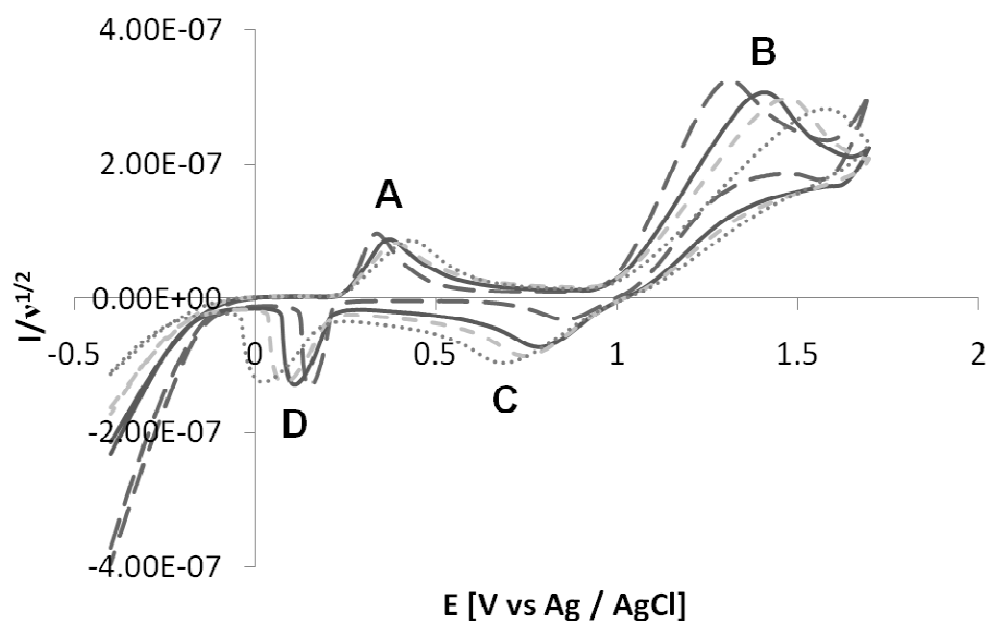
Figure 4.21: 20 mM FeCl$_2$, 0.1 M (dichlorodimethyl)silane and 0.1 M TBACl in THF. Current has been divided by the square root of the scan rate. Scan rates shown are 40 mVs^{-1} (long dash), 120 mVs^{-1} (solid line), 200 mVs^{-1} (short dash) and 400 mVs^{-1}(dotted line)

However, due to the above mentioned electrochemical irreversibility of the reactions taking place here, this does not occur and there is still a shift to higher potentials with increasing scan rate. The oxidation current maxima, however, do become similar (as for peaks A and D) if irreversibility is taken into account. What is significant though here is that the normalised reduction current maxima increases with scan rate. Such a behaviour is anomalous for an EC (electron transfer - chemical reaction) mechanism. Thus an oxidation of R, the intermediate species [I] gives rise to the following process shown as

$$R \rightleftharpoons n\ e^- + O$$

$$O \longrightarrow P$$
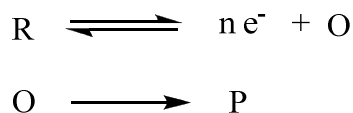
This yields the species O which can undergo chemical reaction to give an electrochemically inactive species P. The amount of O available for the reverse reduction process to give peak C depends on the rate of the chemical reaction of O converting to P. If the latter process is very fast, then there will never be any O available to give the peak C. On the other hand, for very slow conversion of O to P, the reverse reaction will not be affected at all except at the very slow scan rates. The reality for the first step of the kinetic model is the (dichlorodimethyl)silane is consumed in the electrochemical step, thus giving rise to the irreversible process.

In the context of our system, the effect of this is to change the kinetic equation associated with the overall reaction shown in Scheme 4.6. The initial reaction step 1 proceeds as shown:

$$Cl-\overset{|}{\underset{|}{Si}}-Cl \quad + \quad FeCl_3 \quad \xrightarrow{\quad k_1 \quad} \quad Cl-\overset{|}{\underset{|}{Si}}\oplus \left[FeCl_4^- \right]$$
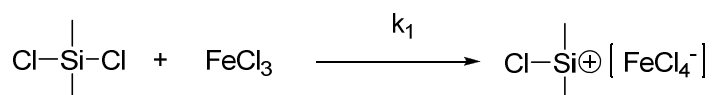
where the rate of the reaction is now solely dependent on k_2 and the kinetics are as follows:

$$\frac{d[P]}{dt} = k_2[I][C]$$

In this instance the amount of species [I] will be small in line keeping with steady state approximation. Therefore, the rate change in the equation collapses to a first order equation as was confirmed in the resulting NMR plots of concentration of the methoxy capped PDMS, i.e.

$$\frac{d[P]}{dt} = k_2[C]$$

4.6 Chapter Conclusion

The synthesis of carborane-siloxane copolymers was achieved using $FeCl_3$. TGA analysis of the $FeCl_3$ copolymer network material showed remarkable thermal stability as predicted in the literature. The thermal degradation cycle of the material was investigated by use of thermal volatilisation analysis. The main degradation process is dehydrogenation of the carborane, possibly to produce boron carbide and reduction of the siloxane fragments to form low molecular mass silanes.

By use of a methoxy capped PDMS polymer the replacement of $FeCl_3$ in the much discussed copolymerization reaction was investigated. It was shown that other Lewis acids may give rise to copolymers without the added complication of cross-linking, namely $AlCl_3$ and $ZnCl_2$. The kinetics associated with the $FeCl_3$ polymerization have been extensively investigated. It was found that the activation energy was +43.6 kJ mol^{-1} with an activation entropy of -198.2 J K^{-1} mol^{-1}. The results of this study have recently been published in the Journal of Applied Polymer Science.[10]

In the next Chapter the focus is changed from inorganic condensation catalyst salts, to organic hydrosilylation addition catalysts. Will the use of this alternative catalyst lead to cleaner, better defined network elastomers and will dehydrogenation still occur during thermal degradation?

4.7 References

1. Bayers, F.D., Dudley, M.A., *"Method for production of mica based insulation"* US Patent 4107358

2. Greef, R., Peat, R., Peter, L.M., Pletcher, D., Robinson, J., *"Instrumental Methods in Electrochemistry"*, Ellis Horwood Limited 1990: 183

3. Tillekaratne, A., Siap, D., Trenary, M. *"Adsorption and dehydrogenation of ortho-carborane on the Pt(111) surface"* Journal of Physical Chemistry C 2008 **112**: 8682

4. Ruhl, E., Riehs, N.F., Behera, S., Wilks, J., Liu, J., Jochims, H.W., Caruso, A.N., Boag, N.B., Kelber, J.A., and Dowben, P.A., *"Photofragmentation of the closo-Carboranes Part II: VUV Assisted Dehydrogenation in the closo-Carboranes and Semiconducting $B_{10}C_2H_x$ Films"* Journal of Physical Chemistry: Part A 2010 **114**: 7284

5. Morgenstern-Badarau, I., Lambert, F., Renault, J.P., Cesario, M., Marechal, J.D., Maseras, F., *"Amine conformational change and spin conversion induced by metal-assisted ligand oxidation: from the seven-coordinate iron(II)–TPAA complex to the two oxidized iron(II)–(py)3tren isomers. Characterization, crystal structures, and density functional study"* Inorganica Chimica Acta 2000 **297**: 338

6. Harris, W.R., Messori, L., *"A comparative study of aluminum(III), gallium(III), indium(III), and thallium(III) binding to human serum transferrin"* Coordination Chemistry Reviews 2002 **228**: 237

7. Atkins, P., De Paula, J *"Physical Chemistry – 8th Edition"* Oxford Press 2006: 886

8. Blairs, S. *"Sublimation studies of anhydrous ferric chloride"* Journal of Chemical Thermodynamics 2006 **38**: 1484

9. Avery, H.E. *"Basic Reaction Kinetics and Mechanism"* Macmillan Press 1974: 67

10. Apedaile, A., Liggat, J.J., Parkinson, J., Nikiforidis, G., Berlouis, L., Patel, M., *"Lewis acid mediated polymerisation of poly(dimethylsiloxane) polymers: Investigating reaction kinetics using both NMR spectroscopy and cyclic voltammetry"* Journal of Applied Polymer Science 2012 **123** (5): 2601-2608

Chapter 5

Carborane Containing Polydimethylsiloxane Elastomers Formed *Via* Hydrosilylation

5.0 Chapter Introduction

In this final Chapter attention is turned from condensation catalysts to addition catalysts. Hydrosilylation is the method of producing carbon-silicon bonds by addition of a silane to a vinyl functional group. These reactions have been used in the formation of silicone networks for over ten years, however, publications where carborane-siloxane networks have been formed via hydrosilylation are far less prominent.

The work carried out by Keller and Kolel-Veetil is one of the few examples that employ hydrosilylation to form a cross-linked carborane siloxane network.[1] The networks they created showed remarkably high onset of degradation temperatures between 530 – 590 °C. This reaction will be studied in this Chapter with revisions made to the reaction detailed in their paper. First the carborane used will be replaced with 1,7-diallyl-*m*-carborane. Secondly no solvent will be used in the reaction as by removing the solvent the subsequent thermal degradation study will be simplified further. The key to this Chapter will be to produce carborane and non-carborane containing silicone networks to compare the thermal degradation of these materials. The nature of the dehydrogenation of these silicone materials will be revealed. Finally by varying the cross-link density the true nature of the thermal stability of these materials will be investigated.

5.1 Synthesis of a Carborane-Siloxane Network Using 1,7-Diallyl-*m*-Carborane and a Low Molecular Mass Silane Monomer

To a 25 ml beaker 5.0 g poly(dimethylsiloxane-*co*-methylhydrosiloxane) with an average molar mass (M_n) ~950 g mol^{-1} was added. To this solution 1,7 bis(allyl)*m*-carborane (1.18 g, 5.26 mmol) was added. Karstedt's catalyst (platinum(0)-1,3-divinyl-1,1,3,3-tetramethyldisiloxane) in 0.1M vinyl terminated PDMS which was loaded onto the end of a pipette and three drops were added to the solution containing the monomers. The reaction mixture was stirred for ten seconds using a high shear stirrer. After a short delay the material started to harden and turn dark brown, during this time the temperature of the sample rose to about 80 °C. The material was allowed to cool then post-cured in an oven at 60 °C overnight. A light yellow opaque rubber was obtained as the final product.

The reaction has been repeated several times in which the molar ratio of the carborane to the polymer has been varied from 1:1 through to 1:6.

Experimental Data:

1:1 Carborane Siloxane Network

Yield = > 99 %

Thermogravimetric analysis:

Run	Onset Degradation Temperature / °C	Temperature Maximum Mass Loss / °C	Char Residue / % @ 800 °C
Non-oxidative	448	615	70.0
Oxidative	395	613	82.0

5.1 Synthesis of a Carborane-Siloxane Network Using 1,7-Diallyl-m-Carborane and a Low Molecular Weight Silane Monomer

DSC analysis (non-oxidative):

Transition	Onset Temperature / °C	Peak Maximum / °C	Enthalpy of Transition / J g^{-1}
Exotherm	98.1	108	0.322

Solid State NMR:

^{13}C NMR data (100.5 MHz, δ): -1.94 (Si(CH$_3$)$_3$); 1.59 (t, SiCH$_3$); 17.60 (s, SiCH$_2$); 24.16 (s, CH$_2$); 40.80 (s, CH$_2$ next to carborane); 76.34 (s, BCB carborane carbon)

^{11}B NMR data (128 MHz, δ): -4.13, -11.09, -13.87, -15.45 (q (b), BH)

FTIR (ν/cm^{-1}[45° reflectance]): 2970 (aliphatic CH$_3$); 2600 (B-H); 2160 (Si-H bond); 1275 (Si-CH$_3$); 1100 (Si-O stretch); 915 (B-H rock); 850 (Si-(CH$_3$)$_2$);

2:1 Carborane Siloxane Network

Yield = > 99 %

Thermogravimetric analysis:

Run	Onset Degradation Temperature / °C	Temperature Maximum Mass Loss / °C	Char Residue / % @ 800 °C
Non-oxidative	553	570	73.9
Oxidative	569	571	81.1

DSC analysis (non-oxidative):

Transition	Onset Temperature / °C	Peak Maximum / °C	Enthalpy of Transition / J g^{-1}
T$_g$	-58.6	-58.2	-
Exotherm	107	121	1.86

5.1 Synthesis of a Carborane-Siloxane Network Using 1,7-Diallyl-m-Carborane and a Low Molecular Weight Silane Monomer

Solid State NMR:

^{13}C NMR data (100.5 MHz, δ): 1.69 (t, Si$\underline{C}$H$_3$); 17.70 (s, Si$\underline{C}$H$_2$); 24.20 (s, $\underline{C}$H$_2$); 40.80 (s, C$\underline{H}_2$ next to carborane); 76.39 (s, B$\underline{C}$B carborane carbon)

^{11}B NMR data (128 MHz, δ): -4.55, -11.09, -13.87, (t (b), $\underline{B}$H)

FTIR (ν/cm^{-1}[45° reflectance]): 2970 (aliphatic CH$_3$); 2600 (B-H); 2160 (Si-H bond); 1275 (Si-CH$_3$); 1100 (Si-O stretch); 915 (B-H rock); 850 (Si-(CH$_3$)$_2$);

3:1 Carborane Siloxane Network

Yield = > 99 %

Thermogravimetric analysis:

Run	Onset Degradation Temperature / °C	Temperature Maximum Mass Loss / °C	Char Residue / % @ 800 °C
Non-oxidative	535	569	60.0
Oxidative	520	550	78.3

DSC analysis (non-oxidative):

Transition	Onset Temperature / °C	Peak Maximum / °C	Enthalpy of Transition / J g^{-1}
T$_g$	-27.9	-14.7	-

Solid State NMR:

^{13}C NMR data (100.5 MHz, δ): 1.83 (t, Si$\underline{C}$H$_3$); 18.18 (s, Si$\underline{C}$H$_2$); 24.35 (s, $\underline{C}$H$_2$); 40.50 (s, C$\underline{H}_2$ next to carborane); 76.53 (s, B$\underline{C}$B carborane carbon)

^{11}B NMR data (128 MHz, δ): -11.25, -13.63 (d (b), $\underline{B}$H)

5.1 Synthesis of a Carborane-Siloxane Network Using 1,7-Diallyl-m-Carborane and a Low Molecular Weight Silane Monomer

FTIR (ν/cm^{-1}[45° reflectance]): 2975 (aliphatic CH_3); 2600 (B-H); 1275 (Si-CH_3); 1100 (Si-O stretch); 915 (B-H rock); 850 (Si-$(CH_3)_2$)

4:1 Carborane Siloxane Network

Yield = > 99 %

Thermogravimetric analysis:

Run	Onset Degradation Temperature / °C	Temperature Maximum Mass Loss / °C	Char Residue / % @ 800 °C
Non-oxidative	514	556	63.5
Oxidative	519	552	72.9

DSC analysis (non-oxidative):

Transition	Onset Temperature / °C	Peak Maximum / °C	Enthalpy of Transition / J g^{-1}
T_g	-24.3	-12.0	-

Solid State NMR:

^{13}C NMR data (100.5 MHz, δ): 1.93 (t, Si$\underline{C}H_3$); 18.08 (s, Si$\underline{C}H_2$); 24.54 (s, $\underline{C}H_2$); 41.19 (s, $\underline{C}H_2$ next to carborane); 76.82 (s, B$\underline{C}$B carborane carbon)

^{11}B NMR data (128 MHz, δ): -13.33 (s (b), $\underline{B}$H)

FTIR (ν/cm^{-1}[45° reflectance]): 2975 (aliphatic CH_3); 2600 (B-H); 1275 (Si-CH_3); 1100 (Si-O stretch); 915 (B-H rock); 850 (Si-$(CH_3)_2$)

5:1 Carborane Siloxane Network

Yield = > 99%

5.1 Synthesis of a Carborane-Siloxane Network Using 1,7-Diallyl-m-Carborane and a Low Molecular Weight Silane Monomer

Thermogravimetric analysis:

Run	Onset Degradation Temperature / °C	Temperature Maximum Mass Loss / °C	Char Residue / % @ 800 °C
Non-oxidative	510	557	64.1
Oxidative	523	553	67.5

DSC analysis (non-oxidative):

Transition	Onset Temperature / °C	Peak Maximum / °C	Enthalpy of Transition / J g^{-1}
T$_g$	-29.3	-23.0	-

Solid State NMR:

^{13}C NMR data (100.5 MHz, δ): 1.93 (t, SiC̲H$_3$); 18.08 (s, SiC̲H$_2$); 24.35 (s, C̲H$_2$); 40.60 (s, C̲H$_2$ next to carborane); 76.73 (s, BC̲B carborane carbon)

^{11}B NMR data (128 MHz, δ): -12.14 (s (b), B̲H)

FTIR (ν/cm^{-1}[45° reflectance]): 2975 (aliphatic CH$_3$); 2600 (B-H); 1275 (Si-CH$_3$); 1100 (Si-O stretch); 915 (B-H rock); 850 (Si-(CH$_3$)$_2$)

6:1 Carborane Siloxane Network

Yield = > 98 %

Thermogravimetric analysis:

Run	Onset Degradation Temperature / °C	Temperature Maximum Mass Loss / °C	Char Residue / % @ 800 °C
Non-oxidative	466	569	51.2
Oxidative	493	549	62.8

5.1 Synthesis of a Carborane-Siloxane Network Using 1,7-Diallyl-m-Carborane and a Low Molecular Weight Silane Monomer

DSC analysis (non-oxidative):

Transition	Onset Temperature / °C	Peak Maximum / °C	Enthalpy of Transition / J g^{-1}
T_g	-32.0	-25.2	-

Solid State NMR:

^{13}C NMR data (100.5 MHz, δ): 1.93 (t, Si$\underline{C}$H$_3$); 18.18 (s, Si$\underline{C}$H$_2$); 24.74 (s, $\underline{C}$H$_2$); 41.09 (s, $\underline{C}$H$_2$ next to carborane); 76.82 (s, B$\underline{C}$B carborane carbon)

^{11}B NMR data (128 MHz, δ): -11.84 (s (b), $\underline{B}$H)

FTIR (ν/cm^{-1}[45° reflectance]): 2975 (aliphatic CH$_3$); 2600 (B-H); 1275 (Si-CH$_3$); 1100 (Si-O stretch); 850 (Si-(CH$_3$)$_2$)

5.1.1 Extraction of Residues from 6:1 Carborane Siloxane Network

About 200 mg of the 6:1 carborane siloxane network material was weighed out accurately. This was then added to a two dram tall screw cap vial, 5 ml of THF was then added to the vial, the contents were shaken and left overnight to allow the material to swell. After this time the excess solvent was removed and the material dried in an oven for two hours. The dried product was then accurately reweighed. This was carried out in duplicate. The process was also repeated swelling the polymer in deuterated chloroform and performing NMR analysis on the resulting solvent extract.

Experimental Data:

Adjusted Yield = 83.76 % +- 0.32 %

Thermogravimetric analysis:

Run	Onset Degradation Temperature / °C	Temperature Maximum Mass Loss / °C	Char Residue / % @ 800 °C
Non-oxidative	450	553	62.0

DSC analysis (non-oxidative):

Transition	Onset Temperature / °C	Peak Maximum / °C	Enthalpy of Transition / J g^{-1}
T_g	-28.7	-23.8	-

NMR data of extract:

^{1}H NMR data (400MHz, CDCl$_3$; δ): 0.10 (t, 0.53H, C$\underline{H}_3$); 1.63 (s (b), 1H, B$\underline{H}$), 5.03 (q, 0.08H, C$\underline{H}_2$); 5.52 (d, 0.22H, ?); 5.801 (q, 0.22H, C$\underline{H}_2$);

^{11}B NMR data (128MHz, CDCl$_3$; δ): -6.74, -10.75, -12.28, -15.10 (s (b), $\underline{B}$H)

FTIR (v/cm^{-1}[45° reflectance]): 2975 (aliphatic CH_3); 2600 (B-H); 1275 (Si-CH_3); 1100 (Si-O stretch); 850 (Si-$(CH_3)_2$)

5.2 Synthesis of a Carborane-Siloxane Network via Hydrosilylation Using High Molecular Mass Poly(hydrosiloxanes)

To a 25 ml beaker 5.0 g of poly(dimethylsiloxane-*co*-methylhydrosiloxane) with an average molar mass (M_n) ~13,000 g mol^{-1} was added. To this solution 1,7 bis(allyl)*m*-carborane (0.17 g, 0.76 mmol) was added. Karstedt's catalyst (platinum(0)-1,3-divinyl-1,1,3,3-tetramethyldisiloxane) was loaded onto the end of a pipette and three drops were added to the solution containing the reactants. The reaction mixture was stirred for ten seconds using a high shear stirrer. After a short delay the material started to harden and turn dark brown, during this time the temperature of the sample rose to about 80 °C. The material was allowed to cool then post-cured in an oven at 60 °C overnight. A light yellow opaque rubber was obtained as the final product.

The reaction was repeated where the molar ratio of the carborane to the copolymer was increased to 1:6.

Experimental Data:

2:1 Carborane Siloxane Network:

FTIR (ν/cm^{-1}[ATR]): 2965, 2915 (aliphatic CH$_3$); 2600 (B-H); 1410 (C-H bend); 1260 (Si-CH$_3$); 1080, 1000 (Si-O stretch); 915 (B-H rock); 860 (Si-(CH$_3$)$_2$); 785 (Si-CH$_3$)

6:1 Carborane Siloxane Network:

FTIR (ν/cm^{-1}[ATR]): 3430, 3330 (H$_2$O); 2965, 2915 (aliphatic CH$_3$); 2600 (B-H); 1680, 1600 (H$_2$0); 1450, 1410 (C-H bend); 1260 (Si-CH$_3$); 1085, 1010 (Si-O stretch); 915 (B-H rock); 865 (Si-(CH$_3$)$_2$); 785 (Si-CH$_3$)

5.3 Synthesis of a PDMS Network Using a Low Molecular Mass Vinyl Siloxane and a Low Molecular Mass Poly(hydrosiloxane)

To a 25 ml beaker 5.0 g of poly(dimethylsiloxane-*co*-methylhydrosiloxane) with an average molar mass (M_n) ~950 g mol^{-1} was added. To this solution vinyl terminated poly(dimethylsiloxane) (1.95 g, 10.5 mmol) with an average molar mass of ~186 g mol^{-1} was added. Karstedt's catalyst (platinum(0)-1,3-divinyl-1,1,3,3-tetramethyldisiloxane) was loaded onto the end of a pipette and three drops added to the solution containing the reactants. The reaction mixture was stirred for ten seconds using a high shear stirrer. After a short delay the material started to harden and turn dark brown. The material was allowed to react for five minutes then post-cured in an oven at 60 °C overnight. A light yellow opaque rubber was obtained as the final product.

The reaction was repeated where the molar ratio of the vinyl terminated PDMS to the copolymer was increased to 6:1.

Experimental Data:

2:1 Siloxane Network:

FTIR (v/cm^{-1}[ATR]): 2965, 2910 (aliphatic CH$_3$); 1415 (C-H bend); 1260 (Si-CH$_3$); 1080, 1010 (Si-O stretch); 860 (Si-(CH$_3$)$_2$); 785 (Si-CH$_3$)

6:1 Siloxane Network:

FTIR (v/cm^{-1}[ATR]): 2965, 2910 (aliphatic CH$_3$); 1440, 1415 (C-H bend); 1260 (Si-CH$_3$); 1080, 1000 (Si-O stretch); 865 (Si-(CH$_3$)$_2$); 780 (Si-CH$_3$)

5.4 Synthesis of a PDMS Network Using a High Molecular Mass Vinyl Siloxane and a Low Molecular Mass Silane

To a 25 ml beaker 4.52 g of vinyl terminated poly(dimethylsiloxane) with an average molar mass (M_n) ~4305 g mol^{-1} was added. To this solution poly(dimethylsiloxane-*co*-methylhydrosiloxane) (0.5 g, 0.52 mmol) with an average molar mass (M_n) ~950 g mol^{-1} was added. Karstedt's catalyst (platinum(0)-1,3-divinyl-1,1,3,3-tetramethyldisiloxane) was loaded onto the end of a pipette and three drops were added to the solution containing the reactants. The reaction mixture was stirred for ten seconds using a high shear stirrer. After a short delay the material started to harden and turn dark brown. The material was allowed to react for five minutes then post-cured in an oven at 60 °C overnight. A light yellow opaque rubber was obtained as the final product.

The reaction was repeated where the molar ratio of the vinyl terminated PDMS to the copolymer was increased to 6:1.

Experimental Data:

2:1 Siloxane Network:

FTIR (v/cm^{-1}[ATR]): 3350 (H_2O); 2965, 2915, 2880 (aliphatic CH_3); 1640 (H_2O); 1410 (C-H bend); 1260 (Si-CH_3); 1085, 1010 (Si-O stretch); 840 (Si-(CH_3)$_2$); 785, 770 (Si-CH_3)
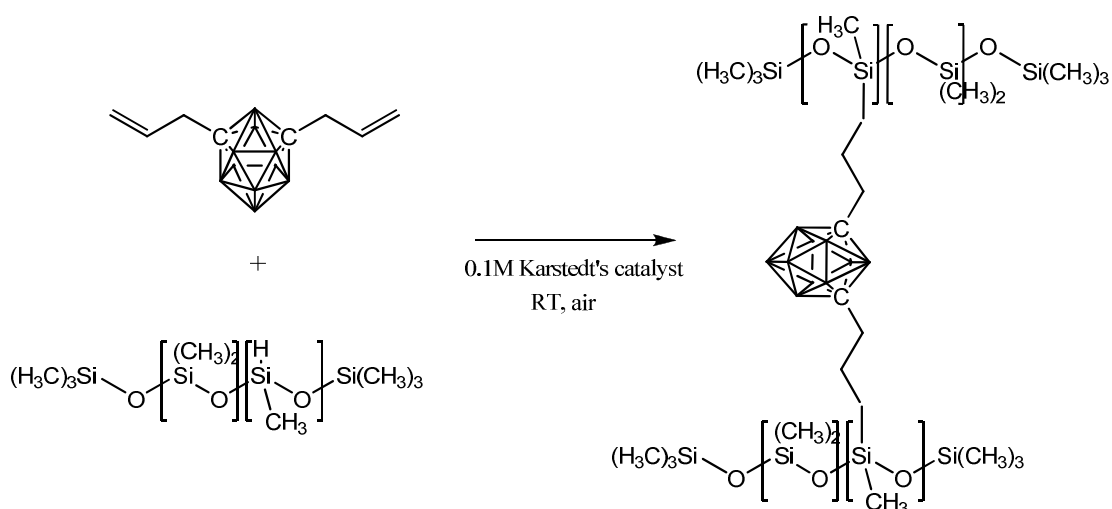
6:1 Siloxane Network:

FTIR (v/cm^{-1}[ATR]): 3440 (H_2O); 2965, 2915, 2880 (aliphatic CH_3); 1600 (H_2O); 1450, 1410 (C-H bend); 1260 (Si-CH_3); 1085, 1010 (Si-O stretch); 840 (Si-(CH_3)$_2$); 785, 770 (Si-CH_3)

5.5 Hydrosilylation Formed Siloxane-Carborane Networks

The use of hydrosilylation in the attempt to link an allyl carborane to a poly(hydrosiloxane) has been successful. Yields for the reaction are high, reaction times are short and the catalyst is not sensitive to oxidising conditions so can be carried out in an open beaker or open mould. By varying the carborane content the amount of cross-linking that can take place will increase until the system is saturated. To study the reaction further synthesis of samples from 1:1 to 6:1 carborane to copolymer by molar ratio have been synthesised and tested, the reaction is shown in Scheme 5.1:

Scheme 5.1: Hydrosilylation of 1,7-diallyl-*m*-carborane with poly(dimethylsiloxane-*co*-methylhydrosiloxane) to form a cross-linked network polymer.

In order to perform a comprehensive study samples have been formed *via* the hydrosilylation route that give a range of different materials. The following samples from Sections 5.1 - 5.4 have been assigned nomenclature found in the Table below for the purpose of comparing the thermal degradation properties of the hydrosilylation networks. They fall into four types of materials, carborane or non-carborane containing networks and open or closed networks:

Sample Identity	1,7-diallyl-*m*-carborane / Molar Mass (g mol^{-1})	Vinyl end capped PDMS / Molar Mass (g mol^{-1})	Poly(dimethylsiloxane-*co*-methylhydrosiloane) / Molar mass (g mol^{-1})
Section 5.1: 6:1 carborane siloxane closed network	224	-	950
Section 5.2: 6:1 carborane siloxane open network	224	-	13,000
Section 5.3: 6:1 siloxane closed network	-	186	950
Section 5.4: 6:1 siloxane open network	-	4305	950

Table 5.1: Identities of all samples in Chapter 5 showing molecular mass of monomers
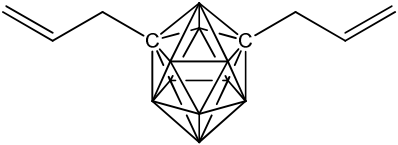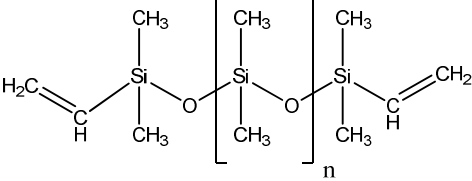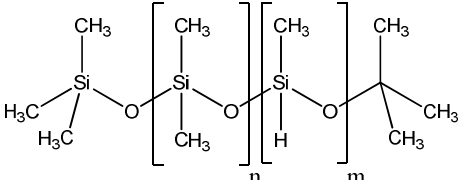
Monomer	Chemical Structure
1,7-diallyl-*m*-carborane	
Vinyl end capped PDMS	
Poly(dimethylsiloxane-*co*-methylhydrosiloane)	

Table 5.2: Structures of Monomer units:

Sample Name	Mass Fraction of vinyl cross-linker	Mass fraction of copolymer
Section 5.1: 6:1 carborane siloxane closed network	0.19	0.81
Section 5.2: 6:1 carborane siloxane open network	0.03	0.97
Section 5.3: 6:1 siloxane closed network	0.28	0.72
Section 5.4: 6:1 siloxane open network	0.90	0.10

Table:5.3: Mass fraction of cross-linker to copolymer in each network sample

Where molecular mass of the two monomer units are low a closed network is formed. When the molecular mass is high for one of the monomers a more open network is formed. The non-carborane containing materials will act as a reference for understanding the behaviour of the carborane containing networks.

Two methods were used to characterise the materials formed. 45° reflectance FTIR of the series of related samples revealed that greater than 2:1 loading of carborane lead to a loss of the absorption at both 2160 and 960 cm^{-1}. These signals correspond to the silane (Si-H) groups on the backbone of the polymer and the loss of intensity shows the carborane reaction has proceeded. Solid state ^{13}C NMR spectroscopy was then used to confirm that all the free vinyl groups had been bound into the system. Initial studies revealed only reacted vinyl groups in the ^{13}C NMR and ^{11}B signals were broad. To further investigate the vinyl groups the contact time was varied for the 3:1 and 6:1 carborane-siloxane closed network samples where the contact time experiment is described in more detail in Chapter 2.7. The results of these experiments are shown below in Figures 5.1-5.2:

Reacted CH$_2$ from vinyl groups

CH$_2$ adjacent to carborane

Carborane carbons

Figure 5.1: Solid state ^{13}C NMR of 3:1 vinyl carborane-siloxane closed network copolymer after varying contact time 0.5 ms (black line) and 10 ms (red line)

Unreacted Vinyl Group

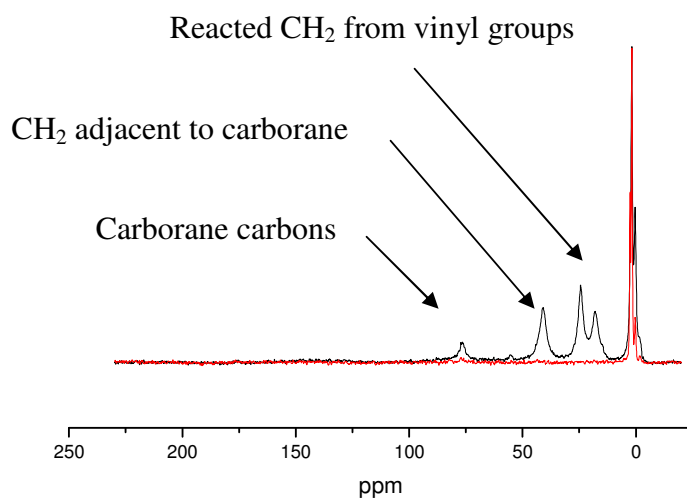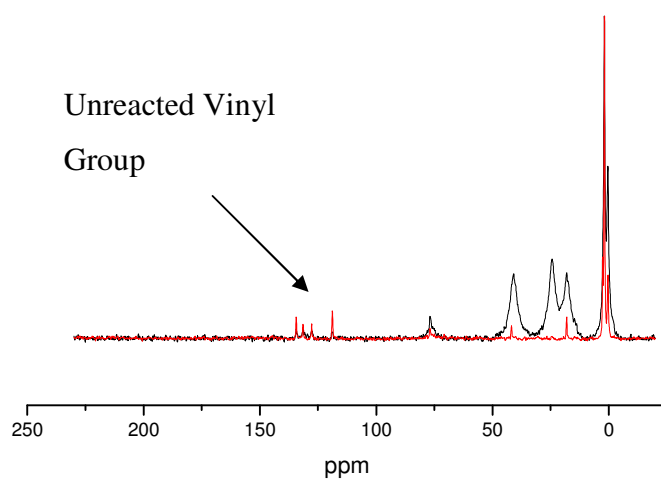**Figure 5.2**: Solid state ^{13}C NMR of 6:1 vinyl carborane-siloxane closed network copolymer varying contact time 0.5 ms (black line) and 10 ms (red line)

5.5 Hydrosilylation Formed Siloxane-Carborane Networks

For the 3:1 carborane-siloxane closed network sample all the vinyl groups on the carborane have been bound to network as no peaks appear at longer contact times. For the 6:1 sample a series of lines appear under the original peaks and around 130 ppm at longer contact times. This indicates there are still free vinyl groups arising from pendant attachment of the carborane where the carborane was unable to react with two polymer units.

The morphology of the samples were compared by use of DSC analysis. The material is completely different to the original PDMS elastomer as shown in Figure 5.3. Whereas there was a large crystalline endotherm in the DSC of the PDMS sample the 2:1 and 6:1 carborane-siloxane closed networks show only a T_g transition. This is probably due to the fast rate of cure preventing any crystalline regions from forming. Also the T_g transition is more pronounced with increasing carborane content due to the increased amorphous content:
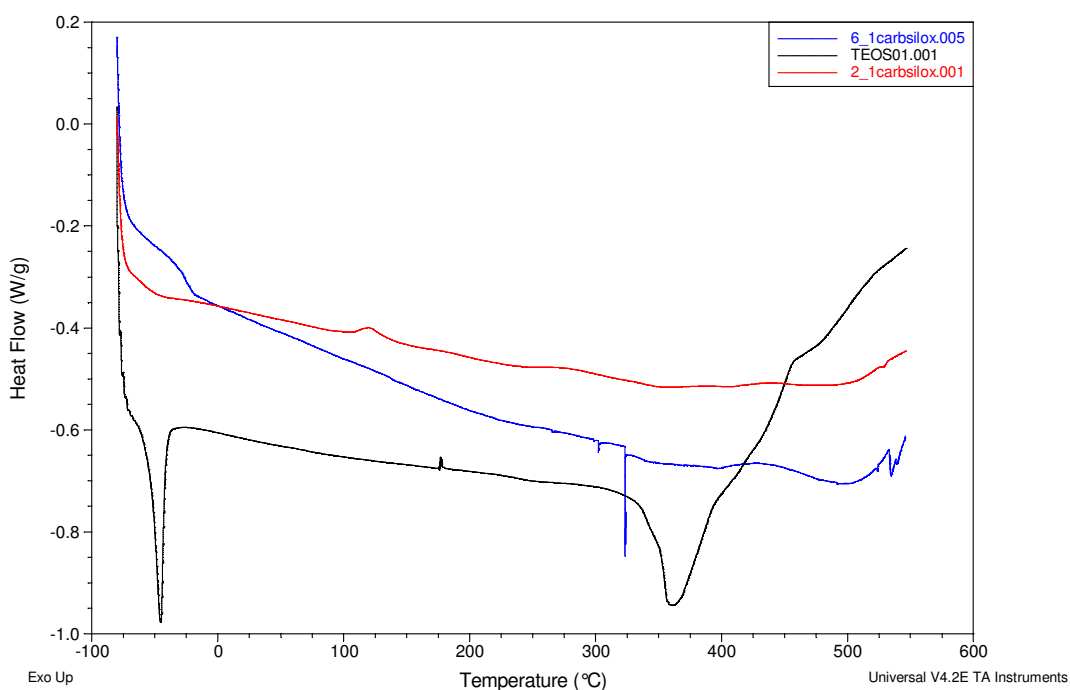
Figure 5.3: DSC comparing PMDS elastomer (black line), 2:1 carborane-siloxane closed network material (red line) and 6:1 carborane-siloxane closed network (blue line). Morphology of the new network material is completely changed

Thermal stability of these materials have been improved over the original formulation of the PMDS elastomer systems used in Chapter 3 and are typical for PDMS polymers bound to carboranes. In order to fully assess the thermal stability of these materials TGA was employed. The results are shown in the non-oxidative TGA plot shown in Figure 5.4:
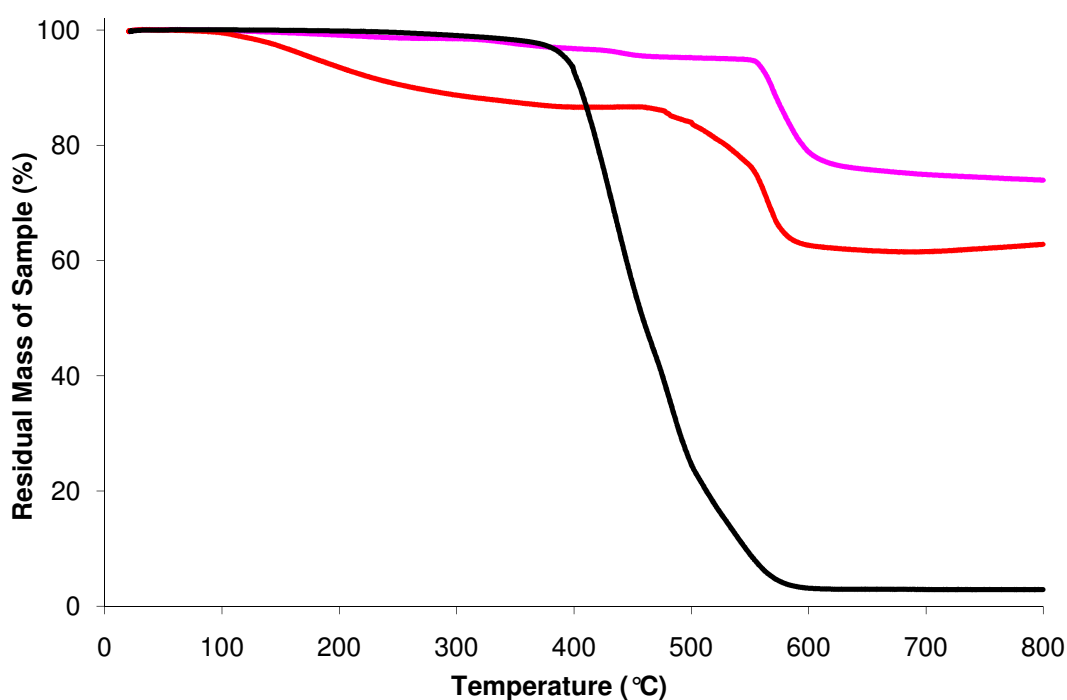
Figure 5.4: Non-oxidative TGA comparing original tin catalysed PDMS elastomer (black line) to 2:1 carborane-siloxane closed network material (pink line) and 6:1 carborane-siloxane closed network material (red line)

From the data, the 2:1 network material shows the highest onset of degradation temperature with high char residues of 80%. The 6:1 network is suffering from volatile loss at reduced temperatures and is similar to that for the vinyl dispersed systems discussed earlier. To further investigate this weight loss a 6:1 carborane-

siloxane closed network sample was extracted with THF and deuterated chloroform. The chloroform was collected after 24 hours of immersing the sample. After this time the polymer was dried in an oven overnight. The TGA of the extracted 6:1 carborane-siloxane closed network is shown in Figure 5.5:
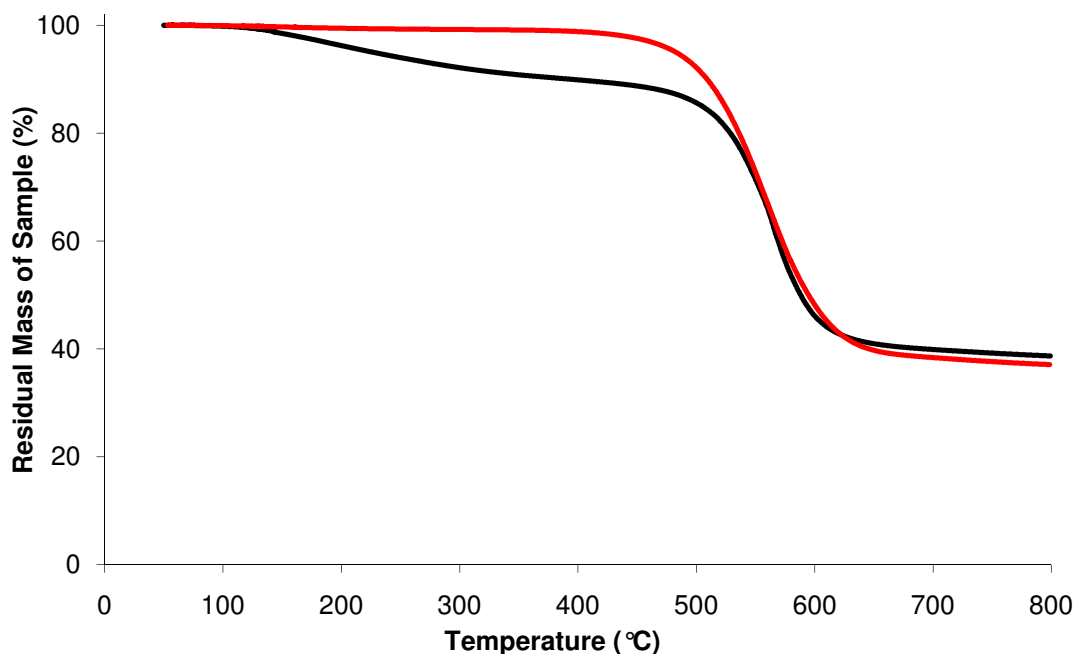
Figure 5.5: Non-oxidative TGA comparing 6:1 carborane-siloxane closed network (black line) against 6:1 washed carborane-siloxane closed material (red line)

Extracting the material removes the initial volatile loss in the sample before the main degradation event occurs, which is unaffected by the extracting process. The ^{1}H NMR of the chloroform extract revealed that unreacted diallyl carborane was present and also some unbound siloxane polymer. The removal of these extractable materials should give a true reflection of the degradation of the bound network.

The next sample to be investigated was the 6:1 carborane-siloxane open network material. The backbone of the silane-siloxane copolymer has been extended to incorporate a large, flexible non-cross-linked region. The effect of this physical change on the thermal degradation behaviour is shown in Figure 5.6:
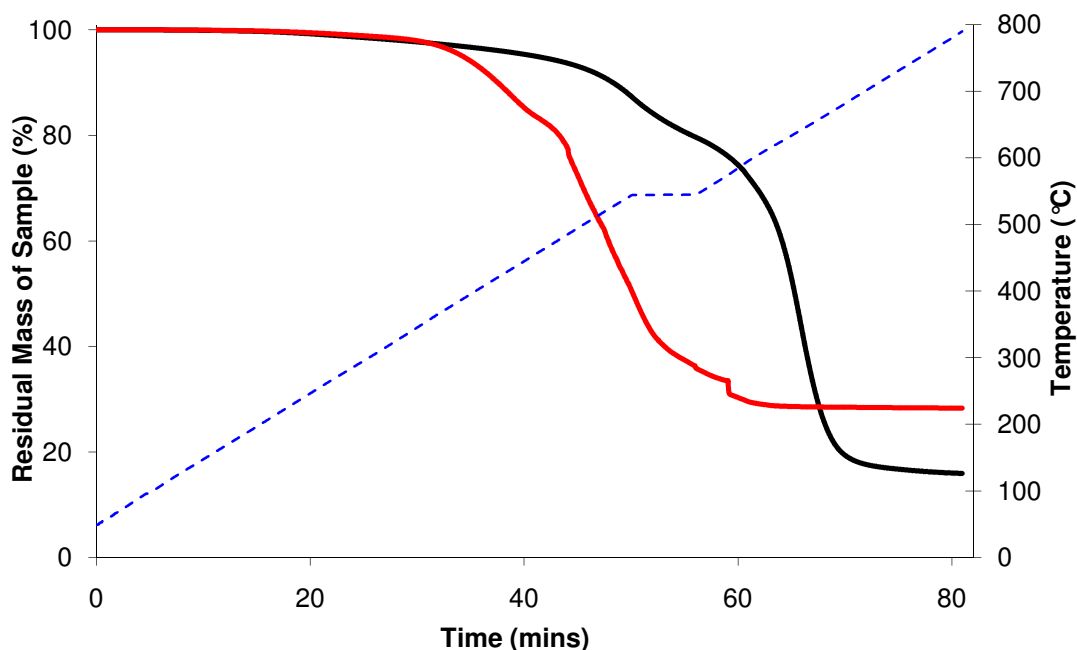
Figure 5.6: TGA analysis of 6:1 carborane-siloxane open network; non-oxidative run (black line) and oxidative run (red line) including temperature profile of run (blue dotted line)

Run	Onset Degradation Temperature / °C	Temperature Maximum Mass Loss / °C	Char Residue / % @ 800 °C
Non-oxidative	447	645	15.9
Oxidative	337	573	28.3

The first problem encountered with this network was sample dropout when approaching the degradation temperatures. Sample dropout occurs when the sample leaves the TGA pan during degradation, either due to foaming of the sample or jumping of the sample due to vigorous volatilisation. The TGA temperature program had to be reduced from 10 °C per minute to 2 °C per minute over the temperature of maximum sample loss (540-550 °C). Although not directly comparable to the TGA data in Figures 5.4-5.5 it is indicative of reduced thermal stability with an increase in amount of volatiles formed during degradation and also reduced onset of degradation temperatures versus the closed network systems.

In order to complete the TGA study the thermal degradation of both the 6:1 siloxane closed network and the 6:1 siloxane open network was investigated and shown in Figure 5.7:
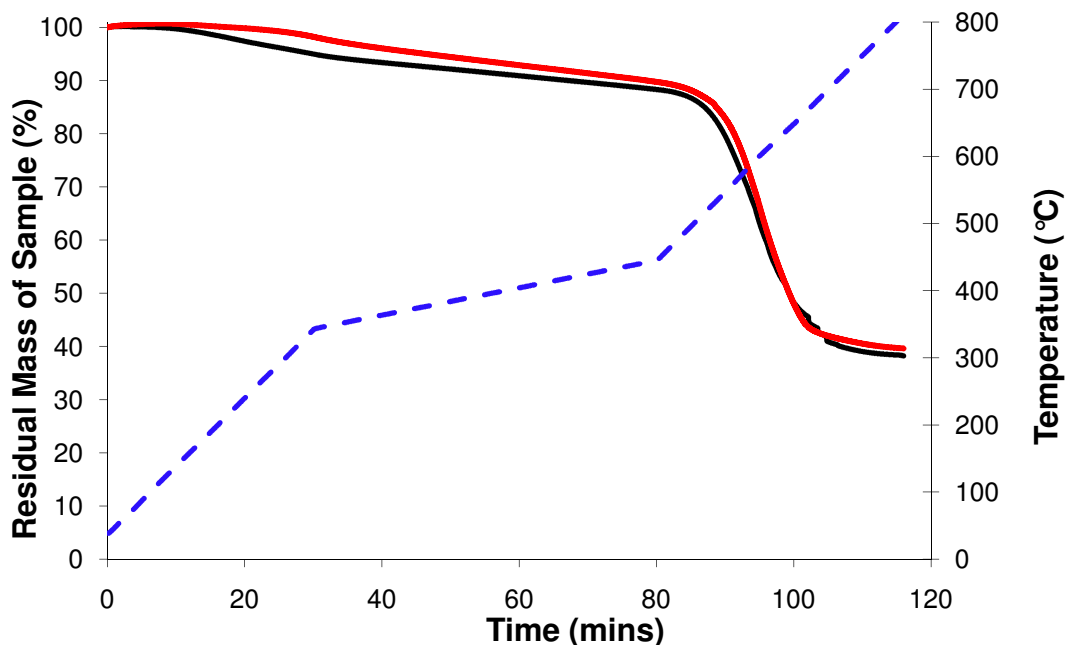
Figure 5.7: Non-oxidative TGA analysis of 6:1 siloxane closed network (black line) and 6:1 siloxane open network (red line) including temperature profile of run (blue dotted line)

Sample	Onset Degradation Temperature / °C	Temperature Maximum Mass Loss / °C	Char Residue / % @ 800 °C
6:1 closed siloxane elastomer	484	670	38.2
6:1 open siloxane elastomer	499	601	39.6

Again problems were encountered when running the TGA, the samples required a slower heating programme to avoid issues with sample dropout. The onset temperatures of degradation of these non-carborane containing networks is

197

remarkable given the carborane is usually thought to contribute to the thermal stability of the networks. The char residues are much smaller for the non-carborane networks which are typical of the observed degradation behaviour in the previous Chapter. In the next Section thermal volatilisation analyses of the hydrosilylation carborane-siloxane networks are investigated.

5.6 Thermal Volatilisation Analysis of Hydrosilylation Formed Carborane Siloxane Networks

In the previous Chapter the presence of carboranes in the material is suggested to have been responsible for the dehydrogenation event as it thermally degrades. The following Sections compare the degradation of all the hydrosilylation materials synthesised in this Chapter in order to assess the origin of the volatiles that form during thermal degradation. Additional data is available in the Appendix.

5.6.1 Degradation Run

The results for the degradation runs show that the carborane-containing networks obtained by hydrosilylation are degrading in a completely different manner from that seen previously for the $FeCl_3$ catalysed carborane-siloxane network in Chapter 4. The degradation runs for the 2:1, 6:1 and 6:1 extracted carborane siloxane closed networks are compared in Figure 5.8:
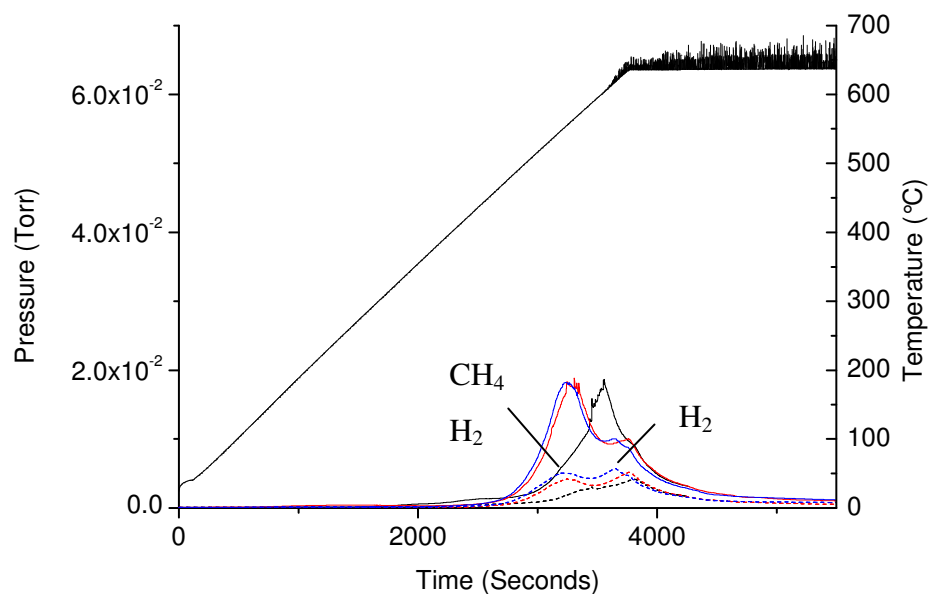
Figure 5.8: Degradation runs comparing the 2:1, 6:1 and 6:1 extracted carborane-siloxane closed network materials. Total volatiles evolved of 2:1 (black line), 6:1 (red line) and 6:1 washed (blue line) closed network materials are shown. Also non-condensable products are shown for 2:1(black dashed line), 6:1 (red dashed line) and 6:1 washed (blue dashed line) where all pressure peaks are shown against time with furnace temperature (dotted line) on second axis

Sample	Onset Degradation Temperature / °C	Peak Temperature of Maximum Volatile Loss (Non-condensable) / °C	Peak Temperature of Maximum Volatile Loss (Condensable) / °C
2:1 closed	279	627	604
6:1 closed	402	621	564
6:1 washed closed	394	604	553

In the degradation step the major non-condensable volatiles detected are hydrogen and methane. The presence of hydrogen is indicative of dehydrogenation occurring, however, this process occurs twice where methane is linked to the first

dehydrogenation event. This was confirmed by the use of single-ion monitoring on the mass spectrometer. By use of online mass spectrometry it is possible to assess semi-quantitatively the amount of analyte being evolved by each polymer sample. The amount of hydrogen and methane given off is shown for the 6:1 carborane-siloxane closed network in Figure 5.9:
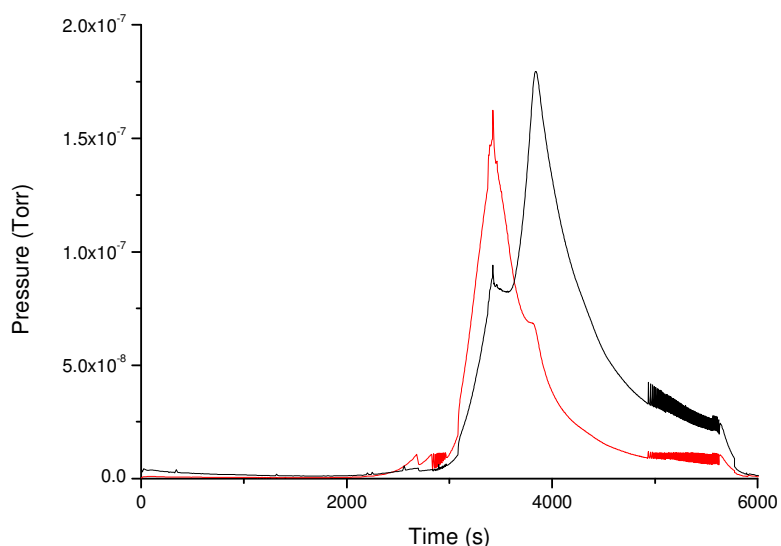
Figure 5.9: Faraday scanning mode on the mass spectrometer for the degradation step of the 6:1 carborane siloxane closed elastomer, running to 650 °C. Total amount of hydrogen m/z 2 (black line) and methane m/z 16 (red line) evolved is shown

From the pressure data in Figure 5.8 it was observed that the degradation event begins at 450 °C for the 6:1 carborane-siloxane network materials with two distinct non-condensable peaks. As Figure 5.9 shows, the first event is the evolution of methane with hydrogen and the second is the result of a separate dehydrogenation event. The second event occurs at higher temperature and is similar to the dehydrogenation event observed in the $FeCl_3$ materials in Chapter 4, but since the events are linked it is not possible to determine the cause of each event in this case. The hydrogen could arise from the thermal degradation of either unreacted silane or the carborane thermally degrading.

5.6.1 Degradation Run

In order to gain a further understanding of the degradation step the siloxane copolymer was increased in dimethylsiloxane content by increasing the molecular mass from 950 g mol^{-1} to 13,000 g mol^{-1}. This would give the material an extended dimethylsiloxane backbone which is more similar to the PDMS type materials studied before whilst also decreasing the cross link density of the material. The degradation of the 6:1 carborane-siloxane open network material is compared to the 6:1 carborane-siloxane closed network material and shown in Figure 5.10:
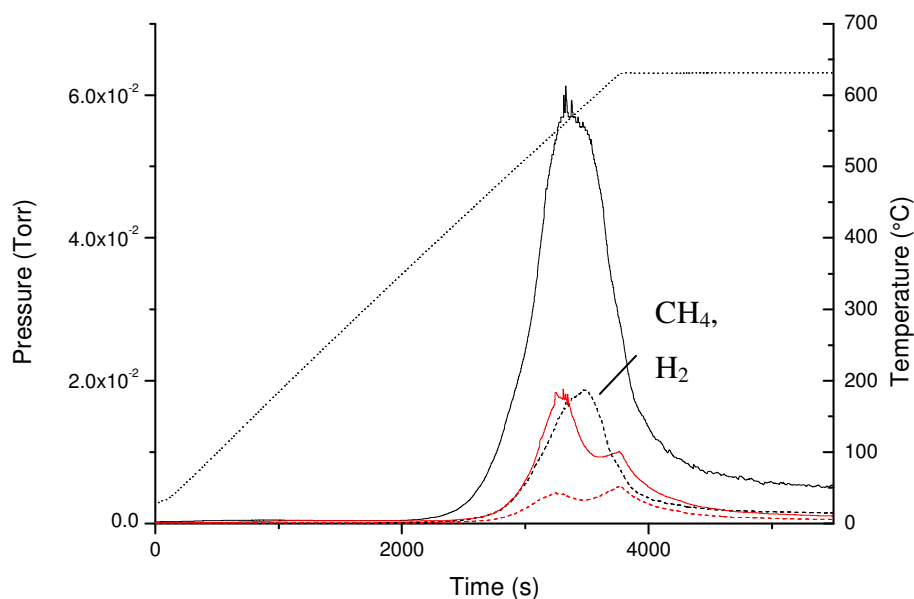
Figure 5.10: Degradation run of the 6:1 carborane-siloxane open network compared to the 6:1 carborane-siloxane closed network material. Total volatiles evolved of 6:1 open (black line) and 6:1 closed (red line) samples are shown. Also non-condensable products are shown for 6:1 open (black dashed line) and 6:1 closed (red dashed line) where all pressure peaks are shown against time with furnace temperature (dotted line) on second axis

5.6.1 Degradation Run

Sample	Onset Degradation Temperature / °C	Peak Temperature of Maximum Volatile Loss (Non-condensable) / °C	Peak Temperature of Maximum Volatile Loss (Condensable) / °C
6:1 open	356	579	562
6:1 closed	402	621	564

Although the molar ratios of carborane and siloxane are the same in both samples due to the similar number of silane groups available for cross-linking, the increased length of the dimethylsiloxane content changes the degradation profile. The increase in molecular mass of the polymer backbone has decreased the onset of degradation of the material from 402 °C to 356 °C. Also, three times the amount of condensable and non-condensable volatiles were obtained. This is in line with the mass loss from the TGA experiment where the 6:1 open network has lower char residues than the 6:1 closed network under non-oxidative degradation. The non-condensable peak was investigated further using the online mass spectrometer and the result is shown in Figure 5.11:
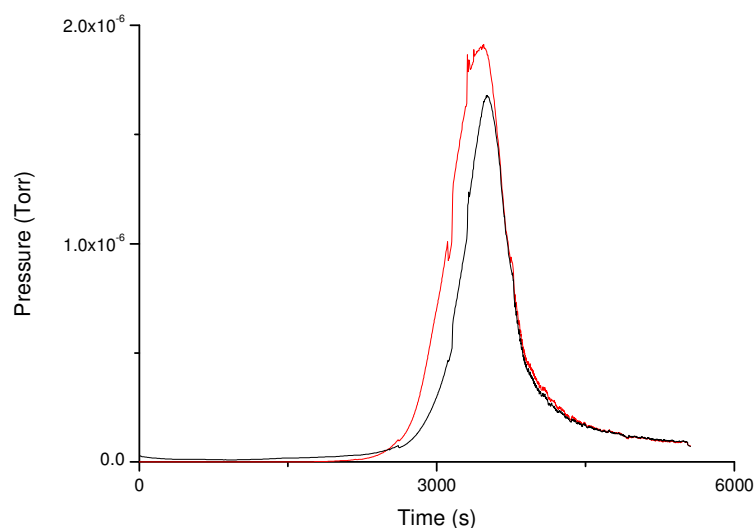
5.6.1 Degradation Run

Figure 5.11: Faraday scanning mode on the mass spectrometer for the degradation step of the 6:1L carborane-siloxane network material, running to 650 °C. Total amount of hydrogen m/z 2 (black line) and methane m/z 16 (red line) evolved is shown

In this case the second dehydrogenation event is no longer observed where the amount of methane evolved is higher than the amount of hydrogen formed. In Figure 5.9 the peak evolution of hydrogen was 1.75×10^{-7} Torr and as the molar ratio of carborane is similar in the open network the second event may no longer be observable as the mass fraction of carborane in the open network is about $1/6^{th}$ of the closed system. This could mean the first dehydrogenation event is linked to the breakdown of the poly(dimethylsiloxane-*co*-methylhydrosiloxane) copolymer and hence by implication the 2nd is due to the dehydrogenation of *m*-carborane.

The last TVA degradation experiment in this subsection compares non-carborane containing hydrosilylation networks to the carborane-siloxane networks. For this comparison two materials have been synthesised, the first 6:1 siloxane closed elastomer where the carborane in the 6:1 closed network was replaced with a vinyl end capped siloxane of comparable molecular mass. The second, 6:1 siloxane open elastomer increases the molecular mass of the vinyl end-capped siloxane elastomer

5.6.1 Degradation Run

from 186 g mol^{-1} to 4300 g mol^{-1} to increase the flexibility in the network. The comparison of the 6:1 siloxane closed network, 6:1 siloxane open network and 6:1 carborane-siloxane network materials are shown in Figure 5.12:
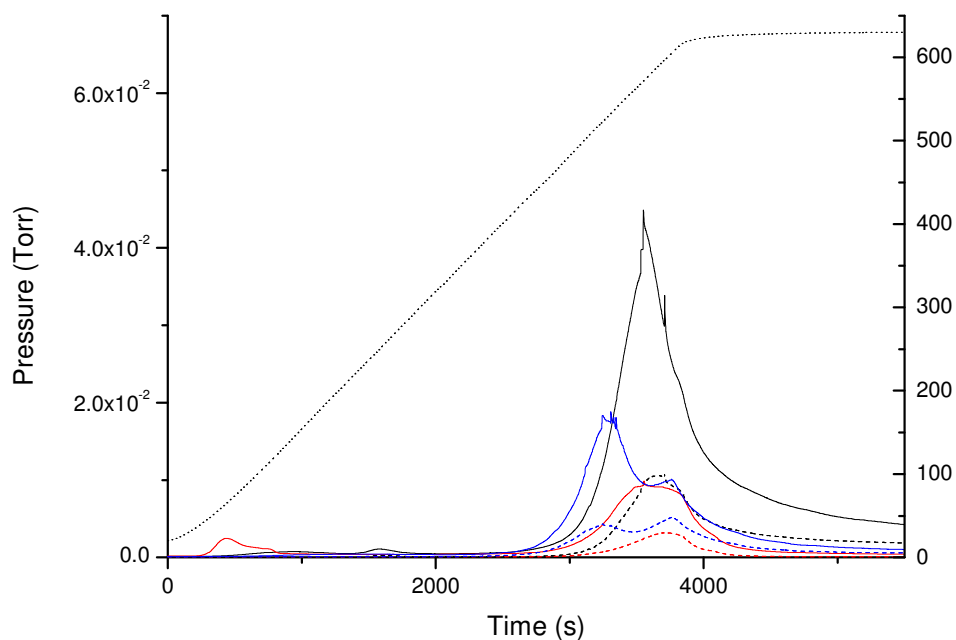
Figure 5.12: Degradation run comparing the 6:1 siloxane closed and 6:1 siloxane open networks to the 6:1 carborane-siloxane network. Total volatiles evolved of 6:1 siloxane closed (black line), 6:1 siloxane open (red line) and 6:1 carborane-siloxane closed (blue line) network materials are shown. Also non-condensable products are shown for 6:1 closed siloxane (black dashed line), 6:1 open siloxane (red dashed line) and 6:1 carborane-siloxane closed (blue dashed line) networks where all pressure peaks are shown against time with furnace temperature (dotted line) on second axis

Sample	Onset Degradation Temperature / °C	Peak Temperature of Maximum Volatile Loss (Non-condensable) / °C	Peak Temperature of Maximum Volatile Loss (Condensable) / °C
6:1 siloxane closed	400	576	571
6:1 siloxane open	423	579	566
6:1 carborane-siloxane closed	402	621	564

The degradation runs show the PDMS only networks are as thermally stable as the carborane containing network due to their comparable onset of degradation temperatures. Also, the maximum evolution of condensable volatiles occurs at higher temperatures for the PDMS only networks. These two inferences lead to the conclusion that the carboranes are not responsible for the high thermal stability of these networks and appear to be less thermally stable. The Faraday scanning mode mass spectrometer of the PDMS networks are compared in Figure 5.13:
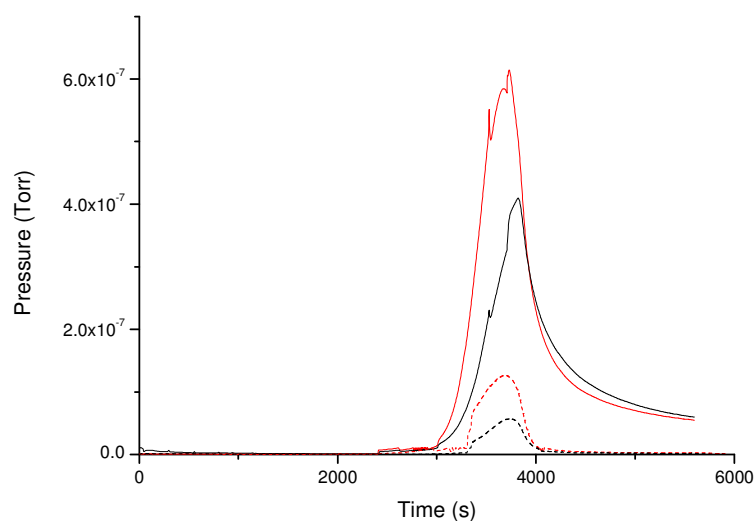
Figure 5.13: Faraday scanning mode on the mass spectrometer for the degradation step, running to 650 °C. Total amount of hydrogen m/z 2 (black line) and methane m/z 16 (red line) evolved where 6:1 siloxane closed (solid lines) and 6:1 siloxane open (dashed lines) networks are shown

The non-condensable volatiles in the PDMS only networks are methane and smaller quantities of hydrogen. The methane is a product of the degradation of the poly(dimethylsiloxane-*co*-methylhydrosiloxane) copolymer. However, there is still a significant source of dehydrogenation in the sample and no carborane present. To elucidate the source of hydrogen in the degrading sample the mass spectrum from the SATVA of the tin catalysed network is shown in Figure 5.14:
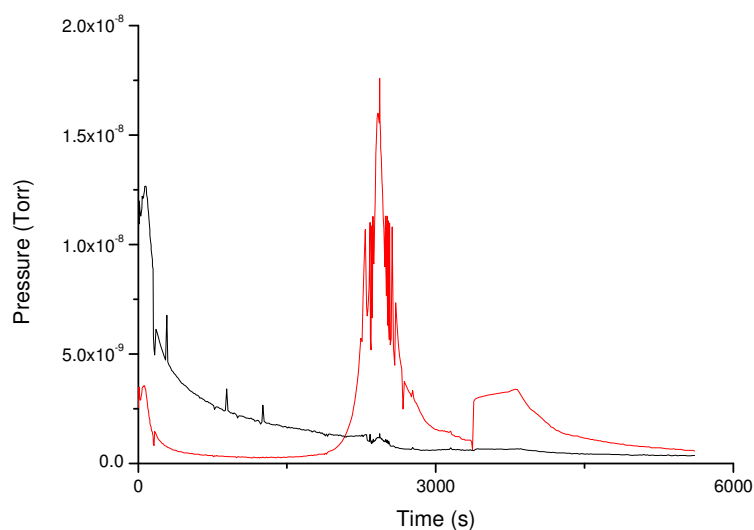
Figure 5.14: Faraday scanning mode on the mass spectrometer for the degradation
step of the tin catalysed PDMS network, running to 650 °C. Total amount of
hydrogen m/z 2 (black line) and methane m/z 16 (red line) evolved are shown

In the tin catalysed PDMS elastomer network the reactive groups are cross-linking
silicon ethers and hydroxyl groups where the polymer backbone consists of $-CH_3$
groups. As there is no dehydrogenation in the tin catalysed PDMS elastomer network
sample it can be assumed the source of hydrogen is coming from unreacted hydride
sites on the backbone of the copolymer.

In the next Section the sub-ambient distillation of the products from degradation of
these materials is studied.

5.6.2 Sub-ambient Distillation

The sub-ambient distillation of the products from the 2:1 carborane-siloxane closed
network was carried out and is shown in Figure 5.15:
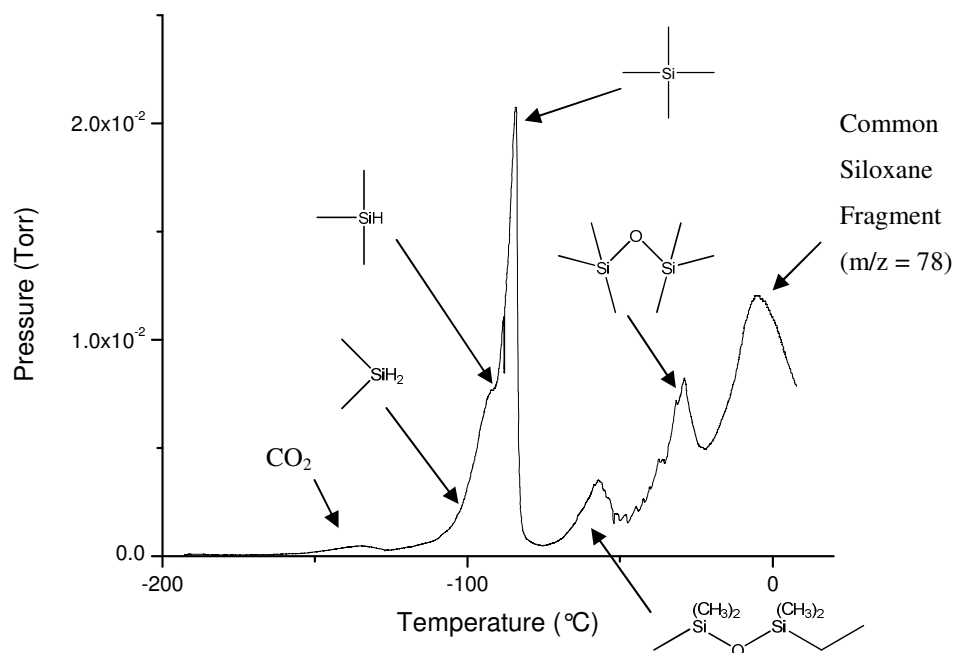
5.6.2 Sub-ambient Distillation

Figure 5.15: Sub-ambient distillation of 2:1 carborane-siloxane closed network material. Exit pressure from trap (black line) plotted against trap temperature

The sub-ambient distillation step reveals a series of low molecular mass silanes are distilled at around -100 °C. These silanes may be generated from breakdown of the silane side groups on the siloxane backbone. Also, small siloxane ring fragments are obtained at the end of the distillation which is similar to the species formed when siloxane only networks form. The formation of D_3 and D_4 siloxane rings are a common degradation fragment in these materials. The common siloxane fragmengt is a breakdown product in the online mass spectrometer, potentially $HSi(OH)_2CH_3$ is the species formed.

The sub-ambient distillation of the 6:1 carborane-siloxane closed network material is shown in Figure 5.16 where the accompanying mass spectrum is shown in Figure 5.17:

Figure 5.16: Sub-ambient distillation of 6:1 carborane-siloxane closed network material. Exit pressure from trap (black line) plotted against trap temperature

Figure 5.17: Faraday scanning mode on the mass spectrometer for sub-ambient distillation step of the 6:1 carborane-siloxane closed elastomer. Total amount of CO_2 m/z 44 (black line), silane m/z 58 (red line), silane 2 m/z 73 (blue line), siloxane m/z 147 (pink line) and water m/z 18 (green line) evolved is shown

5.6.2 Sub-ambient Distillation

The results indicate the amount of free silane evolved during degradation has reduced with increasing carborane content By analysing the mass spectrum in Faraday mode the amount of tetramethylsilane to trimethylsilane is about 6:1 which is a strong indication that the diallyl carborane monomer has reacted with the available silane groups on the siloxane copolymer. Water was detected as a degradation product and can only be present as a result of the degradation process in the reaction as the materials for synthesis are kept dry and post-cured. Also, a carborane peak is detected which could be the result of either unreacted carborane monomer volatilising during degradation or pendant carborane groups on the copolymer breaking off during the degradation event.

The sub-ambient distillation of the 6:1 extracted carborane-siloxane closed material is shown in Figure 5.18 where the accompanying mass spectrum is shown in Figure 5.19:
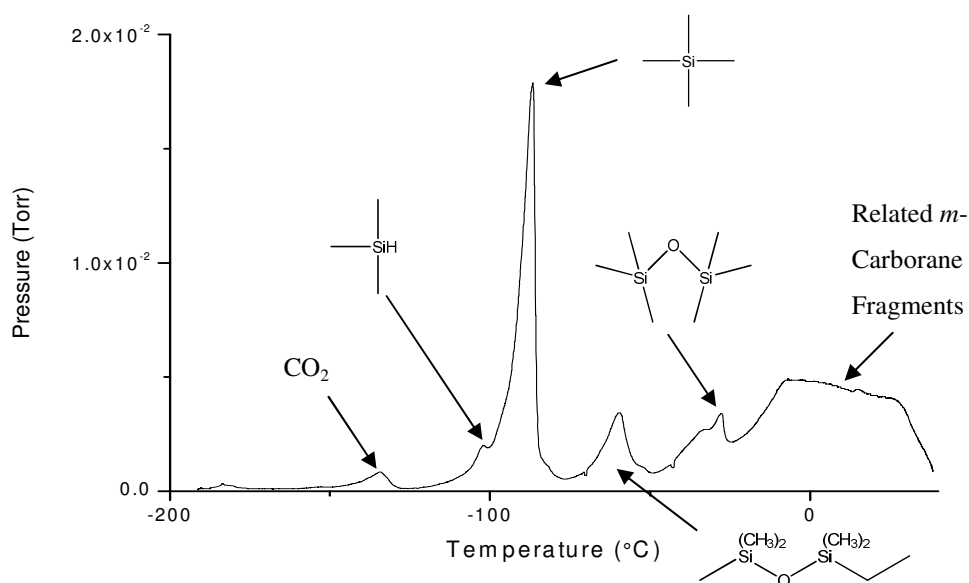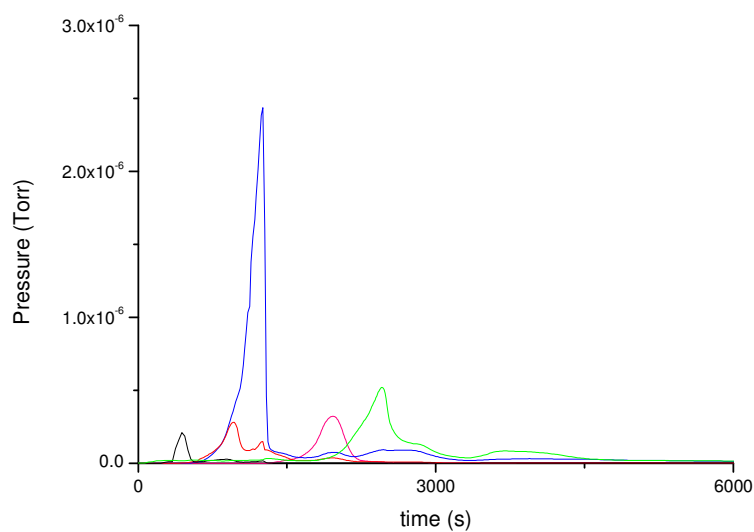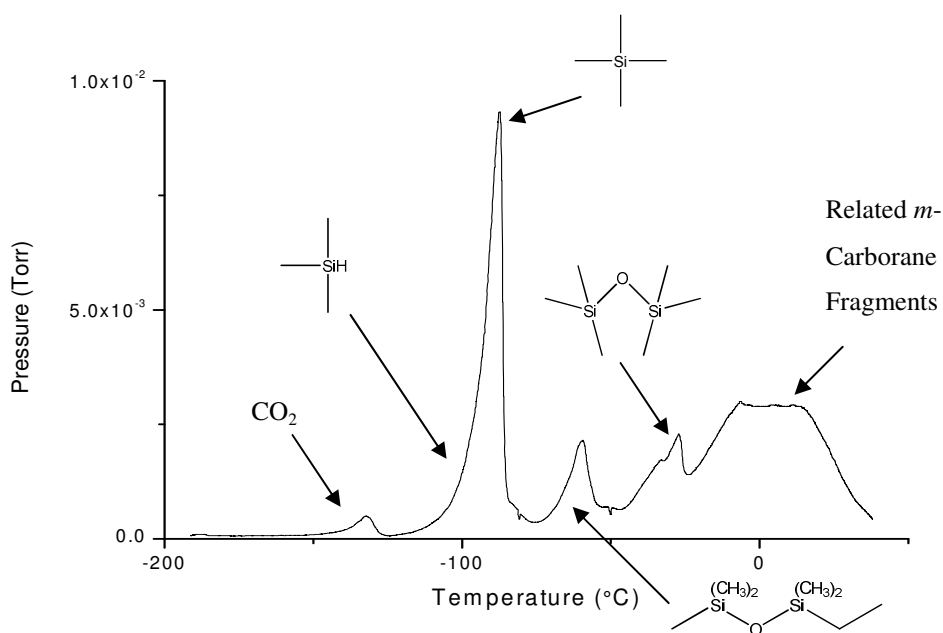

Figure 5.18: Sub-ambient distillation of 6:1 extracted carborane-siloxane closed network material. Exit pressure from trap (black line) plotted against trap temperature
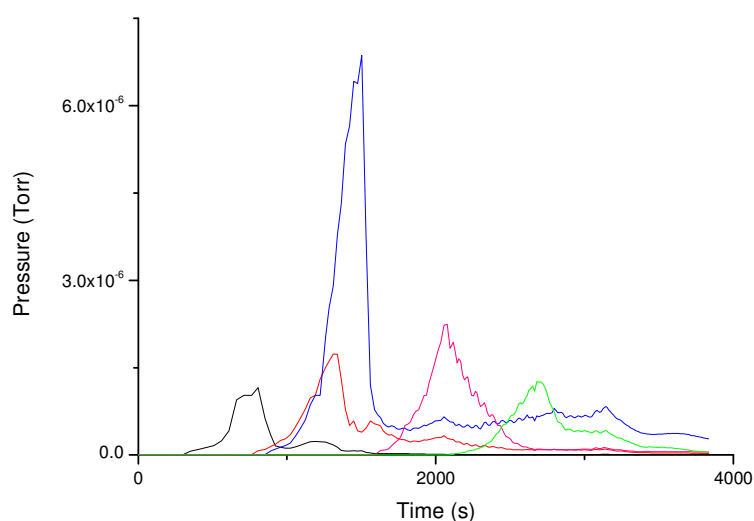
Figure 5.19: Faraday scanning mode on the mass spectrometer for sub-ambient distillation step of the 6:1 washed carborane-siloxane closed material. Total amount of CO_2 m/z 44 (black line), trimethylsilane m/z 58 (red line), tetramethylsilane m/z 73 (blue line) and D_2 siloxane m/z 147 (pink line) and D_3 siloxane m/z 207 (green line) evolved is shown

On comparison of the peak pressures in the mass spectra the effect of extracting the 6:1 carborane-siloxane closed network material is to lower the ratio of tetramethylsilane to trimethylsilane from 6:1 to 4:1. This is most likely due to the removal of species able to migrate from the siloxane copolymer material. Also the overall amount of silane volatiles collected has been reduced by half suggesting a significant amount of polymeric material has been extracted from the network. Carboranes are again detected which indicates that the carboranes decouple from the polymer network under thermal degradation.

The 6:1 carborane-siloxane open network material sub-ambient distillation is shown in Figure 5.20 with the accompanying mass spectrum shown in Figure 5.21:

5.6.2 Sub-ambient Distillation

Figure 5.20: Sub-ambient distillation of 6:1 carborane-siloxane open network material. Exit pressure from trap (black line) plotted against trap temperature

Figure 5.21: Faraday scanning mode on the mass spectrometer for sub-ambient distillation step of the 6:1 carborane-siloxane open elastomer. Total amount of CO_2 m/z 44 (black line), silane m/z 58 (red line), silane 2 m/z 73 (blue line), siloxane m/z 147 (pink line) and siloxane 207 m/z (green line) evolved is shown

5.6.2 Sub-ambient Distillation

By increasing the dimethylsiloxane content of the networks and reducing the cross-link density the sub-ambient distillation of the 6:1 carborane-siloxane open material looks completely different to the previous materials. The amount of tetramethylsilane is now much reduced where the amount of siloxane species has increased significantly. This keeps in proportion of what would be expected when increasing dimethylsiloxane content of the polymer network. The carborane peak normally observed for the closed network towards the end of the distillation is not present. This is probably dwarfed by the siloxane peaks due to the mass fraction of carborane in the sample being 1/6th than in the carborane-siloxane closed network. Also, trace amounts of water have appeared in the distillation which suggests that again water is potentially a product from a degradation process in the material.

The 6:1 siloxane closed network material sub-ambient distillation is shown in Figure 5.22 with the accompanying mass spectrum shown in Figure 5.23:
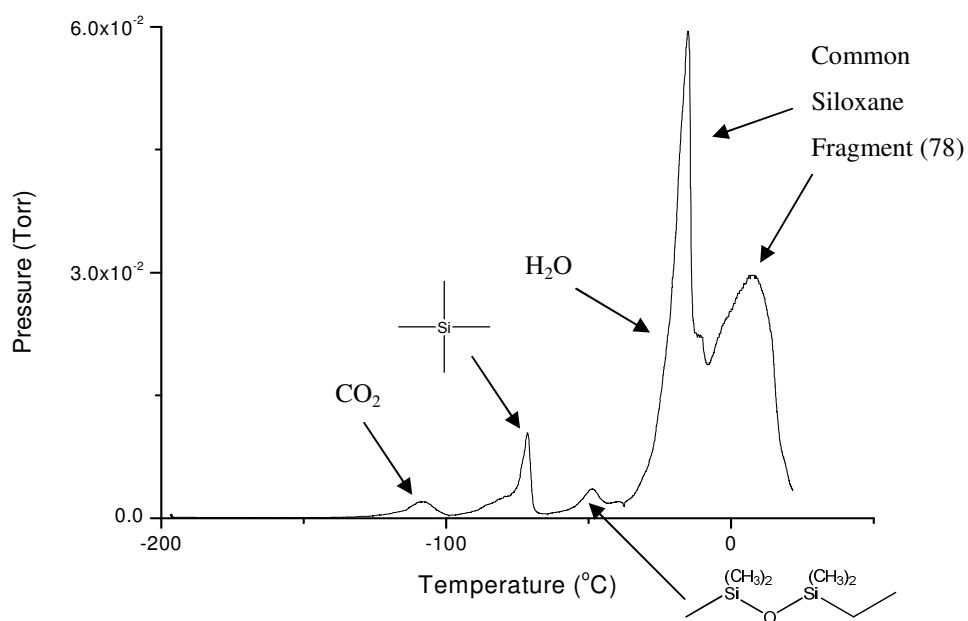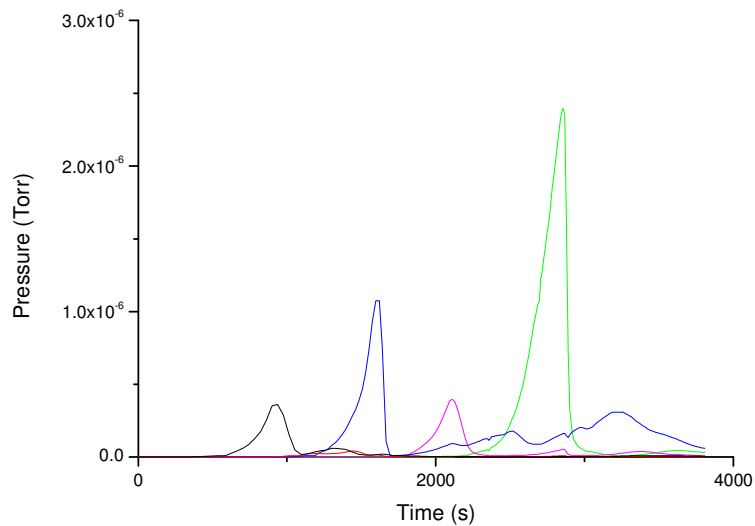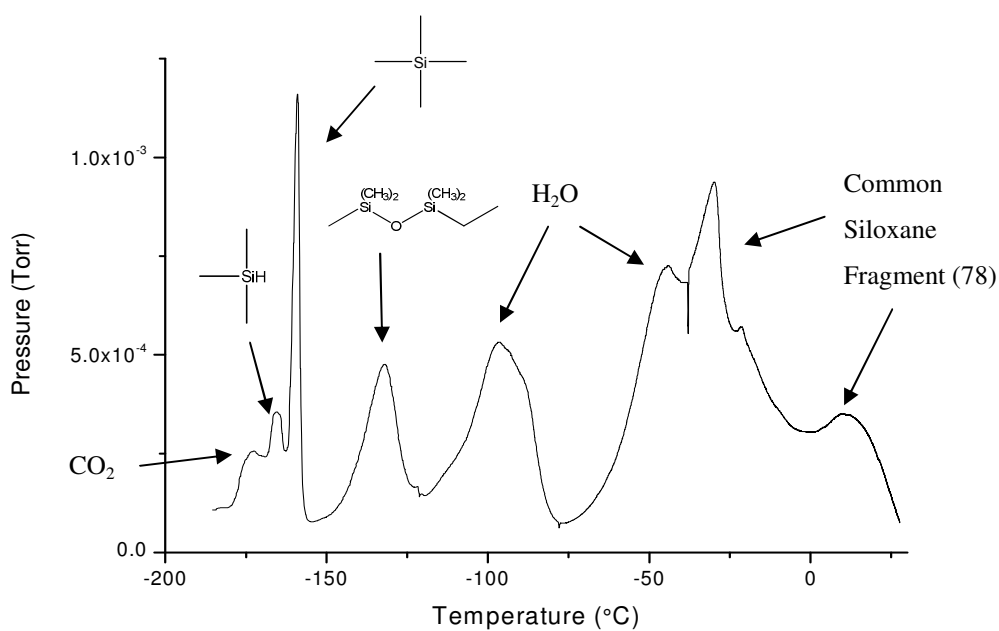

Figure 5.22: Sub-ambient distillation of 6:1 siloxane closed network material. Exit pressure from trap (black line) plotted against trap temperature
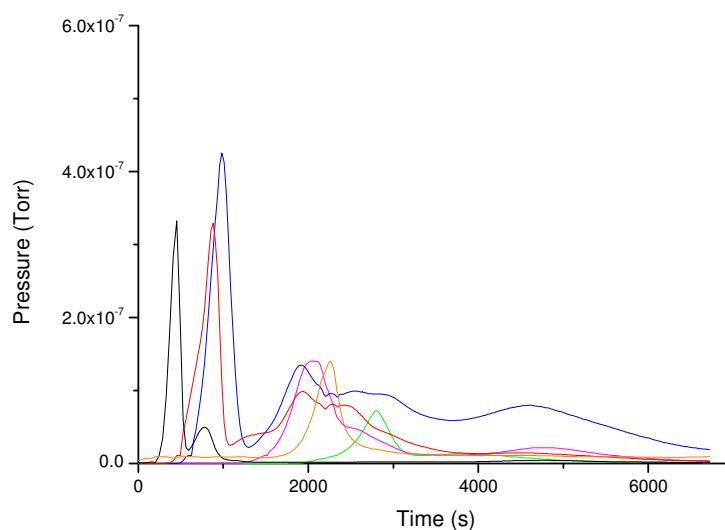
5.6.2 Sub-ambient Distillation

Figure 5.23: Faraday scanning mode on the mass spectrometer for sub-ambient distillation step of the 6:1 siloxane closed elastomer. Total amount of CO_2 m/z 44 (black line), silane m/z 58 (red line), silane 2 m/z 73 (blue line), siloxane m/z 147 (pink line), siloxane 2 m/z 207 (green line) and water m/z 17 (orange line) evolved is shown

The 6:1 siloxane closed material is the siloxane only material that is a direct comparison with the 6:1 carborane-siloxane elastomer material. The 6:1 siloxane closed network sub-ambient distillation has tetramethylsilane and trimethylsilane evolution in common with the 6:1 carborane containing samples. Also small siloxane rings are evolved as part of the degradation event. The major degradation analyte formed is water, which is produced in larger quantities than in previous samples. This would suggest water evolution is unrelated to the presence of carborane in the polymer.

The 6:1 siloxane open network material sub-ambient distillation is shown in Figure 5.24 with the accompanying mass spectrum shown in Figure 5.25:
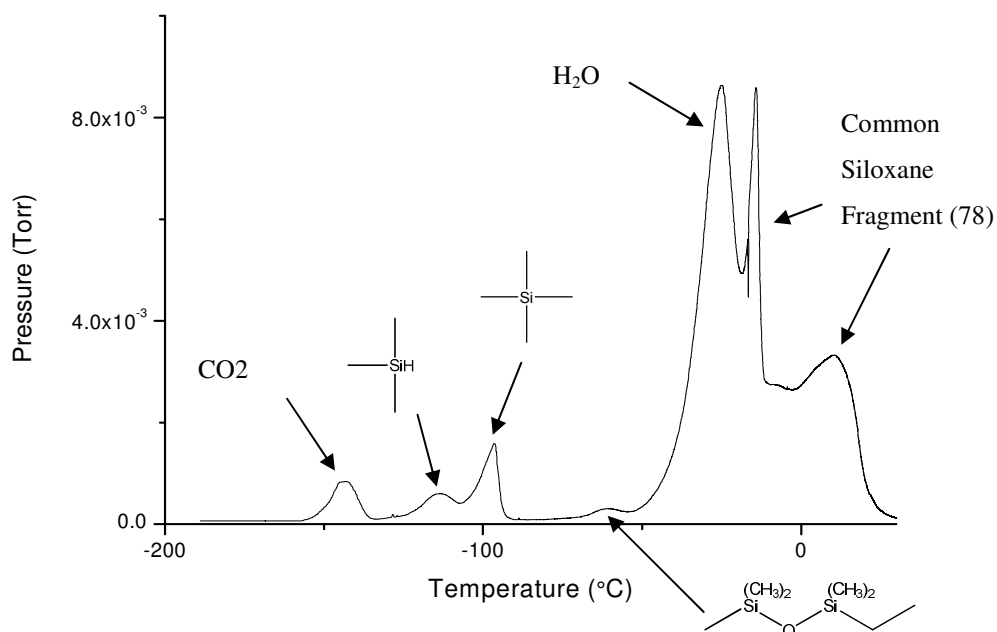
Figure 5.24: Sub-ambient distillation of 6:1 siloxane open network material. Exit pressure from trap (black line) plotted against trap temperature
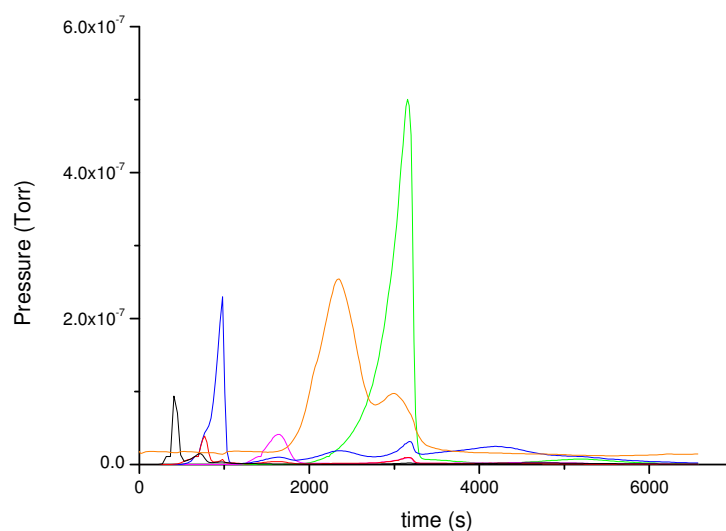
Figure 5.25: Faraday scanning mode on the mass spectrometer for sub-ambient distillation step of the 6:1 siloxane open elastomer. Total amount of CO_2 m/z 44 (black line), silane m/z 58 (red line), silane 2 m/z 73 (blue line), siloxane m/z 147 (pink line), siloxane 2 m/z 207 (green line) and water m/z 17 (orange line) evolved is shown

216

5.6.2 Sub-ambient Distillation

The 6:1 siloxane open network sample has an increase in dimethylsiloxane content and an increase in the open volume of the material compared to the 6:1 siloxane closed sample. The trend is similar to that seen before with the change between 6:1 carborane-siloxane closed sample to 6:1 carborane-siloxane open sample where the amount of tetramethylsilane is now reduced and the amount of siloxane species evolved has increased. Also, the amount of water distilled has increased which could indicate the formation of water is directly linked to the dimethylsiloxane content by previous data in this Section.

The next Section investigates the trends in the degradation products found in the limbs and cold ring during the TVA runs.

5.6.3 Limb and Cold Fraction Analysis

The analysis of the degradation products found in the cold ring and limbs on the TVA has been carried out for all the hydrosilylation networks discussed previously in this Chapter. The analyses of the limbs are the major distillate peaks observed by the pressure gauges which have been re-trapped further down the line and distilled into gas phase IR cells. More usually Limb 4 is a combined FTIR and GC cell that allows for further interrogation of the higher molecular mass fragments. The cold ring analysis consists of preparation of the higher molar mass residues into an appropriate solvent for GC analysis.

As the amount of spectroscopic data generated in this comparative study is considerable the spectroscopic peak data for each limb will be tabulated. The FTIR peaks found for each sample in limb 1 is shown in Table 5.4:

5.6.3 Limb and Cold Fraction Analysis

Sample Identity	Wavenumber (cm^{-1})	Peak Identities
2:1 carborane-siloxane network	2925, 2850, 2350	aliphatic CH_3, CO_2
6:1 carborane-siloxane network	2925, 2850	aliphatic CH_3,
6:1 washed carborane-siloxane network	3300, 2925, 2850,	OH group, aliphatic CH_3
6:1L carborane-siloxane network	2925, 2850	aliphatic CH_3
6:1S carborane-siloxane network	2950, 2925, 2850	aliphatic CH_3
6:1V carborane-siloxane network	2925, 2850	aliphatic CH_3

Table 5.4: Limb 1 FTIR (v/cm^{-1}[NaCl]):

In limb one, the main degradation component identified was CO_2 in various amounts where strength of absorbance was dependant on amount of CO_2 in each gas phase IR-cell. The peak present at 2950 cm^{-1} appears as a weak shoulder peak in most cases. This is likely to be an indication of the amount of CO_2 degrading from the vinyl containing monomers. The peaks observed in limb two are shown in Table 5.5:

Sample Identity	Wavenumber (cm^{-1})	Peak Identities
2:1 carborane-siloxane closed network	2970, 2925, 2850, 2350, 2145, 2130, 2110, 1250, 915, 900, 875, 700	aliphatic CH_3, CO_2, Si-H, Si-CH_3 stretch, Si-H, Si-$(CH_3)_2$, Si-H
6:1 carborane-siloxane closed network	2970, 2925, 2850, 2125, 1425, 1250, 925, 875, 700	aliphatic CH_3, Si-H, C-H stretch, Si-CH_3 stretch, Si-$(CH_3)_2$, Si-H
6:1 washed carborane-siloxane closed network	2970, 2900, 2825, 2125, 1450, 1250, 920, 915, 875, 700	aliphatic CH_3, Si-H, Si-H stretch, C-H stretch, Si-CH_3 stretch, Si-$(CH_3)_2$, Si-H
6:1 carborane-siloxane open network	2970, 2920, 2850, 2125, 1425, 910, 870, 690	aliphatic CH_3, Si-H, Si-H stretch, C-H stretch, Si-CH_3 stretch, Si-$(CH_3)_2$, Si-H
6:1 siloxane closed network	2970, 2925, 2850, 2125, 1460, 1250, 910, 870	aliphatic CH_3, Si-H, Si-H stretch, C-H stretch, Si-CH_3 stretch, Si-$(CH_3)_2$, Si-H
6:1 siloxane open network	2950, 2925, 2850, 870	aliphatic CH_3, Si-H

Table 5.5: Limb 2 FTIR (v/cm^{-1}[NaCl]):

In limb two, various low molecular mass silanes were isolated from each sample. These silanes are common to all the degrading materials and therefore arise from the breakdown of the silane component in the copolymer. The cold trap was silanated which decreased the separation between similar silane species during distillation. Silanation of the trap is performed to modify the glass in order to increases the hydrophobicity of the glass surface. Without this treatment any water in the system would mask other volatiles of interest. The consequence is that it is not possible to identify the silane compounds as they distil using FTIR. The following FTIR peaks were found in limb 3 and shown in Table 5.6:

Sample Identity	Wavenumber (cm^{-1})	Peak Identities
2:1 carborane-siloxane closed network	2970, 2925, 2850, 2400, 2150, 1450, 1275, 1250, 1075, 875, 750, 700	aliphatic CH_3, CO_2, Si-H, C-H stretch, Si-CH_3, Si-O stretch, Si-$(CH_3)_2$, Si-CH_3,Si-H
6:1 carborane-siloxane closed network	2975, 2920, 2850, 2125, 1475, 1250, 1075, 915, 905, 850	aliphatic CH_3, Si-H, C-H stretch, Si-CH_3, Si-O stretch, Si-H, Si-$(CH_3)_2$
6:1 washed carborane-siloxane closed network	2970, 2920, 2850, 1275, 1075, 850	aliphatic CH_3, Si-CH_3, Si-O stretch, Si-$(CH_3)_2$
6:1 carborane-siloxane open network	2975, 2930, 2850, 1460, 1075, 850,	aliphatic CH_3, C-H stretch, Si-O stretch, Si-$(CH_3)_2$
6:1 siloxane closed network	2970, 2925, 2850, 2125, 1410, 1260, 920, 850, 750	aliphatic CH_3, Si-H, C-H stretch, Si-CH_3, Si-H, Si-$(CH_3)_2$
6:1 siloxane open network	2975, 2925, 2850, 1450, 1260, 1035, 820	aliphatic CH_3, C-H stretch, Si-CH_3, Si-O stretch Si-H, Si-$(CH_3)_2$

Table 5.6: Limb 3 FTIR (ν/cm^{-1}[NaCl]):

In limb three, the introduction of Si-O stretches occurs. This is potentially from the formation of small siloxane ring fragments as seen in previous Chapters (3.4.2 and 4.4.1). The following peaks were observed in limb 4 in Table 5.7:

Sample Identity	Wavenumber (cm^{-1})	Peak Identities
2:1 carborane-siloxane closed network	2975, 2920, 2850, 2300, 1750, 1250, 1075, 800	aliphatic CH_3, CO_2, Si-CH_3, CO_2H stretch, Si-O stretch, Si-$(CH_3)_2$
6:1 carborane-siloxane closed network	3300, 2975, 2920, 2850, 2375, 2125, 1250, 1025, 915, 905, 875, 825	O-H group, aliphatic CH_3, CO_2, Si-H, Si-CH_3, Si-O stretch, Si-H, Si-$(CH_3)_2$
6:1 washed carborane-siloxane closed network	Not Available	Not Available
6:1 carborane-siloxane open network	2950, 2925, 2850, 1460, 1030, 810	aliphatic CH_3, C-H stretch, Si-O stretch, Si-$(CH_3)_2$
6:1 siloxane closed network	3300 (b), 2970, 2925, 2850, 2125, 1265, 1075, 1025, 850, 825	O-H group, aliphatic CH_3, Si-H, Si-O stretch, Si-H, Si-$(CH_3)_2$
6:1 siloxane open network	3300, 2950, 2920, 2850, 1470, 1265, 1030, 820	O-H group, aliphatic CH_3, Si-O stretch, Si-H, Si-$(CH_3)_2$

Table 5.7: Limb 4 FTIR (v/cm^{-1}[NaCl]):

In limb four, the presence of water is detected where the remaining components are siloxane based fragments. No carborane fragments were detected in the IR data for the carborane containing species although their presence was previously observed by the online mass spectrometer.

In order to fully assess the volatiles formed during the degradation event the GC data for limb 4 and the cold ring fraction that is collected during the degradation event is compared for each sample, the analysis for limb 4 is shown in Table 5.8:

5.6.3 Limb and Cold Fraction Analysis

Sample Name	Analytes detected				
	D$_3$ siloxane	D$_4$ siloxane	trisiloxane	Silanes	*m*-carborane
2:1 carborane-siloxane closed network	√	-	-	√	√
6:1 carborane-siloxane closed network	√	√	√	-	√
6:1 wash carborane-siloxane closed network	√	-	-	-	-
6:1 carborane-siloxane open network	-	√	√	-	√
6:1 siloxane closed network	√	-	-	-	-
6:1 siloxane open network	-	√	√	-	-

Table 5.8: GC Mass Spectrometry limb 4:

In limb four, trends in the degradation analytes can be clearly observed. The presence of *m*-carboranes in the mass spectrum is observed for all carborane containing samples except for the extracted sample. As limb fraction four of the 6:1 extracted carborane-siloxane closed sample did not contain *m*-carborane in the mass spectrum it could be an indication that the volatile carboranes arise from unbound carborane monomers. Silane fragments were observed in the 2:1 carborane-siloxane closed sample but not in any of the 6:1 samples. This could be due to the presence of unreacted silane units on the side of the copolymer chain. The last trend is the increase in size of siloxane fragments with increasing dimethylsiloxane content in the polymer network. As the dimethylsiloxane content increases, for example in the 6:1

carborane-siloxane open and 6:1 siloxane open samples, both D_4 and trisiloxane are readily observed. The cold ring analysis is shown in the Table 5.9 below:

	Analytes detected			
Sample Name	D_3 siloxane	D_4 siloxane	D_5 siloxane	bis(allyl)*m*-carborane
2:1 carborane-siloxane closed network	√	√	-	-
6:1 carborane-siloxane closed network	-	√	√	√
6:1 wash carborane-siloxane closed network	-	-	√	-
6:1 carborane-siloxane open network	√	√	√	-
6:1 siloxane closed network	-	-	-	-
6:1 siloxane open network	-	-	-	-

Table 5.9: GC Mass Spectrometry cold ring:

The cold rings generally had decreased concentration of analytes in the GC analysis than the limb fraction, however, trends can still be observed. The major discovery is the presence of the carborane monomer in the 6:1 carborane-siloxane closed network sample and not in any other carborane containing samples. The ratio of diallyl carborane to silane in the 6:1 carborane-siloxane closed sample should give a complete reaction of both monomers with high conversion. The problem of mass transport as the network gels probably stops the complete reaction of all monomers, where although the yield appears high the material is not fully cured. Due to the small mass fraction of carborane in the open carborane-siloxane network it is

probably too dilute in initial carborane concentration to observe the species in the cold ring fraction.

The non-carborane containing networks have no readily detectable analytes which could be an indication that any siloxane degradation fragments are of insufficiently high molecular mass to be trapped in the cold ring.

5.6.4 Residue Analysis

Char residue from a selection of the samples ran were compared to see the changes in the material after thermal degradation. The chars obtained were intractable so analysis was limited to solid state techniques and in some cases not enough material was recovered for analysis. Comparison of the amount of char in selected samples in order to assess trends in the degradation is shown in Table 5.10:

Sample	% Char residue
6:1 carborane-siloxane closed network	36
6:1 carborane-siloxane open network	9.3
6:1 siloxane closed network	23
6:1 siloxane open network	3.0

Table 5.10: Char residues for selected degraded hydrosilylation networks

The presence of carborane in the hydrosilylation networks increases the amount of residue and is reduced with increasing dimethylsiloxane content. Increasing dimethylsiloxane content reduces the amount of char residue observed for the both the carborane and non-carborane containing networks.

5.6.4 Residue Analysis

Solid state ATR diamond FTIR was employed to investigate further some of the char residues that were obtained. The peaks obtained from the samples are compared in Table 5.11:

Sample	Wavenumber / cm^{-1}	Peak Identities
2:1 carborane-siloxane closed network	2975, 2590, 1275, 1030(b), 800	aliphatic CH_3, B-H stretch, Si-CH_3, Si=O stretch, Si-$(CH_3)_2$,
6:1 carborane-siloxane closed network	2970, 2590, 1270, 1030(b), 780	aliphatic CH_3, B-H stretch, Si-CH_3, Si=O stretch, Si-CH_3
6:1 washed carborane-siloxane closed network	2970, 2590, 1450-1410, 1260, 1000(b), 790	aliphatic CH_3, B-H stretch, C-H bend, Si=O stretch, Si-CH_3
6:1 siloxane closed network	2965, 1265, 1020, 800	aliphatic CH_3, Si-CH_3, Si=O stretch, Si-CH_3

Table 5.11: FTIR (v/cm^{-1}[ATR diamond])

The peaks found at 1030 – 1000 cm^{-1} are representative of the material having formed SiO_2 which is a common degradation product in siloxane elastomer thermal degradation. For the carborane containing samples there is a large peak at 2590 cm^{-1} where boron hydride char residue is left *in situ*.

Solid state NMR was also used in order to assess some of the chars to further understand the chemical environments contained within the residues. Generally ^{13}C data were disappointing for each char but the ^{11}B spectra for 6:1 carborane-siloxane closed and 6:1 carborane-siloxane open networks reveal more about the speciation of the boron nuclei. In order to understand these changes with temperature the solid state ^{11}B NMR spectra are compared for the initial material, material degraded to 450 °C and material degraded to 650 °C as shown in Figures 5.25-5.26:
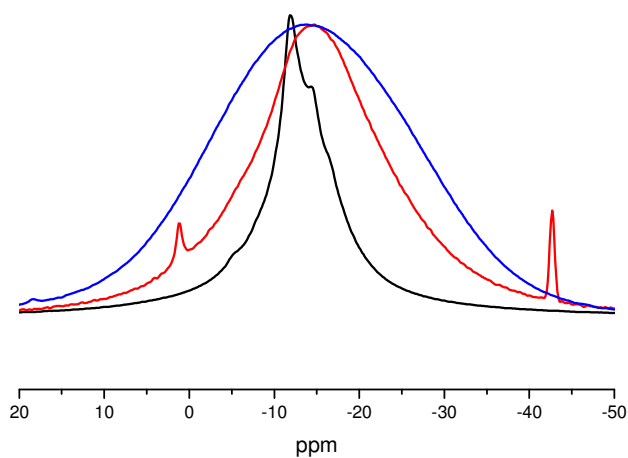
Figure 5.25: Solid state ^{11}B NMR of the 6:1 carborane-siloxane closed network before degradation (black line), degraded to 450 °C (red line) and degraded to 650 °C (blue line)
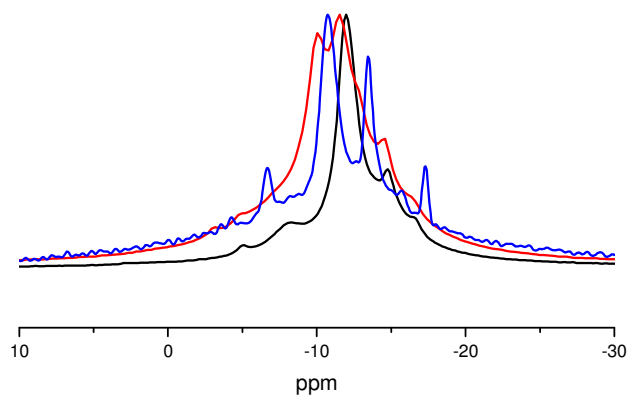

Figure 5.26: Solid state ^{11}B NMR of the 6:1 carborane-siloxane open network before degradation (black line), degraded to 450 °C (red line) and degraded to 650 °C (blue line)

The ^{11}B spectra for the 6:1 carborane-siloxane closed sample show a broadening of the spectra with increased degradation temperature. This is due to the increased disorder of the material as it forms a char residue leading to dipolar broadening. By 650 °C the material is so disordered poor resolution is observed in the spectrum with loss of structural information. However, the spectrum at 450 °C has a doublet peak at 1.2 ppm and -42.7 ppm which is possibly the formation of a boron-metal bond.[2] Although further investigation is needed it could support the formation of boron-platinum bonding in the sample which would indicate the source of the dehydrogenation event that takes place during degradation. If so, this gives a coupling constant $J(^{11}B\text{-}^{195}Pt) = 4086$ Hz.

For the more dilute 6:1 carborane-siloxane open sample the spectra are shifted slightly in the x-axis where the peaks broaden with increased degradation temperature. Again the broadening is probably due to disorder of the carboranes with increased degradation temperature. The important structural feature from the comparable spectra is the cage structure remains intact up to temperatures of 650 °C.

In the next Section the comparable data from each Section are compared to determine the possible mechanisms occurring during degradation.

5.6.5 Inferences Arising From Comparative TVA Study

In this Section the main findings of the TVA study are listed and inferences drawn on the nature of degradation found in hydrosilylation catalysed carborane siloxane networks. Predictions are also made for other carborane containing networks undergoing degradation. The following results were observed in the previous discussions and are discussed in turn:

1. The major degradation event observed for carborane containing siloxane elastomer networks is low molar mass silane formation and demethylation

The first point has not been observed previously for these systems where dehydrogenation has been alluded to in the event of thermal degradation of carboranes under vacuum on a platinum surface.[3] The main degradation products are trimethylsilane, tetramethylsilane, methane and hydrogen. Previous work involving silanes, hydrogen and methane under thermal stress leads to the formation of silicon-carbide films.[4] This process relies on the efficient dissociation of the silane and methane to deposit a thin silicon film on the surface of the silicon wafer substrate. Conversely in the TVA the hydrosilylation networks are undergoing the reverse process. Also, water is observed as a degradation product in this study where a previous study shows silane degradation under oxygen is a driving force of the formation of water on a platinum surface.[5] Although the TVA is carried out under non-oxidative conditions the siloxane backbone is a ready source of oxygen for this degradation reaction.

This author's opinion is the platinum catalyst residues have an important part to play in the degradation of the material. Evidence to this effect discusses the nature of the breakdown of the siloxane under heating and the presence of platinum.[6] This is shown in Scheme 5.1:
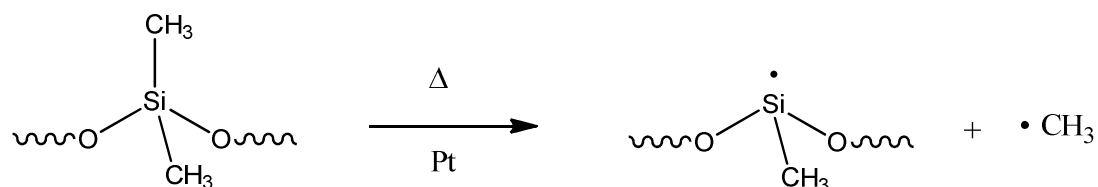
Scheme 5.1: Initation step of thermal degradation on a siloxane polymer backbone in the presence of a platinum metal centre

The breakdown of the polymer then propagates with the formation of methane by abstraction of hydrogen from another –CH$_3$ side group on the polymer backbone.[7] This is shown in Scheme 5.2:
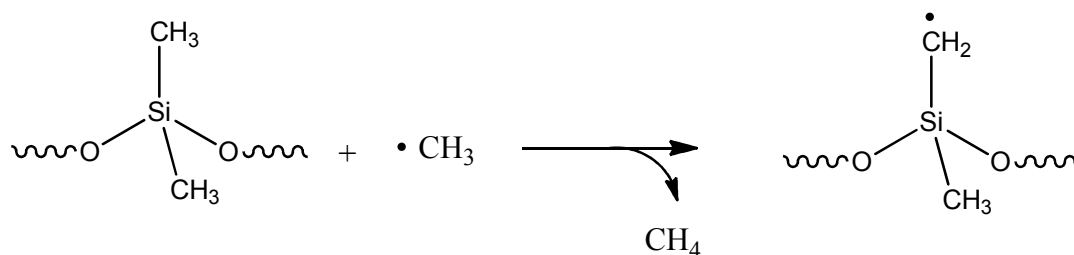
Scheme 5.2: Abstraction of hydrogen to form methane

It is proposed by the present author that a similar process may occur in the presence of silane to generate the formation of hydrogen in the first dehydrogenation event. In this instance the hydrogen radical may abstract with another hydrogen from a nearby $-CH_3$ side group and generate hydrogen gas. This proposed mechanism is shown in Scheme 5.3:
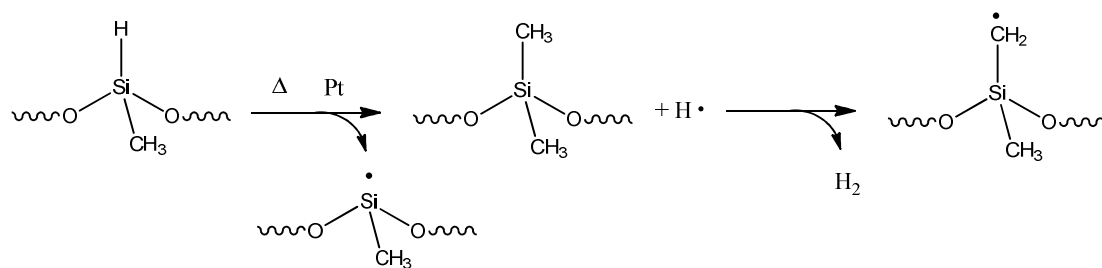
Scheme 5.3: Proposed mechanism for the formation of hydrogen from degradation of unreacted silane in the presence of platinum and methane

The second dehydrogenation event seen in the closed carborane-siloxane networks also can be explained by the presence of catalyst residues. Platinum and other electron rich transition metal species are able to accommodate the addition of C-H bonds on the metal in a Shilov type process where preferential reaction of the metal centre is with strong C-H bonds.[9] This is shown in Scheme 5.4 below:
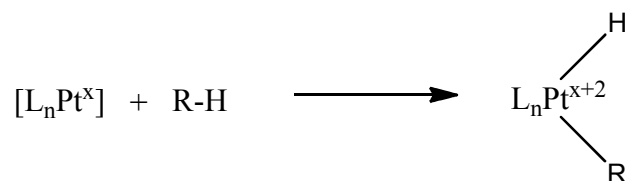
Scheme 5.4: Oxidative addition of R-H bond to a platinum (0) complex

229

These types of systems are used in the production of syngas from methane using metal catalysts of which platinum is commonly used. The main step is the addition of C-H bond across the metal centre.[10] This is shown in Scheme 5.5 below:
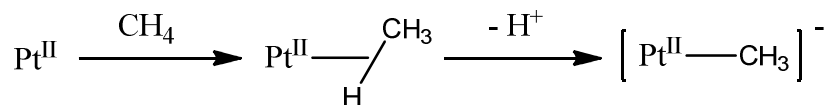
Scheme 5.5: Breakdown of a methane molecule by a platinum (II) centre

The second dehydrogenation event observed for the closed carborane-siloxane hydrosilylation networks is most likely cracking of the remaining carbonaceous residues left in the sample at high temperatures. Cracking of hydrocarbons occurs at temperatures of 600 °C and have been shown to propagate in the presence of platinum metals.[11-12] The cross-linked 1,7-diallyl-*m*-carborane monomer could act as a source of C-H bonding with the platinum residues able to abstract hydrogen. An example of this is shown in Scheme 5.6.
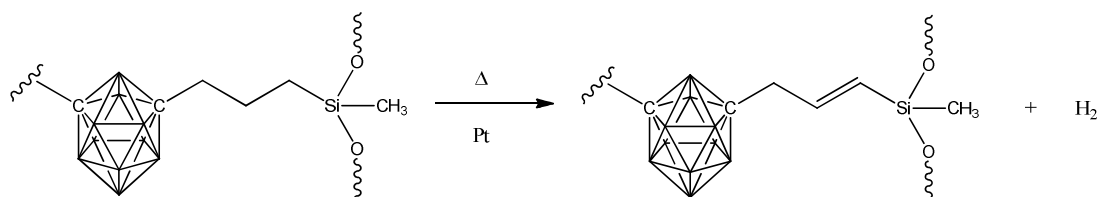
Scheme 5.6: Potential cracking of the aliphatic side group on the bound *m*-carborane. B-H groups are not explicitly shown for clarity

The final but most important requirement is the determination of the mechanisms of formation of tetramethylsilane, trimethylsilane and water observed as degradants during the TVA experiments. These are likely to form from the degradation of the siloxane copolymer under thermal stresses. Water has been previously observed as a degradant in platinum containing silicone systems by MacLaury where methane and CO_2 were also observed.[13] When water is present with a source of protons, PDMS may be hydrolysed under acidic conditions as shown in reaction Scheme 5.7:[14]
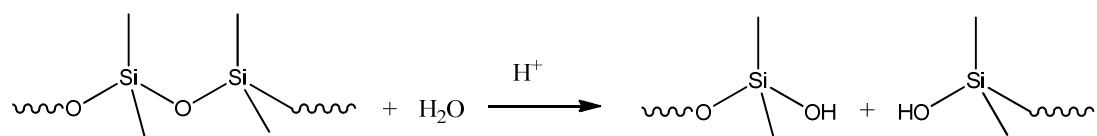
Scheme 5.7: Hydrolytic scission of PDMS in the presence of H$^+$ ions

This cannot happen for three reasons. The first is there is no trace of silanol degradants in the TVA study. Secondly, water is observed as a degradant and would be consumed if this process were to happen. Thirdly, there is unlikely to be a source of protons in the degradation step as hydrogen radical formation is more likely as shown in Scheme 5.3. Free radical breakdown of PDMS to form dimethylsilanone has been observed by Khabashesku *et al.* under vacuum pyrolysis and is shown in Scheme 5.8:[15]
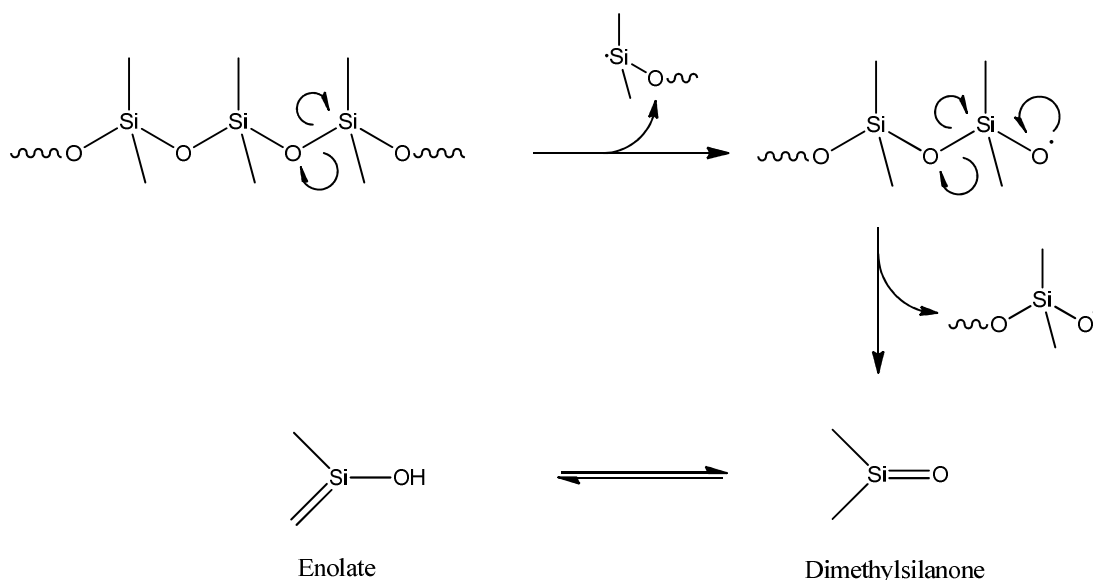
Scheme 5.8: Thermally induced free radical degradation of PDMS to form dimethylsilanone

Although a potential degradation mechanism the lack of dimethylsilanone in the mass spectrum data means this is unlikely to be the reason for the breakdown of the polymer backbone. This author believes that the formation of silanes is due to the presence of the platinum catalyst. Work by Lagarde on the mechanisms associated with the thermal degradation of siloxanes in the presence of platinum suggests that the platinum does not take a direct role in the dissociation of the polymer due to the

lack of metal oxide formation.[16] The conclusion is likely to be that the platinum promotes scission of the Si-O bond through a Shilov coupling process observed in Scheme 5.5 where methane is readily available for C-H bond activation and nucleophilic attack of the CH_3^- into the delta positive silicon centre as shown in Scheme 5.9:
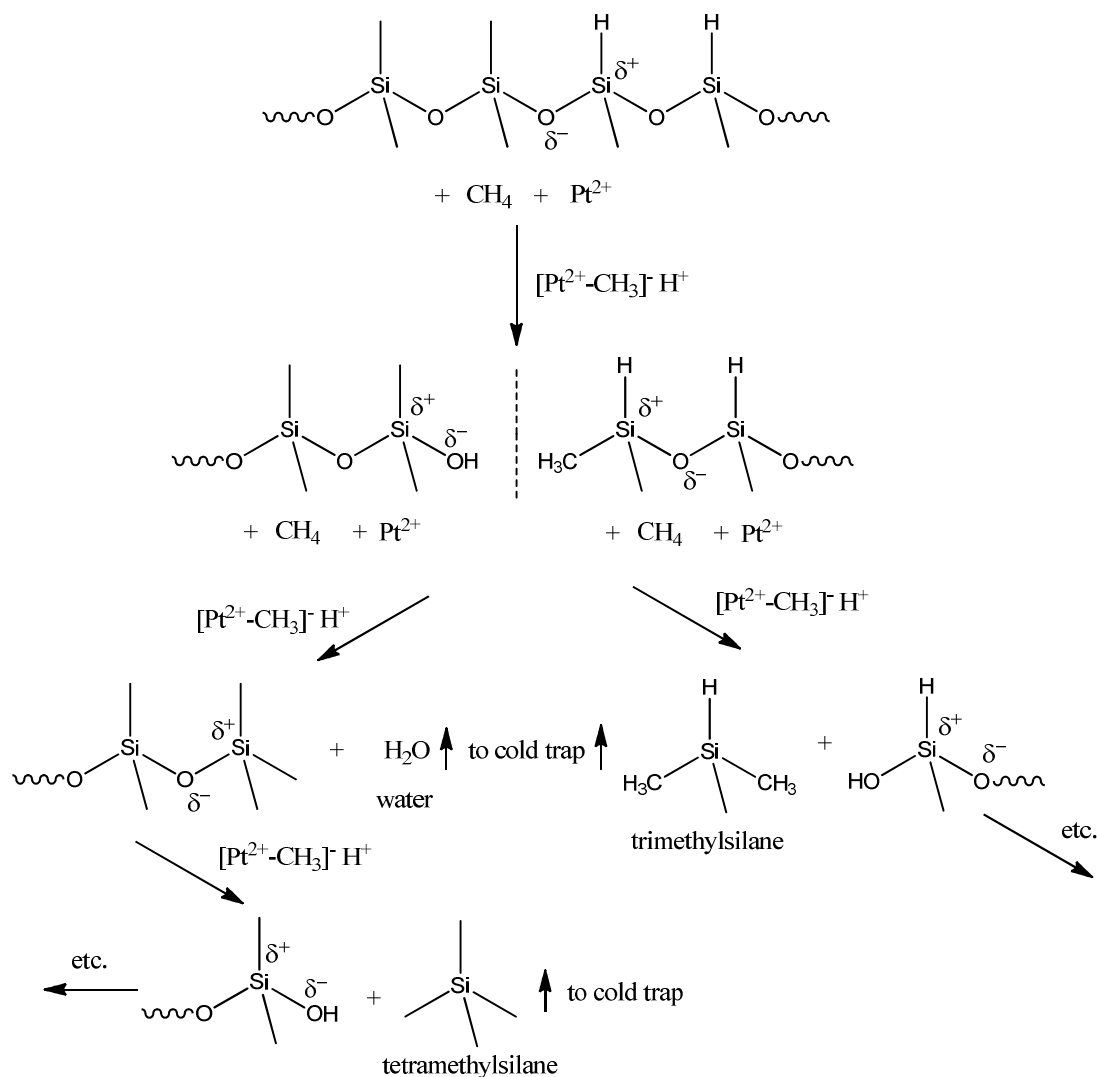
Scheme 5.9: Proposed degradation mechanism leading to the formation of tetramethylsilane, trimethylsilane and water

5.6.5 Inferences Arising From Comparative TVA Study

2. More open elastomer networks lower the thermal stability of the material

Point two has been observed for these types of materials before. The hydrosilylation networks that were produced in the study by Keller and Kolel-Veetil were increasingly thermally stable with increasing cross-link density where the only prediction as to the high char residues being observed was as a result of cross-linking of remaining alkenyl groups. This is a dangerous conclusion based on the results of TGA data where mass transport of volatiles may be affected by surface degradation retarding the volatilisation of the bulk of the sample. Also the evidence supporting the presence of the alkenyl groups in the product could easily come from the Karstedt's catalyst residues or cracking of the remaining carbonaceous residues rather than unbound vinyl carborane groups.

3.Non-carborane containing networks are just as thermally stable as carborane containing networks

In point three the surprise result has been the fact that the onset of degradation of the siloxane elastomer networks is independent of carborane content. The initial research carried out on carborane-siloxane network polymers has maintained the bonding of carborane into the network resulting in high thermal stability.[17-18] The only notable increases observed by the incorporation of carboranes is in the amount of char residue left after the degradation event compared to that of a siloxane-only containing network.

4. Char residues contains disordered carborane residues where carborane cage remains intact

This brings the discussion to point 4 which is supported through evidence found by Tillekaratne *et al.*[19] The initial observations in this study showed dehydrogenation of the carborane under vacuum at raised temperature. The authors made the following comment on this process:

5.6.5 Inferences Arising From Comparative TVA Study

"The fact that boron carbide thin films can be grown by chemical vapor deposition using carborane as a precursor might suggest icosahedral structures are preserved in the process. If so, the boron carbide structure would have to be initially formed from icosahedral units that still retained considerable hydrogen…"

In this study the carborane cage structure is most definitely retained with evidence from the NMR solid state char residue analysis. The broadening observed will most likely arise from the number of symmetries the carborane residues adopt as the sample disorders during degradation.

5.7 Chapter Conclusion

The synthesis of hydrosilylation derived carborane-siloxane networks was successfully achieved using Karstedt's catalyst. TGA analyses of these elastomer network materials showed a high thermal stability as predicted in the literature. The TGA study also revealed that non-carborane containing networks also had high thermal stabilities. The thermal degradation cycle of the material was investigated by use of TVA where the main degradation process is the formation of a series of low molecular mass silanes. Other reactions are the reduction of the siloxane fragments to form low molecular mass siloxane ring structures and dehydrogenation.

The presence of what appears to be transition metal to boron bonding in the char residue gives weight to the theory that the dehydrogenation occurs due to the catalyst residues. The NMR spectra of the char residues broaden with increased degradation temperature, however, the structural information observed in the 6:1 carborane-siloxane open network samples suggest that the carborane cage is intact. Also the thermal stability of these materials is independent of carborane content and is more closely related to the cross-link density.

5.8 References

1. Kolel-Veetil, M.K., Keller, T.M., *"Formation of Elastomeric Network Polymers from Ambient Heterogeneous Hydrosilations of Carboranylenesiloxane and Branched Siloxane Monomers"* Journal of Applied Polymer Science: Part A 2006 **47**:147

2. Hermanek, S., Machacek, J., Fusek, J., Blechta, V., *"Importance of ^{11}B-^1H coupling constants in assigning the ^{11}B signals"* Wiley Interscience, New York, 1998

3. Tillekaratne, A., Siap, D., Trenary, M. *"Adsorption and dehydrogenation of ortho-carborane on the Pt(111) surface"* Journal of Physical Chemistry C 2008 **112**: 8682

4. Das, D., Chattopadhyay, S., Barua, A.K., *"Improved quality a-SiC: H films deposited by a combination of heated filament and rf plasma deposition technique"* Solar Energy Materials and Solar Cells 1998 **51**: 1

5. Kershner, D.C., Zhang, W., Medlin, J.W., *"Investigation of submonolayer SiO_x species formed from oxidation of silane on Pt(1 1 1)"* Surface Science 2008 **602**: 3225

6. Hayashida, K., Tsuge, S., Ohtani, H., *"Flame retardant mechanism of polydimethylsiloxane material containing platinum compound studied by analytical pyrolysis techniques and alkaline hydrolysis gas chromatography"* Polymer 2003 **44**: 5611

7. Delebecq, E., Hamdani-Devarennes, S., Raeke, J., Lopez Cuesta, J.M., Ganachaud, F., *"High Residue Contents Indebted by Platinum and Silica Synergistic Action during the Pyrolysis of Silicone Formulations"* Applied Materials and Interfaces 2011 **3**: 869

8. Carcassi, M.N., Fineschi, F., *"Deflagrations of H_2–air and CH_4–air lean mixtures in a vented multi-compartment environment"* Energy 2005 **30**: 1439

9. Labinger, J.A., Bercaw, J.E., *"Understanding and exploiting C–H bond activation"* Nature 2002 **417**: 507

10. Crabtree, R.H., *"Aspects of methane chemistry"* Chemical Reviews 1995 **95** (4): 995

11. Kaneko, S., Arakawa, T., Ohshima, M., Kurokawa, H., Miura, H., *"Dehydrogenation of propane combined with selective hydrogen combustion over Pt-Sn bimetallic catalysts"* Applied Catalysis A: General 2009 **356**: 80

12. Insura, N., Onwudili, J.A., Williams, P.T., *"Catalytic pyrolysis of low-density polyethylene over alumina-supported noble metal catalysts"* Energy Fuels 2010 **24**: 4231

13. MacLaury, M.R. *"Influence of platinum fillers and cure on the flammability of peroxide cured silicone-rubber"* Journal of Fire and Flammability **10** (3): 175

14. Lewis, F.M., *"The science and technology of silicone rubber"* Rubber Chemistry and Technology 1962 **35**: 1222

15. Khabashesku, V.N., Kerzina, Z.A., Maltsev, A.K., Nefedov, O.M., *"Matrix IR spectroscopic study of the vacuum pyrolysis of octamethylcyclotetrasiloxane, allyloxy and allyl(allyloxy)dimethylsilanes as well as 2,2,6-trimethyl-2-silapyrane as potential sources of dimethylsilanone"* Journal of Organometallic Chemistry 1989 **364** (3): 301

16. Lagarde, R., Lahaye, J., *"Mechanisme d'ignifugation d'elastomers organosiliques par le platine"* European Polymer Journal 1977 **13**:769

17. Andrianov, K.A., Pavlova, S.-S.A., Zhuravleva, I.V., Tolchinskii, Yu.I., Astapov, B.A., *"Thermal breakdown of polydi-organocarborane siloxanes"* Polymer Chemistry in the USSR 1976 **19** (9): 1037

18. Hedaya, K., Kawakami, J.H., Kopf, P.W., Kwiatkowski, G.T., McNeil, D.W., Owen, D.A., Peters, E.N., Tulis, R.W., *"D_2-meta-carborane-siloxanes. IV. Synthesis of linear, high molecular weight polymers"* Journal of Polymer Science 1977 **15**: 2229

19. Tillekaratne, A., Siap, D., Trenary, M. *"Adsorption and dehydrogenation of ortho-carborane on the Pt(111) surface"* Journal of Physical Chemistry C 2008 **112**: 8682

Chapter 6

Conclusion and Appendix

6.0 Thesis Conclusion

A tin catalysed PDMS network has been successfully synthesised and tested for thermal stability. The primary degradation process is "reversion" in which the polymer chain backbites and forms cyclic siloxane species. By addition of functionalised carboranes as composite fillers the increase in thermal stability is minimal.

In order to improve the thermal stability this route to degradation must be blocked and the use of carboranes bound to the elastomer network is one way of achieving this. In the literature $FeCl_3$ copolymer network material showed remarkable thermal stability. The primary degradation process is dehydrogenation of the carborane to produce boron carbide. By use of a methoxy capped PDMS polymer the replacement of the Lewis acid catalyst gives rise to linear copolymers without the added complication of cross-linking using $AlCl_3$ and $ZnCl_2$. The kinetic behaviour associated with the $FeCl_3$ polymerization was extensively investigated where the activation energy was +43.6 kJ mol^{-1} with an activation entropy of -198.2 J K^{-1} mol^{-1}.

The synthesis of hydrosilylation carborane-siloxane networks was successfully achieved using Karstedt's catalyst. TGA analyses of these elastomer network materials showed a high thermal stability as predicted in the literature. The thermal degradation of the material was investigated by use of both thermogravimetric analysis and thermal volatilisation analysis. The study was extended to include non-carborane containing samples and adjustment of dimethylsiloxane content of the networks. The main degradation process is formation of low molecular mass silanes evolved from the breakdown of the poly(siloxane) block copolymer.

Finally the thermal stability of the carborane-siloxane elastomers is more closely related to the cross-link density of the samples. The electron-withdrawing effect of the carborane is not significantly stabilising to these materials. It is the author's opinion where previous papers on the thermal stability of carborane-siloxane elastomers show remarkable increases in char residue using TGA that the thermal

stability of these novel elastomers is only slightly improved by the inclusion of carboranes as non-carborane containing siloxane networks can be as thermally stable.

6.1 Suggested Future Work

More work is required to further investigate the replacement of $FeCl_3$ in the reaction of both 1,7 bis(dimethylmethoxysilyl)*m*-carborane and (dichlorodimethyl)silane. The replacement of the catalyst in the model reactions suggests that the use of either $AlCl_3$ or $ZnCl_2$ would lead to the formation of high molar mass d_2-carborane siloxane polymers. Also this would results in a material without the unwanted cross-linking reaction that turns the $FeCl_3$ material into a rubber upon cooling. The activation energies and activation entropies using alternative Lewis acid catalysts would be of interest to see if they are more favourable than the traditional $FeCl_3$ catalyst.

The other area of interest would be to characterise further the resulting char residues found in both the $FeCl_3$ and hydrosilylation catalyst reactions. The true nature of the boron carbide conformations and symmetries in the unit cell of the chars are yet to be explicitly observed.

Finally comparison of the thermal stability of carborane siloxane networks formed by non-metal catalysts against the metal containing catalysts discussed in this thesis is required. This will help further understand the role of the catalyst residues on the degradation of these materials.

Appendix

The data below are to show that the OMe capped PDMS had its number average molar mass determined by NMR. The methoxy capped carborane was checked for purity as a starting material.

NMR data for the determination of the molar mass (M_n) of the starting OMe end capped PDMS polymer:
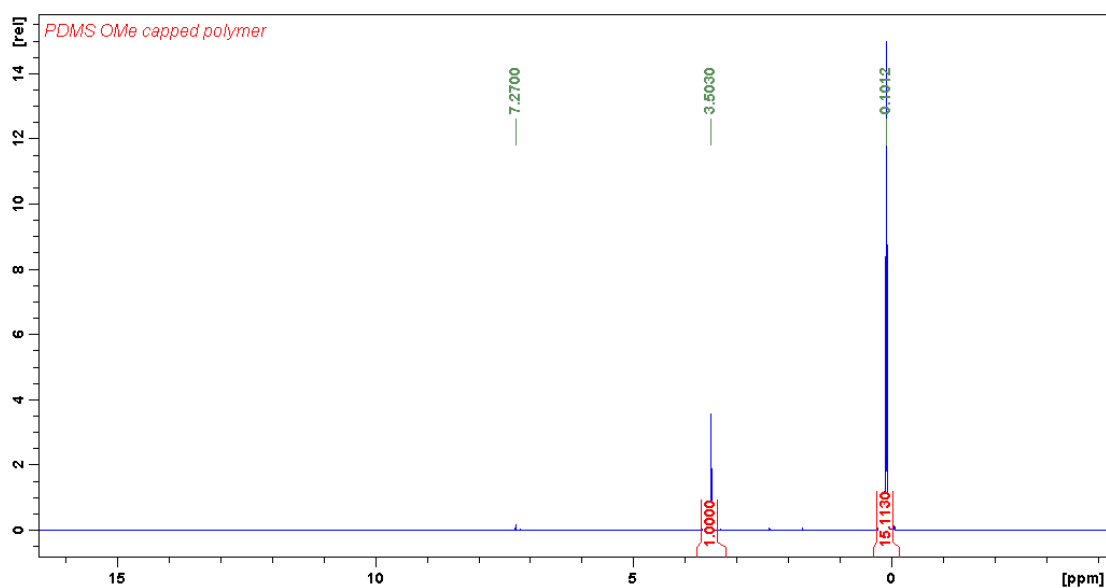
Figure 6.1: ^{1}H NMR of OMe capped PDMS polymer

^{1}H NMR data (400MHz, CDCl$_3$; δ): 0.10 (t, 15H, CH$_3$); 3.50 (t, 1H, OCH$_3$)
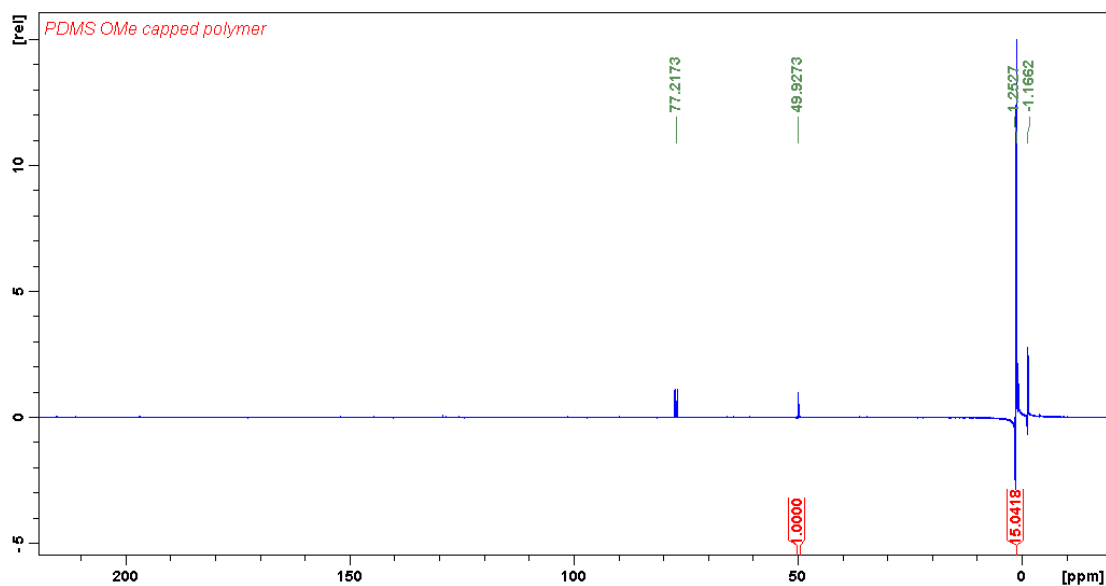
Figure 6.2: ^{13}C-^{1}H decoupled NMR of OMe capped PDMS polymer

^{13}C-^{1}H dec NMR data (100MHz, CDCl$_3$; δ): 1.25 (s, 15H, CH$_3$); 49.9 (s, 1H, OCH$_3$)

Integration OMe:CH$_3$ 1:15 therefore MW = ~1174 (C$_{32}$, H$_{96}$, O$_{17}$ Si$_{15}$)

Determination of purity of 1,7 bis(dimethylmethoxy)*m*-carborane by microanalysis, gas chromatography and ^{1}H NMR

Microanalysis of C$_8$ H$_{28}$ O$_2$ B$_{10}$ Si$_2$:

Element	C	H
% Expected	29.97	8.80
% Found	29.82	8.60

GC analysis (chloroform): Expected M/z = 320.579

Found M/z = 305.2

Expected value (-CH$_3$) = 307.232
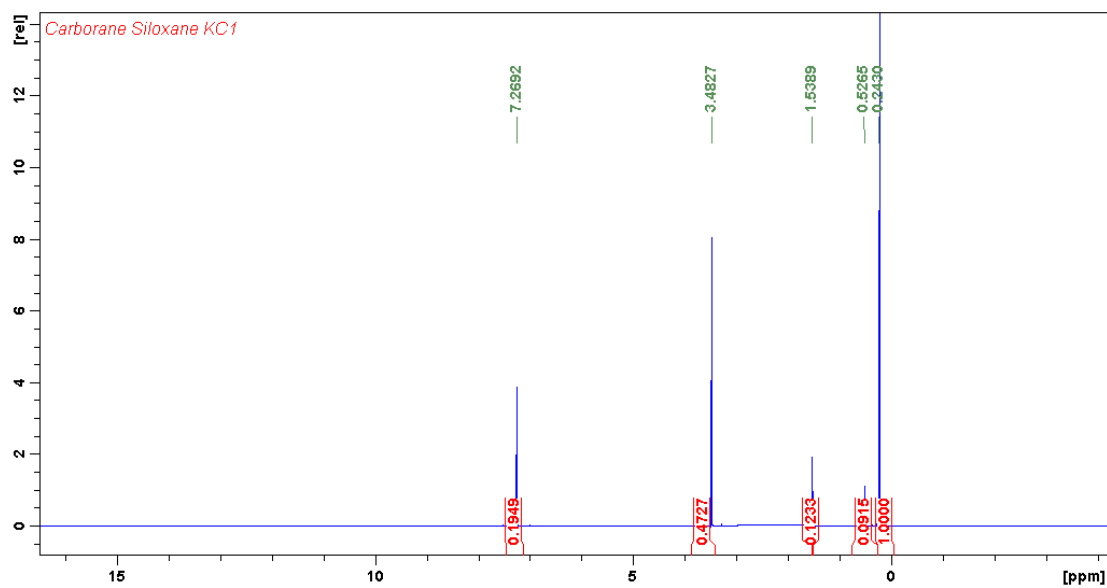
Figure 6.3: ^{1}H NMR of 1,7 bis(dimethylmethoxy)*m*-carborane

^{1}H NMR data (400MHz, CDCl$_3$; δ): 0.24 (t, 1H, CH$_3$); 3.48 (t, 0.47H, OCH$_3$)

Integration OMe:CH$_3$ 1:2 = expected ratio

Calibration of Thermal Volatilisation Analysis Tube

As part of the utilisation of sub-ambient TVA it is important to calibrate the glass tubes such that when quoting degradation temperatures for major events the actual sample temperature is quoted and not the furnace temperature. The reason for this is the thermal differences inside the tube and of the furnace vary firstly due to a lag in temperature increase between the heating furnace and glass tube then secondly due to thermal losses between the glass tube and sample. Therefore it is important to calibrate the actual temperature inside the tube with respect to the furnace temperature programme. This is made difficult as the glass tube is kept under low vacuum so to probe the temperature using a thermocouple requires a special setup which is shown in Figure 6.4.
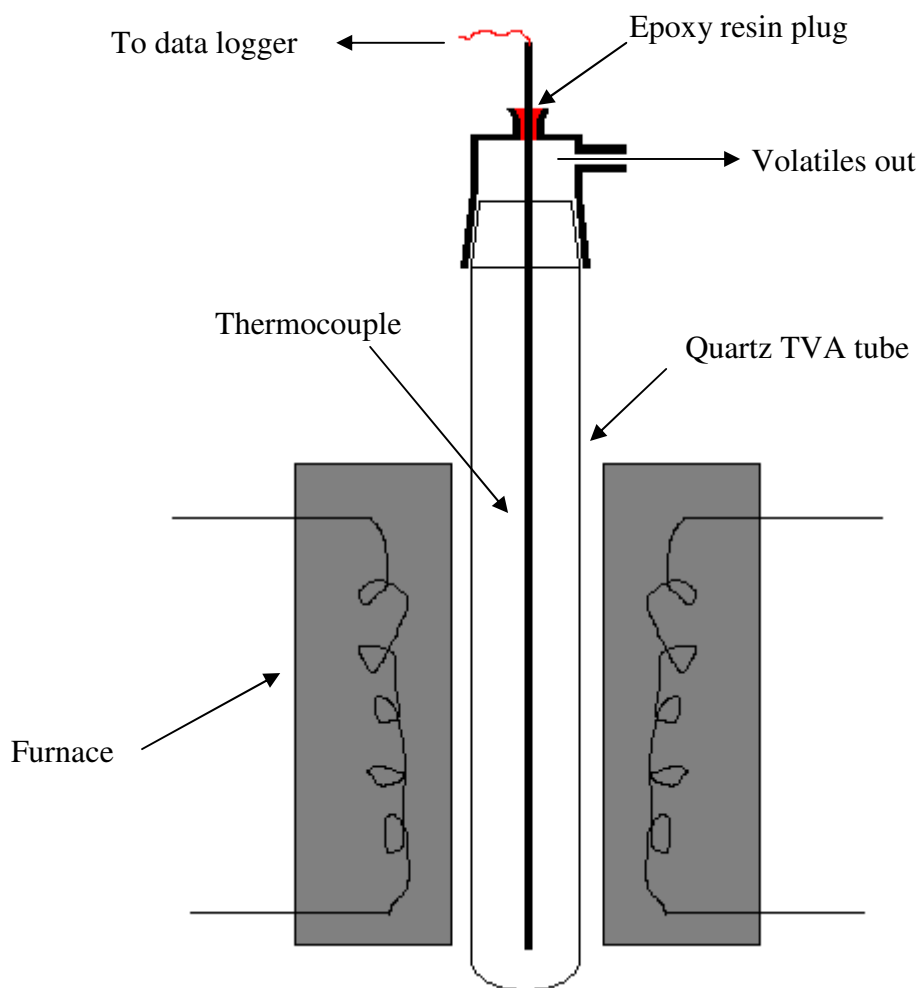
Figure 6.4: Experimental setup of thermocouple used to calibrate a TVA tube

In this setup the thermocouple is fed through a small opening on the top of the tube head to a depth close to the base of the TVA tube. To prevent leaks from occurring under high vacuum the opening is then sealed using epoxy resin which provides a barrier whilst holding the thermocouple in place. In order to calibrate for a selected run the temperature programme of interest is then set on the TVA furnace and the data logger records both the temperature of the furnace and the thermocouple against run time. An example of the plot obtained is shown in Figure 6.5.
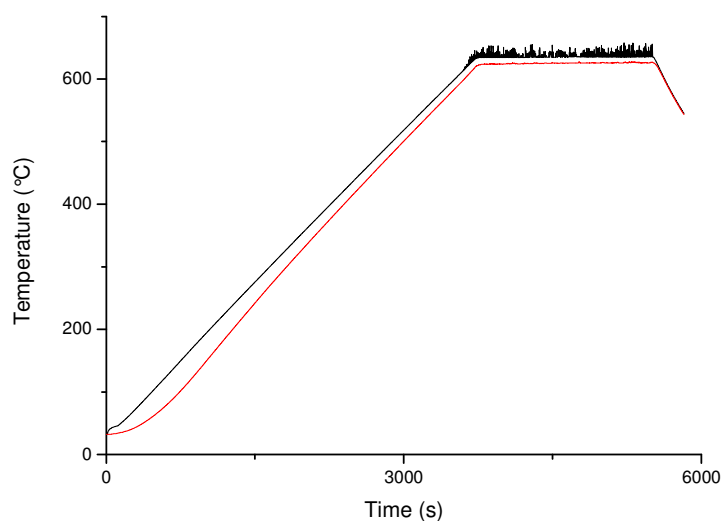
Figure 6.5: Example of tube calibration showing both furnace temperature (black line) and thermocouple temperature (red line) plotted against time

The quartz tube used in all the experimental work in this thesis has been calibrated and the corrected temperatures are shown for key temperatures in the Table below.

Furnace Temperature / (°C)	Calibration Run 1 / (°C)	Calibration Run 2 / (°C)	Corrected Temperature / (°C)
300	269	269	269.0
400	376	377	376.5
500	481	481	481.0
650 (Initial)	613	618	615.5
650 (After 30 mins)	626	626	626.0

Additional TVA Data From Chapter 5

Further supplementary data from the TVA study in Chapter 5 is presented below:
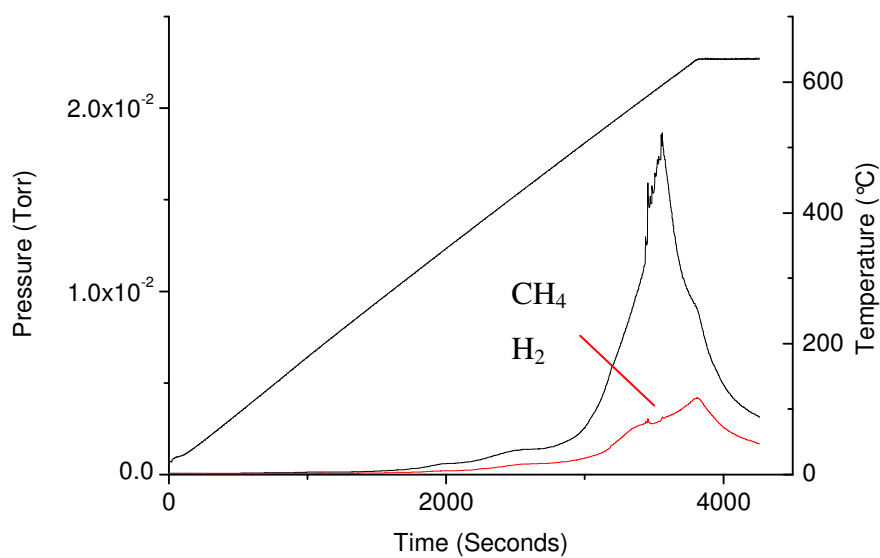
Figure 6.6: Degradation run of 2:1 carborane-siloxane closed network material. Total volatiles (black line) and non condensable (red line) pressure peaks shown against time with furnace temperature (dotted line) on second axis
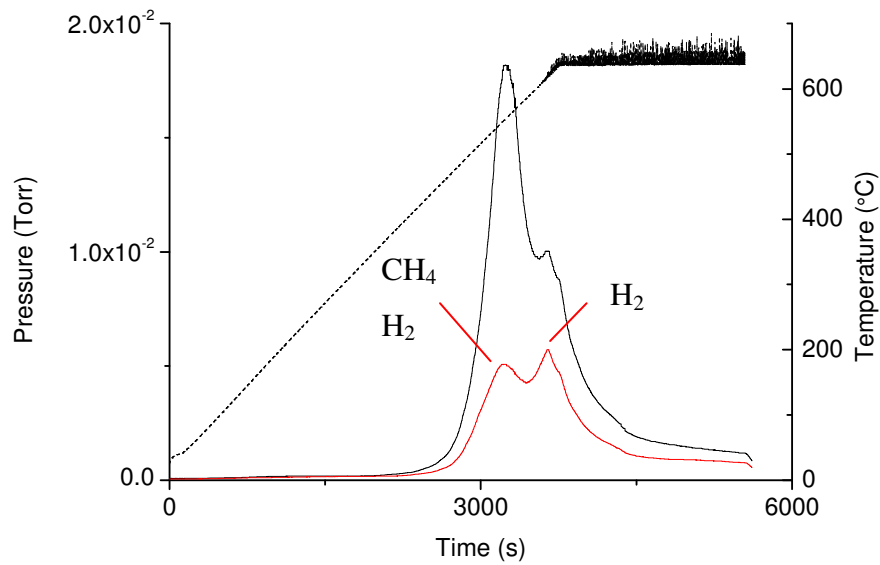
Figure 6.7: Degradation run of 6:1 carborane-siloxane closed network material. Total volatiles (black line) and non condensable (red line) pressure peaks shown against time with furnace temperature (dotted line) on second axis
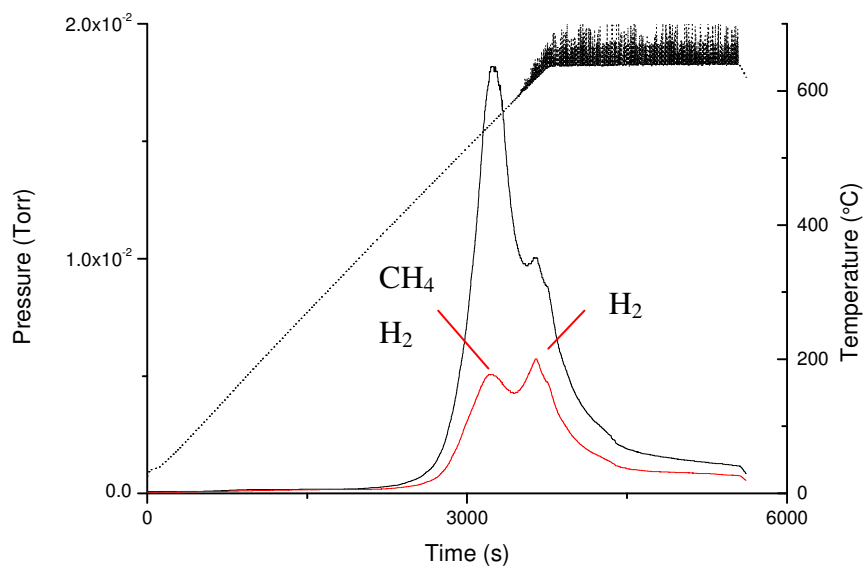
Figure 6.8: Degradation run of 6:1 washed carborane-siloxane closed network material. Total volatiles (black line) and non condensable (red line) pressure peaks shown against time with furnace temperature (dotted line) on second axis
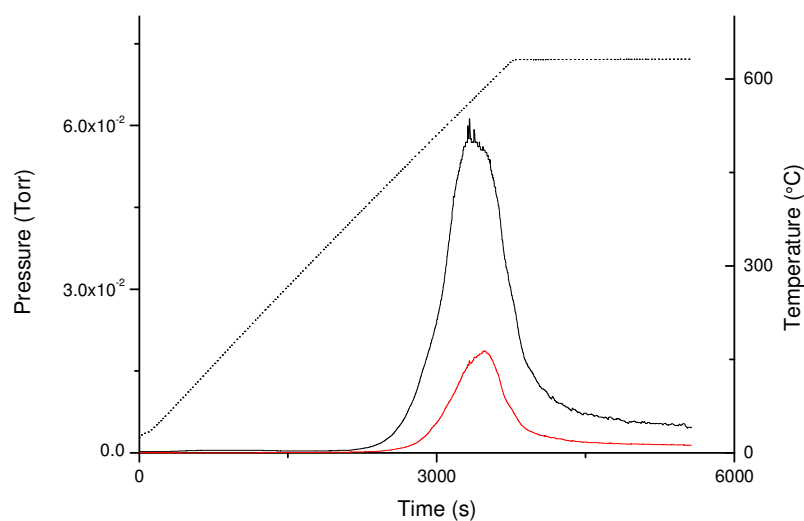
Figure 6.9: Degradation run of the 6:1 carborane-siloxane open network material where the silane-siloxane copolymer is 13,000 g mol^{-1}. Total volatiles (black line) and non condensable (red line) pressure peaks shown against time with furnace temperature (dotted line) on second axis
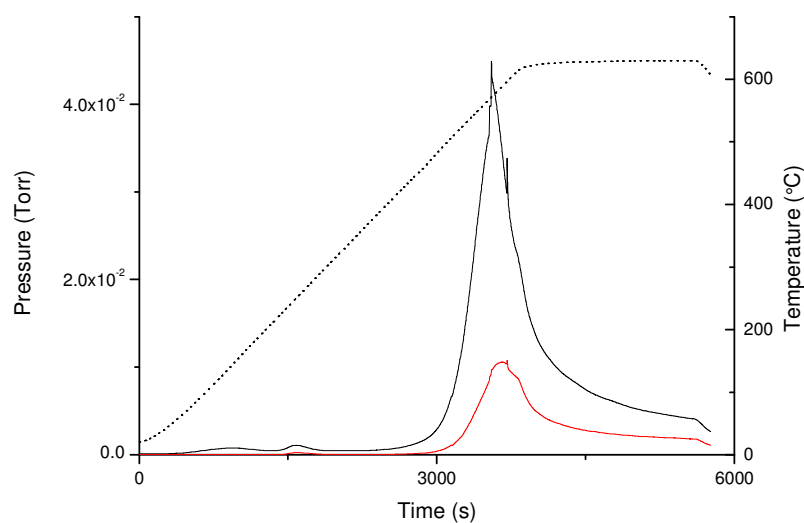
Figure 6.10: Degradation run of the 6:1 siloxane closed network material. Total volatiles (black line) and non condensable (red line) pressure peaks shown against time with furnace temperature (dotted line) on second axis
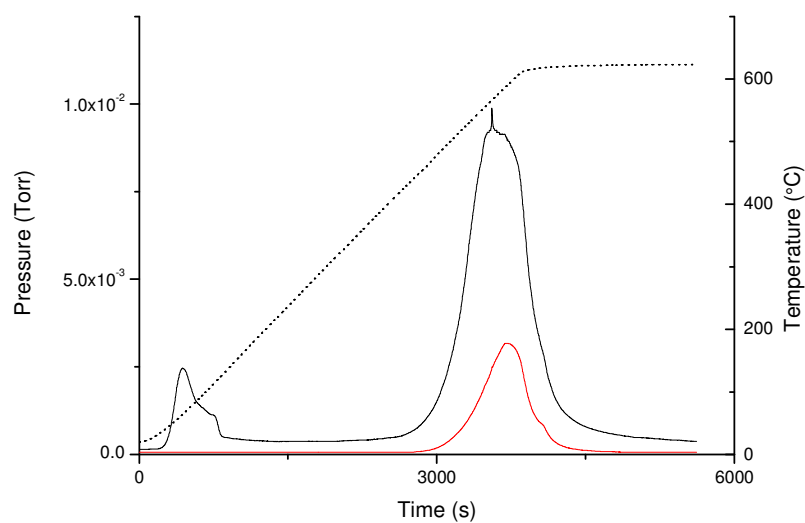
Figure 6.11: Degradation run of the 6:1 siloxane open network material. Total volatiles (black line) and non condensable (red line) pressure peaks shown against time with furnace temperature (dotted line) on second axis
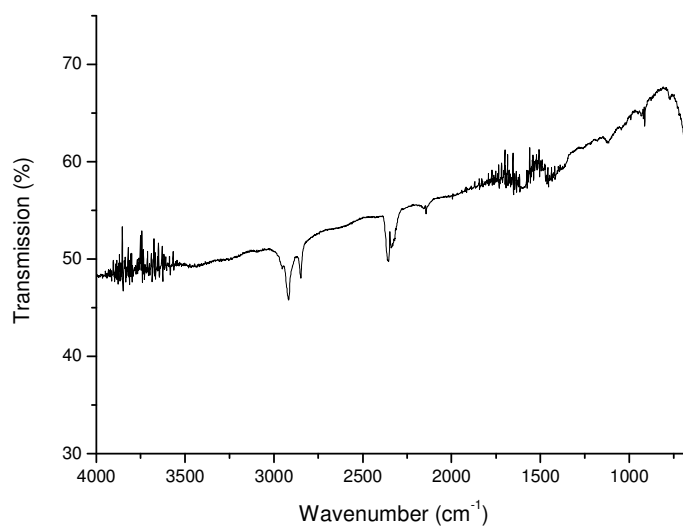
Figure 6.12: 2:1 carborane-siloxane closed network sample gas phase FTIR of TVA limb 1
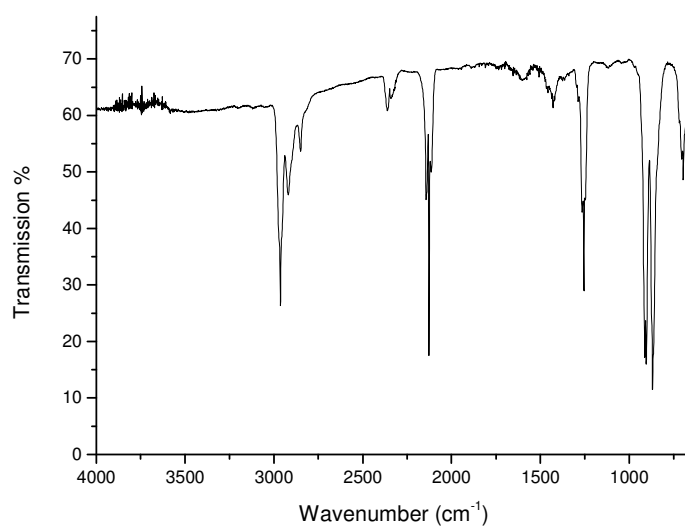
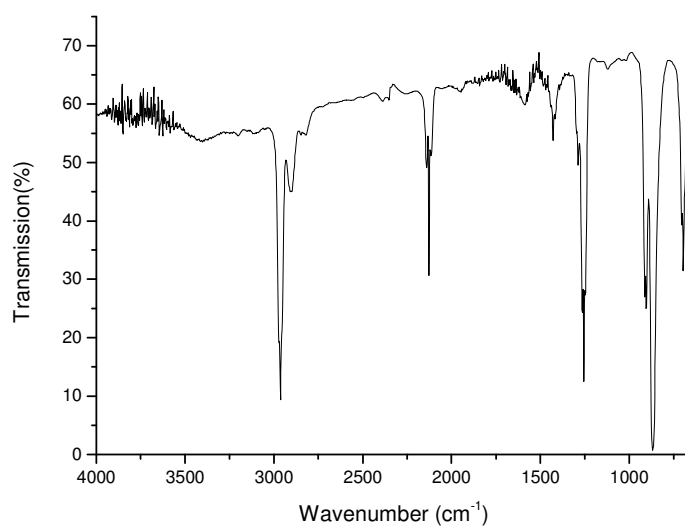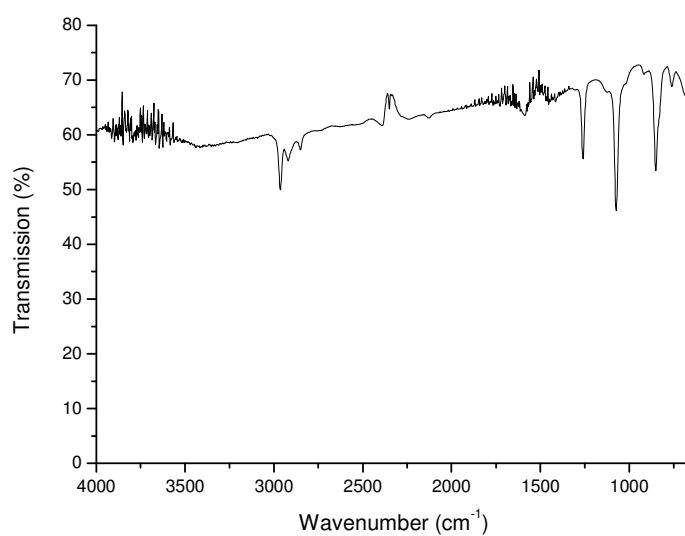**Figure 6:13**: 2:1 carborane-siloxane closed network sample gas phase FTIR of TVA

limb 2
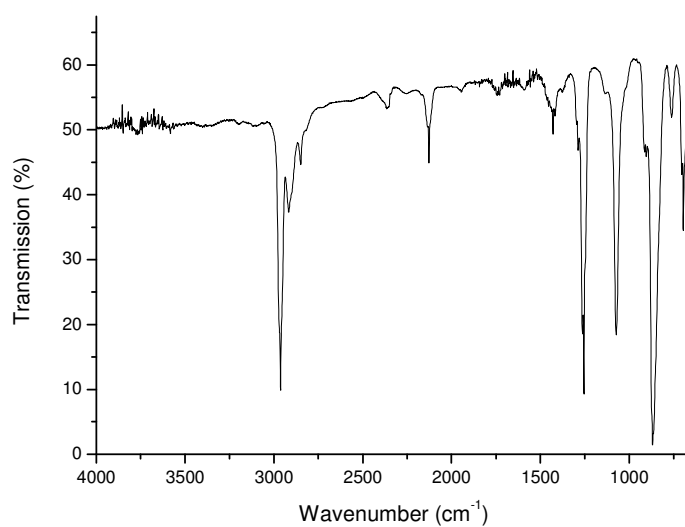
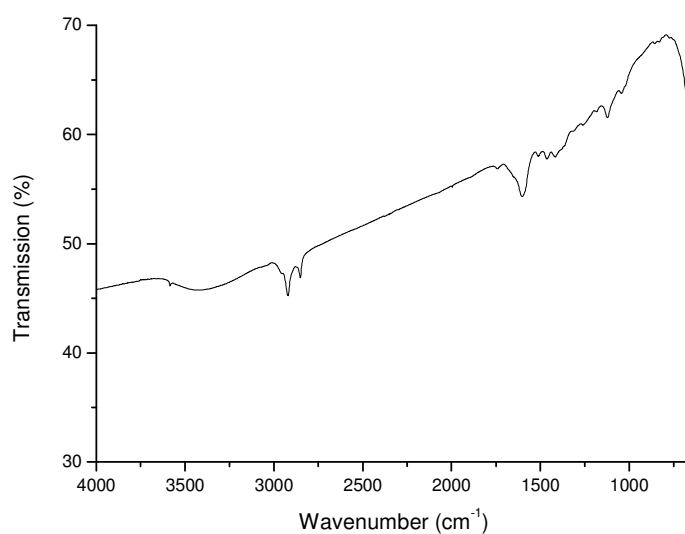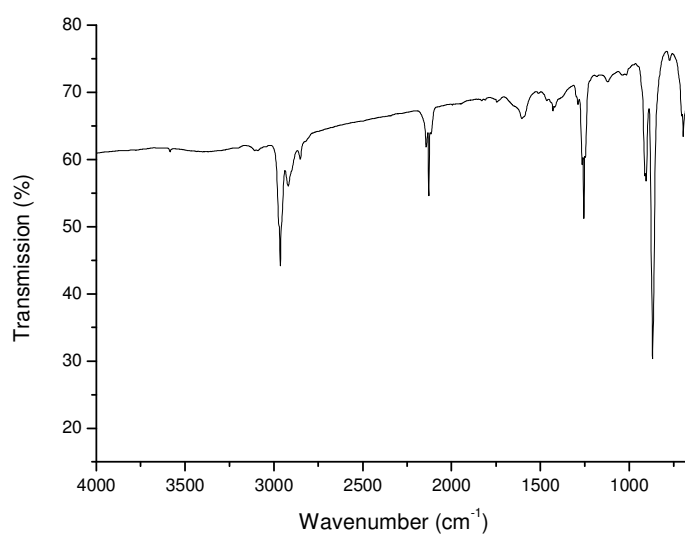**Figure 6.14**: 2:1 carborane-siloxane closed network sample gas phase FTIR of TVA

limb 3
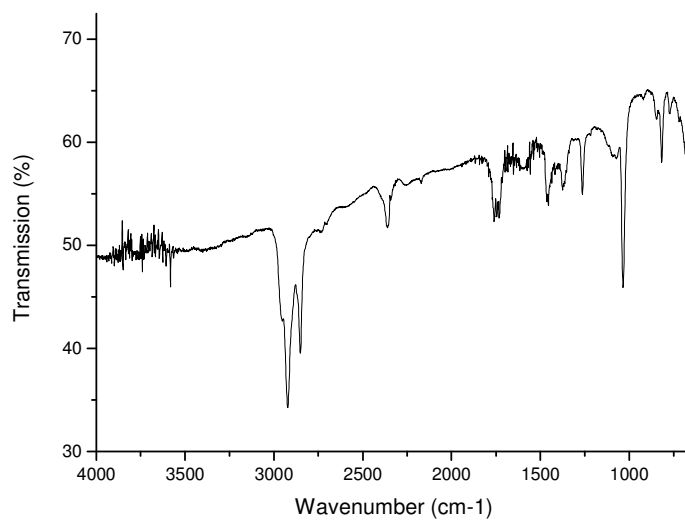
Figure 6:15: 2:1 carborane-siloxane closed network sample gas phase FTIR of TVA limb 4
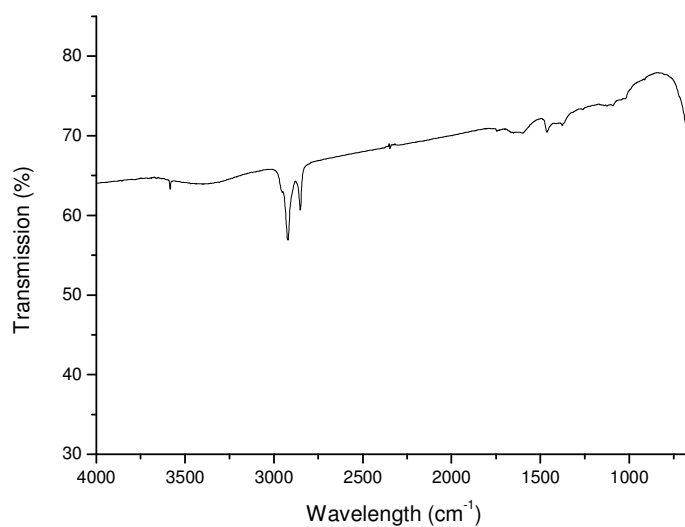
Figure 6:16: 6:1 carborane-siloxane closed network sample gas phase FTIR of TVA limb 1
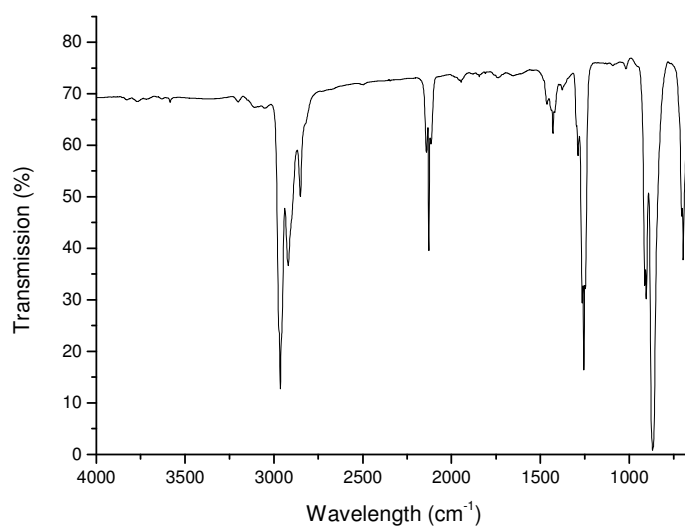
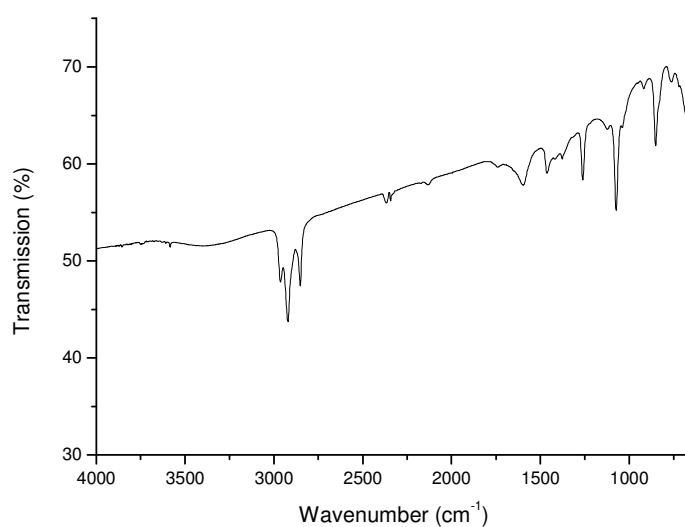**Figure 6:17**: 6:1 carborane-siloxane closed network sample gas phase FTIR of TVA

limb 2
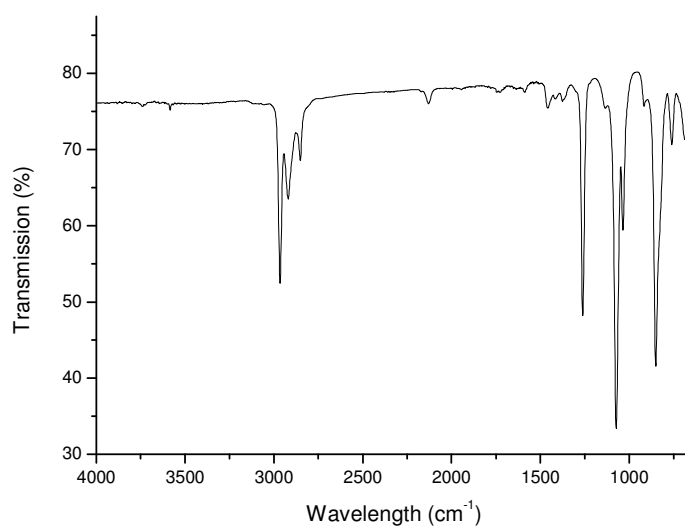
Figure 6.18: 6:1 carborane-siloxane closed sample network gas phase FTIR of TVA

limb 3
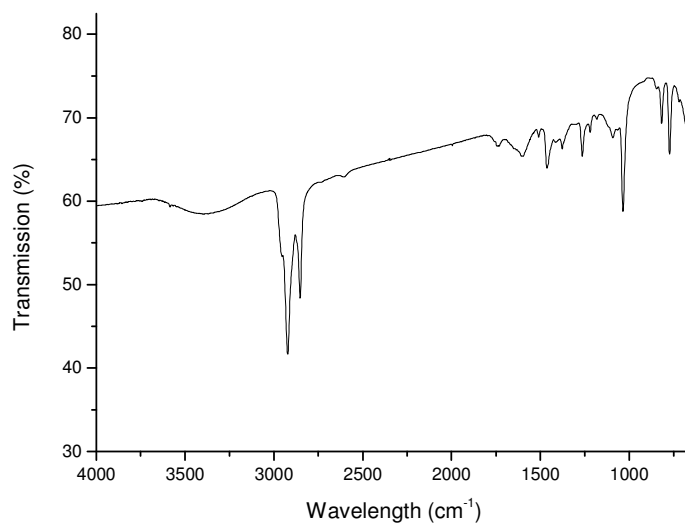
Figure 6.19: 6:1 carborane-siloxane closed network sample gas phase FTIR of TVA

limb 4
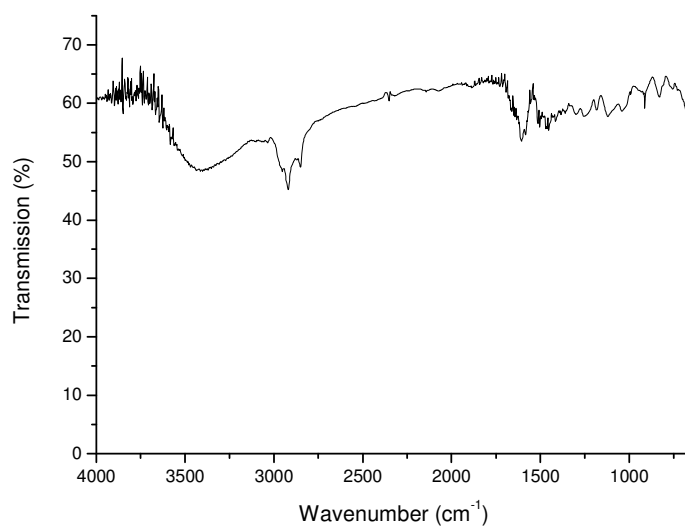
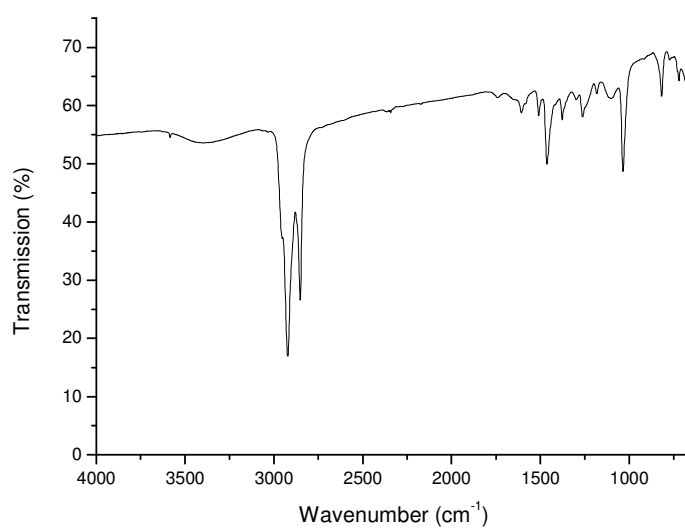**Figure 6.20**: 6:1 wash carborane-siloxane closed network sample gas phase FTIR of

TVA limb 1

Figure 6.21: 6:1 wash carborane-siloxane closed network sample gas phase FTIR of

TVA limb 2

Figure 6.22: 6:1 wash carborane-siloxane closed network sample gas phase FTIR of

TVA limb 3

Figure 6.23: 6:1 carborane-siloxane open network sample gas phase FTIR of TVA limb 1

Figure 6.24: 6:1 carborane-siloxane open network sample gas phase FTIR of TVA limb 2
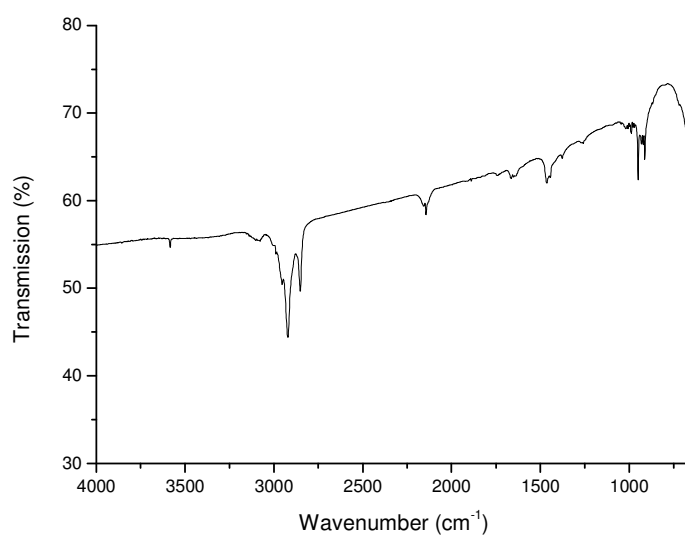
Figure 6.25: 6:1 carborane-siloxane open network sample gas phase FTIR of TVA
limb 3

Figure 6.26: 6:1 carborane-siloxane open network sample gas phase FTIR of TVA
limb 4

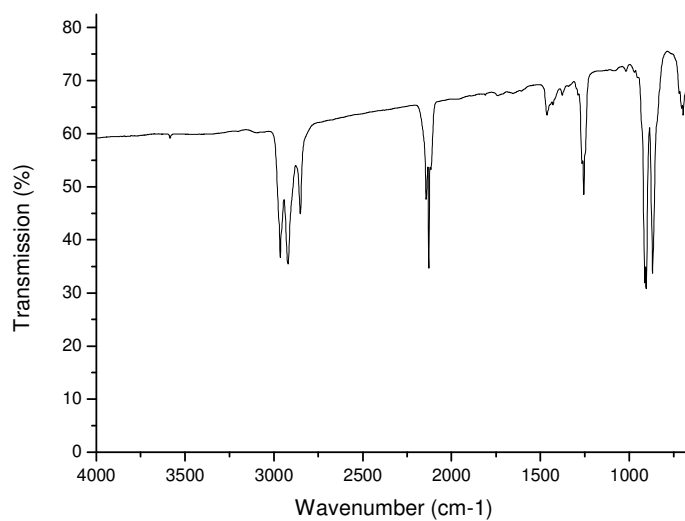**Figure 6.27**: 6:1 siloxane closed network sample gas phase FTIR of TVA limb 1

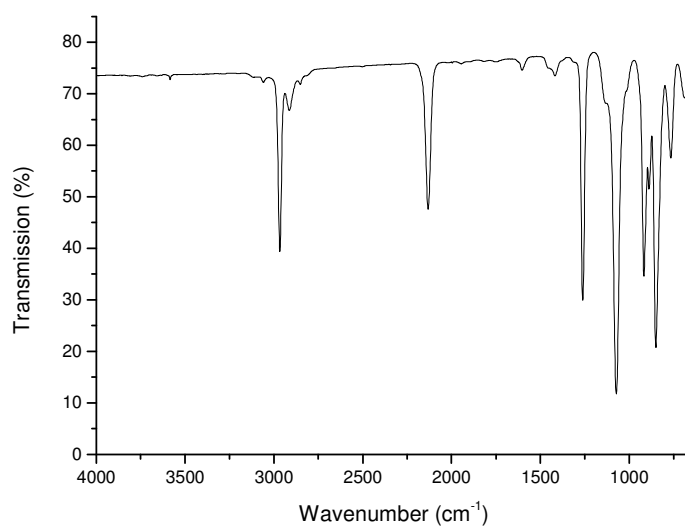**Figure 6.28**: 6:1 siloxane closed network sample gas phase FTIR of TVA limb 2

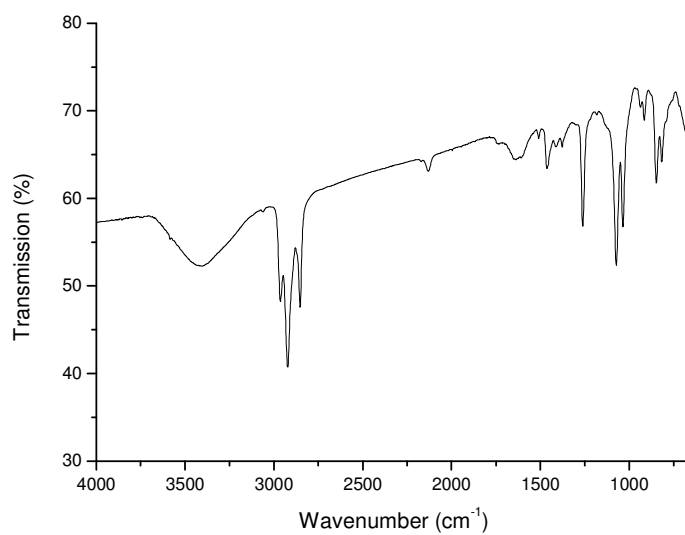**Figure 6.29**: 6:1 siloxane closed network sample gas phase FTIR of TVA limb 3

Figure 6.30: 6:1 siloxane closed network sample gas phase FTIR of TVA limb 4
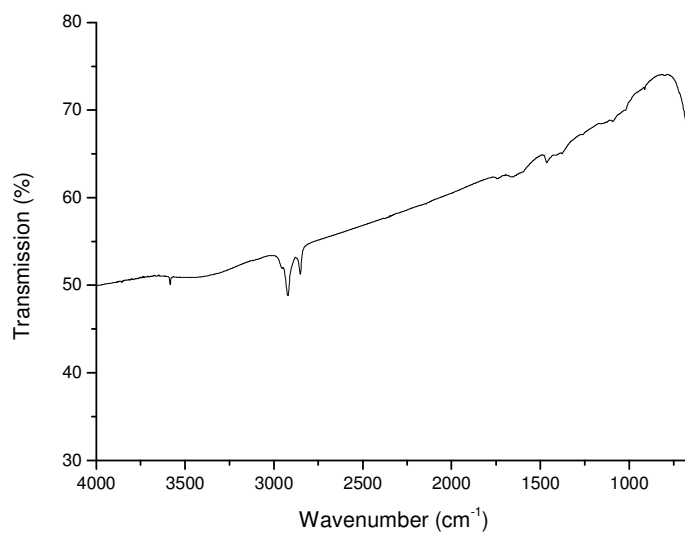
Figure 6.31: 6:1 siloxane open network sample gas phase FTIR of TVA limb 1
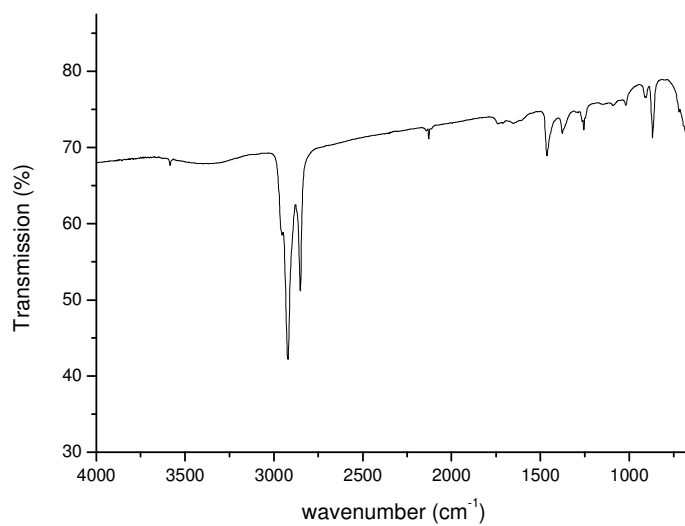

Figure 6.32: 6:1 siloxane open network sample gas phase FTIR of TVA limb 2
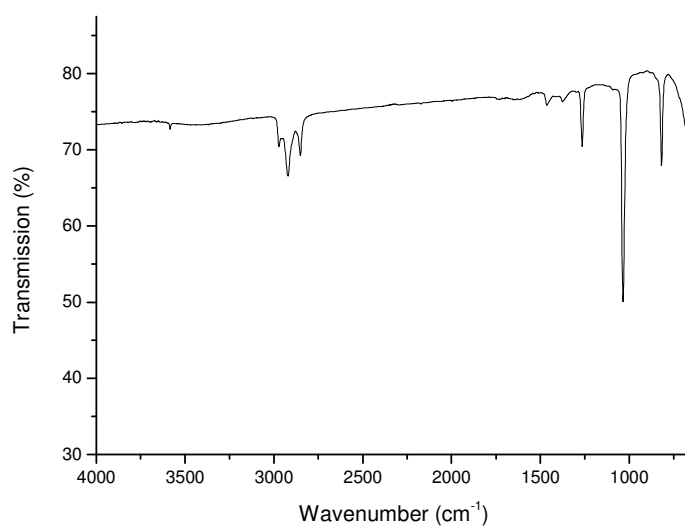
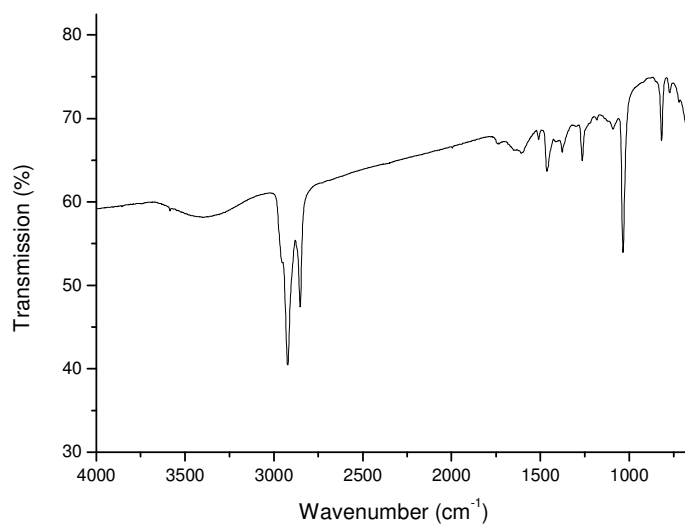**Figure 6.33**: 6:1 siloxane open network sample gas phase FTIR of TVA limb 3

Figure 6.34: 6:1 siloxane open network sample gas phase FTIR of TVA limb 4

2:1 carborane siloxane closed network copolymer GC Mass Spectrometry (m/e, M+):

Retention Time	Molar Mass	Identity
Cold Ring Fraction		
12.79	207.2	D_3 siloxane ring
13.96	281.2	D_4 siloxane ring
Limb 3		
4.23	131.3	Silane fragment
4.87	145.2	Small silane fragment
4.52	147.2	di-siloxane fragment
4.34	159.1	Karstedt's catalyst residue
4.37	193.1	hydride capped siloxane
Limb 4		
8.22	142.4	*m*-carborane cage
8.33	156.4	*m*-carborane + CH
9.04	170.4	*m*-carborane + C_2H_4
10.49	182.4	*m*-carborane + ?
4.37	193.2	siloxane disilane terminated
Retention Time	Molar Mass	Identity
6.10	205.2	D_3 siloxane ring
4.97	207.2	silane disiloxane end capped

6:1 carborane siloxane closed network GC Mass Spectrometry (m/e, M+):

Retention Time	Molar Mass	Identity
Cold Ring Fraction		
11.46	221.2	1,7 bis(allyl)*m*-carborane
14.72	281.1	D_4 siloxane ring
14.83	355.1	D_5 siloxane ring
Limb 4		
8.20	143.2	*m*-carborane cage
8.31	156.2	*m*-carborane + CH
8.39	171.2	*m*-carborane + C_2H_4
7.41	207.1	D_3 siloxane ring
5.63	221.2	trisiloxane
6.75	281.1	D_4 siloxane ring

6:1 washed carborane-siloxane closed network GC Mass Spectrometry (m/e, M+):

Retention Time	Molar Mass	Identity
Cold Ring Fraction		
14.82	354.9	D_5 siloxane ring
Limb 4		
4.93	207.0	D_3 siloxane ring

6:1 carborane-siloxane open network GC Mass Spectrometry (m/e, M+):

Retention Time	Molar Mass	Identity
Cold Ring Fraction		
4.81	207.1	D_3 siloxane ring
6.64	281.1	D_4 siloxane ring
8.25	355.1	D_5 siloxane ring
Limb 4		
4.85	429.1	D_8 siloxane ring
5.50	221.2	trisiloxane
6.64	281.1	D_4 siloxane ring
8.09	143.2	*m*-carborane cage
8.19	156.2	*m*-carborane + CH
8.27	171.2	*m*-carborane + C_2H_4

6:1 siloxane closed network GC Mass Spectrometry (m/e, M+):

Retention Time	Molar Mass	Identity
Cold Ring Fraction		
No peak	-	-
Limb 4		
5.95	207.1	D_3 siloxane ring

6:1 siloxane open network GC Mass Spectrometry (m/e, M+):

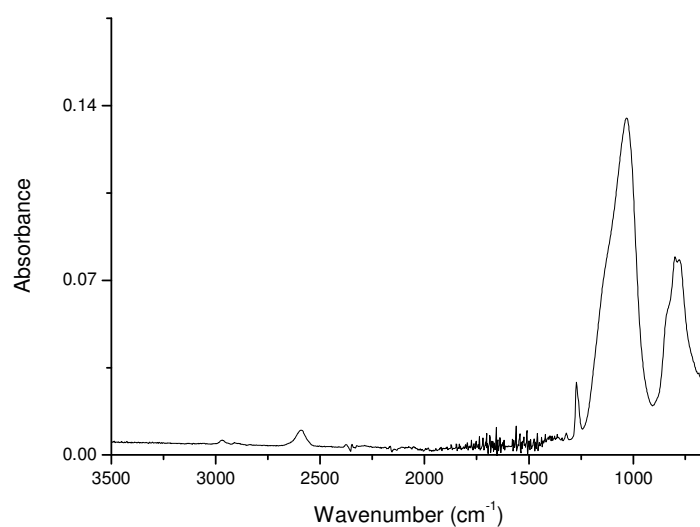| Retention Time	Molar Mass	Identity
Cold Ring Fraction		
No peak	-	-
Limb 4		
5.45	221.2	trisiloxane
6.62	281.1	D_4 siloxane ring

Figure 6.35: ATR FTIR spectrum of 2:1 carborane-siloxane closed network char residue
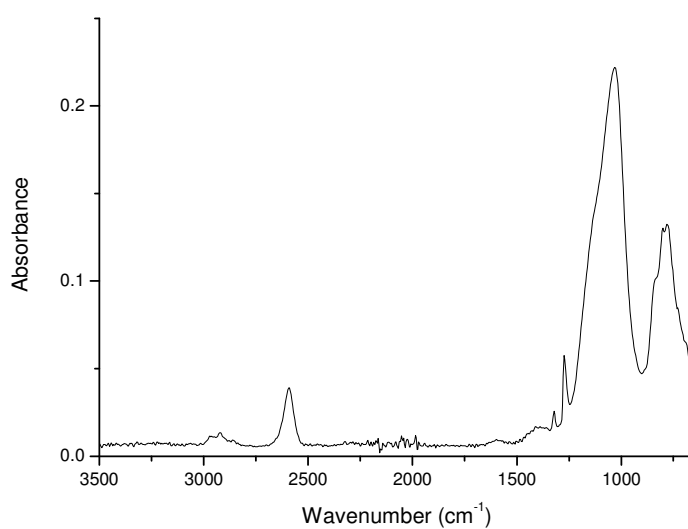

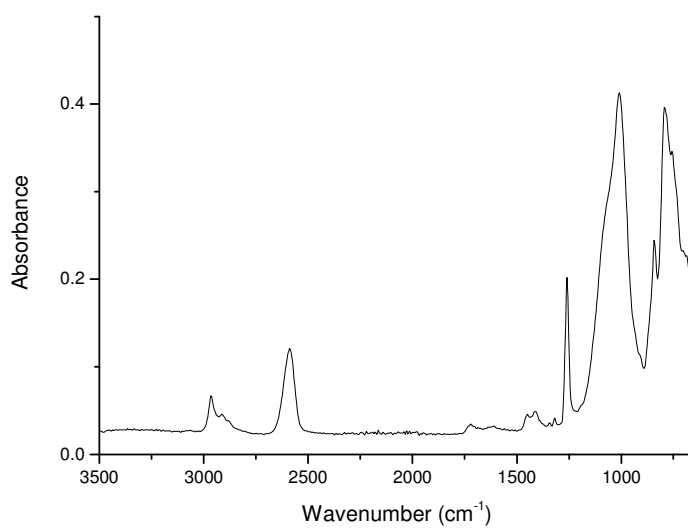**Figure 6.36**: ATR FTIR spectrum of 6:1 carborane-siloxane closed network char residue

Figure 6.37: ATR FTIR spectrum of 6:1 carborane-siloxane closed network washed
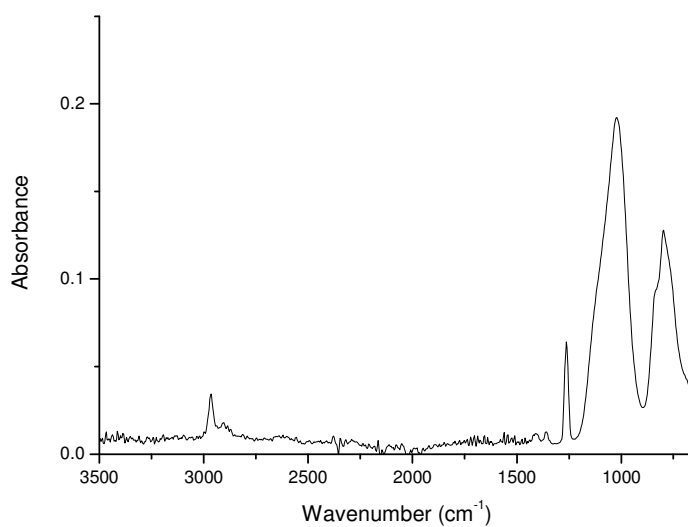
char residue

Figure 6.38: ATR FTIR spectrum of 6:1 siloxane closed network char residue